



## **TRINITY RIVER RESTORATION PROGRAM**

P.O. BOX 1300, WEAVERVILLE, CALIFORNIA 96093

PHONE: 530-623-1800, FAX: 530-623-5944

**Technical Report: TRRP-2021-1**

# History of Fine Sediment and Its Impacts on Physical Processes and Biological Populations in the Restoration Reach of the Trinity River, CA

**Prepared by:**

**Todd H. Buxton  
Trinity River Restoration Program  
Weaverville, California**

**February 2021**



US Department of the Interior  
Bureau of Reclamation

## Contents

LIST OF FIGURES	4
LIST OF TABLES	8
ACKNOWLEDGEMENTS	9
ABSTRACT	9
1. Purpose, scope, and definitions	12
2. Overview of fine sediment in stream ecosystems	12
2.1 Pathways for fine sediment delivery	14
2.2 Fine sediment storage in river corridors	15
2.3 Sediment transport in river channels	15
2.4 Fine sediment effects on flow and physical processes	17
2.5 Fine sediment effects on stream ecology	18
3. History of fine sediment in the Trinity River watershed	19
3.1 Sources of fine sediment	20
3.1.1 Geology	20
3.1.2 Hydraulic mining	21
3.1.3 Dredger mining	22
3.1.4 Timber harvest and roads	23
3.1.5 Wildfire	24
3.1.6 Landslides and mass wasting	26
3.1.7 Fluvial processes	27
3.2 Dam and flow regulation effects on fine sediment	28
3.3 Actions to reduce fine sediment in the Trinity River	31
3.3.1 Regulatory	31
3.3.2 Watershed restoration	33
3.3.3 Riffle cleansing	33
3.3.4 Riffle construction	33
3.3.5 Pool dredging and bar scalping	36
3.3.6 Sediment mining	37
3.3.7 Flushing flows	37
3.3.8 Geomorphic (high) flow releases	38
4. Fine sediment targets for the Trinity River	40
4.1 Instream biology	40
4.1.1 Holding habitat for adult salmon	40
4.1.2 Salmonid spawning gravels	40
4.1.3 Salmonid egg incubation	41
4.1.4 Juvenile rearing and adult salmon	42
4.1.5 Benthic macroinvertebrates	44
4.1.6 Ammocoete rearing	45
4.1.7 Nutrient storage	45
4.2 Floodplains	45
4.3 Geomorphic processes	46
4.3.1 Fine sediment budget	46
4.3.2 Coarse sediment mobility	46

4.3.3 Channel meandering -----	47
4.4 Summary of targets-----	48
5. Fine sediment in major tributaries -----	48
5.1 Deadwood Creek and Hoadley Gulch -----	49
5.1.1 Deadwood Creek flows-----	49
5.1.2 Deadwood Creek delta-----	50
5.1.3 Sediment loads and grain-size distributions-----	51
5.1.4 Carr fire effects -----	53
5.2 Rush Creek-----	54
5.2.1 Annual suspended and bed loads -----	54
5.2.2 Grain-size distributions for bed load -----	56
5.2.3 Rush Creek delta -----	58
5.3 Grass Valley Creek-----	59
5.3.1 Wellock and Hamilton ponds-----	60
5.3.2 Buckhorn reservoir-----	64
5.3.3 Carr fire effects -----	66
5.4 Indian Creek -----	67
5.4.1 Annual suspended and bed loads -----	67
5.4.2 Grain-size distributions for bed load -----	69
5.4.3 Indian Creek delta -----	71
6. Fine sediment in the Trinity River-----	71
6.1 Summary of fine sediment storage-----	71
6.1.1 Pools-----	71
6.1.2 Streambed -----	72
6.2 Sediment transport-----	77
6.2.1 Thresholds of mobility-----	78
6.2.2 Hiding effects and Shields stresses -----	87
6.2.3 Median bed material to bed load ratios -----	91
6.2.4 Fine sediment to coarse bed load ratios (S*)-----	95
6.2.5 Suspended load and bed load estimates-----	96
6.2.5.1 Spring flows -----	96
6.2.5.2 Fall and winter flows -----	100
6.2.5.3 Annual load estimates -----	106
6.2.6 Turbidity -----	113
7. Application of fine sediment targets -----	118
8. Summary of findings -----	126
9. Recommendations-----	128
9.1 Release flows for sediment routing and salmonid protection-----	128
9.2 Add fine sediment to the channel between Lewiston Dam and Rush Creek -----	129
9.3 Undertake analyses to remove Trinity River listing as sediment impaired -----	130
9.4 Monitor sediment transport and storage-----	131
9.5 Cease dredging Hamilton Ponds -----	131
10. Conclusions-----	133
REFERENCES -----	134

APPENDIX A. HISTORIC PHOTOS OF HYDRAULIC MINING IN THE TRINITY RIVER BASIN. -----	147
APPENDIX B. HISTORIC (1964–2018) FIRE ACTIVITY IN THE RESTORATION REACH OF THE TRINITY RIVER.-----	150
APPENDIX C. AERIAL VIEWS OF GRASS VALLEY CREEK DELTA AND WELLOCK AND HAMILTON PONDS.-----	152
APPENDIX D. PLANMAPS OF SEDIMENT TRANSPORT MONITORING LOCATIONS ON THE TRINITY RIVER.-----	155
APPENDIX E. CROSS SECTIONS SURVEYED PRIOR TO SPRING FLOW RELEASES AT THE SEDIMENT MONITORING STATIONS. -----	159
APPENDIX F. BED LOADS MEASURED DURING SPRING FLOW RELEASES. -----	160
APPENDIX G. CRITICAL DISCHARGES AND HYSTERESIS FOR BED LOADS AND SUSPENDED LOADS MEASURED DURING SPRING FLOW RELEASES. -----	174
APPENDIX H. SUSPENDED SEDIMENT LOADS MEASURED DURING SPRING FLOW RELEASES.-----	175
APPENDIX I. FRACTIONAL SUSPENDED SEDIMENT AND BED LOADS MEASURED DURING SPRING FLOW RELEASES.-----	189
APPENDIX J. DISCHARGES ABOVE THRESHOLDS FOR SEDIMENT TRANSPORT AT TRAL, TRLG, AND TRDC.-----	190
APPENDIX K. EXPONENTIAL CURVES RELATING DISCHARGES THAT EXCEED CRITICAL FLOWS FOR SUSPENDED SEDIMENT TO CONCENTRATIONS AT TRAL, TRLG, AND TRDC. -----	193
APPENDIX L. TURBIDITY AND DAILY AVERAGE DISCHARGES FOR SPRING FLOW RELEASES AT TRLG AND TRDC.-----	196
APPENDIX M. TURBIDITY AND DAILY AVERAGE DISCHARGES AT TRLG, RUSH CREEK, AND GRASS VALLEY CREEK.-----	209
APPENDIX N. TURBIDITY AND DAILY AVERAGE FLOWS ON THE TRINITY RIVER ABOVE THE NORTH FORK TRINITY RIVER.-----	212

## List of Figures

Figure 1.	Restoration reach of the Trinity River, California.-----	13
Figure 2.	Fine sediment stored at the base of a hillslope at RM 87.1 (a.), in an alcove and floodplain at RM 99.2 (b.), and in the lee of a boulder near RM 76.2 (c.), and stored in the bed, below the surface armor layer at RM 79.7 (d.).-----	15
Figure 3.	Schematic showing modes of fine sediment transport.-----	16
Figure 4.	Gully erosion from a road surface (a.) and a typical sample of decomposed granite (b.) in the Grass Valley Creek watershed.-----	21
Figure 5.	Hydraulic mining in the Trinity River watershed.-----	22
Figure 6.	View of Oregon Gulch from the old road grade.-----	22
Figure 7.	Dredger operating in the Trinity River corridor.-----	23
Figure 8.	View of Trinity River upstream of Oregon Gulch.-----	23
Figure 9.	Acreages in wildfires exceeding 5 acres and with recorded start dates in the restoration reach of the Trinity River for 1964–2018.-----	24
Figure 10.	Watershed area contributing flow and sediment to the restoration reach of the Trinity River.-----	25
Figure 11.	Aerial photographs of the Trinity River at Dark Gulch (RM 106.3-107.0) showing riparian berm formation that began in November 1960 with dam closure, continued through 1997, and started to be reversed by Record of Decision flows as pictured in 2019.-----	29
Figure 12.	Alder that stabilize banks along the Trinity River (RM 86.6 shown here) are being undercut by bank erosion in many areas of the channel.-----	30
Figure 13.	Flow volumes on the Trinity River at Lewiston (WY 1912–2019) before and after Trinity Dam closure in November 1960.-----	30
Figure 14.	Nearly three feet of fine sediment accumulation near Poker Bar (RM 103.0) in August 1975.-----	30
Figure 15.	Map of major tributary watersheds in the Trinity River restoration reach showing number of restoration projects undertaken in different categories.-----	34
Figure 16.	A bulldozer scarifying a riffle to loosen the streambed and flush fine sediments (a.) and a riffle sifter purging fines from a riffle in the Trinity River in 1971 (b.).-----	35
Figure 17.	Bulldozers constructing an artificial riffle on the Trinity River in 1971.-----	35
Figure 18.	Volume of coarse and fine sediment dredged from pools and removed from bar surfaces in the Trinity River from 1976 to 1991.-----	36
Figure 19.	A dragline (left panel) and excavator increasing depths in constructed pools used to trap fine sediment in the mainstem Trinity River from 1976 to 1991.-----	37
Figure 20.	A large sand delta at the confluence with Hoadley Gulch (RM 110.1) in August 1999 (left panel), and the same view in August 2019.-----	38
Figure 21.	Sand on the channel bed surface at Society Pool tail (RM 101.7) in September 1989 (a.), and relatively few fines on the restored coarse bed surface in 2013 (b.).-----	39
Figure 22.	Sand on the bed surface in August 1975 downstream of Poker Bar Hole at DWR cross section 17 (RM 102.3; a.) and the same area in 2013 showing a lack of fines on the bed (b.).-----	39
Figure 23.	Reo Stott pool (RM 102.5) largely filled with fine sediments in May 1977 (a.) and the same pool with its dimensions restored by evacuation of fine sediments in November 2019 (b.).-----	39

Figure 24. Relationship between percentages of grains smaller than 0.85 and 9.5 mm and Chinook egg-to-fry survival measured by Tappel and Bjornn (1983).-----	41
Figure 25. Schematic showing the embeddedness calculation as the ratio of a particle’s embedded height above the local plane of the bed ( $D_e$ ) to the total height of the particle ( $D_t$ ) in the bed.-----	45
Figure 26. Annual fine sediment load estimates for Deadwood, Grass Valley, Rush, and Indian Creeks.	49
Figure 27. Estimated rate of sediment filling a pool on the Trinity River near Lewiston by Deadwood Creek. -----	51
Figure 28. Suspended sediment load estimates for Deadwood Creek in WY 1997-1998, 2000-2004, and 2006. -----	52
Figure 29. Percent by weight of particles $\leq 8$ mm and daily estimates of fine bed loads estimated for Deadwood Creek in 1998–2001 and 2004.-----	52
Figure 30. Deadwood Creek watershed impacted by the Carr fire (a.) and the Deadwood Creek channel after a rainfall event (0.56 inches) that occurred October 2-4th, 2018. -----	53
Figure 31. Deadwood Creek delta on March 25, 2019 when flow at TRAL was 300 cfs.-----	54
Figure 32. Daily average flows and estimated cumulative annual suspended sediment loads for the period of record on Rush Creek. -----	55
Figure 33. Annual suspended sediment loads estimated with measured transport rates on Rush Creek for WY 1997–2006, excluding WY 2002.-----	55
Figure 34. Annual fine and coarse bed loads estimated with measured transport rates on Rush Creek for WY 1997-2006, excluding WY 2002 and 2003. -----	56
Figure 35. Daily average flows and percent of total bed load samples (by weight) $\leq 8$ mm in diameter (a.), and sorting (b.), skewness (c.), and median grain diameters ( $D_{50}$ , d.) for bed load sampled on Rush Creek December 1996 through May 2006. -----	57
Figure 36. Grain-size distribution for bulk samples collected on Rush and Indian Creek deltas in November 2002. -----	58
Figure 37. Grain-size distributions for bulk sediment samples obtained from Hamilton Ponds by GMA in 2009 and this author in 2018.-----	61
Figure 38. Cumulative volume of sediment infilling Hamilton ponds from dates of construction to the latest survey of the ponds in June 2018. -----	63
Figure 39. Peak daily average flow-normalized rates of sediment infilling Hamilton ponds for periods that contribution estimates are available. -----	63
Figure 40. Carr fire impacts in Little Grass Valley Creek above Buckhorn Dam (a.) and turbidity in Buckhorn reservoir on December 6, 2018 (b.) resulting from runoff in fire-burned areas in the watershed for the dam.-----	64
Figure 41. Area of Grass Valley Creek at the confluence with Buckhorn reservoir that was surveyed in July through September 2018.-----	65
Figure 42. Banded elevations showing surveyed topography of Grass Valley Creek at the confluence with Buckhorn reservoir. -----	66
Figure 43. Daily average flows and estimated cumulative annual suspended sediment loads for the period of record on Indian Creek. -----	68
Figure 44. Annual suspended sediment loads estimated with measured transport rates on Indian Creek for WY 1997–2006, excluding WY 1999 and 2002.-----	68

Figure 45. Annual fine and coarse bed loads estimated with measured transport rates on Indian Creek for WY 1998-2006, excluding WY 2001–2003.-----	69
Figure 46. Daily average flows plotted with $D_{84}$ and median grain diameters ( $D_{50}$ ; a.), percent of total bed load samples $\leq 8$ mm in diameter (b.), and sorting (c.) and skewness (d.) parameters for bed load sampled on Indian Creek December 1996–May 2006. -----	70
Figure 47. Percentages of fine sediment ( $\leq 8$ mm) in Wolman (1954) samples taken at sediment monitoring stations at TRAL, TRLG, and TRDC in 2006–2019. -----	73
Figure 48. Diameters of framework particles ( $D_{84}$ ), median grains ( $D_{50}$ ) and the 16th percentile of grain-size distributions ( $D_{16}$ ) from Wolman (1954) samples taken before and after spring flow releases at TRAL, TRLG, and TRDC from WY 2006–2019. -----	74
Figure 49. Sorting coefficients computed as $(D_{84}/D_{16})^{0.5}$ for Wolman (1954) samples were taken at TRAL, TRLG, and TRDC in 2006–2019. -----	75
Figure 50. Percent fines and grain-size distributions from bulk samples of the streambed surface and subsurface domain at stations on the Trinity River.-----	77
Figure 51. Critical discharges for fine and coarse bed load in WY 2006–2019. -----	81
Figure 52. Median grain size, skewness, and percentage of fine sediment ( $\leq 8$ mm) in bed load sampled at TRAL, TRLG, and TRDC. -----	82
Figure 53. Lateral bar 0.3 miles upstream of TRDC with the armor layer removed in a patch to show fine sediment that is sheltered in the subsurface domain. -----	84
Figure 54. Peak discharges that occurred outside the spring flow season at TRAL, TRLG, and TRDC (a.) and WY 2019 discharges showing winter flows experienced at these stations this year (b.).-----	86
Figure 55. Cumulative addition of coarse sediment to the channel upstream of TRAL and transported from the reach by spring flow releases.-----	87
Figure 56. Hiding exponents ( $b$ ) and Shields stresses for the median grain size ( $\tau_{c50}^*$ ) estimated with the hiding function of Parker et al. (1982) for WY 2006–2019.-----	89
Figure 57. Shields stresses for the median grain size ( $\tau_{c50}^*$ ) and associated Reynolds particle numbers ( $Re_c^*$ ) from Plate 1 in Buffington and Montgomery (1997) and for TRAL, TRLG, and TRDC, which occurred in rough turbulent flow ( $Re_c^* > 350$ ).-----	90
Figure 58. Shear stress partitioned for the granular bed ( $\tau_{\text{grain}}$ ) at discharges that bed load transport was measured at TRAL, TRLG, and TRDC. -----	91
Figure 59. Energy slopes (a.) and cross section average flow velocity for discharges that bed load transport was measured at TRAL, TRLG, and TRDC.-----	92
Figure 60. Diameters of the $D_{65}$ particle in Wolman (1954) samples taken prior to spring flow releases and used in estimates of $\tau_{\text{grain}}$ at TRAL, TRLG, and TRDC. -----	93
Figure 61. Values of $D_{\text{surface}}^*$ by year for 2008–2019 ( $D_{\text{surface}}^*$ ; a.) and $D_{\text{subsurface}}^*$ for 2006–2019 (b.). ---	93
Figure 62. Values of $D_{\text{surface}}^*$ and $D_{\text{subsurface}}^*$ versus discharge at TRAL, TRLG, and TRDC. -----	94
Figure 63. Ratios of the total fine sediment loads to coarse bed loads ( $S^*$ ) measured during spring flow releases at TRAL, TRLG, and TRDC.-----	96
Figure 64. Suspended loads and fine and coarse bed loads estimated for the spring flow period (April 1–July 31) in 2004 through 2019 by GMA. -----	97
Figure 65. Fractional loads of fine sediment estimated for spring flow releases on the Trinity River and associated flow volumes that occurred during the computational period (April 1–July 31) for water years 2004–2019. -----	98

Figure 66. Suspended sediment loads and daily average flows at TRLG for April 1981–September 1991. -----	99
Figure 67. Total suspended sediment loads measured at TRLG during tributary flow events and late winter or early spring high flow releases from Lewiston Dam for 1981–1992. -----	102
Figure 68. Power estimates of loads estimated for around the peak discharge, increasing limb of the hydrograph, or decreasing limb and steady flows at TRLG in winter in WY 1981–1991. ---	103
Figure 69. Suspended loads (<0.5 mm) measured during winter and spring flows in WY 2006 at TRLG and TRDC. -----	103
Figure 70. Fine bed load measured during winter and spring flows in WY 2006 at TRLG and TRDC. -	104
Figure 71. Suspended loads and fine and coarse bed loads estimated for times of year outside the computational period for spring flow releases in WYs 2006–2019. -----	106
Figure 72. Annual (left panels) and flow-normalized loads (right panels) of suspended sediment and fine and coarse bed load at TRAL, TRLG, and TRDC (left panels). -----	107
Figure 73. Daily average flows for the period of record that sediment loads were calculated at TRAL, TRLG, and TRDC. -----	108
Figure 74. Percentages of the total annual load and fractional loads transported during spring flow releases at TRAL, TRLG, and TRDC. -----	109
Figure 75. Deltas in March 2019 (left panels) where Deadwood Creek (a.) Hoadley Gulch (b.), and Indian Creek (c.) confluence with the Trinity River. -----	110
Figure 76. Flow normalized suspended sediment loads at TRAL before and after Trinity Dam closure in November 1960. -----	111
Figure 77. Peak annual discharges at TRAL for WY 1950–2018. Data labels indicate annual floods that occurred the first year after Trinity Dam closure (WY 1961) and dry water years after 2006 with suspended load estimates that are compared to the critically dry WY in 1961. -----	111
Figure 78. Suspended sediment loads at TRLG and Grass Valley Creek at Fawn Lodge. -----	112
Figure 79. Annual suspended loads at TRLG and Grass Valley Creek at Fawn Lodge (a.) with values standardized by drainage area and annual flow volumes at TRLG (b.). -----	113
Figure 80. Median daily average flow and turbidity at TRLG during high spring flow releases from Trinity and Lewiston Dams and for periods outside the high flow releases. -----	115
Figure 81. Daily average turbidity (top panel) and flow normalized turbidity at TRLG. -----	116
Figure 82. Median daily average flow and turbidity at TRNF during high spring flow releases from Trinity and Lewiston Dams and for periods outside the high flow releases. -----	117
Figure 83. Daily average turbidity (a.) and flow normalized turbidity at TRNF (b.). -----	118
Figure 84. Ammocoete survey results on the Trinity River between RM 86.8-84.8 and RM 83.7-81.4 .	125
Figure 85. Aerial view showing the preferred location for adding fine sediment to the Trinity River across from Trinity Hatchery and the weir hole site for additions. -----	132

## List of Tables

Table 1. z-values and associated severity-of-ill impacts to juvenile and adult salmonids in lotic waters.	44
Table 2. Fine sediment targets.	48
Table 3. Estimated volumes of sediment contributed by Deadwood Creek to the Trinity River.	50
Table 4. Rush Creek delta survey dates, changes in delta volume, and ratios of peak flow on the Trinity River and Rush Creek between surveys.	59
Table 5. Sediment volumes delivered to Wellock (W) and Hamilton (H) ponds, 1985–2018.	62
Table 6. Percentages of years that hysteresis was or not observed in suspended sediment and bed load transport at TRAL, TRLG, and TRDC from WY 2006–2019.	101
Table 7. Percent of sediment $\leq 2$ mm in bulk subsurface samples used to evaluate targets for substrate quality for salmonid egg incubation (<15%) and benthic macroinvertebrates (<30%).	119
Table 8. Percent egg-to-fry survival estimated for Chinook with equation (1) by Tappel and Bjornn (1983).	120
Table 9. Suspended loads normalized by the sum of discharges (tons/cfs) during the egg incubation period (October-March) on the Trinity River.	121
Table 10. Percent of time in the juvenile rearing period (January–July) that daily average turbidity was measured at stations on the Trinity River and percent of the available data that values were <30 NTU for >85% of the rearing period.	122
Table 11. Percentages of time that daily average values of severity-of-ill (z) were $\leq 5$ in the juvenile rearing and adult spawning periods for salmonids in the Trinity River.	123
Table 12. Percentage of grains $\leq 2$ mm in Wolman (1954) samples taken at sediment monitoring stations before and after spring flow releases on the Trinity River.	124
Table 13. Percentages of grains $\leq 2$ mm in bulk surface samples at stations on the Trinity River.	124
Table 14. Percentages of sediment $\leq 2$ mm in bulk subsurface samples used to evaluate the target range for gravel mobility (16-24%).	124

## Acknowledgements

Contributions from several individuals aided completion of this report. Andreas Krauss (Yurok Tribe) helped draft the outline for this report and provided helpful comments on the draft document. James Lee (Trinity River Restoration Program) provided information on fine sediment requirements for riparian plants. Wes Smith (NOAA contractor with Ocean Associates, Inc.) contributed to the section on the history of fine sediment sources in the Trinity River and geology. Jeanne McSloy (Trinity River Restoration Program) developed Figure 1 and Kathy Martens (Trinity River Restoration Program) formatted the document. This manuscript was substantially improved with input from four anonymous reviewers.

## Abstract

Land use activities, including mining, logging, and road building substantially altered sediment regimes in the Trinity River and tributary watersheds beginning in 1848 with the discovery of gold on the Trinity River. These actions increased sediment delivery to streams and caused channel aggradation that exceeded several meters in some areas of the Trinity River. Completion of Trinity Dam and the start of flow regulation in November 1960 eliminated the supply of sediment from the upper watershed before Lewiston Dam and Carr Tunnel were completed for use in diverting Trinity water to the Central Valley of California starting in April 1963. The reduction in Trinity River flows enabled fine sediments delivered by tributaries to accumulate in the channel and in berms along the riparian fringe of the river. In response, fine sediment reductions in the river were attempted with pool dredging, riffle cleansing, and bar scalping in the 1970s to reverse noticeable declines in salmonid populations, but with almost no lasting improvements. Source treatments were also implemented in the 1970s to reduce the fine sediment supply from tributaries, especially Grass Valley Creek. Revegetation, road improvements, construction of Buckhorn dam, and operation of sediment retention ponds near the confluence with the Trinity River were successful and largely eliminated Grass Valley Creek as a fine sediment source. Watershed restoration also reduced or maintained fine sediment inputs from Deadwood, Rush, and Indian creeks within ranges that appear normal for the period that data are available (late 1990s to mid-2000s). Meanwhile, a flushing flow study undertaken in the early 1990s recommended discharges that scour fines from depths that salmonids lay their eggs in the Trinity River. The Trinity River flow study further proposed hydrographs in the late 1990s to restore the Trinity River fishery by promoting ecosystem processes, including bed scour, bar construction, and riparian plant establishment, to name a few. The hydrographs were adopted in the Record of Decision (ROD, 2000) and first implemented in spring 2004 to meet a host of restoration objectives, including re-creation of a gravel channel bed and transporting fine sediment at rates that exceed supplies from tributaries.

These objectives were increasingly met on the restoration reach of the Trinity River between Lewiston Dam and the North Fork Trinity River beginning shortly after the start of ROD flow releases in spring 2004, as indicated by Wolman pebble counts and bulk sediment samples at repeat sites showing strong declines in fine sediment ( $\leq 8$  mm) and progressive armoring of the bed. Reduction in fines has also been documented in bed load sampled on the Trinity River during high flow releases from Trinity and Lewiston dams in spring (hereafter “spring flows”)

since 2006. The samples show skewness of the grain-size distributions increased (lower skew=fewer fines) along with median bed load diameters, and fine sediment as a proportion of the total load dropped. These changes were most apparent on the Trinity River at Limekiln Gulch (TRLG) and Douglas City (TRDC), and somewhat less apparent on the Trinity River at Lewiston (TRAL), which has exhibited a chronic deficit in fine sediment since 2006, outside of pulse inputs from channel reconstruction projects upstream of TRAL in 2008 and the Carr fire in 2019. Loads for grain-size fractions (i.e., fractional loads) varied between years depending on their supply and discharges available for transport them in the river. Linear regressions fit to fractional loads normalized by the volume of the spring flow release and discharges in excess of stability thresholds indicated that coarse bed load increased at TRDC, fine bed load decreased at TRLG, and suspended loads decreased at TRDC in 2006–2019 and increased slightly at TRAL in 2006–2016. The latter finding likely resulted from reservoir bank erosion in 2014–2016 and not contemporary supplies of fines since turbidity and suspended sediment transport was not measured at TRAL in 2017–2019.

Transport threshold analyses indicate that fine bed load ( $\geq 0.5$  mm and  $\leq 8$  mm) requires higher discharges for entrainment than coarse bed load ( $> 8$  mm) at TRAL due to the paucity of fines in the Lewiston reach. The counter-intuitive finding that large grains move before small particles at TRAL results from most fine sediment in the reach being sheltered under a coarse surface layer. This same arrangement explains the higher critical discharges estimated for fine bed load at TRDC since water year (WY) 2012, which suggests a deficit of fine sediment has developed in the Douglas City area. Analysis of the relative mobility of grain-size fractions using a hiding function by Parker et al. (1982) supports these results and shows that higher mobility has alternated between fine and coarse grains through time at TRAL and TRDC, with average results indicating approximately equal mobility since 2006. At TRLG, critical conditions for grain size fractions and threshold analysis indicate fine sediment is substantially more mobile than coarse grains, with threshold discharges for fines averaging 33% of those for coarse grains. Reconnaissance is needed to explain this result, with a possible reason being the apparent supply limitation in coarse sediment in the reach requiring relatively high flows to entrain enough material to reach the dimensionless transport rate for estimating critical conditions.

Annual estimates of Shields stress for the median grain size ( $\tau_{c50}^*$ ) plot within the range of expected variation with Reynolds particle number for all years at TRDC and TRLG, excepting WY 2009 and 2013 at TRLG. In these dry water years, fractional loads and their flow normalized values were a record or near record low at this station, but not the others. At TRAL, all values of  $\tau_{c50}^*$  were below the expected range except in WY 2008 (normal WY) and 2019 (wet WY). The cause for higher than normal  $\tau_{c50}^*$  for TRAL in WY 2008 is unclear but may have resulted in WY 2019 from an influx of fines from Deadwood Creek after the Carr fire stabilizing the bed through partial burial and cementation of coarse grains. This explanation aligns with the likelihood that relatively low  $\tau_{c50}^*$  at TRLG resulted, in part, from fine sediment being relatively unavailable for stabilizing the bed in comparison to years when values were in the common range. Higher  $\tau_{c50}^*$  occurs on more stable beds, so the predominately low values of  $\tau_{c50}^*$  at TRAL may seem to disagree with critical flows at TRAL commonly exceeding values for the other stations. Rather, low  $\tau_{c50}^*$  and high critical discharges occur at TRAL because the bed requires comparatively low shear stress for entrainment but relatively high discharges to increase energy slopes and flow velocities to levels that generate critical shear stress on the granular bed.

Annual loads of suspended sediment and fine and coarse bed load computed by adding spring loads measured by Graham Mathews and Associates (GMA) to winter and fall loads estimated by applying entrainment thresholds to sediment rating curves for TRAL, TRLG, and TRDC, and adjusting suspended loads for tributary contributions that occur in winter. In most years since 2006, >60% of the annual load and nearly all bed load transport occurs during spring flow releases at these stations, indicating most coarse sediment delivered by tributaries in winter is deposited and immobile in the mainstem channel until high flows in spring. This unusual dynamic results from flow regulation and may impede fish passage across tributary deltas and negatively effects egg incubation in fall and winter. Suspended sediments (<0.5 mm) are comparatively mobile in winter due to tributary accretions of flow in the mainstem channel and low entrainment thresholds, and thus may pose little threat to egg incubation in most years. However, in winter 2019, marginal areas of the channel upstream of Rush Creek were capped with silt from Deadwood Creek that impacted egg incubation where ~80% of Chinook salmon spawn in the river. A recommendation is to increase flow from Lewiston Dam to remediate these conditions as needed in the future to avoid mortality at this early life stage in winter as currently done with flows released on the Trinity River to safeguard the adult life stage in summer.

Fine sediments in the Trinity River have been dramatically reduced in the past 20 years by watershed restoration, sediment abatements in Grass Valley Creek, and high flow releases from Lewiston Dam. As a result, biological targets that require minimization of fines in the channel have been overwhelmingly met upstream of Junction City since 2009. The target for suspended sediment transport intended to promote salmonid egg incubation was met in all years at TRAL and the majority of years that transport was measured at TRLG and TRDC, and turbidity targets for benefitting juvenile rearing have been met in the restoration reach with only one exception since 2014. Based on this evidence, restoration actions have reduced fine sediments in the Trinity River to levels that are no longer detrimental to ecosystem functioning and salmonid populations. Indeed, repeat photos provide clear evidence of success meeting this goal, and findings herein suggest the supply limitation in fines first noted by McBain and Trush (1997) has increased to a degree that lack of fines may be limiting the health and functionality of the upper restoration reach of the Trinity River in present day.

The deficit in fines is particularly strong upstream of TRAL (river mile (RM) 110.2) and extends at least to Rush Creek (RM 107.9), and a recommendation is to add fine sediment near Trinity River hatchery to remedy the shortage. Additional recommendations are to resume suspended sediment and turbidity measurements at TRAL during high flow releases in spring from Trinity and Lewiston Dams and systematically conduct bulk sampling and facies monitoring in the Lewiston reach to adaptively manage the proposed fine sediment augmentations. Assuming spring high flow releases are continued from Lewiston Dam, an additional suggestion is to curtail dredging Hamilton ponds on Grass Valley Creek and conduct analyses to delist the Trinity River from its status as sediment impaired according to the Total Maximum Daily Load (TMDL) analyses by US EPA (2001). This action necessarily relies on reduced sediment supply from the South Fork Trinity River which has not yet been analyzed, yet is appropriate given success meeting fine sediment targets in the Trinity River restoration reach and timely since Trinity County instituted a grading ordinance in April 2019 so the TMDL is no longer the first defense against unnatural (human caused), high sediment inputs to the Trinity River. Such delisting will benefit restoration activities by potentially easing turbidity limits for channel

reconstruction projects and sediment augmentations that will, in turn, help ease the limited availability of fine sediment in the Trinity River.

## 1. Purpose, scope, and definitions

The purpose and scope of this document is to summarize available information and conduct analyses on fine sediment storage and transport effects on physical processes and biological populations in the 40-mile restoration reach of the Trinity River that extends between Lewiston Dam and the North Fork (NF) Trinity River (Figure 1). Definitions of fine sediment in the literature vary by particle size, mode of transport, and aspect of the stream biome. In this report, grains that transport in suspension on the Trinity River are considered fine sediment and delineated by size as  $<0.063$  mm (wash load),  $\geq 0.063$  to  $<0.5$  mm (fine suspended load), and  $\geq 0.5$  mm (coarse suspended load). Fine sediment that transports as bed load is termed fine bed load and was delineated by size as  $<0.5$  mm and  $\geq 0.5$  to  $\leq 8$  mm prior to water year (WY) 2015 and simply  $\leq 8$  mm thereafter. Fine bed load ( $\leq 8$  mm) is classified as pebble-sized grains by Wentworth (1922) but considered fine sediment on the Trinity River because this material is often decomposed granite that rapidly abrades to grains in the size range of sand ( $\leq 2$  mm) and silt (0.002 mm). Completing the size range of sediment in the Trinity River, grains that are larger than fine bed load are referred to as coarse bed load and assigned the size range  $\geq 8$  mm.

## 2. Overview of fine sediment in stream ecosystems

Fine sediment influences hydrologic and physical processes in streams when in storage and transport, and both phases can have profound influences on a stream's biome depending on the location and volume of fine sediment deposition. Where overly abundant, fine sediments can increase particle mobility, degrade aquatic habitat, and threaten biological populations. Grain mobility is increased by fine sediments when they are sufficiently available to deposit between large grains and smooth the bed, which increases flow velocities and drag forces on the partially exposed, large grains. Mobility of large grains can also be increased where fines are lacking and so unavailable for depositing amongst gravel to increase their stability by partial burial and cementation (Yager et al., 2018). In both cases, the relatively mobile bed can threaten egg incubation from mechanical crushing by mobile sediment or bed scour (e.g., Rennie and Millar, 2000; Montgomery et al., 1996), and fines that deposit on salmon nests (redds) can restrict intragravel flow and impede the flushing of metabolic wastes and lead to suffocation of embryos incubating in the stream bed (Chapman, 1990). A deficit of fines can also negatively impact nutrient cycling by restricting the availability of particles for flocculation, which occurs when nutrients aggregate on wash load that can settle on the bed surface and catalyze primary production in streams. Too few fines in floodplain areas can also inhibit germination of riparian plants by not providing sufficient media on which plants can establish (Dietrich et al., 2015). The mechanics for this is that fines exhibit low hydraulic conductivity and so retain moisture to support riparian root growth to water tables that sustain plants through the long, hot Mediterranean summers on the Trinity River. In this way, low availability of fine sediments can limit the resilience of riparian plant communities following disturbance and inhibit their regeneration following floods, mechanical restoration, beaver activity, and other disturbances in floodplain areas (Helfield et al., 2012).

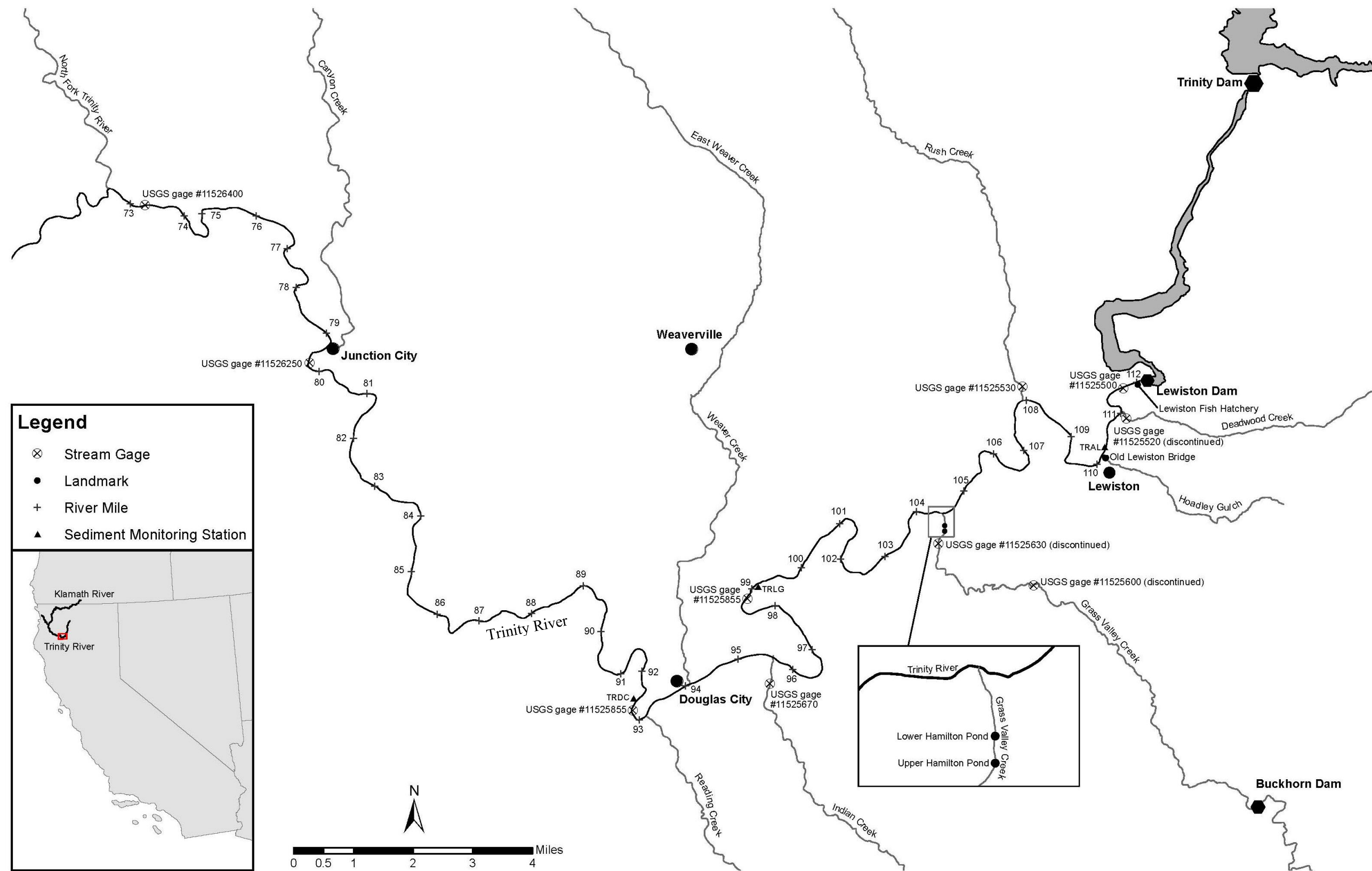


Figure 1. Restoration reach of the Trinity River, California. Acronyms in the figure indicate locations where sediment transport monitoring stations are located on the Trinity River at Douglas City (TRDC), Trinity River at Limekiln Gulch (TRLG), and Trinity River at Lewiston (TRAL), and where gaging stations are operated or were operated in the past by the U.S. Geological Survey (USGS).

A range of targets for managing the presence of fine sediment in stream ecosystems is necessary because fines differentially influence biological populations (macroinvertebrates, lamprey, and salmonids) and physical (bed load transport, channel migration) and riparian (plant colonization and growth) processes in stream ecosystems. For example, fine sediment deposits in slackwater areas of the channel provide rearing habitat for juvenile Pacific Lamprey (*Entosphenus tridentatus*) and fines deposited in the lee of point bars or in the up- or downstream end of chute channels that occur between point bars and the adjacent floodplain can promote channel meandering by restricting flow in the chutes (Braudrick et al., 2009; Parker et al., 2011). Another morphodynamic process involving fine sediment occurs when deposits form on bar tops near the inner bank on meander bends (Leopold and Wolman, 1960) and increase the bar's elevation to the adjacent floodplain for colonization by riparian plants that help maintain flow in the bend to erode the outer bank and promote further meandering. On a smaller scale, where fine sediment is overly abundant, it can fill interstitial spaces on the stream bed surface and increase near-bed flow velocities and promote coarse bed mobility (Wilcock et al., 2001; Wilcock and Crowe, 2003; Curran and Wilcock, 2005). However, fine sediments in abundance can endanger salmon reproduction. Research by Chapman (1990) determined where fines (defined as 0.8 to 6.3 mm by the author) compose 10% or more of the streambed sediments (by weight), egg-to-fry survival of Pacific salmon (*Oncorhynchus* spp.) is reduced. Also, fines that exceed 30% of the grain-size distribution in subsurface areas of the channel can reduce benthic macroinvertebrate populations (Relyea et al., 2000). These considerations highlight the availability of fine sediment must necessarily vary with location in a river corridor. Furthermore, after beneficial levels of fine sediment are restored in a corridor, a long-term balance between fine sediment delivery, storage, and transport is needed to promote healthy river functioning (Trush et al., 2000), which is an objective for restoration of salmonid populations in the Trinity River.

## 2.1 Pathways for fine sediment delivery

Fine sediment is delivered to rivers by multiple pathways. Hillslopes, particularly those with roads, are often major sources of fine sediment delivered to stream channels (Platts et al., 1989). Fine sediment delivery from hillslopes and roads occurs from landslides, road prism failures, road surface erosion, stream crossing failures, and gulying associated with channelization of water by roads (Furniss et al., 1991). Hillslope erosion and delivery of fines to stream channels are also increased in logged and wildfire areas where heat from fire or high summer temperatures may create a hydrophobic condition in the soil (DeBano, 2000), shelter from water impacting the slope is reduced by tree canopy removal (Mohammad and Adam, 2010), or mechanical stability of the hillslope from plant roots is lowered by tree removal (Sidle, 1992). In the Trinity Basin, relic mining ditches have and continue to deliver fines to tributaries and the mainstem river when gully erosion occurs downslope from where a ditch is breached (Madej, 2007). These modes of sediment delivery involve variable-term storage of material on hillsides, terraces, and floodplains for later contribution to stream channels or they can input directly to streams. Stream bank erosion is an additional direct contributor of fines (Abernathy and Rutherford, 2001) along with grazing impacts to floodplains, urbanization, and transport of fines to river channels by overland flow, frost heaving, and wind (Walters et al., 2003; Meehan and Platts, 1978; Dunne and Leopold, 1978).

## 2.2 Fine sediment storage in river corridors

Hillslopes, floodplains, and terraces are significant areas for storage of fine sediments in river corridors (Walling, 1997; Figure 2a). Hillslopes are source areas for fine sediments due to the weathering of colluvial materials and presence of vegetation that promotes organic soil development (Slattery and Burt, 1998). Floodplain storage of fines can then occur where hillslope failures or rainfall runoff transports this material, or when overbank flows access floodplain surfaces and are slowed by roughness that reduces the transport capacity of flow and promotes deposition of the transported load. In-channel areas where large amounts of fine sediment can be stored include interstitial spaces between coarse sediments on the bed, in pools, and in ponds (Lisle and Hilton, 1999), lee areas associated with wood jams and boulders, and in zones of backwater (e.g., alcoves; Figure 2b). Fine sediment storage also occurs below the armor layer on the streambed (Figure 2d). Perhaps the only area in a river corridor that fine sediment is not stored in appreciable quantities is in bedrock dominated areas of the channel.



Figure 2. Fine sediment stored at the base of a hillslope at RM 87.1 (a.), in an alcove and floodplain at RM 99.2 (b.), in the lee of a boulder near RM 76.2 (c.), and stored in the bed, below the surface armor layer at RM 79.7 (d.).

## 2.3 Sediment transport in river channels

Fine sediment ( $\leq 8$  mm) is mobilized when the basal shear stress exceeds the stability threshold of these sized grains. Following mobilization, fines can be transported as bed load or suspended in flow depending on the particle size involved and the magnitude of shear stress in excess of the

mobilization threshold. Wash load ( $<0.063$  mm) primarily travels in suspension and is typically present in small quantities so tends to be supply limited in streams. Because of its small size, wash load experiences low fluid drag that results in slow settling velocities, even in still water. In water with any kind of movement, wash load remains suspended by turbulence and Brownian motion (erratic motion of microscopic particles that results from molecular interactions in the fluid) and transports downstream at a rate that is approximately equal to the mean flow velocity (Biedenharn et al., 2006). Particles that transport in suspension but are larger than wash load (i.e.,  $\geq 0.063$  mm to  $<0.5$  mm) are held in the water column by turbulence and particle drag until forced into the bed by flow or until they settle in slackwater or lee areas in the channel (Figures 2b and 2c). Bed load are clasts in the size range of fine ( $\leq 8$  mm) and coarse ( $>8$  mm) sediment that are transported along the bed in a pivoting, rolling, or sliding motion or in saltation whereby particles alternately exhibit these motions and move downstream suspended in flow (Francis, 1973; Komar and Li, 1988). At high shear stresses, bed load is transported in the forementioned ways often while conglomerated in sheets (Recking et al., 2009), translating bars (Lisle et al., 2001), or migrating dunes (Dinehart, 1989).

Movement of fine sediment into stream beds can occur through open, connected pore spaces between large clasts. Even if most pore spaces are disconnected or clogged with fines, detritus, or biomatter, infiltration can still occur via “spontaneous percolation” or settling, whereby grains on the bed fall under gravity through a stationary bed of larger particles (Gibson et al., 2009; Bridgewater et al., 1969). Once in upper areas of a stream’s bed, horizontal, advective transport of fines can occur to produce a Brinkman load (Casas-Mulet et al., 2017; Figure 3). Horizontal transport that occurs below the Brinkman load area is called the interstitial load. Flume studies have estimated the Brinkman load can be  $\sim 90\%$  of the total subsurface load of fines (Brinkman + interstitial loads). Brinkman loads can exfiltrate from the bed by upwelling hyporheic flow for transport downstream by surface water (Casas-Mulet et al., 2018). Exfiltrated fines are accounted for in suspended and bed load sampling on the Trinity River, but Brinkman and interstitial loads are not measured by the Trinity River Restoration Program (TRRP).

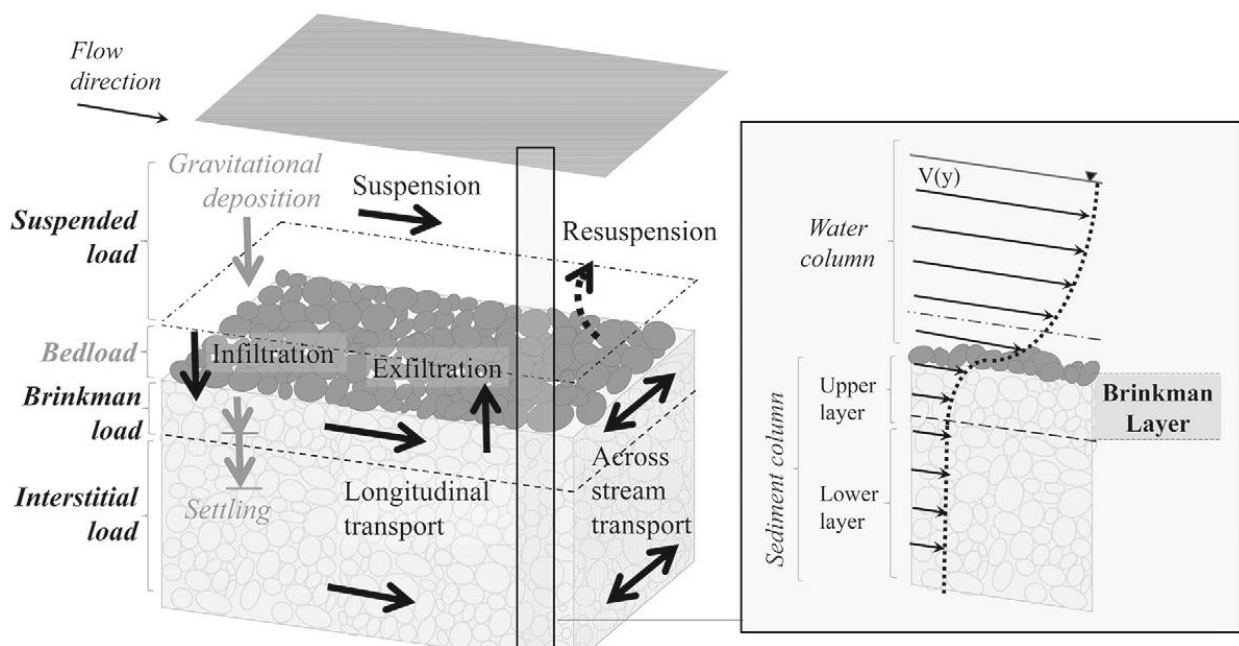


Figure 3. Schematic showing modes of fine sediment transport (from Casas-Mulet et al., 2017).

## 2.4 Fine sediment effects on flow and physical processes

The presence or absence of fine sediments differentially influence groundwater hydrology in river valleys by affecting water exchange between surface and subsurface flow in the channel, banks, and floodplains areas. Where fines are lacking, groundwater and surface water elevations are tightly coupled even when surface flows are highly variable. Such coupling was measured during the spring flow release in 2016 by Bradley (personal communication) at RM 90.0 and 83.1, where no difference between river flow and adjacent groundwater elevations was measured due likely to a lack of fines enabling pressure changes in surface water to immediately transmit water to subsurface areas in floodplains. Such rapid coupling has the advantage of increasing water in subsurface areas with brief increases in flow, but negative impacts of such quick response are numerous. Where fines are abundant in pore spaces between larger clasts, flow paths are inhibited by decreases in the porosity and hydraulic conductivity of the sediments. Such clogging limits the ability of flow velocity pressure and head to pump groundwater between clasts and into floodplain and terrace formations. Reduced rates of recharge in these areas during the rising limb of hydrographs can then result in time lags between increases in river stage and subsurface water levels that, in turn, can lessen the dampening effect of groundwater storage on flood magnitudes. As a result, where fine sediments are overly abundant in subsurface sediments, longer periods of high flows may be required to fill groundwater reservoirs. Attenuated groundwater recharge couples with slow groundwater release and baseflow maintenance in streams, which helps prevent high water temperatures in summer and low water temperatures in winter from negatively impacting the aquatic system's health.

By affecting bed porosity and hydraulic conductivity, fine sediments also influence the hyporheic zone in stream channels, which is the biologically and chemically active interface between surface water and groundwater that occurs along stream banks, bars, and riparian areas (Edwards, 1988). Reduction in porosity and conductivity can lead to modified characteristics of hyporheic exchange, including exchange rate (i.e., flux), volume, and residence time. These parameters have different ecological roles in streams. Hyporheic flux controls the rate of exchange of nutrients in surface flow for uptake and processing in the hyporheic ecotone (O'Keefe and Edwards, 2002). Hyporheic volume controls the spatial extent for nutrient processing (Valett et al., 1996). Residence time controls the temporal availability of nutrients for biochemical processing to occur (Marzadri et al., 2012). As with the continuity equation for surface flow, change in one aspect of hyporheic exchange has a direct influence on behavior of the others. For example, reduced hyporheic flux from abundant fines increases the residence time of solutes for biochemical processing and decreases the hyporheic volume so that fewer nutrients are available for uptake and storage while in transit in the bed. The extent to which these changes influence nutrient processing and upper trophic organisms that rely on the processing for aspects of their lifecycle depends on the biogeochemical processing rate of the nutrients that are present. Therefore, fine sediments in hyporheic areas can have positive or negative impacts to rearing salmonids depending on multiple factors.

Fine sediments that are sufficiently available to exceed the transport capacity of the subsurface environment will fill interstitial spaces in the bed and accumulate on the bed surface. In these occurrences, the increased range of coarse to fine particle sizes on the bed reduces grain sorting and the depth of resting pockets in which particles can reside, sheltered from flow (Buffington et al., 1992; Einstein, 1950). Fines in excess abundance can also smooth the bed surface, which lowers roughness and increases flow velocities near the bed, as mentioned before (Venditti et al., 2010). This in combination with suspended sediment raising the effective density of water increases shear stress on

the bed, which can result in bed instability and increased sediment transport. However, this outcome from excessive fines is not certain. For example, fines that infiltrate the bed and fill interstitial spaces between coarse particles may instead stabilize coarse particles by reducing exposure of grains to flow (Kirchner et al., 1990) and increase particle resistance from intergranular friction, enhanced weight on larger particles, cementation, and packing (Perret et al., 2017; Yager et al., 2018).

## 2.5 Fine sediment effects on stream ecology

Fine sediments have a diverse influence on stream biomes and are important for nutrient processing. Suspended particles that cause turbidity in streams are media for nutrients to flocculate (aggregate) in formations of particles called flocs (Petticrew et al., 2011). Flocs facilitate conveyance and storage of marine nutrients that are delivered to streams by adult salmon and processed by lower trophic levels to benefit aquatic food webs (Buxton et al., 2015b; Power and Dietrich, 2002). The trophic base that is directly aided by flocculation is biofilm (algae, bacteria, fungi, and protozoans), which dominate microbial life in stream ecosystems (Battin et al., 2016). Biofilm secrete polymers that enable flocculation to provide beneficial feedbacks to higher trophic organisms. For instance, biofilm is the primary food for macroinvertebrate grazers and scrapers, including caddisfly, mayfly, and freshwater snails (Hax and Golladay, 1993). These organisms can, in turn, function as the primary food for rearing juvenile salmonids. Therefore, turbid flows are an indication that the physical structure (inorganic sediment) for nutrient storage and cycling via flocculation is available to benefit fish production in streams.

High, protracted turbidity from suspended sediments can also be deleterious to biofilm and juvenile salmonids. High turbidity limits light penetration and can reduce primary productivity with resultant effects on lotic food chains (Wood and Armitage, 1997). Also, because salmonids are visual feeders, elevated turbidity can limit a fish's ability to locate prey for consumption and growth. Further limitations in prey occur where fines deposit on the bed in high concentrations, which can shift the macroinvertebrate community from surface dwelling organisms to burrowing taxa that are unavailable as prey for salmonids (Suttle et al., 2004). Alternatively, elevated turbidity can benefit fish survival by providing visual shelter from predation by piscivorous fish (e.g., Brown Trout (*Salmo trutta*) and Steelhead (*Oncorhynchus mykiss*)) and birds (see Hostetter et al. (2012), Strod et al. (2008), and Gregory and Livings (1998). Limits that define the duration and magnitude of suspended loads that benefit or weaken trophic cascades are unpublished, but limits that impact juvenile salmonids have been defined by research that is summarized in Section 4.1.4.

Reductions in the median size of surface grains and the exposed area of coarse particles by fines on stream beds can impact Foothill yellow-legged frogs (FYLF, *Rana boylei*, a species of special concern in California (see Lind et al. 1996)) and macroinvertebrate assemblages by lowering the exposed area of grains that are stable during non-flood flows (Wood and Armitage, 1997; Railsback et al., 2016). Both these effects often decrease FYLF populations and the density, diversity, and distribution of macroinvertebrates by restricting areas of suitable benthic habitats. Large wood and other roughness elements in the channel can mitigate some of these effects by promoting flow convergence and hydraulics that generate a topographically diverse bed that exhibits a patchwork of different grain-size distributions (Paola and Seal, 1995). For example, young FYLF prefer large, stable substrates and adult FYLF prefer grain patches with a range of particle sizes that generally exhibit intermediate mobility and are proximal to bedforms (Yarnell,

2000) that often coexist with large wood deposits and irregularity in stream banks (Buffington and Montgomery, 1999).

Deposition and infiltration of fine sediments on and in stream beds also impacts salmonid egg incubation. Fine sediments in ambient stream beds are mitigated to an extent by methods female salmon use to construct spawning nests (redds). To construct a redd, the female uses rapid undulations of her caudal fin to excavate a pit in the bed. In this process, fine sediments are flushed from larger clasts and into the water column for transport downstream (Buxton et al., 2015a; Montgomery et al., 1996). The relatively fine-sediment free gravel that remains to receive the deposited eggs provides them protection from predation in media that exhibits high hydraulic conductivity to support egg respiration and flush metabolic waste from the nest. After spawning is complete, egg mortality may result from abrasion caused by turbulence jiggling eggs in large, open interstitial spaces in the redd. Egg mortality can also occur if fine sediment infiltrates into the area of redds where eggs are deposited in quantities that reduce intergravel flow and leads to suffocation of embryos. This can be avoided if sand-sized sediments (<2 mm) are the first to deposit on the redd and block deeper infiltration of fines to protect the eggs from sedimentation (Lisle, 1989; Meyer et al., 2005).

Fines <2 mm are also important for germination and establishment of riparian plants. Here, the primary function is for fine sediments in combination with coarser materials to hold water long enough to support root growth to water table depths. In the absence of fines providing these soil-water conditions, plants are unable to survive through the long, hot, Mediterranean climate on the Trinity River.

### 3. History of fine sediment in the Trinity River watershed

Resource extraction that has intensively occurred the past 150 years has significantly altered the vegetation, soils, and sediment erosion and deposition regimes in the Trinity River watershed. Hydraulic mining for gold occurred in the watershed began in 1854 and lasted until the 1970s, and dredger mining in the mainstem river valley lasted from the early-1900s until the mid-1960s. Industrial logging also began in the watershed in the early-1900s, and with mining wholly altered the sediment regime in the Trinity River by introducing large quantities of material to the river by hydraulic mining hillslopes and terraces and altering the composition of existing sediment in the channel and floodplain areas with dredging. The historic flow regime was likely able to move a large portion of the increased supply of fine sediments downstream until flow regulation on the Trinity River began with closure of Trinity Dam in November 1960. Lewiston Dam was then completed in April 1963, which allowed flow diversions to the Central Valley via Carr Tunnel. The flow regulation and diversions significantly decreased sediment transport capacity in the Trinity River and caused fine sediment to accumulate in the channel and in tributary delta areas. To help reduce the storage and supply of fine sediments, rehabilitation work on the mainstem Trinity River began in the late 1970s and continues to this day. This section describes the primary sources of fine sediment, areas of accumulation, and management actions that promoted fine sediment erosion and its later abatement. Available quantitative and quality measures of fine sediment are presented, and the scale of impacts from land management on the fine sediment regime in the Trinity River watershed are emphasized in photographs presented below.

## 3.1 Sources of fine sediment

### 3.1.1 Geology

The watershed that contributes flow and sediment to the Trinity River restoration reach is underlain by portions of the Klamath Mountains Province, which is composed of five major Paleozoic and Mesozoic oceanic terranes that extend from east of Shasta Reservoir to just west of Willow Creek (see Irwin (2009) and geologic maps at <https://pubs.er.usgs.gov/>). The province is divided into the Eastern Klamath, Central Metamorphic, Western Paleozoic, Triassic, and Western Jurassic terranes. The eastern Klamath sub-province occupies the majority of Trinity and Lewiston reservoirs and tributaries that contribute flow to the restoration reach of the Trinity River (GMA, 2001). The sub-province consists of geology that is stable and erosion-resistant, except for serpentinites in the ultramafic rocks that are susceptible to mass movement. Two medium to high-grade metamorphic rock units occur in the sub-province, including the Salmon Hornblende Schist and Abrams Mica Schist, which are moderately erodible (Irwin, 2009). The Jurassic to Permian Sub-province underlies the North Fork Trinity River watershed, which consists of serpentinite, gabbro, and diabase along the western side and rocks further east include silicious tuff, chert, mafic volcanic rock, with minor lenses of limestone, phyllite, and local pebble conglomerates. The igneous rocks and sediments produce moderately stable slopes, and the serpentinites produce unstable slopes. Several plutons have intruded the Canyon Creek pluton, Granite Peak pluton, Shasta Bally Batholith, and Weaver Bally Batholith. The former two plutons are primarily diorite and created the Trinity Alps. These plutons do not contribute significant amounts of fine sediment to tributary streams. The Shasta and Weaver Bally batholiths consist of coarse-grained diorites and granodiorites composed of plagioclase feldspar, orthoclase feldspar, quartz, and mica (GMA, 2001). As feldspar weathers, it chemically transforms into the clay mineral kaolin that absorbs moisture, leading it to fracture and crumble into sand-sized particles of silica (Diller, 1910; Figure 4). Hillslopes underlain by these granitic-type rocks are composed of deeply weathered granodiorite, or decomposed granite. Hillslopes with decomposed granite retain little moisture, are non-cohesive and highly erodible, and produce large volumes of fine sediment when disturbed. Weathered granodiorite exists in most of Grass Valley Creek watershed and portions of Indian Creek, Rush Creek, Hoadley Gulch, and hillsides along the mainstem Trinity River. Aggressive timber harvest and road building in the mid-19<sup>th</sup> century caused large scale erosion of decomposed granite (Figure 4) that motivated rehabilitation efforts in Grass Valley Creek. Section 5.3 describes the extensive sediment erosion that has occurred upstream of Buckhorn Dam and Hamilton Ponds. Both were constructed to trap the eroded decomposed granite transported by Grass Valley Creek, as discussed below.



Figure 4. Gully erosion from a Grass Valley Creek watershed road surface and fill (a.) and a typical sample of the grain-size distribution of decomposed granite (b.).

### 3.1.2 Hydraulic mining

Gold mining began on the Trinity River in 1848 when the predominant method was to remove or “scalp” the upper portions of river bar material for sluicing and gold removal. Later, hydraulic mining with low pressure jets of water was used to erode stream banks, terraces, and hillsides into sluices for gold recovery beginning around 1854. Following a large flood in 1861, high pressure water jets came into use and continued until the early 1970s (Figure 5; Krause, 2012). This type of mining persisted in the region for 116 years as opposed to about 40 years in the Sierra-Nevada area because the Trinity watershed was not subject to the Gold Run Decision of 1882 nor the Sawyer Decision of 1884, which respectively issued and upheld an injunction against placement of mining debris in Sierra-Nevada and Central Valley Rivers. Because the Trinity River does not flow in these areas, hydraulic mining was not at issue in these rulings. Therefore, such mining continued for some time using water supplied to the jets by elaborate infrastructures for water delivery. The infrastructures included water pipes and water bridges and series of low head dams on tributaries or was more simply supplied by diversions from the Trinity River into ditches, which themselves contributed sediments to stream channels and floodplain areas (Bailey, 2008). When operational, the La Grange mine at Oregon Gulch and Union Hill mine near Douglas City were the two largest hydraulic mines in the world. In its lifetime, the La Grange Mine produced approximately 110 million cubic yards (cy) of sediment that nearly filled Oregon Gulch to its hilltops (Figure 6; Bailey, 2008). Over time, these sediments were delivered to the Trinity River and impounded material transported by the river and caused the channel to aggrade up to 16 ft for miles up- and downstream of Oregon Gulch (Krause, 2010). Besides the La Grange and Union Hill mines, 307 additional mines were registered in Trinity County. Amongst these, notable mines included the Sykes hydraulic mine near Trinity Center and the Cie Fse Mine near Junction City (Appendix A; Bailey, 2008).



Figure 5. Hydraulic mining in the Trinity watershed (courtesy of the Trinity Historical Society).



Figure 6. Oregon Gulch viewed from the old road grade (courtesy of the Trinity Historical Society).

### *3.1.3 Dredger mining*

Dredger mining in the Trinity River started in the early 1900s and continued until 1959. Dredgers were essentially bucket excavators that dug pools up to 40 ft deep, processed the extracted sediment for gold, and then returned sediment to the river in mounds deposited at the rear of the dredge (Figure 7; Krause, 2012). Dredgers worked between hillslopes wholly disrupting the natural stratigraphy of the river valley by scooping up and sorting riverbed sediments and then dumping the fines at the bottom of dredger pools and capping them with coarse sediments. It is unclear whether dredging resulted in a net addition or deficit of fines

sediments in the Trinity River, but it undoubtedly modified processes that regulate fine sediment deposition and storage in the river corridor (Figure 8).



Figure 7. Dredger operating in the Trinity River corridor (courtesy of the Trinity Historical Society).



Figure 8. View of Trinity River upstream of Oregon Gulch (courtesy of the Trinity Historical Society).

#### 3.1.4 Timber harvest and roads

Forest road networks were built to support mining, timber harvest, and development in rural and urban areas of the Trinity watershed beginning in the late 1800s. Between this time and 2001, GMA (2001) estimated that 1,340 miles of roads were constructed in watershed areas of the Trinity River restoration reach. From these roads, the estimated average mass rate per unit area of sediment production is 130 tons/mi<sup>2</sup>/yr (GMA, 2001). In the Rush Creek watershed alone, Madej (2007) estimated that total surface erosion from roads was 277,000 tons from 1924 to

1998. Extensive timber harvest in the 1940s through 1990s further increased sediment contributions to streams where skid trails on hillsides intercepted subsurface flow and accelerated soil erosion. Harvest areas were also destabilized by clear cuts that nearly eliminated rainfall interception and generated hillslope instability from loss of mechanical stability from tree roots as stumps rotted. These cumulative effects increased water yields that further increased surface erosion and mass failures on hillslopes and groundwater interception by road and skid trails. Timber harvest areas and roads have not been assessed for erosion potential in the Trinity River watershed since 2001. Nonetheless, sediment contributions from harvest activities have likely been substantially reduced since implementation of the Northwest Forest Plan on federal lands in 1994 and the California Forest Practices in 2017.

### 3.1.5 Wildfire

Fine sediment delivery to streams is typically increased by wildfire disturbance to landscapes that can superheat the forest floor and induce formation of a water repellent soil layer by forcing hydrophobic substances from leaf litter into the soil profile (Woods et al., 2007). The hydrophobicity can block water infiltration and increase the bulk density of soils, which together promote surface runoff on hillslopes and increase soil erosion. This in combination with the elimination of leaf litter and reduced canopy cover are some of the main causes of increased fine sediment delivery to streams following wildfire events. In the Trinity River restoration reach, the number and size of wildfires exceeding 5 acres in 1964–2018 have varied markedly between years. In decreasing order of acreage burned (in parenthesis), years with the largest total burned area with recorded ignition dates were 1987 (40.1 mi<sup>2</sup>), 1964 (26.7 mi<sup>2</sup>), and 2018 (24.5 mi<sup>2</sup>; Figures 9 and 10, Appendix B). Extended periods when fires did not exceed 5 acres were recorded in 1965–1986 (21 years) and 1988–1991, 2002–2005, and 2010–2013 (3 years each).

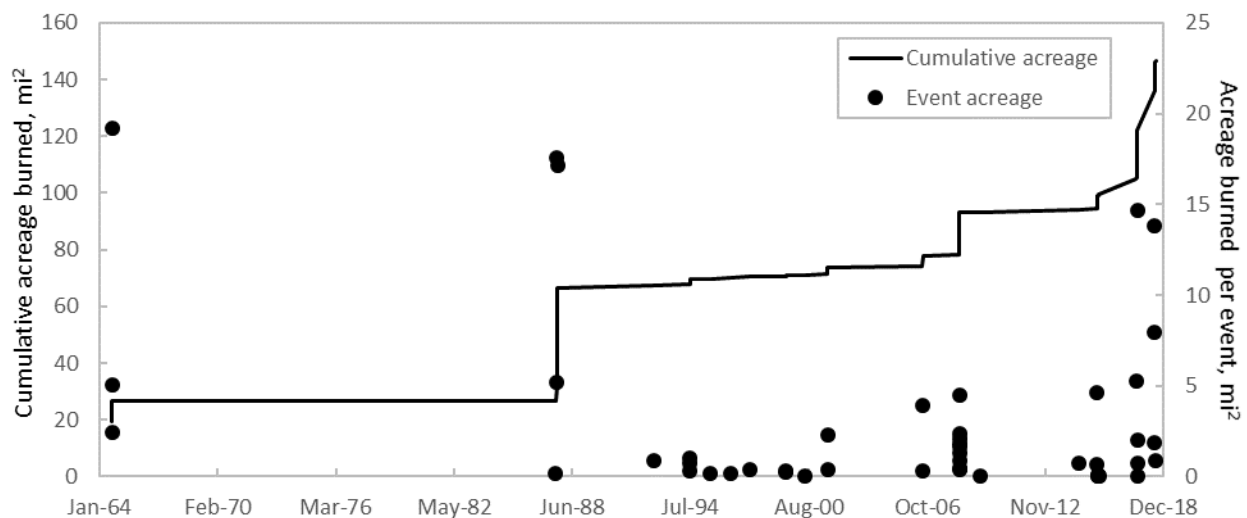


Figure 9. Acreages in wildfires exceeding 5 acres and with recorded start dates in the restoration reach of the Trinity River for 1964–2018.

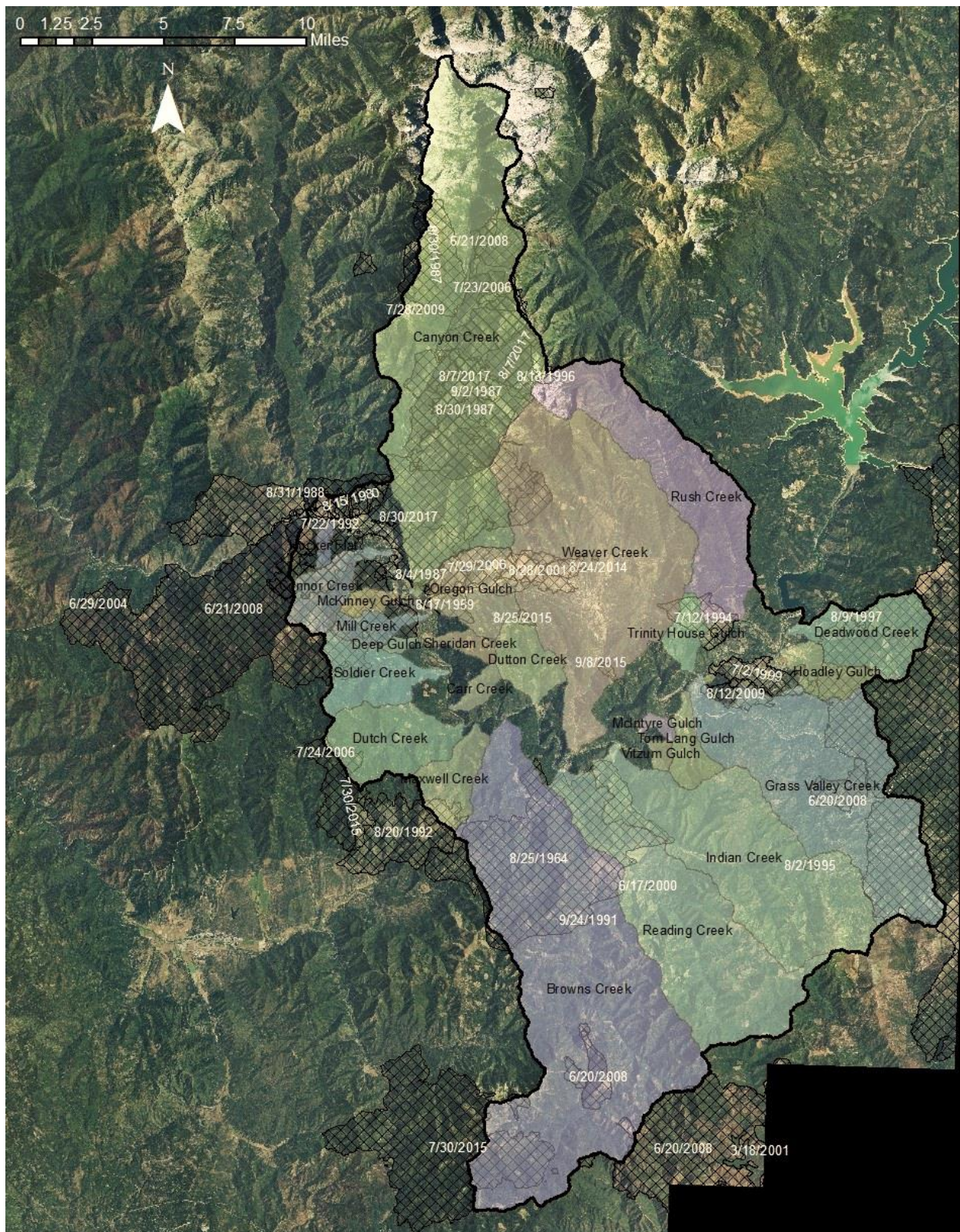


Figure 10. Watershed area (black outline) contributing flow and sediment to the restoration reach of the Trinity River. Named tributaries are colored and wildfires that exceeded 10 acres in 1964–2018 are shown hatched and labeled with their ignition dates.

Despite pauses in activity, wildfire is a common disturbance on the landscape that affects channel evolution and functioning. A recent outcome of fire in the Trinity basin has been increased fine sediment supply from fire-affected tributaries and formation of large delta deposits at tributary confluences with the mainstem channel. The occurrence of both from fire is discussed in Section 5, and it is important to note that both can have profound influences on salmonid habitats for incubation, rearing, and spawning. In the short term, accreted deltas can prevent salmonid spawners access to tributaries when tributary flows shallow beyond minimum depth requirements for fish migration (see Bjornn and Reiser, 1991). Longer term influences of delta growth from fire are the deposits can affect the spatial distribution of mainstem channel substrates for fish spawning by increasing channel gradients downstream of their lobe and lowering gradients upstream as a result of their partial blockage to flow (Benda et al., 2003). Upstream of deltas, in fire-affected tributaries, reductions in the water retention capacity of soils can lower summer flows, which in combination with decreased canopy and shade from burning can increase water temperatures and reduce the availability of habitats for fish (Isaak et al., 2010). This along with channel aggradation from accelerated inputs of sediments can extend throughout a tributary basin and effectively exacerbate negative influences of fire on fish (Moody and Martin, 2001). Tributaries in the restoration reach are not monitored for their change in sediment production and availability of fish habitat following wildfire disturbance. The literature on these topics is consistent on points made above, such that wildfire effects on streams exert both a physical and biological influence that can vary in magnitude and duration through time ranging from decades to centuries depending on numerous factors (Clague et al., 2003).

### *3.1.6 Landslides and mass wasting*

Aerial photograph analyses by GMA (2001) indicated that landslides and mass failures in the Trinity River watershed generally increased between 1944 and 2000 (). A total 64 slides were identified in 1944, 50 slides were identified in 1979 as having occurred since 1944, and an additional 250 slides were identified in 2000 as having occurred since 1979. GMA (2001) further discovered that more slides occurred in the 21 years between 1979 and 2000 than in the 35 years between 1944 and 1979, which included the series of floods that were generated by rain on snow events between December 19, 1964 and January 11, 1965 (see USBR, 1965). The heaviest rains in this period fell on a 10-20 ft deep snowpack in the Trinity and Klamath mountains the week of December 19–26, 1964 and generated a peak inflow to Trinity Reservoir of 84,000 cfs while outflow from the dam was maintained at 224 cfs. Flows from tributaries downstream of the dam were nonetheless sufficient to generate a record 231,000 cfs at Hoopa (U.S. Bureau of Reclamation, 1965) and cause the Trinity River to migrate laterally as much as 140 ft and aggrade up to 11 ft (Ritter, 1968). Major tributaries (see Figure 1) themselves experienced -1.7 to +4.6 ft change in elevation and up to 270 ft of lateral migration near their confluence with the Trinity River due in part to landslides causing aggradation and debris flows on the streams (Ritter, 1968).

Returning to the landslide inventory by GMA (2001), Reading Creek had the largest number of slides occur between 1979 and 2000 (49), followed by Browns Creek (46), Indian Creek (40), and Grass Valley Creek (38). Of the total volume of landslides inventoried from 1944 to 2000, volumes generated by roads were 37% in 1944, 23% in 1979, and 27% in 2000. Timber harvest-related landslide volumes were almost non-existent in 1944 and 23% of the historic volume in 1979 and 21% in 2000. Landslide volumes in forested areas were 63% of the historic total in

1944 and 54% and 52% respectively in 1979 and 2000. Weaver Creek and Indian Creek were the two largest producers of landslide volumes between 1979 and 2000. Notably, Rush Creek and Weaver Creek were dominated by non-management related landslides in this period (both 94% of the total), likely related to rain-on-snow debris torrents and slides generated by the large storm event in 1997. In most of the remaining sub-watersheds, the combined management-related landslides (roads and harvests) generated 50 to 90% of inventoried landslides. GMA (2001) provides comprehensive details on the methods and sediment inputs by various land management activities, but grain-size distributions for the source materials is not provided.

### *3.1.7 Fluvial processes*

Fine sediments are stored on stream beds and beneath coarse armor layers on gravel beds (see Figure 2d). Consequently, elevated flows that initiate movement of the bed surface can expose significant amounts of fine sediment for redistribution in the channel and on floodplain surfaces. Mobility of coarse grains in the armor layer of the Trinity River has been measured by several researchers (e.g., Wilcock et al., 1995; McBain and Trush, 1997; USFWS and HVT, 1999), and the earliest known marked rock study was undertaken in 1991 (TRA, 1993). The studies typically involved painting rocks of a desirable size (usually the local median grain size ( $D_{50}$ ) or the surface particle that is coarser than 84% of grains on the bed,  $D_{84}$ ) a distinguishable color, labeling them with a unique identifier, and placing them at known locations on the surface of the bed and returning after one or more high flow events to see if movement occurred. Inaccuracies with this approach were that 1) a rock's first movement was unlikely to represent thresholds for similar particles in the area of placement because the marked grain was not fluvially arranged (imbricated or packed) on the bed; 2) if several high flow events occurred before the monitored site was revisited, the highest flow was associated with the rock's movement even though it may have transported at a lower discharge; and 3) if a rock mobilized a significant distance or was buried, it was often difficult or impossible to find, which reduced the sample size for determining probabilities of particle movement. Particle mobility studies have more recently been undertaken using rocks embedded with Passive Integrated Transponders (PIT). The PIT in each tagged rock is dormant until excited by a magnetic coil in a wand the researcher hovers over the bed. The excited PIT tag emits a unique radio frequency uniquely identifying the particle even when buried up to a meter deep. On the Trinity River near Lowden Meadows (Gaeuman, 2019), PIT tagged rocks were used to track particles and largely avoid inaccuracy from 3) but PIT tag studies are still affected by 1) and 2). Results from both techniques have provided results that are highly variable between locations and time, so are not summarized here. Instead, thresholds of mobility for fine and coarse sediment are addressed in Section 6.2.1.

Stream flows that mobilize the bed surface can lead to scour of the bed. Bed scour undoubtedly varied widely between the pre- and post-dam periods due to significant changes in flow and sediment regimes on the Trinity River. Unfortunately, bed scour data is only available for the post-dam period, including WYs 1991–1993 by Wilcock et al. (1996) at Poker Bar (RM 103.7) and Bucktail (RM 106.1), WYs 1996–1997 by McBain and Trush (1997) at Sheridan Creek (RM 82.0), Steiner Flat (RM 91.1), and Bucktail, and on point bars in the restoration reach by Hales et al. (2020) in WY 2009–2013. In Wilcock et al. (1996) and McBain and Trush (1997), scour was highly variable between years and discharges due to the spatial and temporal variability in shear stress and sediment supply and transport that have first-order effects on scour. Results from Wilcock et al. (1996) were that scour of the surface armor layer generally occurred at a Shields

stress for the  $D_{50}$  of 0.06, and the value that McBain and Trush (1997) measured was 0.063. Statistical evaluation of scour measurements for WY 2009–2013 by Hales et al. (2020) indicated scour depths increased with Shield Parameter, and that a discharge of around 8,500 cfs was required to mobilize 80% or more of the bed surface and that around 10,000 cfs is needed to scour to a depth equal to the diameter of the local  $D_{84}$ .

Adjustments to the dimensions of the Trinity River channel's have also varied widely through time. Before Trinity and Lewiston Dams significantly decreased flood magnitudes and flow variability, the Trinity River meandered broadly and displayed an active width of around 500 ft in the vicinity of Dark Gulch (RM 107; August 1944 and September 1960 panels in Figure 11 below). Less than a decade later, in May 1971, flow regulation and sediment retention by the dams enabled riparian vegetation to colonize the channel margins and fix the river in a largely stable planform (see Figure 11). Channel migration restarted when allocation of water to the river was increased by the Secretarial Decision of 1981, followed by a large tributary-dominated flood in 1997 (McBain and Trush, 2000) and implementation of the “feather edge” concept that involved removal of riparian berms and grading the river's banks to a gentle slope (Curtis et al., 2015). As a result of these actions, channel widths normalized by channel length and time in 1980–1997 were higher than any period since ( $0.30 \text{ m}^2/\text{m}/\text{yr}$ ; Curtis et al., 2015). Curtis et al. (2015) also found that normalized values (in parenthesis) were positive in subsequent time frames, indicating channel widening also occurred in 1997–2001 ( $0.24 \text{ m}^2/\text{m}/\text{yr}$ ), 2001–2006 (0.23), 2006–2009 (0.08), and 2009–2011 (0.27). This trend continued in 2011–2019 (0.12), as determined from active channel width measurements made from aerial photos by the author. In the past year, the increase in active channel area almost exclusively resulted from channel rehabilitation work undertaken summer 2020. In viewing the aerial photos and rafting the restoration reach in 2020, the author observed alder that have encroached on the channel being undercut by bank erosion (see Figure 12). An expectation is the undercutting banks will collapse and increase channel migration rates in the medium term (10-15 years) assuming Himalayan blackberry and reed canarygrass do not establish in denuded areas where trees fall before high flows cause bank erosion and channel migration (Hook et al., 2009; Hough-Snee et al., 2010).

### 3.2 Dam and flow regulation effects on fine sediment

Following closure of Trinity Dam in November 1960, nearly all sediment from upper watershed areas was impounded. Only wash load passed the dam 1) during large rain events that triggered emergency flow releases in WYs 1963 and 1974 to avoid a full reservoir from overtopping the dam and 2) during periods of low reservoir pools in WYs 1977, 1991, and 2015 when erosion of the exposed banks by wind and rain introduced wash load that remained suspended in the reservoirs for downstream release. In April 1963, Lewiston Dam was completed and became operational and Carr tunnel began diverting Trinity water to the Central Valley. The storage of sediment by dams and reduction in river flows by regulation and diversions cause a deficit of fine sediments to develop between Lewiston Dam (RM 112.2) and Deadwood Creek (RM 111.0). However, below Deadwood Creek, unnaturally low, year-round flows released from Lewiston Dam until the first year of ROD flows in spring 2004 (see Figure 13) caused fine sediments from tributaries to exceed the storage capacity of the bed and the transport capacity of regulated flows. Negative effects of the resulting sedimentation to salmon spawning areas were recognized almost immediately. The earliest published observations of fine sedimentation on the Trinity River following dam closure known to the author was by the U.S. Geological Survey

(USGS) between 1961 and 1965 (USGS, 1968). Observations included impacts from the record 1964 flood that accelerated “tremendous natural erosion process[es]...in the Trinity River watershed” that were catalyzed by mining, road building, and logging. This coupled with up to 92% of the total annual Trinity Flow being diverted to the Central Valley and discharges being maintained at 150-300 cfs year-round (McBain and Trush, 1997) caused particle-size distributions and channel bed elevations near tributary junctions to respectively transition from primarily pebble and cobble to sand at 15 of 17 stations where aggradation averaged 2.2 ft (USGS, 1968; see Figure 14). These changes resulted in a spawning habitat loss of ~80% between Lewiston Dam and Grass Valley Creek and ~50% in the following 6 miles, according to LaFaunce (1968; Krause, 2012).

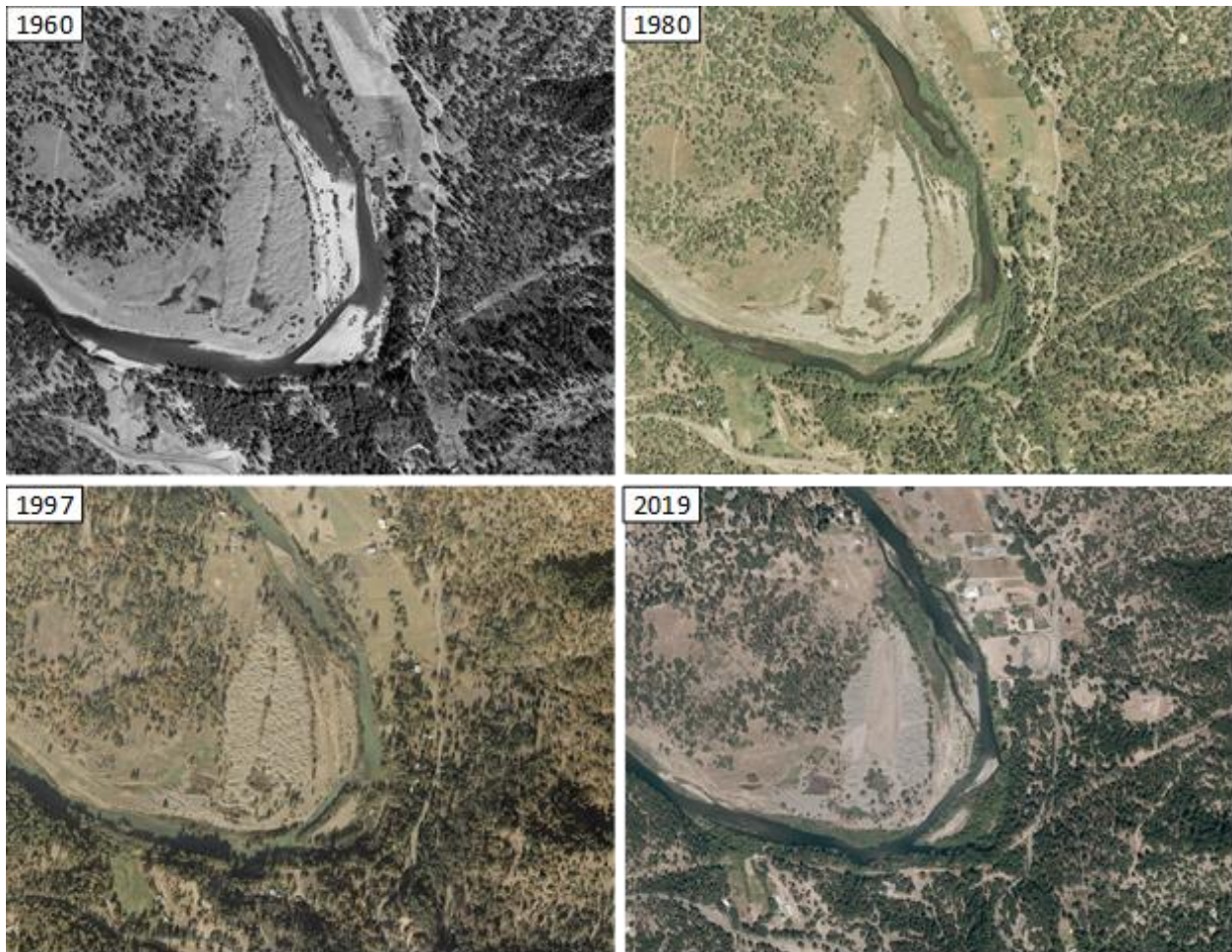


Figure 11. Aerial photographs of the Trinity River at Dark Gulch (RM 106.3-107.0) showing riparian berm formation that began in November 1960 with dam closure, continued through 1997, and started to be reversed by Record of Decision (ROD, 2000) flows as pictured in 2019.

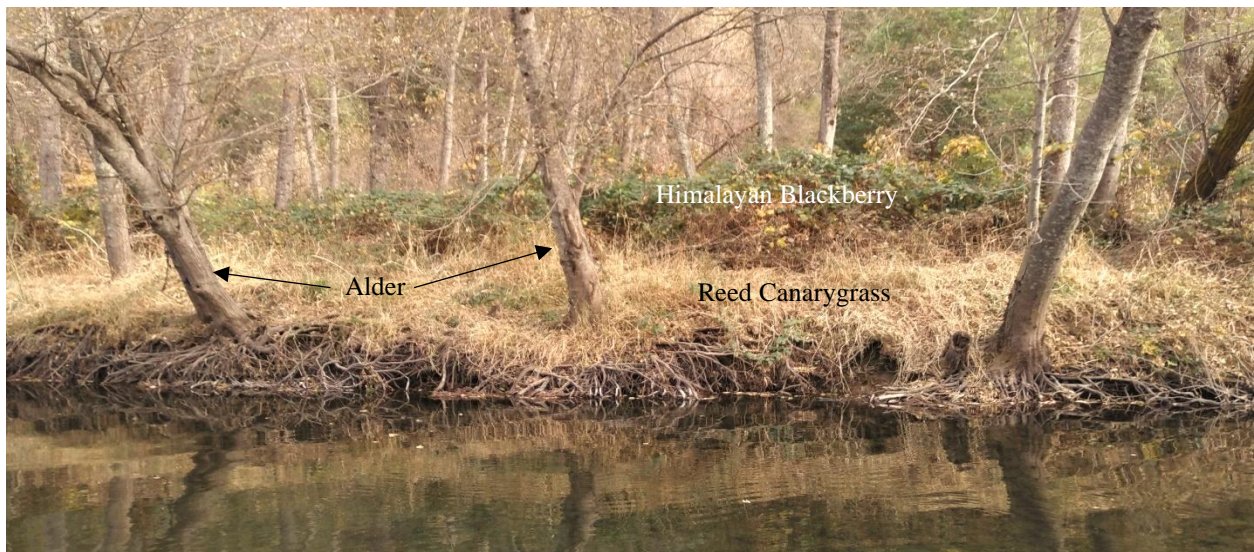


Figure 12. Alder that stabilize banks along the Trinity River (RM 86.6 shown here) are being undercut by bank erosion in many areas of the channel.

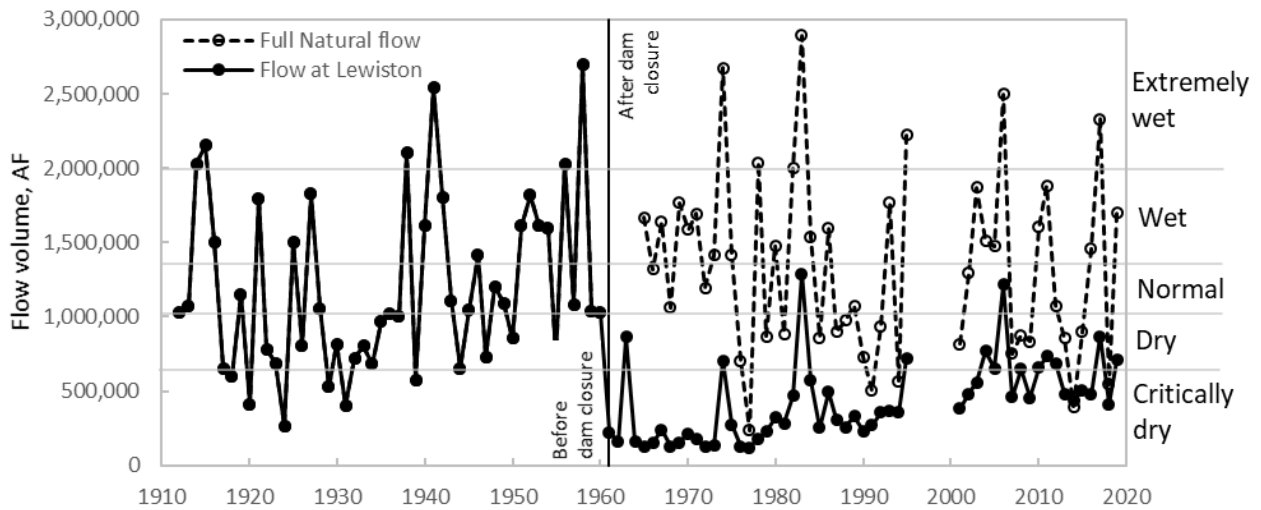


Figure 13. Flow volumes on the Trinity River at Lewiston (WY 1912–2019) before and after Trinity Dam closure in November 1960. Water year designations for full natural flows are also shown.



Figure 14. Nearly three feet of fine sediment accumulation near Poker Bar (RM 103.0) in August 1975.

By 1967, coarse granitic sand blanketed the channel 8 miles downstream of Lewiston Dam, and habitat degradation from the accumulations extended 30 miles downstream of the dam in 1977 (TRT, 1978). The U.S. Bureau of Reclamation recognized the siltation problem in 1967 and concluded the dams benefitted spawning gravel quality by eliminating floods that would have dispersed sand from Grass Valley Creek and degraded spawning areas further downstream (CRA, 1970). In this same year, the Army Corps of Engineers concluded differently when they described the combination of flood suppression and sand contributions from Grass Valley Creek were jointly responsible for degrading spawning areas. Later, in 1970, flood suppression enabled root mats from aquatic vegetation to grow in sand on spawning riffles (unpublished notes, 1970). Such plant growth stabilized fine sediments in these areas and contributed roughness that promoted deposition of additional fines that furthered degraded habitat (CRA, 1970).

Flood suppression also helped riparian vegetation establish on low flow channel margins (see Figure 11). The increased roughness from vegetation promoted deposition of fines during overbank flows and resulted in construction of berms or levees. These features naturally occur on regulated (Klasz et al., 2014) and unregulated (Church, 1972) alluvial rivers and can benefit instream habitat in meandering channels. Indeed, berm erosion by channel migration recruits woody material that is an important component of fish habitat in streams (Hafs et al., 2014). However, suppression of floods occurred to a degree and duration on the Trinity River that riparian trees were able to establish networks of roots that armored the banks, essentially locking the channel in place (see Figure 11). The berms ranged in height above the low water channel margin to 8 ft and caused an entrenched, nearly rectangular channel dimension to form (McBain and Trush, 1997). The berms remain largely in place until they are removed with mechanized equipment, such as bulldozers. The first of the removals occurred in nine “feather edge” projects between 1991 and 1993 (Krause, 2012) and the removals have continued in projects that began in the post-ROD period and continue to this day (Curtis et al., 2015).

### 3.3 Actions to reduce fine sediment in the Trinity River

#### 3.3.1 Regulatory

Flood suppression by Lewiston and Trinity Dams enabled large quantities of fine bed material ( $\leq 8$  mm) delivered by tributary channels to accumulate in and on the banks of the mainstem Trinity River, as mentioned above (e.g., FKA, 1980). This largely transformed the gravel-bed river to a sand bed stream and imperiled salmon populations. The first instream flow study that attempted to identify actions to remediate flow regulation impacts to salmonids was undertaken in 1978 (USFWS, 1980a). The study recommended that to improve juvenile Chinook habitat, Lewiston Dam releases to the river should be increased from 150 to 250 cfs to higher base levels ranging 300 to 500 cfs. The subsequent environmental impact statement recognized that while increasing river flows was necessary, watershed restoration, mechanical improvements to streambed conditions, and increased regulation of fish harvests would be necessary to return salmon populations to pre-project levels (USFWS, 1980b). These recommendations helped motivate passage of the Trinity River Stream Restoration Act in 1981 (also known as the Secretarial Decision of 1981) that authorized minimum instream flows for the Trinity River be increased from 120 thousand acre-feet (AF) to 340 thousand AF and directed the USFWS to undertake a 12-year study of the effectiveness of increased flows and other habitat rehabilitation efforts that may be implemented through the newly formed TRRP. The study began in 1984 with Congressional authorization of the Trinity River Basin Fish and Wildlife Management Act that

enabled watershed restoration and construction of sediment retention ponds and Buckhorn Dam on Grass Valley Creek in 1988 and 1990, respectively. The Central Valley Project Improvement Act of 1992 then authorized implementation of increased flow on the Trinity River for water years 1992 through 1996 to not less than 340 thousand AF per year for restoration efforts.

The Trinity River Flow Evaluation study (USFWS and HVT, 1999) subsequently reported that flows authorized in 1992 were insufficient to restore biologic and geomorphic processes and fish populations in the Trinity River. This led to development of the Environmental Impact Report for Trinity River Mainstem Fishery Restoration (TREIR, 1999), which concluded that restoration of fish populations would most likely occur through implementation of preferred alternative recommendations made in the flow study (USFWS and HVT, 1999). These recommendations were subsequently implemented through adoption of the 2000 Record of Decision (ROD, 2000), which authorized mechanical channel rehabilitation, coarse sediment augmentations, annual flow releases, and watershed restoration to reestablish conditions that promote a healthy alluvial river and associated fish populations, among other objectives that included fine sediment reduction. Annual flows allocated to the Trinity River under the ROD are based on forecasted hydrology for the basin as of April 1 and range from 369 to 815 thousand AF in critically dry to extremely wet years. Watershed restoration and allocated flows have multiple objectives that concern fine sediment, including reduction of fines in tributaries and transporting fines in the mainstem river at rates that exceed contributions from tributaries.

Soon after finalization of the ROD, further recognition was given to sediments in the size range of fines that were observed to be overly present in the mainstem Trinity River and several tributary streams. This recognition resulted in the Trinity River being listed under section 303(d) of the Clean Water Act for sediment total maximum daily load (TMDL; US EPA, 2001). Water quality standards of concern listed in the TMDL are turbidity and suspended material, excepting wash load, and the generic identifier “sediment” without a defined behavior or size definition. Beneficial uses impacted by these sediments were cold water fish habitat for spawning, rearing, and migration, and environmental indicators for these beneficial uses were listed as spawning gravel quality and permeability, turbidity, pool depth, and geomorphic indicators of a healthy alluvial river, including attributes 1 and 3-6 in USFWS and HVT (1999) and TREIR (1999).

The requirement for delisting the Trinity River and impacted tributaries from the TMDL is that sediment delivery cannot exceed 125% of background (unimpacted) rates that occur in reference watersheds in the Trinity Basin (see Table 5-1 in US EPA (2001)). Unfortunately, sediment monitoring no longer occurs on the reference streams, which precludes a contemporary comparison between fine sediment transport rates on these streams and the Trinity River. Nonetheless, actions to address tributary contributions of fine sediment to meet this requirement included 1) reducing sediment production from roads and timber harvest in sediment-impaired sub-watersheds; 2) continuing sediment preventative measures in reference watersheds through implementation of road maintenance, tree planting, and other beneficial actions; and 3) implementing the flow schedule, restoration measures, and adaptive management program in the Trinity River that is called for in the ROD (ROD, 2000; US EPA, 2001). These steps were indeed implemented in the Trinity River watershed and reduced fine sediments at several locations in the basin to targeted levels, as demonstrated in following sections.

### 3.3.2 Watershed restoration

Rehabilitation work in the Trinity River basin has focused on hydrologically disconnecting road systems from streams and reducing potential for road-stream crossing failures and hillslope failures. To meet these objectives, work has mostly focused culvert maintenance, construction of rolling dips to divert water from road surfaces to inboard ditches, road grading to eliminate surface and channelized flow on roads, and restoration of hillslope profiles by road removal. These types of efforts were particularly active in watersheds with substantial areas of exposed granite, which is thought to be the largest source of fine sediment that impacted the mainstem Trinity River. For instance, in Grass Valley Creek, where 65% of the area is composed of decomposed granite, watershed restoration activities mentioned above and construction of Buckhorn Dam and sediment retention ponds near the confluence with the Trinity River were implemented to reduce the large volume of fine sediment produced in the watershed (see Section 5.3). Other restoration projects in tributary watersheds that contribute flow and sediment to the Trinity River restoration reach have addressed fish passage issues, instream habitat needs, revegetation, riparian rejuvenation, invasive weed removal, wetland rehabilitation, and water conservation (Figure 15; Rupp, 2019). Opportunities for future restoration work has included protection of water sources for instream and human uses, continued reclamation of mining impacts, and restoration of fish passage at culverts identified as barriers to anadromous fish passage (Rupp, 2019).

### 3.3.3 Riffle cleansing

The use of bulldozers and riffle sifters to improve the quality of salmon spawning riffles for egg incubation started in the 1970s and continued to the early 1980s (Figure 16). The riffle sifter was developed by the U.S. Forest Service to be pulled along the bed by a cable winch while using high pressure water jets mounted in a tube that was dragged through the bed to flush fines from gravels to a depth of 14 inches while also using suction to remove fines (USFWS, 1979). The riffle sifters were plagued by mechanical problems that included the pull cables breaking from the force required to pull the flushing bars through the bed and the suction system was easily plugged with sediment and organic debris. Despite these challenges, intergravel flow improved where the sifter was applied, yet the improvements were short lived because the over availability of fine sediment that degraded habitat in riffles in the first place was not addressed by this method (USFWS, 1979). Scarification of the bed using tines attached to bulldozers was also used to loosen sediment in riffles for redd construction by salmonids and to enable river flows to flush fine sediments downstream (Kondolf and Mathews, 1991a). The scarification effectively loosened the bed by breaking up the compacted sediments, but it did not reduce the quantity of sand in riffles and had a negative effect on the benthic community (Turek, 1986). Because of this and the lack of lasting benefits to spawning conditions from riffle sifting and tilling, both operation ceased in the late 1980s.

### 3.3.4 Riffle construction

In the same period that riffle cleansing was attempted, spawning riffles were constructed on the Trinity River to provide salmonids clean gravel in areas with suitable flow depths and velocities for spawning and egg incubation (Figure 17). As explained by Krause (2012), the first spawning riffles were constructed in 1972 with coarse sediment placements near Lewiston Dam (RM 112.2) and by 1977 a total of 14 artificial riffles had been between the dam and Grass Valley Creek (RM 104.4). Construction of the riffles involved scarifying the channel bed to loosen it and remove substrate that exceeded the size targeted by spawning salmon (see Kondolf and Wolman, 1993). The oversized material was then used in grade-control structures that provided up- and downstream hydraulic controls

to help prevent erosion of the riffles and to construct berms to confine flow over the riffles. The suitability of the riffles for spawning was invariably reduced by fine sediment deposition and the riffles were often damaged by tributary-driven flows. After such events, coarse sediment augmentations were used to replenish the riffles through 1990 when the effort was abandoned.

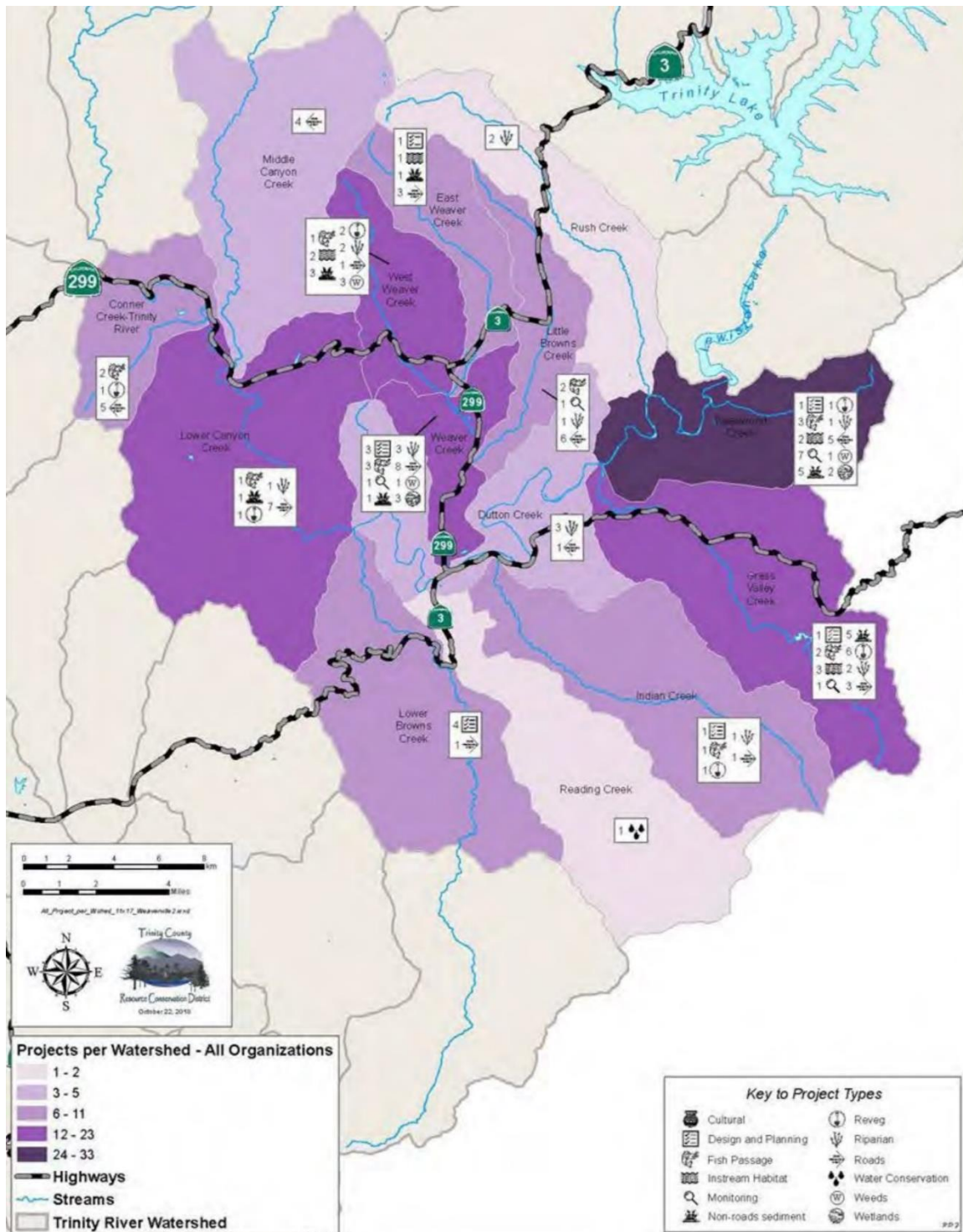


Figure 15. Map of major tributary watersheds in the Trinity River restoration reach showing number of restoration projects undertaken in different categories (from Rupp, 2019).

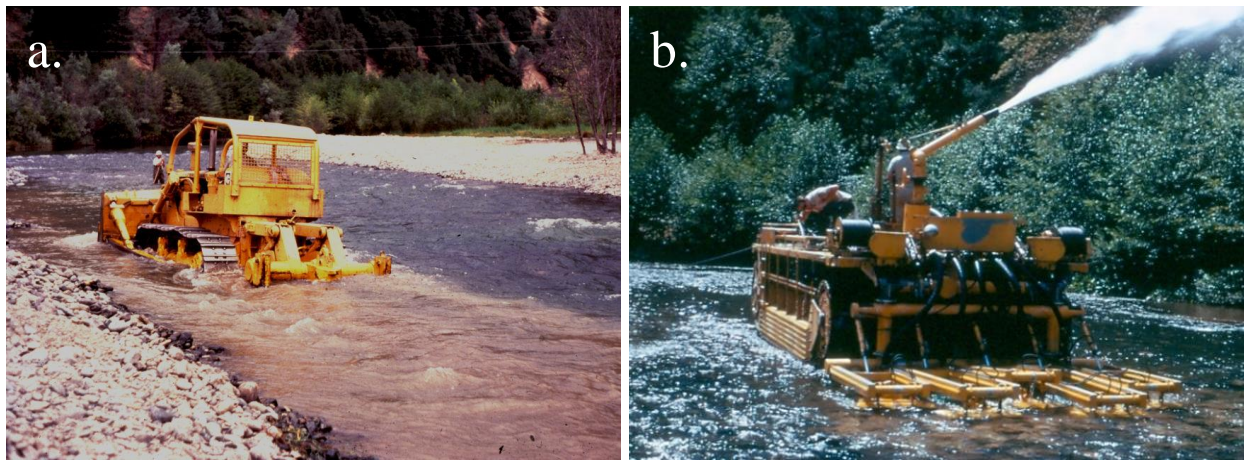


Figure 16. A bulldozer scarifying a riffle to loosen the streambed and flush fine sediments (a.) and a riffle sifter purging fines from a riffle in the Trinity River in 1971 (b.).



Figure 17. Bulldozers constructing an artificial riffle on the Trinity River in 1971 (from Krause, 2012).

### 3.3.5 Pool dredging and bar scalping

Removal of fine sediment from pools in the Trinity River was another primary focus of early restoration efforts. This was because the majority of large pools between Grass Valley Creek (RM 104.4) and Steel Bridge (RM 99.0) that were formerly 10-20 ft deep were reduced in depth to 3-6 ft by sand deposition (Nelson et al., 1987). Most significantly, Reo Stott pool (RM 102.5) that had a surveyed depth of 20 ft deep in 2009 (Woolpert, 2010) exhibited a depth of only less than a foot in 1966 due to filling by sand (LaFaunce, 1968; Krause, 2012). To restore Reo Stott pool depths, fine sediment was hydraulically pumped with suction dredges to a nearby holding barge in 1976–1977 (Barnes, 1978). Pumping was expanded to a location about 1.8 river miles upstream from Reo Stott pool to near the confluence with Grass Valley Creek with construction of a sediment retention pool at this location in 1978. The constructed pool capacity was rapidly exceeded by the sand supply in the river that primarily originated from Grass Valley Creek but also upstream areas on the river, so several more catchment pools were constructed (Krause, 2012). The constructed pools were typically 300 to 500 ft long and 10 to 15 ft deep and were either enlarged natural pools or were built in areas where pools did not previously exist. Observed refill of the pools enabled infill rates to be estimated. Denton (1980) reports that measured infill rates at Reo Stott pool in 1979 increased from 22 cy/day at 300 cfs, to 33 cy/day at 300 to 450 cfs, and 100 cy/day at 300 to 600 cfs. In response to the over-supply of fine sediments, suction dredges, excavators and draglines were also used to remove around 223,000 cy of sediment from the pools and an additional 7,200 cy of sediment was scalped from bar surfaces and used for gravel augmentations after fines were removed. The total volume of fine sediment extracted from the Trinity River by pool dredging and bar scalping between 1976 and 1991 was around 173,100 cy according to Krause (2012; Figures 18 and 19).

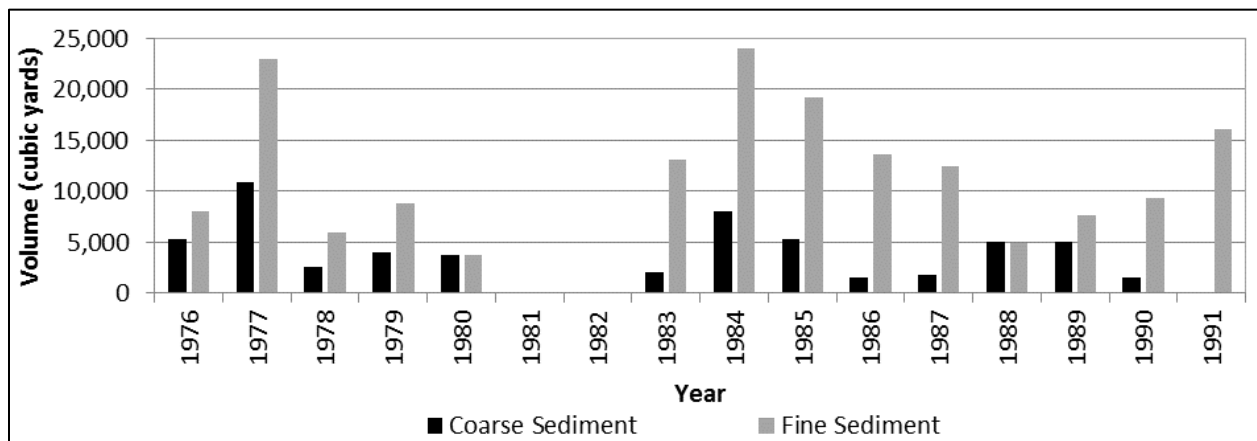


Figure 18. Volume of coarse and fine sediment dredged from pools and removed from bar surfaces in the Trinity River from 1976 to 1991 (from Krause, 2012).

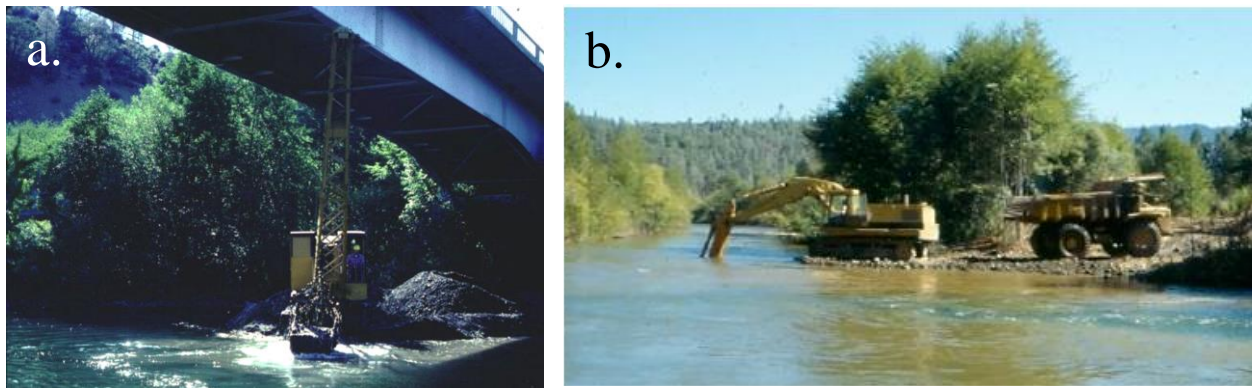


Figure 19. A dragline (a.) and excavator (b.) increasing depths in constructed pools used to trap fine sediment in the mainstem Trinity River from 1976 to 1991.

### 3.3.6 Sediment mining

Sediment was mined from the Trinity River channel and floodplain areas for Trinity Dam and Lewiston Dam construction and other commercial purposes from at least 1912 to 1974. The end date is probably an early estimate since sediment mining was not tracked on the Trinity River after 1974. Sediment extraction from the Trinity River channel primarily occurred at Lewiston and near the outlets of Grass Valley, Indian, Weaver, and Reading creeks. Tributary delta removal was often a consequence of the mining, and Indian Creek was channelized across its delta in 1978 to facilitate mining. The most detailed records of sediment mining from the Trinity River were kept by the Trinity Sand and Gravel company in Douglas City that supplied sand and gravel locally until it ceased operation in 1980. Mining source areas for the company extended from Weaver Creek (RM 94.0) to near Reading Creek (RM 92.5). In this area, around 35,000 cy of material was extracted primarily from floodplains, but also the main channel when necessary to maintain the company's supply of sediment (Krause, 2012). Assuming fine sediments composed 30% of the extracted sediment, around 202,000 cy of fines was removed by the company in the time between Lewiston dam closure and 1980.

### 3.3.7 Flushing flows

The failure of mechanical treatments to remedy the transport limitation and consequent accumulation of fine sediment in the Trinity River led to the reluctant adoption of a flushing flow strategy to mobilize fine sediments downstream. The reluctance stemmed from recognition by the Trinity River Task Force that the expense of lost revenue from power generation and irrigation water supply that would result from the use of Trinity water to transport the accumulated fines would be significant (Nelson et al., 1987). Nonetheless, test flow releases were made in 1991, 1992, and 1993 to investigate minimum flows for removal of fine sediment between Grass Valley Creek (RM 104.4) and Steel Bridge (RM 99.0) to depths that salmon spawners lay their eggs without causing a deficit in coarse sediment in this reach (USFWS and HVT, 1999). Individually, none of the trial releases produced a substantial reduction in fine sediment, but cumulative results from the releases provided a basis for flow recommendations to help remedy the overabundance of fines (Wilcock et al., 1995). The results were that releases of 2,800 cfs removed sand from the bed surface, but not from any depth in the bed. A release of 5,800 cfs for 5 days mobilized the surface gravel layer and entrained the underlying fine sediments. From these observations, the recommendation was that a minimum release of 6,000

cfs for 5 days would be needed to entrain the bed surface and flush fine sediments to targeted depths. Flushing flow recommendations by Wilcock et al. (1995) were reflected in the flow record for Trinity River at Lewiston until the first geomorphic flow release from Lewiston Dam occurred in spring 2004 with implementation of the ROD.

### 3.3.8 Geomorphic (high) flow releases

Flushing flows reduced the amount of fine sediment in the Trinity River, as evidenced by supply limitations observed by McBain and Trush (1997) in the mid-1990s, but flushing flows lacked attributes of natural hydrographs that are important for healthy river functioning. In recognition of this, a flow study was undertaken on the Trinity River in 1996 and 1997 to determine flow magnitudes, durations, and timings needed to restore attributes of a healthy alluvial river (USFWS and HVT, 1999). Findings in the study resulted in adoption of the ROD (2000), which required implementation of winter (300 cfs) and summer (450 cfs) baseflow discharges and spring flow hydrographs from Lewiston Dam that vary in magnitude and volume (based on the annual unimpeded water yield in the basin) to achieve multiple biologic and geomorphic objectives. After litigation opposing the flow releases on the Trinity River was resolved, the first geomorphic high flow release in 2004 was implemented to transport fine sediment at rates greater than tributary inputs, among several other objectives. Repeat photos provide clear evidence of success meeting this goal (Figures 20-23). With this and complimentary results presented below, it is proposed that the fine sediment management objective of the TRRP change to promote a balanced fine sediment regime in the river and floodplain areas. The management objective would be evaluated with targets addressing key biologic and physical components of the Trinity River ecosystem. These targets are presented in the following section and evaluated for the Trinity River to the extent that available data allows in Section 7.



Figure 20. A large sand delta at the confluence with Hoadley Gulch (RM 110.1) in August 1999 (a.), and the same view in August 2019 (b.).

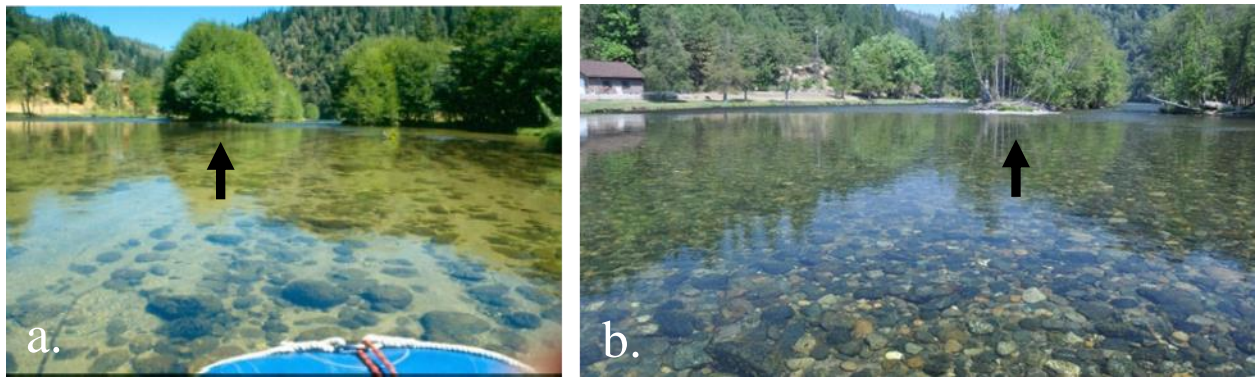


Figure 21. Sand on the channel bed surface at Society Pool tail (RM 101.7) in September 1989 (a.), and relatively few fines on the restored coarse bed surface in 2013 (b.). The arrow in each figure shows the same mid-channel island. The arrows point to the same location in both photos to orient the reader between panels.



Figure 22. Sand on the bed surface in August 1975 downstream of Poker Bar Hole at DWR cross section 17 (RM 102.3; a.) and the same area in 2013 showing a lack of fines on the bed (b.).

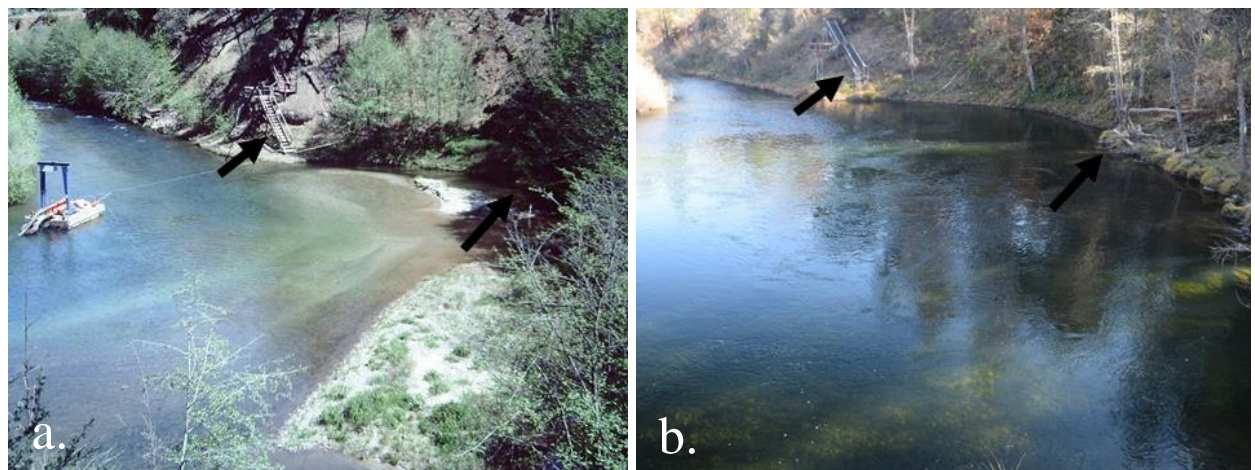


Figure 23. Reo Stott pool (RM 102.5) largely filled with fine sediments in May 1977 (a.) and the same pool with its dimensions restored by evacuation of fine sediments in November 2019 (b.). The arrows point to the same location in both photos to orient the view of the pool between panels.

#### 4. Fine sediment targets for the Trinity River

Fine sediment targets for the Trinity River mainstem and floodplain areas are published in the Trinity River flow study (USFWS and HVT, 1999), Trinity River mainstem fishery restoration environmental impact statement (EIS, 2000), and Integrated Assessment Plan (TRRP and ESSA, 2009). These documents report similar targets, namely to

- 1) Decrease fines to increase median and geometric mean diameters;
- 2) Reduce fine sediment storage in the Trinity River channel and riparian berms;
- 3) Lower fine sediment supply from tributaries; and
- 4) Deposit fine sediment on floodplains.

The published targets were derived with the expectation they would be adjusted as channel and floodplain restoration progressed and new information became available. Both these conditions have been met and updated fine sediment targets for specific biologic, hydrologic, and physical functions that impact river's ecosystem processes and salmonid populations are presented in following sections and summarized in Table 2. The updated targets were developed referencing published work and provide quantifiable targets that are tractable and physically and biologically meaningful.

##### 4.1 Instream biology

###### 4.1.1 *Holding habitat for adult salmon*

The life history strategy for spring Chinook salmon is to enter natal streams in early summer and reside in deep, cold water pools until spawning in fall. Fall Chinook, coho, and steelhead also use pools for resting during migration to spawning grounds, and pools provide juvenile salmonids safety when depths exceed the effective fishing depth of predators like kingfishers and herons. For these reasons, deep pools are critical habitat for salmonids in their juvenile and adult life stages, but pool habitats are reduced when fine sediments fill void spaces in the bed, accumulate on the bed surface, and reduce pool depths. A measure of impacts of fine sediment storage on the capacity of pools to provide habitat for fish is captured in  $V^*$ , defined as the ratio of fine sediment volume in a pool to the pool volume during summer low flows that would be present in the absence of fines (Lisle and Hilton, 1992). Values of  $V^*$  vary with the lithology of a basin, and  $V^*$  targets for the Franciscan formation are  $\leq 0.21$  and  $< 0.10$  for other basin lithologies (US EPA, 2001). Franciscan lithology is only present on Grouse Creek, which is a tributary to the South Fork Trinity River, so the  $V^*$  target of  $< 0.10$  applies to pools in the Trinity River.

###### 4.1.2 *Salmonid spawning gravels*

Substrate composition affects salmon spawning and incubation initially by influencing the location where a female salmon chooses to construct a redd and later when fine sediment affects substrate permeability and water flow through redds, which is necessary for egg respiration and flushing metabolic wastes from the nest. Jensen et al.'s (2009) meta-analyses on fine sediment impacts to salmon egg-to-fry survival reports the probability of Chinook and coho egg-to-fry survival respectively decreases 17 to 18% with every 1% increase in fines  $< 0.85$  mm above 10%. Bjornn and Reiser (1991) also report that salmon egg-to-fry survival rapidly decreases when the fine sediment ( $< 0.85$  mm) content in redds exceeds 10%. Sediment  $> 0.85$  mm also adversely influences egg-to-fry survival. For example, Hall and Lantz (1969) and Phillips et al. (1975) demonstrate that when 1-3 mm grains comprised 10-20% of bulk samples, steelhead and coho fry emergence was reduced (Jong, 1994), presumably by egg suffocation or entombment in the bed. In line with these findings, the target is fines

$\leq 2$  mm be  $<15\%$  (by weight; see Bunte and Abt, 2001) in bulk samples of subsurface sediments where salmon spawn. For bulk sampling to evaluate this target, the subsurface domain extends below the active layer of the bed, which itself ranges from the bed surface to a depth that is equal to the diameter of the local  $D_{84}$ .

#### 4.1.3 Salmonid egg incubation

Tappel and Bjornn (1983) used a laboratory study to measure Chinook salmon egg-to-fry survival in variable sediment mixtures and found that survival was predicted with around 93% accuracy using a quadratic equation of the form

$$S = 93.4 - 0.171s_{9.5}s_{0.85} + 3.87s_{0.85} \quad \text{Eqn. 1}$$

where  $S$  is the percent survival of Chinook embryos and  $s_{9.5}$  and  $s_{0.85}$  are percentages of subsurface bulk samples that are respectively smaller than 9.5 mm (-0.3 phi) and 0.85 mm (4.3 phi; where  $\phi = -\log_2 D$ , with  $D$  as grain diameter in mm). Bulk samples on the Trinity River are sieved in half-phi size classes and for the size class  $<0.85$  mm, so percentages  $<9.5$  mm were determined by linear interpolation between percentages of grains that bound this size class. Results in Tappel and Bjornn (1983) show that when percentages of 9.5 and 0.85 mm grains respectively increase above 30% and 10%, egg-to-fry survival steeply declines (Figure 24). From this, the target for percent egg-to-fry survival estimated with equation (1) is  $\geq 85\%$  where repeat bulk sampling and pebble counts are made on the Trinity River (see GMA, 2020b).

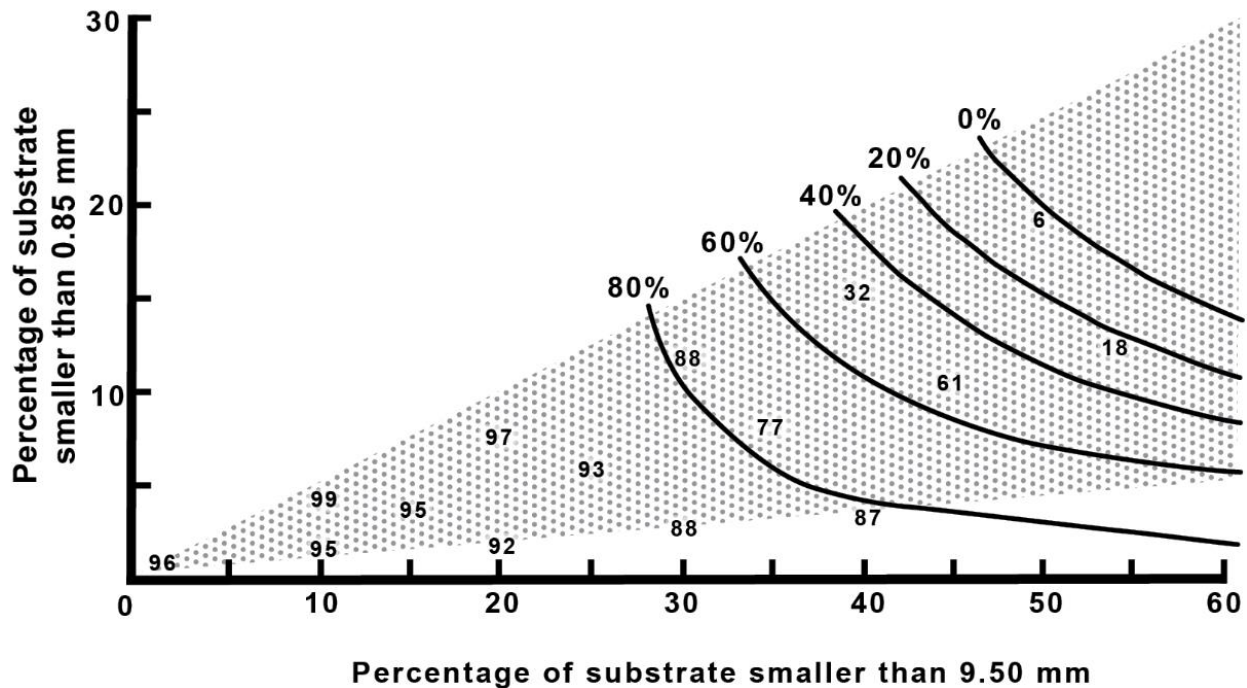


Figure 24. Relationship between percentages of grains smaller than 0.85 and 9.5 mm and Chinook egg-to-fry survival measured by Tappel and Bjornn (1983). The scattered numbers are measured percent survivals and the shaded area is the range of sediment compositions in rivers that were modeled in laboratory tests by Tappel and Bjornn (1983).

Once spawned, eggs in redds may be protected from suffocation and entombment when sand seals block infiltration of fines to embryos in nests (Meyer et al., 2005). Sand seals form in the

upper portion of redds when small grains fill interstices and restrict infiltration of fines further into the redd (Lisle, 1989). Sand seals reduce pumping exchange that supplies water to embryos (Tonina and Buffington, 2009) but decrease the probability of mortality by preventing entombment of alevins. Meyer et al. (2005) report that when total suspended sediment transport ( $Q_s$ , in tons) normalized by the cumulative discharge ( $Q$ , in cubic feet per second, cfs) in the period when salmon eggs are incubating in redds is  $>0.05$  tons/cfs, sand seal protections are overwhelmed and egg-to-fry survival is reduced to near zero. Therefore, maintaining  $\sum Q_s / \sum Q \leq 0.05$  tons/cfs in the incubation period (October–March) at the sediment monitoring stations is targeted to help safeguard salmon eggs from mortality.

#### 4.1.4 Juvenile rearing and adult salmon

Turbidity from fine sediments suspended in flow can affect fish health and is commonly used to track disturbance in watersheds (see Klein et al., 2012), with lower turbidity occurring in more pristine areas. Turbidity has been measured on the Trinity River in Nephelometric Turbidity Units (NTU) and Formazin Nephelometric Units (FNU; Turner and Boner, 2004). Both NTU and FNU quantify turbidity according to the amount of infrared light that is scattered by particles suspended in the flow, but values for the same turbidity vary between units due to differences in how the respective readings are converted (ISO 7027 method for FNU and EPA method for NTU). GMA (2020a) measured turbidity in both units during the spring flow release in 2019 on the Trinity River below Limekiln Gulch (TRLG) and at Douglas City (TRDC; see Figure 1) to derive equations for converting turbidity readings between units that it has been measured on the Trinity River through time. The relationships are exclusive to a station because the composition of organic and inorganic particles in turbid flow varies between channel location. The relationships and correlation coefficients ( $r^2$ ) between units measured at TRLG are

$$\begin{aligned} \text{NTU}_{\text{TRLG}} &= 0.671 * \text{FNU} + 0.11 && \text{if FNU} < 6 \quad (r^2 = 0.92) \\ \text{NTU}_{\text{TRLG}} &= 0.951 * \text{FNU} - 1.15 && \text{if FNU} \geq 6 \quad (r^2 = 1.0) \end{aligned} \tag{Eqn. 2}$$

and for TRDC

$$\begin{aligned} \text{NTU}_{\text{TRDC}} &= 0.707 * \text{FNU} + 0.36 && \text{if FNU} < 20 \quad (r^2 = 0.92) \\ \text{NTU}_{\text{TRDC}} &= 1.204 * \text{FNU} - 11.64 && \text{if FNU} \geq 20 \quad (r^2 = 0.91). \end{aligned} \tag{Eqn. 3}$$

Fine sediment affects juvenile salmon physiology and behavior where suspended sediments increase turbidity to high values. Physiological effects of high turbidity and total suspended sediment concentrations include gill trauma at ~60 NTU (Berg and Northcote, 1985) or 3,148 mg/L (Servizi and Martens, 1987) and elevated blood glucose and cortisol levels at ~500 mg/L (Servizi and Martens, 1987, 1992) that indicates stress and potential decreased immunological competence (Bash et al., 2001). Juvenile fish behaviors that accompany high suspended loads include changes in avoidance, territoriality, and foraging habits. Avoidance behavior occurs when juvenile salmonids circumvent areas where turbidity is 60-70 NTU (Berg, 1982; Bisson and Bilby, 1982) or suspended concentrations are ~7,000 mg/L (Servizi and Martens, 1992) and seek refuge where higher water clarity is present (Sedell et al., 1990). Since spring flow releases on the Trinity River are typically mistimed with elevated flows on tributaries, this behavior may

imperil juvenile fish by motivating them to seek clearer water at tributary junctions where piscivorous brown trout (*Salmo trutta*) may reside. Decreased territoriality and collapse in social structure can also result from high turbidity (>60 NTU; Berg 1982), which can decrease some fishes' growth and feeding rates (Bash et al., 2001). For example, Berg and Northcote (1985) noted that a dominant fish positioned in a superior feeding station is often displaced from its territory by turbidity pulses between 30 and 60 NTU. Being visual predators, reduced visibility from turbidity lessens the ability of fish to see prey, and prey consumption at 60 NTU is around 35% of that in clear water (Berg, 1982), which can lead to decreased growth and lower fish health (Gardner, 1981). However, clear water may also not be preferable, as Sigler et al. (1984) observed that juvenile salmonids sought slightly turbid water in an apparent trade between predation risk and reduced feeding success. In certain cases, fish (in this case, brook trout, *Salvelinus fontinalis*) were observed showing less reliance on overhead cover when turbidity was 7 NTU (Gradall and Swenson, 1982). Given these considerations, the turbidity target for juvenile salmon rearing in the restoration reach of the Trinity River is <30 NTU for >80% of the rearing period (January–July) at TRLG, TRDC, and TRNF (see Figure 1).

Point measurements of turbidity can be evaluated relative to the above standards, but this neglects the impact of duration of exposure to fish health. To address this, Newcombe and Jensen (1996) conducted a meta-analysis of studies and related the duration of exposure to concentrations of suspended sediment to estimate severity-of-ill ( $z$ ) impacts on adult and juvenile salmonids during their freshwater life stage. Values of  $z$  are binned by effects that range from no impact at  $z=0$  to 100% mortality at  $z=14$  (Table 1), and the target value of  $z$  for both life stages is  $\leq 5$ . The equation for  $z$  is

$$z = 1.0642 + 0.6068 \log_e x + 0.7384 \log_e y \quad \text{Eqn. 4}$$

where  $x$  is the duration of exposure (hrs) and  $y$  is the concentration of suspended sediment  $\leq 0.25$  mm in mg/L. Suspended sediment is measured on the Trinity River as  $<0.5$  mm, which over-estimates impacts to salmonids that are projected by this approach. To account for this, the target  $z$ -value was increased to  $\leq 5$  for  $\geq 80\%$  of the rearing (January–July) and spawning period (September–January) for adult and juvenile salmonids, respectively (USFWS and HVT, 1999). A value of 5 is associated with “minor physiological stress and increased rates of coughing and respiration”, but the actual impact to fish resulting from suspended sediments  $\leq 0.25$  mm on the Trinity River would be lower because suspended loads in this size range are less than values for  $<0.5$  mm used in the calculations. The actual impacts to fish are therefore conservatively expected to fall under the next lower  $z$ -value of 4 that is associated with a “short term reduction in feeding success” at sediment transport monitoring locations on the Trinity River (i.e., TRAL, TRLG, and TRDC; see Figure 1).

Table 1. z-values and associated severity-of-ill impacts to juvenile and adult salmonids in lotic waters.

z value	Description of effects	Class of effects
0	No behavior effects	Nil effect
1	Alarm reaction	Behavioral effects
2	Abandonment of cover	
3	Avoidance response	
4	Short term reduction in feeding success	Sub-lethal effects
5	Minor physiological stress and increased rates of coughing and respiration	
6	Moderate physiological stress	
7	Moderate habitat degradation and impaired homing	
8	Indications of major physiological stress and reductions in feeding rate and success	Lethal effects
9	Reduced growth rate and fish density and delayed hatching	
10	0-20% mortality, increased predation, and moderate to severe habitat degradation	
11	>20-40% mortality	
12	>40-60% mortality	
13	>60-80% mortality	
14	>80-100% mortality	

#### 4.1.5 Benthic macroinvertebrates

Fine sediment affects benthic macroinvertebrates by exerting control on the amount of interstitial habitat available for colonization and the types of species present, generally delineated as surface or subsurface dwelling organisms. Studies report the biomass of surface-dwelling invertebrates that are available as prey for salmonids inversely relates to percent fines in streambeds (Relyea et al., 2000; Sylte and Fischenich, 2002; Suttle et al., 2004; Cover et al. 2008). For example, Relyea et al. (2000) measured that macroinvertebrate abundance was greatest when fines  $\leq 2$  mm were  $<30\%$  of bulk subsurface samples, which is the target adopted here for riffles, glides, and runs where repeat bulk sampling and pebble counts are made on the Trinity River (see GMA, 2020b). Pools are excluded because the aforementioned areas are where macroinvertebrates are most abundant and because deep water in pools precludes bulk sampling sediments from them.

Because fine sediments can fill interstices between gravel and reduce the exposed surface area of coarse particles that are habitat for macroinvertebrates, gravel embeddedness (Figure 25) is an additional measure for detecting fine sediment effects on benthic habitats. To avoid reductions in macroinvertebrates and shifts in species composition to burrowing organisms that are difficult for salmonids to prey on, Relyea et al. (2000) suggest embeddedness be maintained at  $<20\%$  and Bjornn et al. (1974, 1977) propose embeddedness be  $\leq 33\%$ . Similarly, Koschersberger (2008) found macroinvertebrate abundance decreased 50% when embeddedness was  $>33\%$ . From these studies, the embeddedness target on the Trinity River is set as  $\leq 33\%$  outside of pool habitats to promote macroinvertebrate species assemblages that are prey for salmonids. This update is used in place of the embeddedness target in US EPA (2001;  $\leq 25\%$ ).

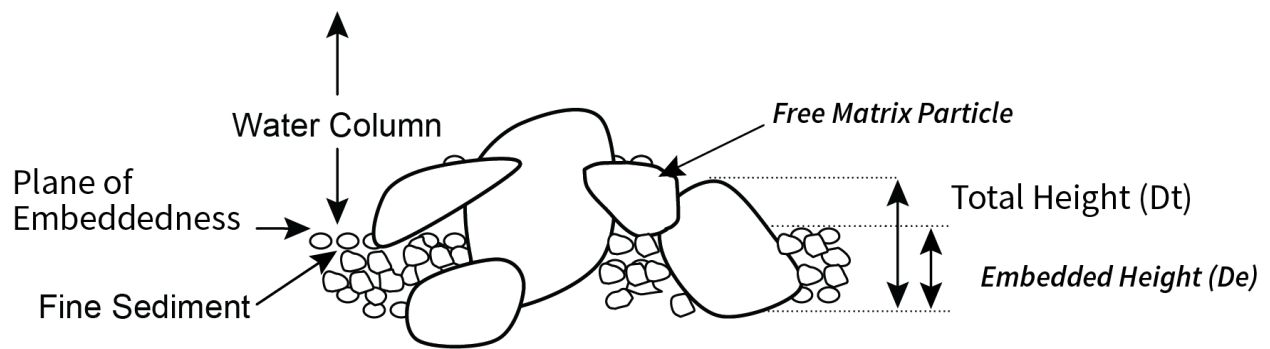


Figure 25. Schematic showing the embeddedness calculation as the ratio of a particle's embedded height above the local plane of the bed ( $D_e$ ) to the total height of the particle ( $D_t$ ) in the bed.

#### 4.1.6 Ammocoete rearing

Prior to migrating to sea as adult lamprey, ammocoetes rear for 4 to 7 years in low velocity areas where silt and sandy substrate ( $\leq 2$  mm; Torgerson and Close, 2004) accumulate, including pools, alcoves, and side channels (Stillwater Science, 2014). Stone et al. (2002) measured correlation between ammocoete densities and percentages of fines (here  $< 9$  mm) that exceeded 28%. Additionally, Claire (2003) measured ammocoete densities increased in substrate with percent fines ( $\leq 2$  mm)  $> 23\%$ . For consistency with size definitions for other fine sediment criterion, the fine sediment ( $\leq 2$  mm) target for ammocoete rearing in slack water areas of the Trinity River is  $> 28\%$  by weight in bulk grain-size distributions, as indicated by Stone et al. (2002). Where these data are unavailable, presence of fine sediment deposits in lee areas of the winter baseflow channel sufficiently satisfies this target.

#### 4.1.7 Nutrient storage

Marine-derived nutrients (MDN) delivered to streams by salmon bolster primary and benthic macroinvertebrate production at times of year when prey for fish is less available than other times of year due to spawning disturbance to substrate and water temperatures and sun angles that are low in early spring and fall (Rinella et al., 2013). Buxton et al. (2015b) modeled that residence times of marine nutrients in hyporheic areas of the bed are short and reduce with increasing densities of spawning due to the effect of redd construction increasing hydraulic conductivity in the bed. Therefore, a potentially more important pathway for MDN storage occurs when microbial processes bind MDN to fine sediment for storage until release by bacterial processing (Rex and Petticrew, 2008), especially in gravel bar deposits (Ock et al., 2015). Nutrients that bind to fine sediment ( $< 0.4$  mm in the literature, represented as  $< 0.5$  mm here) form flocs that can be stored in hyporheic areas for processing by biofilm, which is the base of stream food webs. To enhance this storage function, the target is for sediment  $< 0.5$  mm to be available in the suspended load at TRLG, TRDC, and TRNF.

#### 4.2 Floodplains

Deposition of fine sediment on floodplains removes fine sediment from the channel and promotes soil conditions for riparian plant establishment and growth. This is especially important on Trinity River floodplains that have been disturbed by historic dredger mining (Section 3.1.3) that sorted and deposited material to form unnaturally coarse surfaces. Consequently, floodplains on the Trinity River are typically deficient in fine sediments that are necessary for retaining and

processing nutrients, providing media for root holding strength, maintaining soil moisture for plant germination, and increasing capillary flow of water from the water table to the plant rooting zone. An investigation of woody riparian seed germination on floodplains on the Trinity River by Bair (2001) indicated the number of seedlings sharply increases when the percentage of surface and subsurface fines >15% in Wolman (1954) pebble counts and >20% in subsurface bulk samples, which are fine sediment targets for floodplain surfaces. Sampling protocol to quantify these metrics should be uniquely designed to provide statistically meaningful results for each floodplain surface that is assessed.

#### 4.3 Geomorphic processes

##### 4.3.1 *Fine sediment budget*

A balanced fine sediment ( $\leq 8$  mm) budget ensures that fines are neither overly abundant nor in deficit in the Trinity River and its floodplains. These end points are undesirable because they can respectively lead to a host of undesirable effects, including suffocation of salmonid eggs in redds, reduced macroinvertebrate populations, and pool filling, or restrict riparian colonization on floodplains and tops of point bars, decrease availability of ammocoete rearing habitat, and suppress nutrient cycling. Achieving quasi-equilibrium between the amount of fine sediment supplied to the river and the river's capacity to transport fines helps avoid these ends. Bounds of quasi-equilibrium in fine sediment budgeting are defined by fine sediment targets in the river and on floodplain surfaces. Acceptably high bounds occur where the availability of fines does not exceed the upper targeted values. Avoidance of a deficit in fine sediment is also desirable and results where fine sediment targets for ammocoete rearing, riparian plants on floodplains, and channel meandering are met. A numeric target for fine sediment budgeting is therefore not provided, but the budget is considered balanced when targets for fine sediment in channel and floodplain areas are largely met in the restoration reach of the Trinity River.

##### 4.3.2 *Coarse sediment mobility*

Fine sediments can increase the mobility of coarse substrate by filling interstitial spaces on the bed, which can smooth the bed surface, lower friction angles resisting particle movement, and increase near-bed velocities and shear stress on grains exposed to flow (Venditti et al., 2010; Curran and Wilcock, 2005; Wilcock and Crowe, 2003; Wilcock et al., 2001; Buffington et al., 1992). In experiments by Wilcock and Kenworthy (2002), these effects reduced Shields (1936) stresses by 2.8 times, from 0.034 on bed surfaces without sand ( $\leq 2$  mm diameter) to 0.012 on beds with sand contents that exceeded around 25%. Alternatively, Yager et al. (2018) and Buxton (2014) found that critical conditions for gravel can increase as fine sediments deposit around coarse grains and reduce particle exposure and enhance intergranular friction, cementation, and the weight of particles on grains embedded with half or more of their diameter in the bed (e.g., Barzilai et al., 2013). These opposing effects on gravel mobility suggest a threshold content of fines may exist at which the bed is either stabilized or destabilized by fine sediments, certainly with respect to the biophysical requirements of the stream biome. For example, over-stabilizing the channel surface can lead to biomatter accumulation in the bed and reduced intergravel flow that supports the biology in the subsurface environment; under-stabilizing the bed surface can lead to salmonid egg scour and macroinvertebrate population shift to species that reside deeply in the bed and are generally unavailable as prey for salmonids. To possibly avoid these effects, the target for fines  $\leq 2$  mm is set as 5-12% in Wolman (1954) and

bulk surface samples, which should promote intermediate values of critical Shields (1936) stresses. Subsurface grains also influence surface gravel mobility by generating intergranular friction with the underside of embedded grains. To account for this and achieve comparable decreases in critical Shields stress that Wilcock and Kenworthy (2002) measured with increasing surface sand contents, the target is fines  $\leq 2$  mm compose 16-24% of subsurface bulk samples. Both surface and subsurface contents of fines should be measured for evaluation of these targets at sediment transport monitoring locations (i.e., TRAL, TRLG, and TRDC) and where repeat bulk sampling and pebble counts are made on the Trinity River (see GMA, 2020b).

#### 4.3.3 Channel meandering

Meander building is perhaps most affected by fine sediments that deposit on the tops of point bars and are colonized by riparian plants. The plants increase roughness and promote additional fine sediment deposition and further colonization by riparian plants, which can direct flow toward the outer bank to promote further meandering (Leopold et al., 1960). This process commonly results in a gradient of age classes in riparian trees, from old to young, extending toward the outside of the bend from the top surface on point bars on actively meandering streams. Another meandering process that is fine-sediment dependent results when deposition occurs in meander cut-off, or chute channels that form on the inside of meander bends. The fines accumulate and plug the chute channels and cause flow to be more intensely directed toward the outer bend, which promotes channel migration (Braudrick et al., 2009). Targets to initiate these meander processes is for fine sediments  $\leq 2$  mm to deposit in chute channels and on the tops of point bars to depths that exceed the diameter of the local surface  $D_{84}$ , which is the approximate critical rooting depth of riparian seedlings (USFWS and HVT, 1999). Following initiation, both processes require surfaces be in proximity to groundwater for plant hydration and fine sediment to continue to be deposited amongst the increasingly established vegetation or in the cut-off channel, which could be monitored following initiation of these processes. Bars for evaluating these criteria are located at RMs 73.1, 79.4, 82.0, 104.2, 106.1. These sites were chosen because they are located away from future planned reconstruction areas and bedrock and hillslopes preventing channel migration and are in predominantly alluvial sections of river.

#### 4.4 Summary of targets

Table 2. Fine sediment targets.

Indicator	Target
Spawning gravel quality and incubation success	Fines $\leq 2$ mm $< 15\%$ in subsurface bulk samples in spawning areas Chinook egg-to-fry survival $\geq 80\%$ estimated with equation (1) $\sum Q_s / \sum Q \leq 0.05$ tons/cfs in the Chinook egg incubation period (October – March)
Juvenile rearing	Turbidity $< 30$ NTU for $> 80\%$ of the juvenile rearing period (January – July) $z \leq 5$ for $> 80\%$ of the rearing period (January – July)
Adult holding and spawning	$V^*$ for pools $< 0.10$ $z \leq 5$ for $\geq 80\%$ of the spawning period (September – January)
Benthic macroinvertebrates	Fines $\leq 2$ mm $< 30\%$ in subsurface bulk samples on riffles, runs, and glides Embeddedness $\leq 33\%$ outside of pools
Ammocoete rearing	Fines $\leq 2$ mm $> 28\%$ in composite bulk samples from slack water areas Presence of fine sediment deposits in lee areas of the winter baseflow channel
Nutrient storage	Presence of fines $< 0.5$ mm in suspended sediment samples
Floodplains	Fines $\leq 2$ mm $> 15\%$ in Wolman (1954) samples Fines $\leq 2$ mm $> 20\%$ in subsurface bulk samples
Coarse sediment mobility	Fines $\leq 2$ mm 5-12% on the bed in Wolman (1954) and bulk surface samples Fines $\leq 2$ mm 16-24% in subsurface bulk samples
Channel meandering	Deposit fines $\leq 2$ mm on the upper surface and in cut-off channels on bars at RM 73.1, 79.4, 82.0, 104.2, 106.1 to the depth of the local surface $D_{84}$

#### 5. Fine sediment in major tributaries

The drainage area that contributes flow and sediment to the restoration reach of the Trinity River is 420 square miles ( $\text{mi}^2$ ), as determined by subtracting the drainage area upstream of Lewiston Dam ( $718.4 \text{ mi}^2$ ) from the drainage area upstream of the NF Trinity River ( $1138.4 \text{ mi}^2$ ). Named tributaries compose 90% of the drainage area for the restoration reach and are primary sources of flow and sediment in the Trinity River (see Figures 1 and 10), including Hoadley Gulch and Deadwood, Rush, Grass Valley, and Indian creeks. These tributaries are the focus of this section because information is available for them and because they are partially underlain by granitic soils, the primary contributor of fine sediment to the Trinity River (Madej, 2007).

Annual loads of fine sediment on Deadwood, Rush, Grass Valley, and Indian creeks show considerable scatter, but exhibit lines of best fit that suggest their sediment contributions to the Trinity River decreased in the period that data are available (1996-2007; Figure 26), except suspended loads increased in the latter end of the period of record for Deadwood Creek (2000–2006; Section 5.1.2) and Rush Creek (1999–2006; Sections 5.2.1). Sediment delivered by Grass Valley Creek to Hamilton Ponds also decreased between 1998 and summer 2018, but watershed disturbance from the Carr Fire in 2018 profoundly increased sediment production in both Grass Valley and Deadwood creeks (see Figure 10 and Appendix B). The sediment pulse from the fire in Grass Valley Creek was captured in Hamilton Ponds, and sediment from Deadwood Creek formed a large delta in the Trinity River and blanketed the most the baseflow channel with up to 0.3 ft of soil and silt for around 1.3 miles downstream of the delta. Past episodic contributions of fines to above Rush Creek delta have caused the fine sediment content in subsurface areas of the bed to fluctuate widely between bulk sample events at Lewiston (Section 6.1.2). Between episodic events, a deficit of fine sediments exists at and upstream of TRAL, and likely extends to Rush Creek, the first major tributary below Lewiston Dam, as demonstrated in later sections.

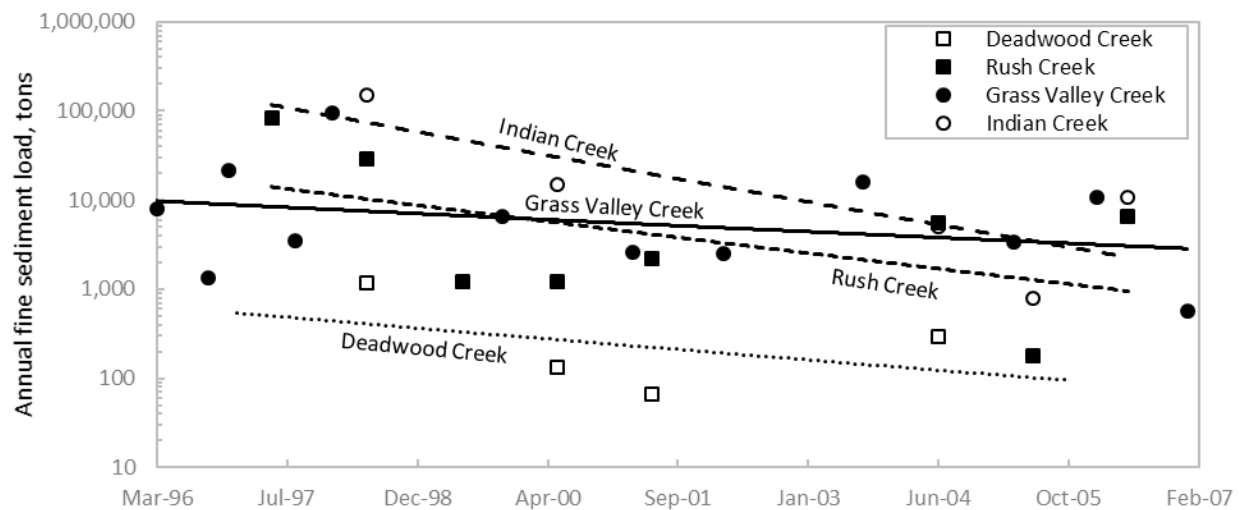


Figure 26. Annual fine sediment load estimates with lines of best fit to the data by eye for Deadwood, Grass Valley, Rush, and Indian creeks. Loads for Deadwood, Rush, and Indian creeks are estimated by summing suspended sediment and fine bed loads estimated with measured transport relationships on these creeks. Loads for Grass Valley Creek are estimated by topographic differencing accumulated sediment in Hamilton ponds.

### 5.1 Deadwood Creek and Hoadley Gulch

Deadwood Creek watershed is 9.2 mi<sup>2</sup> in area and conflues at the outside of a bend in the Trinity River at a location 1.2 miles downstream of Lewiston Dam. Hoadley Gulch conflues with the river an additional 0.9 miles downstream near Old Lewiston Bridge and has a watershed area of 3.6 mi<sup>2</sup>. Land use in the Deadwood Creek watershed was historically dominated by mining and logging, and approximately 75% of Hoadley Gulch was logged between 1977 and 1990 (USDA, 1990). Soils derived from decomposed granite occupy around 74% of Hoadley Gulch and 10% of Deadwood Creek. In both watersheds, logging roads historically contributed approximately half the sediment delivered to the creeks, and the remaining sediment yield resulted from landslides, rilling and gullyng on hillslopes, and bank erosion (GMA, 2001). An inventory of sediment source areas by USDA (1990) indicated that most of Hoadley Gulch was largely stable and non-eroding. Alternatively, sediment from roads and hillslopes were found in a July 1989 survey to compose around 20% of substrate in fish habitats and cause embeddedness of gravels in riffles and pool tails to average 59% and 47% in upper and lower Deadwood Creek, respectively (Ebasco Env., 1990). This information is not available for Hoadley Gulch, where studies are limited to a sediment source inventory by USDA (1990), a fish habitat assessment by Ebasco Env. (1990), and cursory sediment source analysis by GMA (2001). Due to the sparsity of information on Hoadley Gulch, the remainder of this section focuses on fine sediment in Deadwood Creek.

#### 5.1.1 Deadwood Creek flows

Daily average flows on Deadwood Creek were measured by the Hoopa Valley tribe for most of water years 1998 through 2004, and discharge estimates were used to provide missing data for the August 1, 1996 through December 31, 2006 period that sediment transport and delta analyses were undertaken. The estimates were made by normalizing daily average flows gaged on Grass Valley Creek at Fawn Lodge gage by drainage area (30.8 mi<sup>2</sup>) and scaling the result by the Deadwood Creek drainage area at

the confluence with the Trinity River (9.1 mi<sup>2</sup>) and then scaling the result by the average ratio of flows on these creeks when their discharge records overlapped. The Fawn Lodge gage is located 4.3 linear miles from the gaging location on Deadwood Creek. The missing flow record at Fawn Lodge between September 30 through December 2005 required estimating these flows with a linear relationship ( $r^2=0.99$ ) between flows at Fawn Lodge and on Grass Valley Creek near Lewiston (drainage area 36.2 mi<sup>2</sup>) in the period when both gages were operational (10/1/2004–9/29/2005). Estimated flows at Fawn Lodge were then adjusted to discharges expected at Deadwood Creek as described above.

### 5.1.2 Deadwood Creek delta

Deadwood Creek forms a delta in wetter water years where a large pool is located immediately upstream of new Lewiston Bridge. This pool was first dredged in 1976 and then again in 1980 and an estimated 3 to 5 thousand cy of sediment were removed in each of these years despite historically low winter flows on the Trinity River in this period (USDA, 1990). Later, in August 1996 through December 2006, nine elevation surveys were used to estimate the volume of sediment contributed to the pool by Deadwood Creek using topographic differencing (GMA, 2007). The surveys likely captured most coarse sediment delivered to the pool by Deadwood Creek in the time between surveys but may have missed a portion of the finer load produced in the watershed. Results from differencing the surveys nonetheless indicated the rates of infill were <1,000 cy/yr in all cases except between January 1998 and February 1998 when the rate was 12,716 cy/yr (Table 3, Figure 27a). This high fill rate occurred in the first winter after the Deadwood fire burned 4% of the watershed in August 1997 (Appendix B). Between seven of the paired delta surveys, Trinity River flows at Lewiston exceeded 5,600 cfs, which would have mobilized sediment from the delta confluence pool. Even so, annual infill rates normalized by the flow volume that occurred on Deadwood Creek between pool surveys suggest that high creek flows destabilize the channel and evacuate large volumes of sediment to the Trinity River (Figure 27b). Following high flow years, the channel stabilizes and annual contributions of sediment per unit volume of flow reduce, as demonstrated in Figure 27b following floods that occurred in 1997 (414 cfs), 1998 (423 cfs), and 2004 (213 cfs).

Table 3. Estimated volumes of sediment contributed by Deadwood Creek to the Trinity River.

Initial survey date	Ending survey date	Duration (days)	Between survey dates		Infill volume <sup>2</sup> (cy)	Annual infill rate (cy/yr)	Normalized annual infill rate (cy/yr/AF)
			Peak daily flow on Trinity River at Lewiston (cfs)	Peak daily flow on Deadwood Creek (cfs)			
Aug-96	Feb-97	184	6,910	414 <sup>1</sup>	440	873	0.106
Feb-97	Jan-98	334	2,040	87	630	688	0.085
Jan-98	Feb-98	31	5,640	423	1,080	12,716	1.211
Feb-98	Sep-00	943	6,100	189	880	341	0.007
Sep-00	Aug-03	1064	5,990	203	260	89	0.003
Aug-03	Apr-04	244	2,100	213	450	673	0.072
Apr-04	Dec-04	244	6,200	71 <sup>1</sup>	150	224	0.049
Dec-04	Nov-05	335	6,960	71 <sup>1</sup>	280	305	0.028
Nov-05	Dec-06	395	10,100	167 <sup>1</sup>	390	360	0.019

<sup>1</sup>Estimated. <sup>2</sup>Not adjusted for porosity.

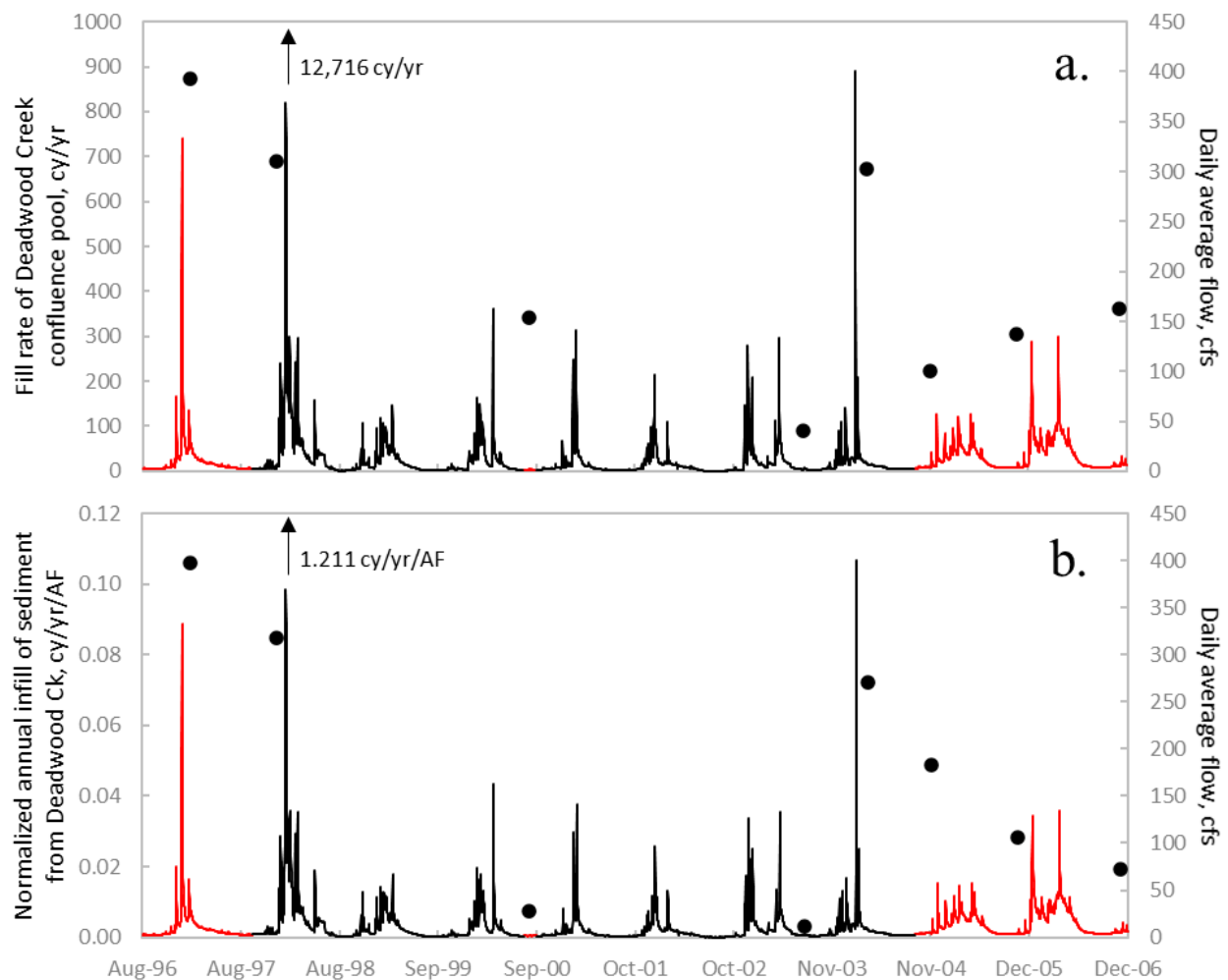


Figure 27. Closed symbols showing estimated annual rates (a.) and flow normalized rates (b.) of sediment filling a pool on the Trinity River near Lewiston by Deadwood Creek. Flows for the normalizations were total volumes that occurred between surveys used to estimate fill rates. Daily average flows in red were estimated as described in Section 5.1.1.

### 5.1.3 Sediment loads and grain-size distributions

Bed load samples were collected on Deadwood Creek in 1997–2001 and 2004 and suspended sediment samples were collected 1997–2006 except 1999. Annual load estimates could only be made for coarse bed load in 1998 and 2000–2001 and also in 2004 for fine bed load because sieve analysis was not undertaken to enable fractional load estimates, discharges were not included with the transport measurement, or too few transport measurements were available to adequately define the discharge to transport relationship. Nonetheless, results for coarse material showed annual loads decreased from 1,374 tons in WY 1998 to 39 tons in WY 2000 and then 56 tons in WY 2001. Fine bed loads were 1180, 134, 66, and 291 tons respectively in WY 1998, 2000–2001, and 2004. Summing the fractional loads provides total load estimates of 2,554, 173, 122, and >291 tons in sequential years noted above, which generally agree with the temporal variations in pool filling (Table 3). The record of suspended sediment transport measurements was more robust than for bed load so these load estimates were made for all water years that data were available except 2005, which was excluded because transport measurements were made

over too narrow a range of flows (40-57 cfs) to enable load calculations the entire year. Here again the computed loads mostly agree with those for pool filling (Table 3, Figure 27), where a record load occurred in WY 1998, followed by a large decline before stabilizing at around 235 tons in 2001–2002 before increasing steadily WY 2000–2006 (Figure 28). These results in combination with sieve analyses of bed load samples taken in WY 1997–2001 and 2004 showing the proportion of fines  $\leq 8$  mm exhibited an overall trend that appears flat (Figure 29) suggest fine sediment contributions from Deadwood Creek in the period of record grew may have slightly increased.

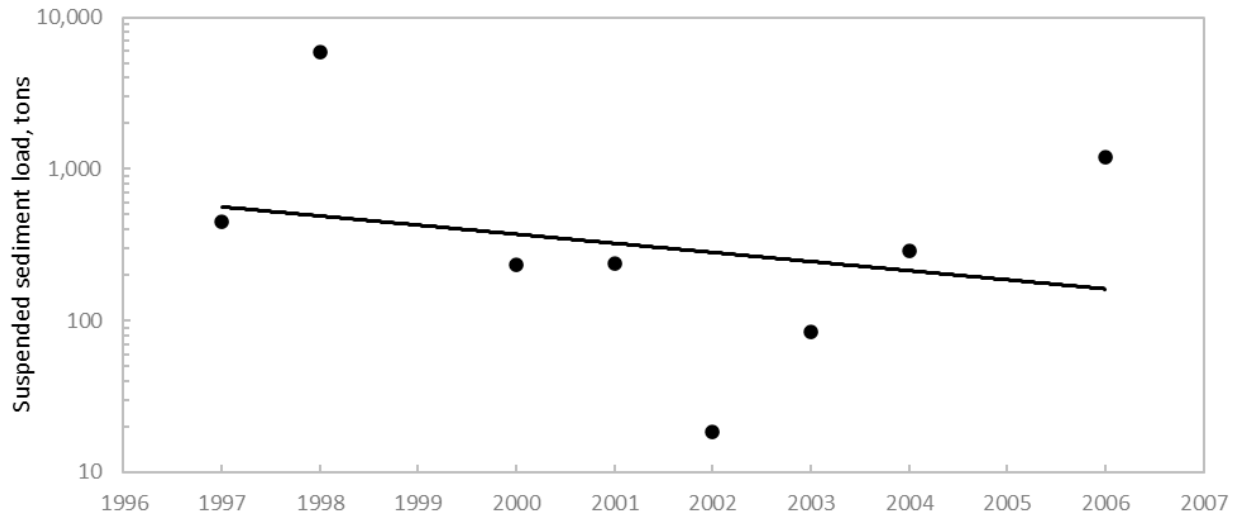


Figure 28. Suspended sediment load estimates for Deadwood Creek in WY 1997–1998, 2000–2004, and 2006. The line was fit by eye to the data.

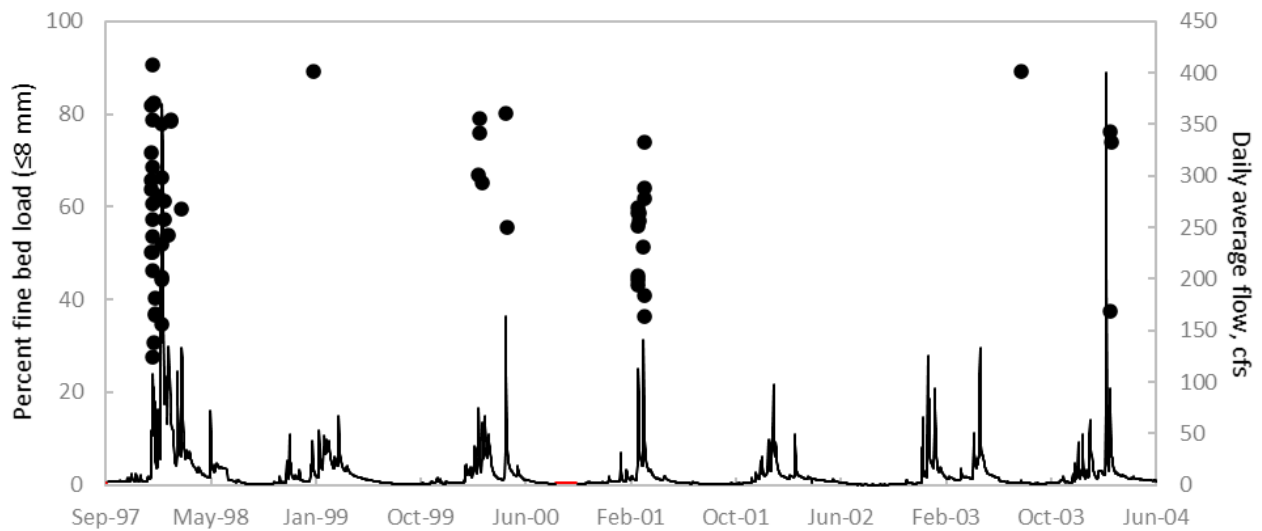


Figure 29. Percent by weight of particles  $\leq 8$  mm and daily estimates of fine bed loads estimated for Deadwood Creek in 1998–2001 and 2004.

### 5.1.4 Carr fire effects

Deadwood Creek was impacted by the Carr fire in summer 2018. More than 80% of the watershed was burned, with 45% of the burn area experiencing low burn severity, 36% moderate severity, and 19% high severity (Appendix B). The U.S. Forest Service modeled runoff from the post-fire topography by a 10-year flood on Deadwood Creek and predicted that sediment production would increase by 1,550% for an unspecified duration in the basin due to the fire. The projections were for sediment production to increase from 2 tons/acre before the fire to 32 tons/acre after the fire. These rates equate to an increase in mass sediment production from 11,724 to 163,404 tons in a runoff event with a 10-year recurrence interval. In support of model predictions, the first post-fire rainfall event in the watershed after the summer dry period delivered 0.56 inches of rainfall between October 2–4<sup>th</sup>, 2018 (Figure 30) was sufficient to generate high flows on Deadwood Creek (see Figure 27), and increase turbidity on the Trinity River from <5 NTU to an event peak of 295 NTU at Limekiln Gulch (USGS gage 11525655) and 216 NTU above the NF Trinity River (USGS gage 11526400).

A site visit in October 2018 indicated that soil erosion from hillslopes, road surfaces, and inboard ditches into Deadwood Creek was extensive. At least a portion of sediments delivered to the channel were routed to a delta deposit on the Trinity River (Figure 31). Based on visual estimates, the delta sediments were primarily fine sediment ( $\leq 8$  mm) with minor contributions of coarse bed load ( $> 8$  mm). As shown in Section 6.2.5.3, substantial fine sediment deposits on the channel bed in the Lewiston area resulted from turbidity plumes from Deadwood Creek that were coincident with delta formation (Figure 31). The deposits capped the gravel-bed in the Trinity River and likely had significant negative consequences for salmonid egg incubation upstream of Rush Creek in 2017–2018. Located between Rush Creek and Lewiston were 733 of the 1853 total Chinook salmon redds constructed in the restoration reach that year, such that 40% of salmon redds constructed in the Trinity River in 2017–2018 were impacted by fines delivered by Deadwood Creek during winter baseflows on the mainstem Trinity River.



Figure 30. Deadwood Creek watershed impacted by the Carr fire (a.) and the Deadwood Creek channel after a rainfall event (0.56 inches) that occurred October 2-4th, 2018 (b.).



Figure 31. Deadwood Creek delta on March 25, 2019 when flow at TRAL was 300 cfs.

## 5.2 Rush Creek

Rush Creek watershed area is 22.6 mi<sup>2</sup> and the channel confluences with the Trinity River 4.3 miles downstream of Lewiston Dam. Land use in the Rush Creek watershed historically involved mining, livestock grazing, logging, and associated road building. Logging was particularly active in the watershed between 1985 and 1990 (USDA, 1990). The road system in the watershed was given the highest rating for potential road impacts to downstream habitats in the Trinity River basin by USEPA (2001). However, Rush Creek watershed has one of the lowest percentages of total watershed acreage burned since 1954 (3% in 1994, see Appendix B). Perhaps owing to this, Rush Creek also exhibited the lowest long-term (1981–2001) sediment yield (266 tons/mi<sup>2</sup>/yr) of all major tributaries to the Trinity River restoration reach, excepting Canyon Creek (GMA, 2001). In 23% of the watershed area, decomposed granite is the parent geologic material (USDA, 1990).

### 5.2.1 Annual suspended and bed loads

Suspended sediment and bed load transport measurements were respectively made on Rush Creek near the confluence with the Trinity River in WY 1997–2006 excepting 2002 and in the same period excepting 2003 and 2004 for coarse and fine bed load. Annual loads for each grain-size class were estimated by applying the measured transport relationships to discharge with the daily average flow record for Rush Creek in these periods with assumed transport thresholds being 10 cfs for suspended sediment, 100 cfs for fine bed load, and 150 cfs for coarse bed load after GMA (2007). Results were that annual suspended loads were typically highest in the first high flow events of the water year (Figure 32) and annual loads may have decreased slightly in the period that data were available, as indicated by a line of best fit by eye (Figure 33). Similar findings occurred with annual fine bed loads, which declined at a rate of -4,143 tons/yr for WY

1997–2006, and a decline was also estimated for WY 1999–2006 as -40 tons/yr (Figure 34). Coarse bed loads for the period of record varied within a smaller range but less systematically than fine bed load and suspended loads; a linear regression of the annual coarse bed loads indicated they increased at an average rate of +64 tons/year (Figure 34). These trends were essentially unchanged when the respective loads were normalized by annual discharge, suggesting the observed variations in loads were independent of streamflow and likely attributed to recruitment of fines by channel disturbance during winter floods in WY 1997 and 1998.

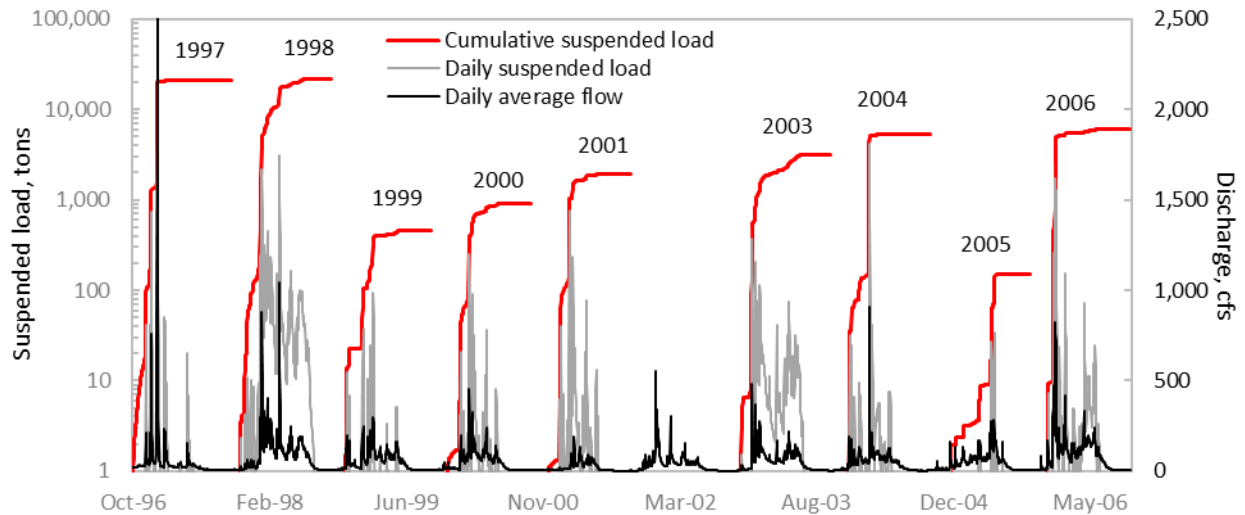


Figure 32. Daily average flows and estimated cumulative annual suspended sediment loads for the period of record on Rush Creek. Suspended sediment transport was not monitored in water year 2002.

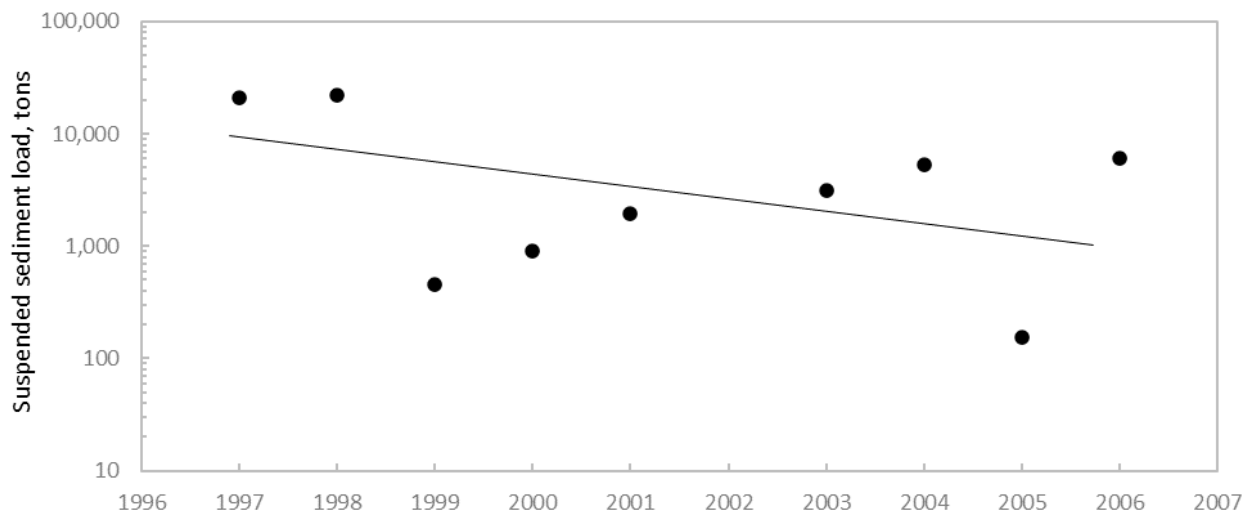


Figure 33. Annual suspended sediment loads estimated with measured transport rates on Rush Creek for WY 1997–2006, excluding WY 2002. The line was fit by eye to the data.

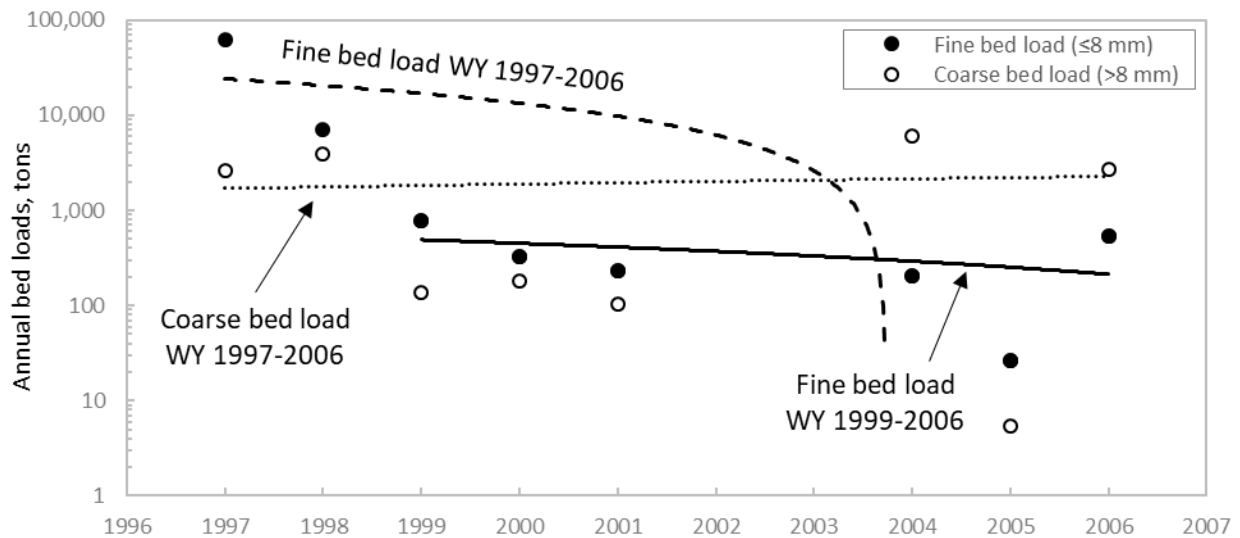


Figure 34. Annual fine and coarse bed loads estimated with measured transport rates on Rush Creek for WY 1997-2006, excluding WY 2002 and 2003. The lines are linear functions for the indicated periods.

### 5.2.2 Grain-size distributions for bed load

Bed load sampled from Rush Creek between December 1996 and May 2006 exhibited a bimodal size distribution in two-thirds of the samples ( $n=68$ ), and sieve analysis of the sampled material indicated grains in the size range of fine bed load ( $\le 8\text{ mm}$ ) dominated the samples (Figure 35a). Sorting parameters computed as the second moment of bed load fractions by weight in half-phi gradations indicated that a slightly narrower range of mobile grain sizes were sampled through time (Figure 35b), and the third moment method indicated skewness of the grain-size distributions and a positive linear slope toward increasing values indicated that smaller grains progressively dominated the bed load samples (Figure 35c; see Bunte and Abt (2001) for descriptions of the moments methods). However, the increasing dominance of fine bed load was apparently not enough to affect the median bed load particle sizes, which varied widely (range 0.5 to 29.5 mm) but remained essentially constant on average at 4.5 mm (Figure 35d).

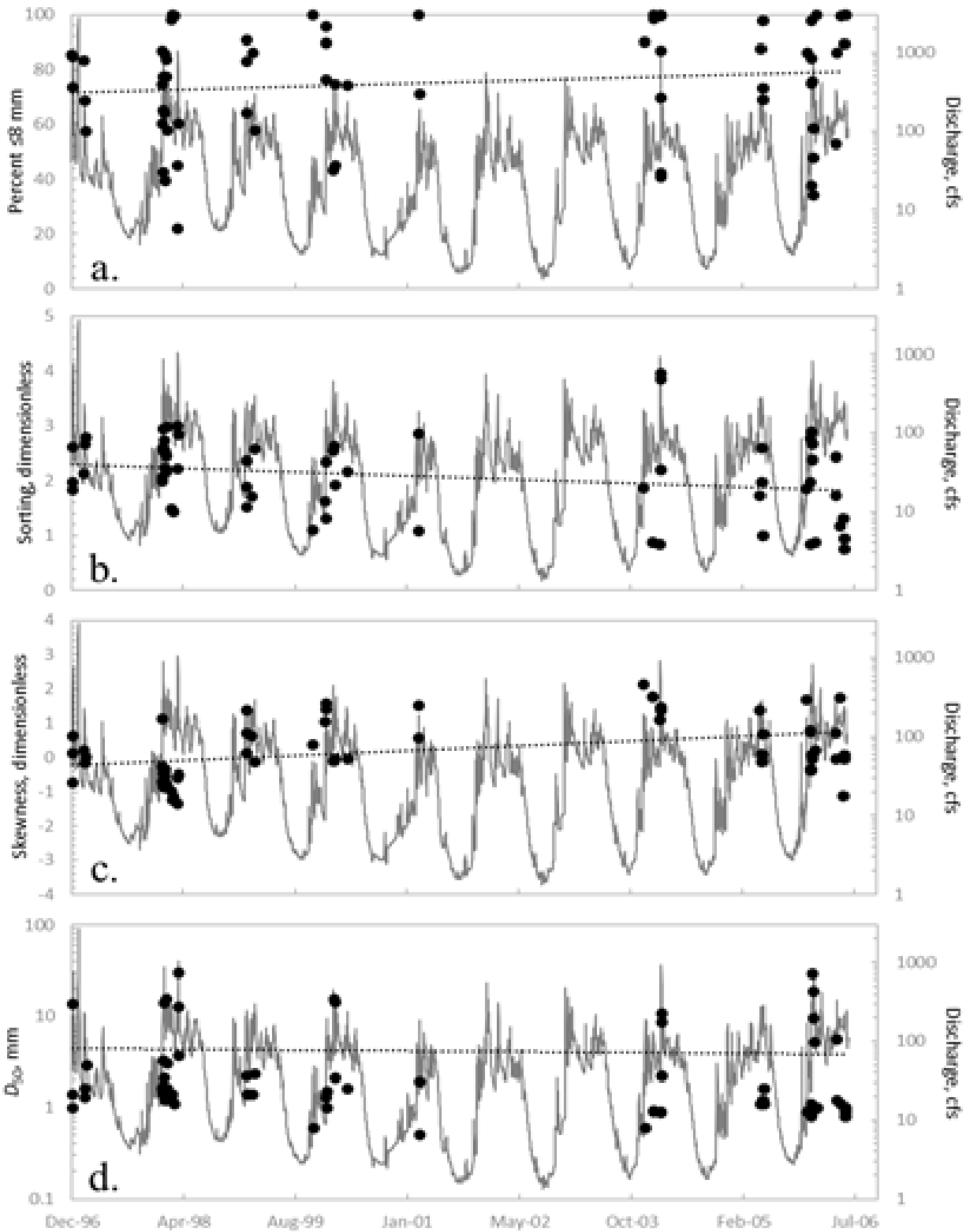


Figure 35. Daily average flows and percent of total bed load samples (by weight)  $\leq 8$  mm in diameter (a.), and sorting (b.), skewness (c.), and median grain diameters ( $D_{50}$ , d.) for bed load sampled on Rush Creek December 1996 through May 2006. Sorting was computed as the second moment and skewness as the third moment of the bed load size fractions. The dotted lines are linear regressions of the data.

### 5.2.3 Rush Creek delta

A bulk sediment sample weighing 18,751 kg was collected from the Rush Creek delta in November 2002 for the purpose of determining the size distribution of delta sediments. A subsample of this material weighing 356 kg was dry sieved and the resulting size distribution indicated fine sediment ( $\leq 8$  mm) composed 19.1% of the sample by weight (Figure 36). In consideration that framework supported beds exhibit 20-30% void space (Carling and Reader, 1982; Milhous, 2001), the Rush Creek delta was partially matrix supported by fines occupying pore spaces between coarse grains. This level of filling restricts but does not prevent intergravel flow. Therefore, a portion of Rush Creek flow would likely have been able to infiltrate the delta in the early 2000s and release relatively cold water to the mainstem Trinity River to moderate water temperatures in the area for juvenile fish rearing. However, it is likely the size distribution of sediment and the availability of open pore space in the delta reduced between 2002 and 2006, based on the percentage of fines and skewness and sorting of grain-size distributions for bed load samples showing increased fine sediment in loads in this period (Figure 35).

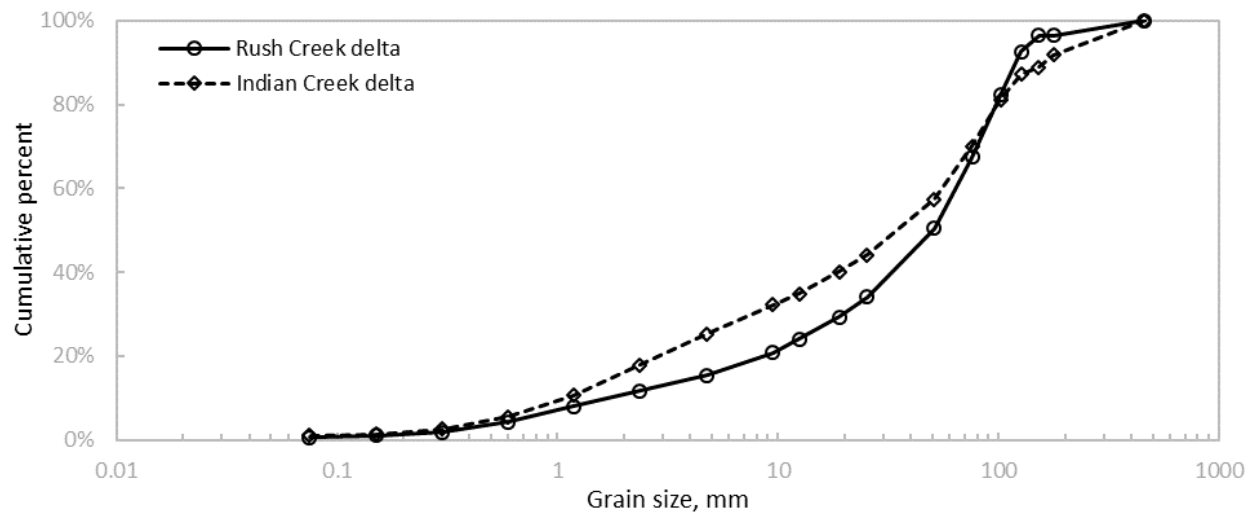


Figure 36. Grain-size distribution for bulk samples collected on Rush and Indian Creek deltas in November 2002.

Differencing elevation surveys of Rush Creek delta made by GMA (2007) and the TRRP indicate the delta's volume varied between +3000 cy and -2700 cy and exhibited an overall increase in volume (+6,400 cy) between October 1996 and May 2013 (Table 4). The duration between delta surveys ranged from 90 to 1400 days, so that it is difficult to explain the observed volume changes except by broad association with flows river flows that disperse delta sediments downstream and Rush Creek flows that deliver sediments to the delta. The differencing results indicated that delta losses occur when the peak discharge on the Trinity River exceeds the peak flow on Rush Creek between surveys by 12.2 time or more, with the only exception occurring between January 1998 and October 2000 when the volume decreased by the largest amount in the period of record (2700 cy) despite a peak flow ratio of 5.9. In all years that delta volume increased, the ratio of peak flows was 10.9 or less.

Table 4. Rush Creek delta survey dates, changes in delta volume, and ratios of peak flow on the Trinity River and Rush Creek between surveys.

Beginning survey	Ending survey	Duration between surveys (days)	Change (cy)	Peak flow Rush Creek	Peak flow TRAL	Peak flow at TRAL / peak flow at Rush Creek	Source
Aug-96	Dec-96	122	760	761	531	0.7	GMA
Dec-96	Mar-97	90	1420	2,710	6,910	2.5	GMA
Mar-97	Jan-98	306	3060	367	2,160	5.9	GMA
Jan-98	Oct-00	1,004	-2680	1,040	6,100	5.9	GMA
Oct-00	Nov-02	761	303	555	6,040	10.9	GMA
Nov-02	Apr-03	151	1690	482	329	0.7	GMA
Apr-03	Apr-04	366	560	909	2,610	2.9	GMA
Apr-04	Dec-04	244	-210	164	6,200	37.8	GMA
Dec-04	Dec-06	730	-750	825	10,100	12.2	GMA
May-06	Nov-06	184	-800	243	10,100	41.6	GMA
Jun-11	Apr-15	1,400	3000	654	6,080	9.3	TRRP

### 5.3 Grass Valley Creek

Grass Valley Creek watershed is 36.9 mi<sup>2</sup> and the creek flows into the Trinity River 7.8 miles downstream of Lewiston Dam. Land use in the watershed was dominated by historic mining and logging in the early 1900s, and logging was particularly aggressive from 1948 to 1993 when most the watershed was clear cut (TRSO, 2004). The timber harvest and associated ground disturbance and road building exposed a portion of the approximately 65% of the watershed area that is underlain by decomposed granite. Mining and logging increased delivery of fine sediment to the creek from colluvial sources, channel incision, stream capture and erosion by skid trails, road and culvert failures, and sheet and rill erosion from exposed soils and road surfaces (USEPA, 2001; Madej, 2007). The increased sediment load is evidenced in a 1944 aerial photo that shows the Grass Valley Creek delta dissected by a braided channel flowing between large deposits of granitic sediment (Appendix C). Prior to closure of Trinity Dam in November 1960 and the beginning of flow diversions to the Central Valley in 1963, Trinity River flows mobilized large amounts of Grass Valley Creek sediment delivered to it (Barnes, 1978), as evidenced by the lack of significant delta forming in the mainstem river. However, flow regulation reduced the sediment transport capacity of the river and enabled the Grass Valley Creek delta to extend across the river by 1965. Continued flow regulation enabled the delta to stabilize with vegetation by as early as 1971, and the delta's stability was apparently sufficient for infrastructures to be constructed on it by landowners around 1980 (Appendix C).

Beginning in 1976, Phase one of a sediment reduction plan to reduce or eliminate contributions of sediment from Grass Valley Creek to the Trinity River began with excavation of large pools in the Trinity River on Southern Pacific land located 0.7 miles downstream of the Grass Valley Creek delta. Jet-pump dredges were operated in the pools to remove fine sediments that accumulated in them. In 1978, the Southern Pacific pool was enlarged by 17 thousand cy because its capacity was exceeded annually by sediment that primarily originated from Grass Valley Creek. In 1980, the U.S. Congress authorized funding for Buckhorn Dam, sediment retention ponds on Grass Valley Creek, and several constructed pools on the mainstem Trinity River (TRSO, 2004). Then in 1984, two sediment retention pools were constructed, one on the Grass Valley Creek delta and another 240 ft upstream on Grass Valley Creek. Each pool had a

retention capacity of 30 thousand cy and were named upper and lower Wellock pools after the owner of land on which they constructed. Upper Wellock pond was periodically dredged until at least 1998, as the 2001 and later aerial photos show the pond filled in and became increasingly vegetated. In 1988, upper Hamilton pond was excavated at a location 260 ft upstream of Wellock pond, and in 1989, lower Hamilton pond was excavated 160 ft downstream of the upper pond. Since their construction, the Hamilton ponds have been dredged around a dozen times, to prevent creek sediments from entering the Trinity River. Construction of a large sediment retention structure, Buckhorn Dam was then completed in 1991. The dam is a run-of-the-river type that captures sediment from 25% of the upper drainage area of Grass Valley Creek and releases year-round flow to Grass Valley Creek via a bottom toe drain and overflows at full reservoir via a top-drain structure.

Implementation of phase two of the sediment reduction plan began in 1992 and involved restoration activities to reduce sediment yields from Grass Valley Creek. The initial step in phase two was the U.S. Bureau of Land Management's purchase of 17,000 acres of highly eroded private timberland for restoration purposes. On this and surrounding lands, an erosion control program was implemented largely by the Trinity County Resource Conservation District and the Natural Resource Conservation Service. The restoration activities included rebuilding stream crossings, stabilizing stream channels, grading and resurfacing road surfaces with crushed rock, hydro mulching critical erosion areas, and reforesting decomposed granitic soils with tree plantings. These treatments were implemented from 1992 to 1996 and estimates are they reduced sediment contributions to Grass Valley Creek by around 133 thousand cy at a cost that was less than half that required to maintain Wellock and Hamilton ponds (Trso, 2004). Watershed restoration continued in the Grass Valley Creek through at least 2004, and in 1997–2003 included over a million tree plantings above Buckhorn Dam.

### *5.3.1 Wellock and Hamilton Ponds*

Sediment yield from Grass Valley Creek can be estimated a number of ways, including application of sediment rating curves measured at Fawn Lodge and near the confluence with the Trinity River, computation of sediment budgets for the watershed, and by adding sediment contributions to Wellock and Hamilton ponds and Buckhorn Dam. Limitations of data from the Fawn Lodge site (USGS gage 11525600) are that periods of record for discharge only include 1975–2005 and for suspended sediment and bed load to 1976–1999, and the site only accounts for sediment contribution from the upper 83% of the watershed, downstream of which exists large erosive areas that contribute sediment to the creek (Trso, 2004). An alternative is to use flow records for Grass Valley Creek near Lewiston (gage number 11525630), which is downstream of 98% of the watershed area, but this gage has a limited period of record for discharge (2004–2018) and sediment transport (water years 2003–2005). Comparing sediment budgets (e.g., Trso, 2004; Madej, 2007) is another option for assessing changes in sediment yield from the basin, except budget values that are the most difficult to quantify are transport and storage in stream channels (Reid and Dunne, 1996), which is of primary interest in this report. Because budget components commonly display errors that exceed  $\pm 50\%$  (Kondolf and Matthews, 1991b) and since total budget estimates typically vary markedly between studies depending on assumptions in the modeling, temporal changes in sediment yield from Grass Valley Creek were evaluated with estimates of infill made for Wellock and Hamilton ponds.

The infill estimates account for all size fractions except wash load conveyed by Grass Valley Creek. The wash load is not accounted for because at least a portion of it remains suspended in flow through the ponds and is delivered to the Trinity River. Moreover, fine and coarse fractions delivered to the ponds are not delineated in the volume estimates because their relative contributions were often not determined when the ponds were dredged. Nonetheless, most sediment contributed to the ponds is in the size range of fine sediment, and the proportion of fines stored in the ponds has increased through time. For example, bulk sampling in 1997 estimated that fine sediments composed 70% of the material in Hamilton ponds (McBain and Trush, 1997), and the proportion increased to 100% in 2009 and 2018 (Figure 37). Between these years, the proportion of bulk samples <1 mm decreased from around 83% in 2009 to about 55% in 2018, which indicates the distribution of grain sizes in the ponds coarsened slightly yet remained in the size range of fines (Figure 37). The dry bulk density of pond sediments sampled in 2018 (average 1.17 tons/cy) was close to the 1.25 tons/cy that is published by Roberts (1996) for Hamilton ponds and referenced in the Trinity River flow study (HVT and USFWS, 1999).

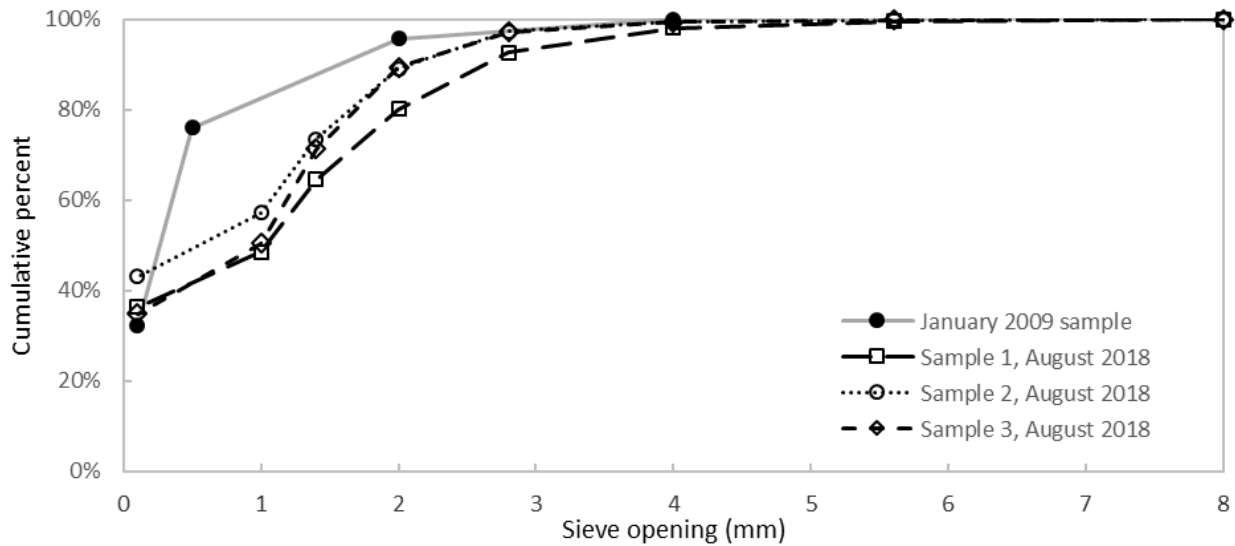


Figure 37. Grain-size distributions for bulk sediment samples obtained from Hamilton Ponds by Graham Mathews and Associates in 2009 and the author in 2018.

Estimates of infill and dredged volumes of sediment for Wellock and Hamilton ponds have been made by topographic differencing elevation surveys and by counting dump truck loads of sediment dredged from the ponds. A variety of entities have estimated the infill rates by these methods and some estimates for the same period have varied substantially between investigators (see Trso, 2004; McBain and Trush, 1997; and GMA, 2007). A major source of uncertainty in the estimates was dates for infill and dredging, which required several assumptions to estimate temporal changes in volumes of fine sediment delivered to the ponds. First, only infill measurements were considered because dredge volumes were subject to substantial error in accounting (Trso, 2004). In this way, estimates of sediment delivery to the ponds are likely conservative because dredging may have occurred between dates when infill volumes were estimated. Also, infill volumes published with a calendar year and not a range of dates were assumed to have resulted from flow on Grass Valley Creek that occurred over the calendar year that was reported.

Infill estimates indicate that just over 206 thousand cy of sediment have been delivered to the ponds since their creation and that sediment contribution rates have decreased through time (Table 5; Figure 38). In the first decade after construction, contribution rates to the ponds were markedly higher (1985–February 1998, average 162.2 cy/d; Table 5) than in the following ten years (February 1998–October 2007 average 5.9 cy/d; Figure 38). Gaeuman (2010) explained the reduction likely resulted from evacuation of sediment from Grass Valley Creek in WY 1995–2000 that were designated wet or extremely wet by the natural hydrology for the Trinity River (see USFWS and HVT, 2001). The reduced rate of pond filling after 1998 also coincides with the timing for completion of the first phase of watershed restoration in the basin. From the most recent survey of the ponds in June 2018, topographic differencing indicated 6,158 cy of sediment was captured in the upper pond and 145 cy in the lower pond since October 2007, which give an average daily rate of infill as 1.6 cy/day, or 584 cy/year for this period. At this rate of infill, the duration to fill both ponds is ~41 years based on the free volume quantified in the 2018 survey. Altogether, sediment delivery rates have varied widely through time, from 1.4 to 2.9 cy/day (Table 5), and normalizing the rates by the observed peak flow on Grass Valley Creek that occurred within each period that volume estimates were made indicate that sediment production has declined as a negative power function of time since pond construction (Figure 39), indicating the objective to reduce sediment yields from Grass Valley Creek watershed has been met.

Table 5. Sediment volumes delivered to Wellock (W) and Hamilton (H) ponds, 1985–2018.

Start date	End date	Duration (days)	Infill volume <sup>1</sup>			Maximum daily flow (cfs)	Unit Infill rate (cy/day/cfs)	Reference; notes
			(cy)	Cumulative (cy)	(cy/day)			
1985		334	2,500	2,500	7.5	62	0.121	2, W only
1986		334	28,000	30,500	83.8	808	0.104	2, W only
1987		334	6,000	36,500	18.0	406	0.044	2, W only
1989		365	4,266	40,766	11.7	121	0.193	3, both H ponds
1992		365	6,600	47,366	18.1	420	0.043	4, both H
1993		365	6,600	53,966	18.1	323	0.056	4, both H
1995		730	70,000	123,966	95.9	1,650	0.046	2, both H
Nov-95	Aug-96	274	3,570	127,536	13.0	182	0.072	5, both H
Aug-96	Dec-96	122	590	128,126	4.8	316	0.015	5, 6, upper H only
Dec-96	Jan-97	31	9,540	137,666	308	1,400	0.220	5, 5, both H
May-97	Jan-98	245	1,540	139,206	6.3	176	0.036	5 <sup>7</sup>
Jan-98	Feb-98	31	42,220	181,426	1,362	1,430	0.400	5, both H
Jan-99	Sep-00	609	2,930	184,356	4.8	553	0.009	upper H only
Sep-00	Oct-01	395	1,140	185,496	2.9	551	0.005	5 <sup>7</sup>
Oct-01	Aug-02	304	1,120	186,616	3.7	686	0.005	5, both H
Aug-02	Sep-04	762	7,080	193,696	9.3	721	0.013	5, both H
Oct-04	Sep-05	335	1,500	195,196	3.7	241	0.019	5, both H
Oct-05	Jun-06	243	4,740	199,936	19.5	566	0.034	5, both H
Oct-06	May-07	212	250	200,186	1.2	125	0.009	5, both H
Oct-07	Jun-18	3,896	6,303	206,489	1.6	680	0.002	both H

<sup>1</sup>Volumes unadjusted for porosity; <sup>2</sup>USDA (1999); <sup>3</sup>Roberts (1996); <sup>4</sup>PWA (2000); <sup>5</sup>GMA (2007); <sup>6</sup>McBain and Trush (1997); <sup>7</sup>unclear which Hamilton pond was dredged.

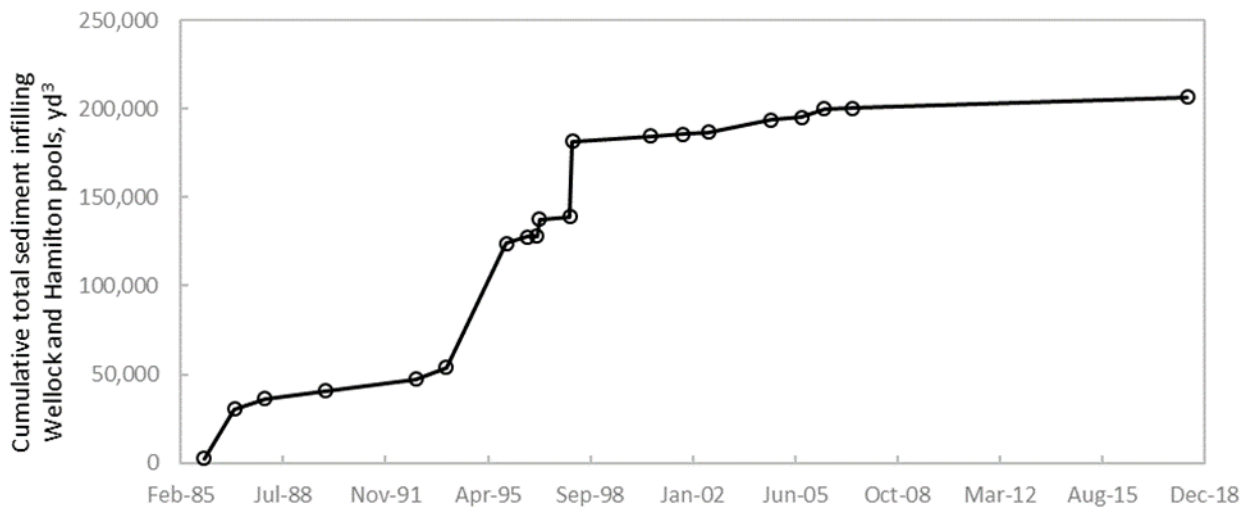


Figure 38. Cumulative volume of sediment infilling Hamilton ponds from dates of construction to the latest survey of the ponds in June 2018.

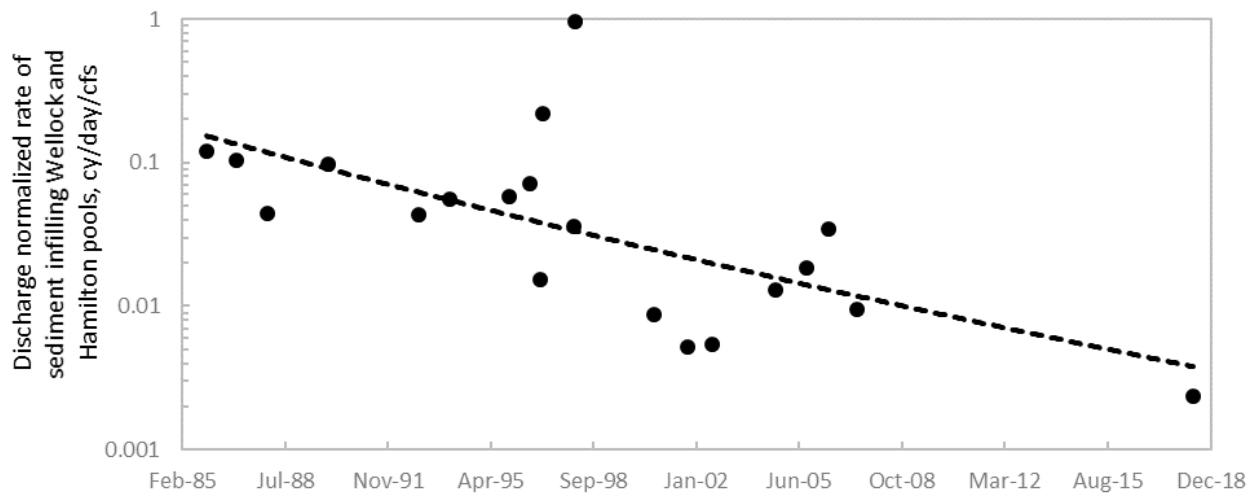


Figure 39. Peak daily average flow-normalized rates of sediment infilling Hamilton ponds for periods that contribution estimates are available. A steeper rate of decline than the one shown resulted when the total flow contributing sediment for each period was used.

In summer 2018, the Carr fire burned 38% of the Grass Valley Creek basin (see Figure 10, Appendix B, and Section 5.3.3) and aerial photographs of Hamilton Ponds indicate that contributions rates of fine sediment increased strongly as a result (Appendix C). The visual evidence shows that the wet winter in WY 2019 that followed the burn mobilized enough sediment to fill the upper pond and form deltas of sediment at inlets to the lower pond (Appendix B). Based on these observations, the time required to fill Hamilton ponds post-fire was first estimated at around 6 years before revision to 20 years based on 1) the lack of substantial fines stored in Grass Valley Creek near the ponds, 2) the occurrence of a critically dry WY 2020 that has provided an additional year for the watershed to stabilize before the return of winter storms, and 3) an inspection of the watershed in spring 2020 that indicated fire burn areas have sparsely revegetated and formed an erosion-resistant crust on the granitic soils (Figure 40). According to Moss (1990), soil crusts develop on granitic soils when rainfall concentrates silt particles on the

ground surface by impact removal of coarser and finer material. Lateral dispersion from the rainfall impacts forms a tightly packed surface that resists deformation and infiltration by subsequent rain. Compaction of the underlying material then proceeds to a depth of around 5 mm as pressure waves from rain impacts propagate from the rigid surface (Moss, 1990). Surface erosion is reduced by the mature soil crust, but material failures at depths beyond the compaction layer may still occur from high intensity rainfall, and so it is unclear how Carr fire impacts will persist through time to effect sediment delivery to Hamilton Ponds and Buckhorn reservoir.



Figure 40. Carr fire impacts in Little Grass Valley Creek above Buckhorn Dam (a.) and turbidity in Buckhorn reservoir on December 6, 2018 (b.) resulting from runoff in fire-burned areas in the watershed for the dam. Similar turbidity levels were exhibited in the toe drain for the dam, indicating wash load occupied the full reservoir. The same view of the fire burned area in April 2020 shows vegetative regrowth from winter rains (c.) that has also formed an erosion-resistant crust on the granite-derived soils (d.).

### 5.3.2 *Buckhorn reservoir*

Grass Valley Creek at the confluence with Buckhorn reservoir was surveyed for the first time after dam closure in July through September 2018 (Figure 41; see GMA, 2019). The surveys used conventional (total station and GNSS surveys) and structure from motion (see Westoby et al. (2012)) analyses to define a point cloud of coordinates with associated elevations for developing a digital terrain model (DTM) of the delta and surrounding terrestrial areas (Figure 42). The DTM serves as a baseline for estimates of fine sediment production from upper areas of the Grass Valley Creek drainage that can be made by topographic differencing future surveys of the same or similar area obtained in the future.



Figure 41. Area of Grass Valley Creek at the confluence with Buckhorn reservoir that was surveyed in July through September 2018. Conventional refers to areas surveyed with total station.

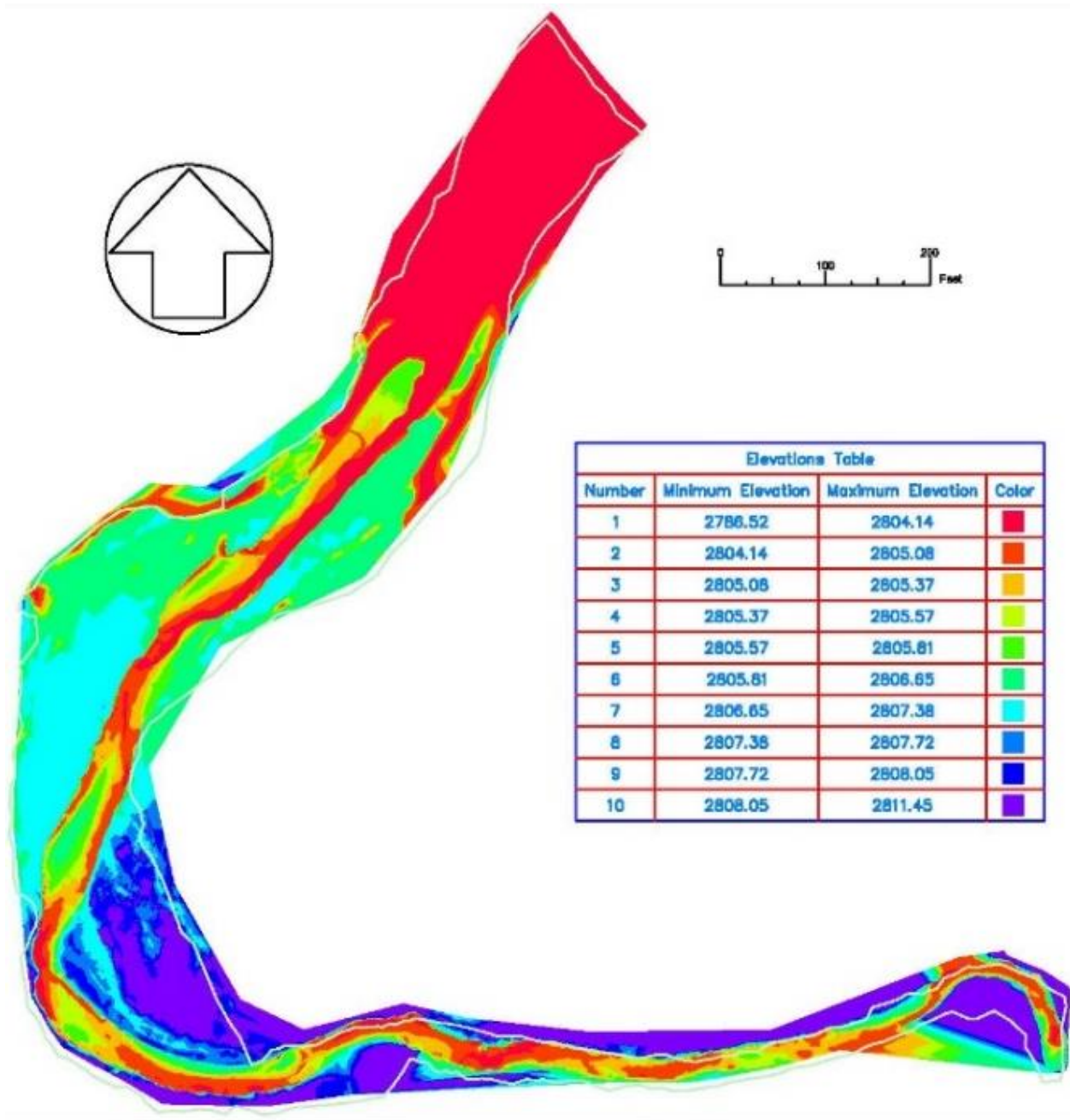


Figure 42. Banded elevations showing surveyed topography of Grass Valley Creek at the confluence with Buckhorn reservoir.

### 5.3.3 Carr fire effects

The Carr fire burnt 13.8 mi<sup>2</sup> of Grass Valley Creek watershed and 57% of this area experienced low burn severity, 36% moderate severity, and 7% high severity. Of the total burn area, 7.2 mi<sup>2</sup> of the affected area was in the 9.4 mi<sup>2</sup> drainage area for Buckhorn Dam, indicating that 77% of this sub-watershed was burnt. The remaining 6.6 mi<sup>2</sup> occupied other sub-basins in the watershed, most predominantly including Little Grass Valley Creek. Similar to the Deadwood Creek watershed, model simulations for a 10-year recurrence interval flow on Grass Valley Creek

predict that sediment production will increase in burned areas of the basin by 1,350% due to the removal of vegetation, hydrophobic soil conditions, and other effects of the Carr fire. From this, projections were for sediment production to increase from 2 tons/acre before the fire to 27 tons/acre after the fire. Based on the total basin area (23,584 acres) and basin area within the fire perimeter (8,854 acres), these rates equate to an increase in mass sediment production from 47,168 to 268,518 tons, or 97,000 cy of sediment. Of this, 56,000 cy are estimated to be retained by Buckhorn Dam, leaving 41,000 cy that could be delivered to the Hamilton ponds in a 10-year runoff event. This estimate does not account for suspended wash load material in Buckhorn reservoir that was released to Grass Valley Creek winter 2018–2019 to increase the fine sediment contribution to Hamilton Ponds and the Trinity River. Peak flows in Grass Valley Creek are estimated to increase by 30% post fire and increase sediment yields from the basin during less extreme precipitation events (USBR, 2018). As mentioned in Section 5.3.1, revegetation and formation of a soil crust has occurred in the burn area since the fire, yet increased production of fines by Grass Valley Creek compared to that observed before the Carr fire is expected to persist for some time. Because of this, a broad estimate of time before Hamilton ponds fill with sediment has been reduced from nearly 41 years before the Carr fire to 20 years after.

#### 5.4 Indian Creek

Indian Creek watershed area is 33.7 mi<sup>2</sup> and confluences with the Trinity River 16.6 miles downstream of Lewiston Dam. At this location, the deficit in coarse sediment in the mainstem channel is assumed to be alleviated by tributary contributions of sediment, though analyses of this possibility has not yet been undertaken. As in other large tributaries upstream of Douglas City, land use in the Indian Creek watershed historically involved mining, livestock grazing, logging and associated road building, and rural development more recently. Logging was particularly active in the watershed between 1985 and 1990 (USDA, 1990). Around 11% of the Indian Creek watershed is underlain by decomposed granitic soils (Trso, 2004), and the estimated mass of sediment contributed by Indian Creek to the Trinity River in 1981–2000 (1,558,226 tons) is second only to Grass Valley Creek for tributaries considered herein (GMA, 2001). For this same period, the mass rate of sediment transport per unit watershed area for Indian Creek near the confluence with the Trinity River (2,103 tons/yr/mi<sup>2</sup>) exceeds values for tributaries upstream of and including Brown's Creek, and notably surpasses normalized mass transport rates for Grass Valley Creek by 62% according to USEPA (2001). Forest roads are the largest source of sediment input to Indian Creek, followed by timber harvest and legacy features that include abandoned roads and mines (GMA, 2001). Sediment contributed from these sources exceeds the background contribution of sediment in the watershed by 707% (USEPA, 2001). Even so, relatively little restoration work has been undertaken to address the elevated levels of sediment production in Indian Creek (see Figure 15). Restoration work has instead focused in Grass Valley Creek, which is the only tributary where fine sediment from human disturbance exceeds background sources by a larger percentage (950%) than Indian Creek. Wildfire has likely not significantly affected sediment production in Indian Creek because only ~7% of the watershed area was burned in 1964, and <0.01% has burned since then (Appendix B).

##### 5.4.1 Annual suspended and bed loads

Annual suspended sediment loads were estimated for Indian Creek using the daily average flow record and measured daily average suspended loads for WY 1997–1998, 2000–2001, and 2003–2006. For these analysis, daily average flows were gaged on Indian Creek WY 2004–2006, and

discharges outside this period were estimated as described for Deadwood Creek using the gage record for Grass Valley Creek at Fawn Lodge. Compared to Rush Creek, suspended loads in Indian Creek are more variable and higher by an average factor of 2.2 (range 0.1 to 5.2) and scaled with daily average flows (Figure 43). The suspended load estimates for WY 1997–2006 (excluding WY 1999 and 2002) appear to have declined in this period, as indicated by a line fit by eye to the data (Figure 44). Additional evidence for a possible decline is that suspended loads lowered by 93% between wet water years that occurred in 2000 and 2005 despite the peak flow in 2000 being only 34% lower. Additionally, a 40% higher peak flow in WY 2004 only transported 36% of the load estimated for WY 2003.

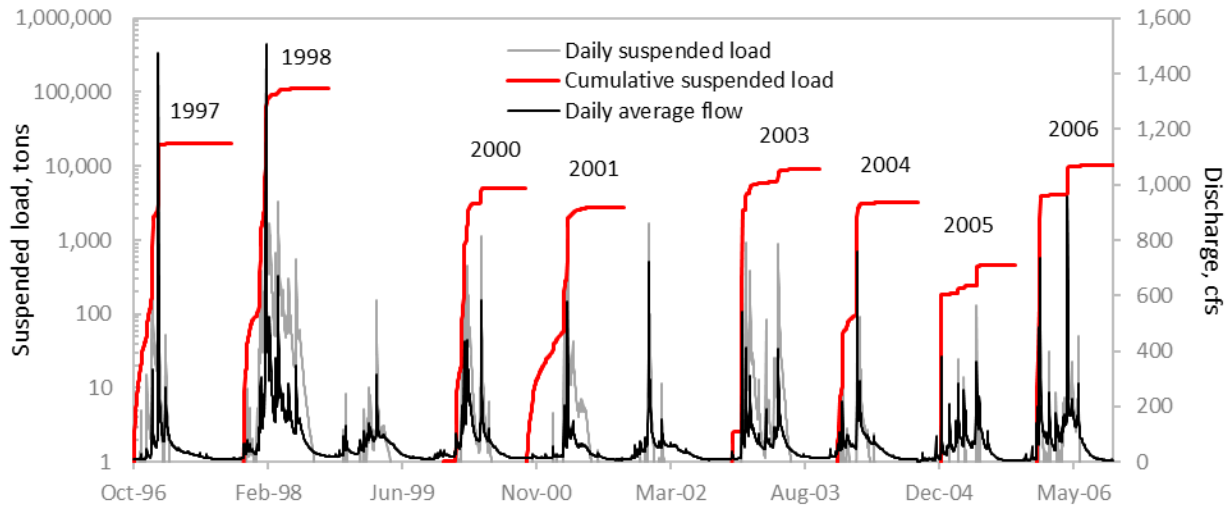


Figure 43. Daily average flows and estimated cumulative annual suspended sediment loads for the period of record on Indian Creek. Labels indicate the water year. Annual loads were not computed for 1999 and 2002 because suspended sediment transport was not monitored these water years.

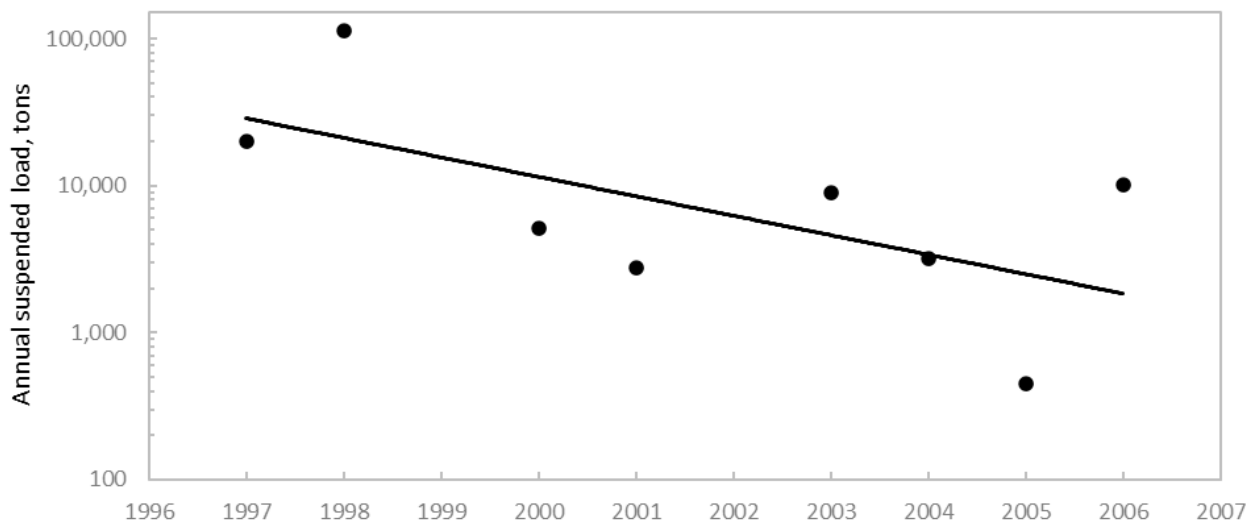


Figure 44. Annual suspended sediment loads estimated with measured transport rates on Indian Creek for WY 1997–2006, excluding WY 1999 and 2002. A line fit by eye to the data suggests load decreased in this time period.

Linear equations fit to annual fine and coarse bed loads provided good fits to the data ( $r^2 \geq 0.76$ ) and indicated that loads decreased at rates of -4,075 and -2,114 tons/yr between WY 1998 and 2006 (Figure 45). Hereto, bed load transport in WY 1998 was extraordinarily high in comparison to other years, so that fine and coarse bed loads respectively decreased at rates of -1,715 and -781 tons/yr when data for WY 2000–2006 are considered. Load declines for both size classes and periods on Indian Creek were substantially greater than on Rush Creek (see Section 5.2.1). Despite this, total fine sediment loads (fine bed load + suspended load) averaged 8.5 times higher (range 0.9 to 19.7) on Indian Creek than Rush Creek in years that estimates were available for both streams. The higher loads result in part from Indian Creek watershed being 33% larger in area than Rush Creek and exhibiting substantially greater disturbance from roads and timber harvest, which apparently overcomes the impacts of a slightly larger area of decomposed granite in Rush Creek (5.2 mi<sup>2</sup>) than Indian Creek (3.7 mi<sup>2</sup>) on sediment production in the basin.

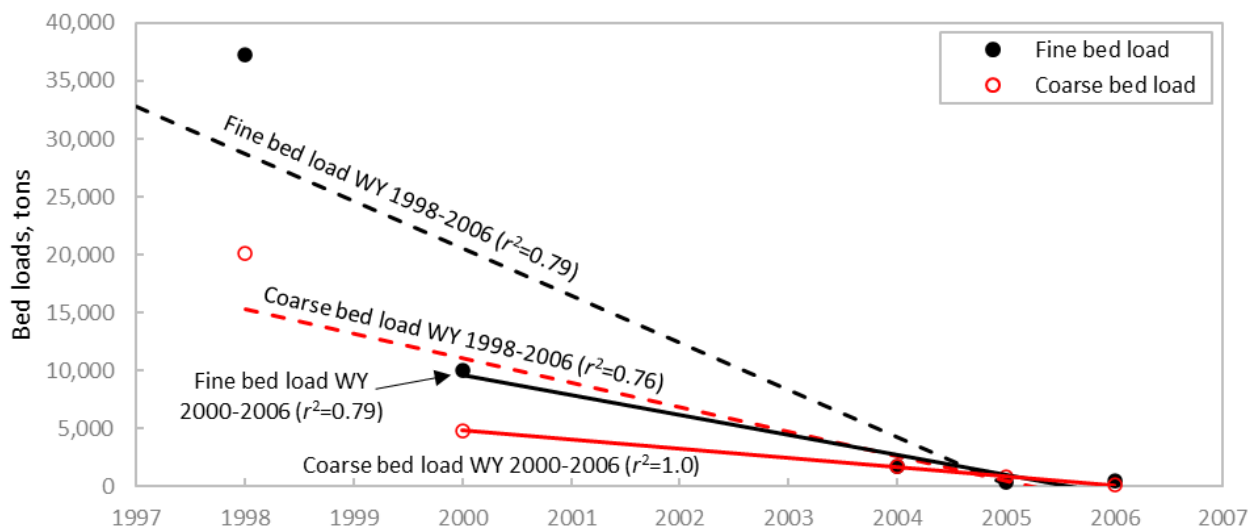


Figure 45. Annual fine and coarse bed loads estimated with measured transport rates on Indian Creek for WY 1998–2006, excluding WY 2001–2003. The lines are linear functions for the indicated periods.

#### 5.4.2 Grain-size distributions for bed load

Bed load sampled from Indian Creek between December 1996 and May 2006 exhibited a bimodal size distribution in half of the samples ( $n=62$ ), and sieve analysis of the sampled material provides conflicting evidence on the direction of change in transport of fine sediments (Figure 45). Evidence suggesting a decrease in fine bed load includes a slight increase in the diameter of the  $D_{84}$  and  $D_{50}$  (Figure 46a) despite the average proportion of fine sediment in bed load samples remaining essentially constant at an average of 79% (Figure 46b). In comparison, the average percentage of fine sediment in bed load samples on Rush Creek was 75%. These differences in the proportion of fines in bed load samples agrees with the slightly finer distribution of bed material sampled from Indian than Rush Creek delta (see Figure 36). Due to the slight increase in the coarse tail of the bed load size distributions and the essentially constant proportion of fine sediment in the samples, sorting decreased in this period (Figure 46c). However, a positive linear slope of skewness through time provides some evidence that reductions in fine sediment may not have occurred in this ten-year period on Indian Creek (Figure 46d).

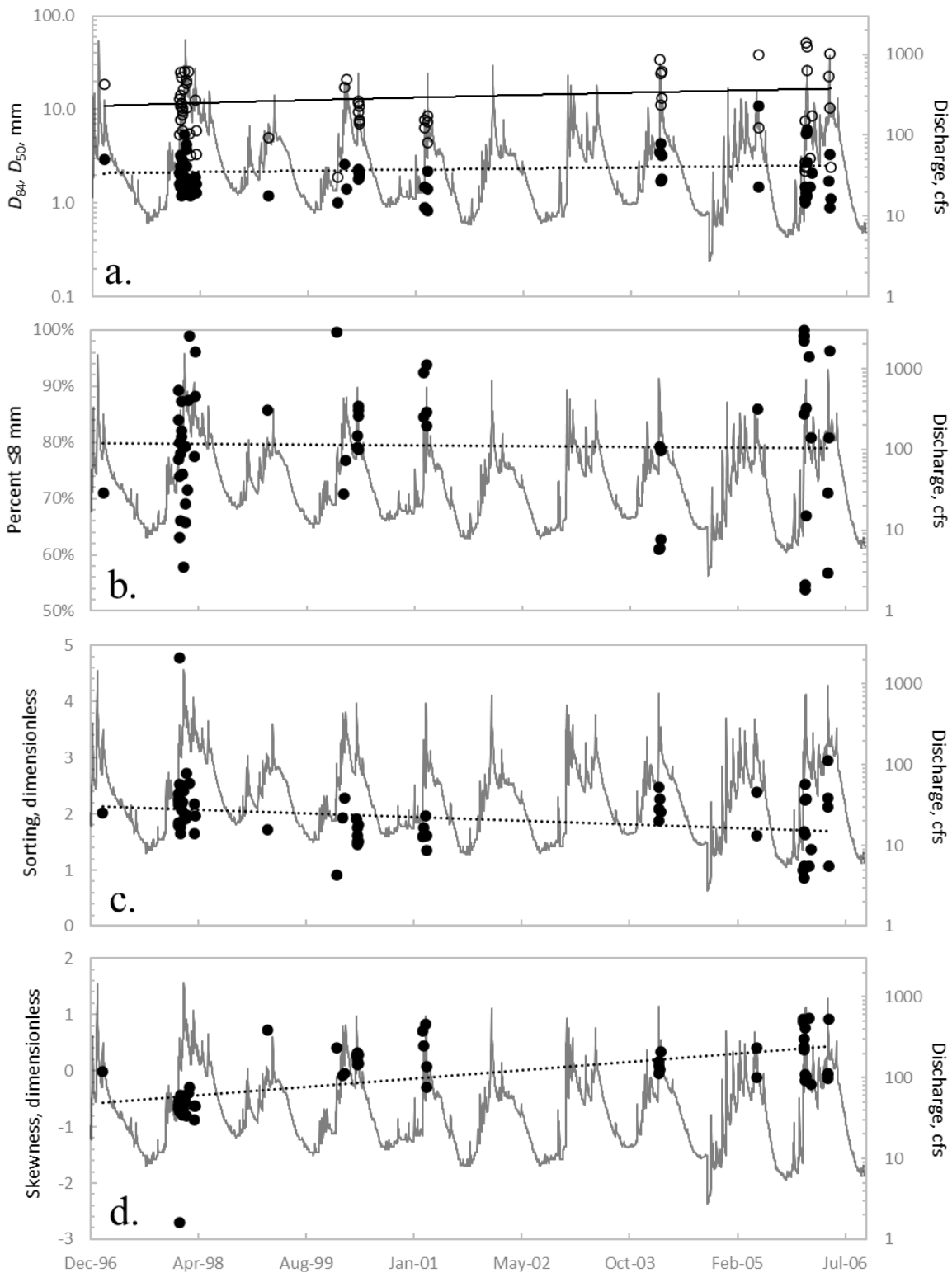


Figure 46. Daily average flows plotted with  $D_{84}$  (open symbols) and median grain diameters ( $D_{50}$  (closed symbols; a.), percent of total bed load samples (by weight)  $\leq 8$  mm in diameter (b.), and sorting (c.) and skewness (d.) parameters for bed load sampled on Indian Creek December 1996–May 2006. Higher skewness indicates a larger proportion of fines. The solid line for  $D_{84}$  and dotted lines are linear regressions of the respective grain size data, with the solid line in (a.) for  $D_{84}$ .

### 5.4.3 Indian Creek delta

A bulk sediment sample weighing 16,846 kg was taken from the Indian Creek delta November 2002 to estimate the grain-size distribution of delta material. A subsample of this material weighing 381 kg was dry sieved and the size distribution indicated that fines ( $\leq 8$  mm) composed 30% of the material (see Figure 36). Again assuming gravel beds exhibit 20-30% void space (Carling and Reader, 1982; Milhous, 2001; Wilcock and Kenworthy, 2002), the availability of fine sediment in the Indian Creek delta in 2002 was sufficient to fill voids and create a matrix supported bed. These beds exhibit substantially lower permeability and intergravel flow than beds that are framework supported. Therefore, a lower proportion of Indian Creek flow would percolate into the bed and release as cold water at the interface with the mainstem channel. This expectation aligns with the linear regression of fines in bed load samples indicating percentage have averaged 80% between 1996 and 2006 and skewness of bed load samples indicating an increasing proportion of fines in this period. Since 2006, it is unclear how the fine sediment composition of delta sediments has changed because bulk samples of this material have not been collected and analyzed.

## 6. Fine sediment in the Trinity River

### 6.1 Summary of fine sediment storage

Restoration flow releases from Lewiston Dam, mechanical rehabilitation of channel and floodplain areas and removal of fine sediment berms (Section 3.3.1), and sediment capture by Hamilton Ponds on Grass Valley Creek (Section 5.3.1) are likely the principal causes for the observed decrease in storage of fine sediments in the Trinity River (Section 7.0). Consequently, bulk samples of streambed sediments show a strong decrease in fine sediment storage on and in the channel bed through time (Section 6.1.2), and most stations currently meet the majority or all fine sediment targets and several stations appear to be in deficit of fine sediment (Section 7). The shortage of fine sediments is particularly strong upstream of Rush Creek and downstream of Steiner Flat (RM 92.0), where percentages of fine sediments in the surface domain are consistently  $<10\%$  and in the subsurface domain  $<30\%$ . Low percentages of fines upstream of Rush Creek at least partly responsible for the long residency and short distances of travel for coarse gravel added to the channel in this reach (see Gaeuman, 2020; Wilcock and Kenworthy, 2002). Concomitant increases in framework particle sizes (Section 6.1.2) have occurred with reduction in fines and restoration of the gravel-bed channel of the Trinity River (Section 3.3.7). Despite coarsening of the bed, incipient threshold for coarse grains have decreased at the sediment monitoring station at Douglas City (Section 6.2.1) potentially due to dilation and loosening of the bed from lack of fines in interstitial spaces between large particles that would increase intergranular friction, if fine sediment were more available (Yager et al., 2018).

#### 6.1.1 Pools

Fine sediments that exceed the storage capacity of voids in the coarse framework of a gravel stream bed may be entrained and transported to pools for transient storage during low flow periods of the year (e.g., Lisle and Hilton, 1999). If sufficiently present, fines can reduce pool depths and volumes and subject larger pool areas to flow turbulence that can reduce temperature stratification and holding habitat for spring Chinook. Gaeuman and Krause (2013) and Gaeuman (2020) differentiated changes in pool bathymetries that were measured during summer baseflow in the Trinity River in 2009, 2011, and 2016 and concluded that depths either remained

unchanged or increased in most pools in the restoration reach between these years. The cause(s) for depth increases was not identified by the authors, but likely varied between pools and included scour by high flows, increased height of hydraulic controls, or reduced fine sediment storage in pool bottoms. In some cases, pool depths decreased, and these occurrences were attributed to mechanical lowering of nearby terraces reducing the competence of flow in combination with nearby additions of gravel to the channel, not increased storage of fines. Anecdotally, these results suggest that storage of fine sediments in pools during low flow periods have remained low and not appreciably changed since 2009, which contrasts with pools filling with fines within days of being dredged in the 1970s (Section 3.3.5).

### 6.1.2 Streambed

Wolman (1954) samples taken before and after spring flow releases at sediment transport monitoring locations at TRAL (RM 110.2), TRLG (RM 98.8), and TRDC (RM 92.7) from 2006 through 2019 indicate that percentages of fine sediment on the bed surface varied widely, exhibited decreasing trends, and were typically lowered by spring flow releases (Figure 47). Causes for wide annual variations in percent fines are unclear but could result from scour of fines from subsurface areas of the streambed or fine sediment inputs from tributaries or floodplain areas. Decreasing trends in fine sediment on the bed surface at these stations reflects that spring flow releases apparently mobilize greater volumes of fine sediment than are delivered to the channel by tributaries between high spring flows events, which is an objective of restoration flow releases. The resulting dynamic involves storage of fine sediments delivered by tributaries to the mainstem channel through winter until spring high flow releases from Lewiston Dam transport them downstream. This temporal storage of fine sediments occurs during the egg incubation period for juvenile salmonids and can have strong negative impacts to fish production in the Trinity River, as previously mentioned (Section 4.1).

On the bed surface at TRAL and TRDC, trends in framework ( $D_{84}$ ) and median particle sizes ( $D_{50}$ ; Figure 48) and sorting coefficients (Figure 49) are largely as can be expected from reductions in fines in the Trinity River. Specifically, at these stations, median grain sizes are increasing, trends in the  $D_{84}$  are mostly flat, and the  $D_{16}$  is increasing. Less difference in size between the  $D_{84}$  and  $D_{16}$  is responsible for increased sorting at these stations. For example, on the bed at TRLG, grain size adjustments that have occurred between 2006 and 2017 include a 46% reduction in the  $D_{84}$  from around 117 mm in 2006 to 64 mm in 2019 and a 35% increase in particle sorting from 2.3 to 1.7 (lower values indicate improved sorting; Figure 49) due to increases in the  $D_{16}$  particle diameter, from 16.0 to 23.0 mm in 2006–2019 (Figure 48). With a larger decrease in the diameter of the  $D_{84}$  (linear slope -3.1) through time than increase in the  $D_{16}$  (linear slope 0.6), the slope of the linear trend in the  $D_{50}$  was -1.3, which represents an overall fining of the bed despite the reduction in grains  $\leq 8$  mm on the bed at this site (Figures 46-47).

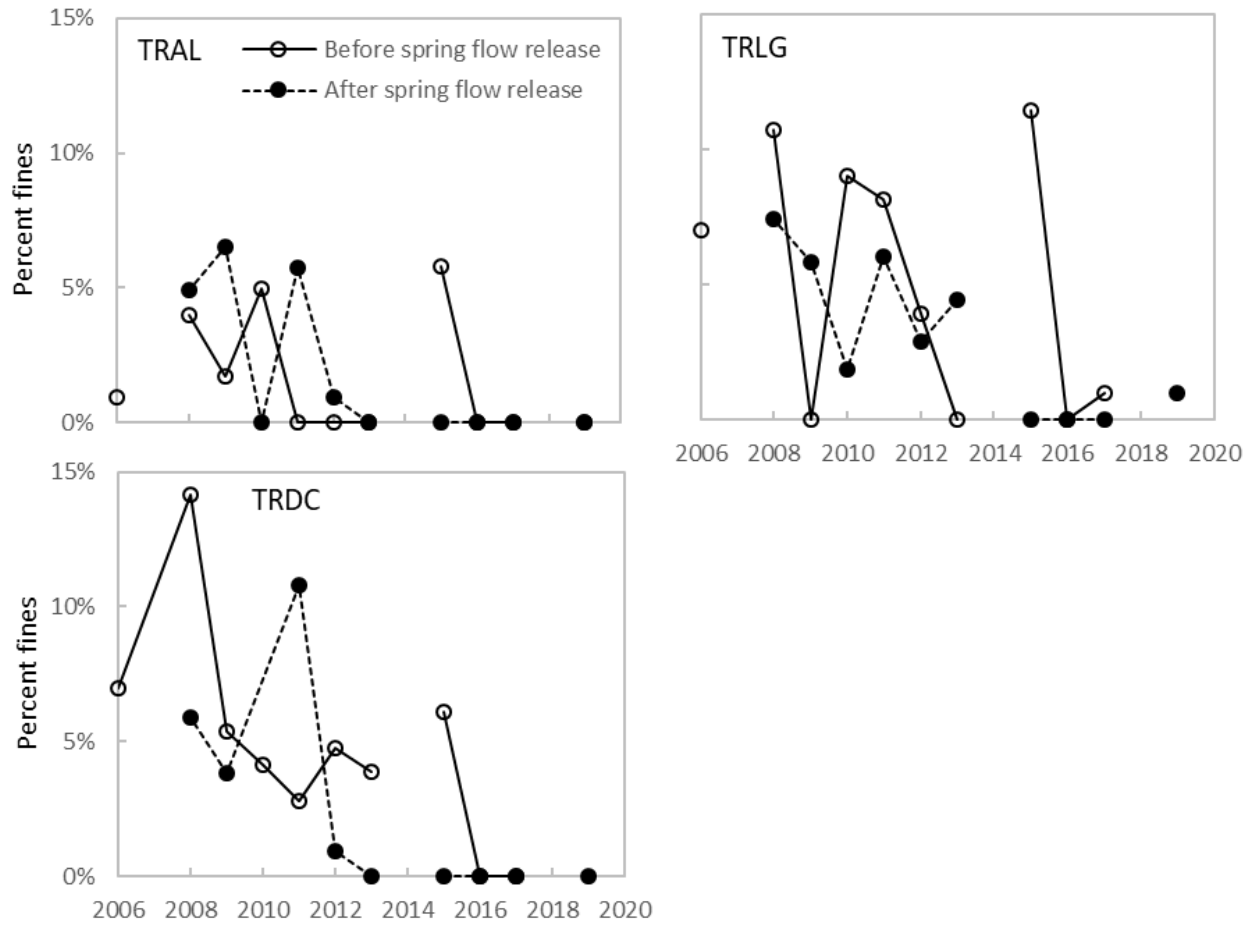


Figure 47. Percentages of fine sediment ( $\leq 8$  mm) in Wolman (1954) samples taken at sediment monitoring stations at TRAL, TRLG, and TRDC in 2006–2019. Samples were not taken after the 2006 flow release for an unknown reason and no samples were taken in the dry water year in 2007 and the critically dry water year in 2014. Lines connect percentages of fines for contiguous years.

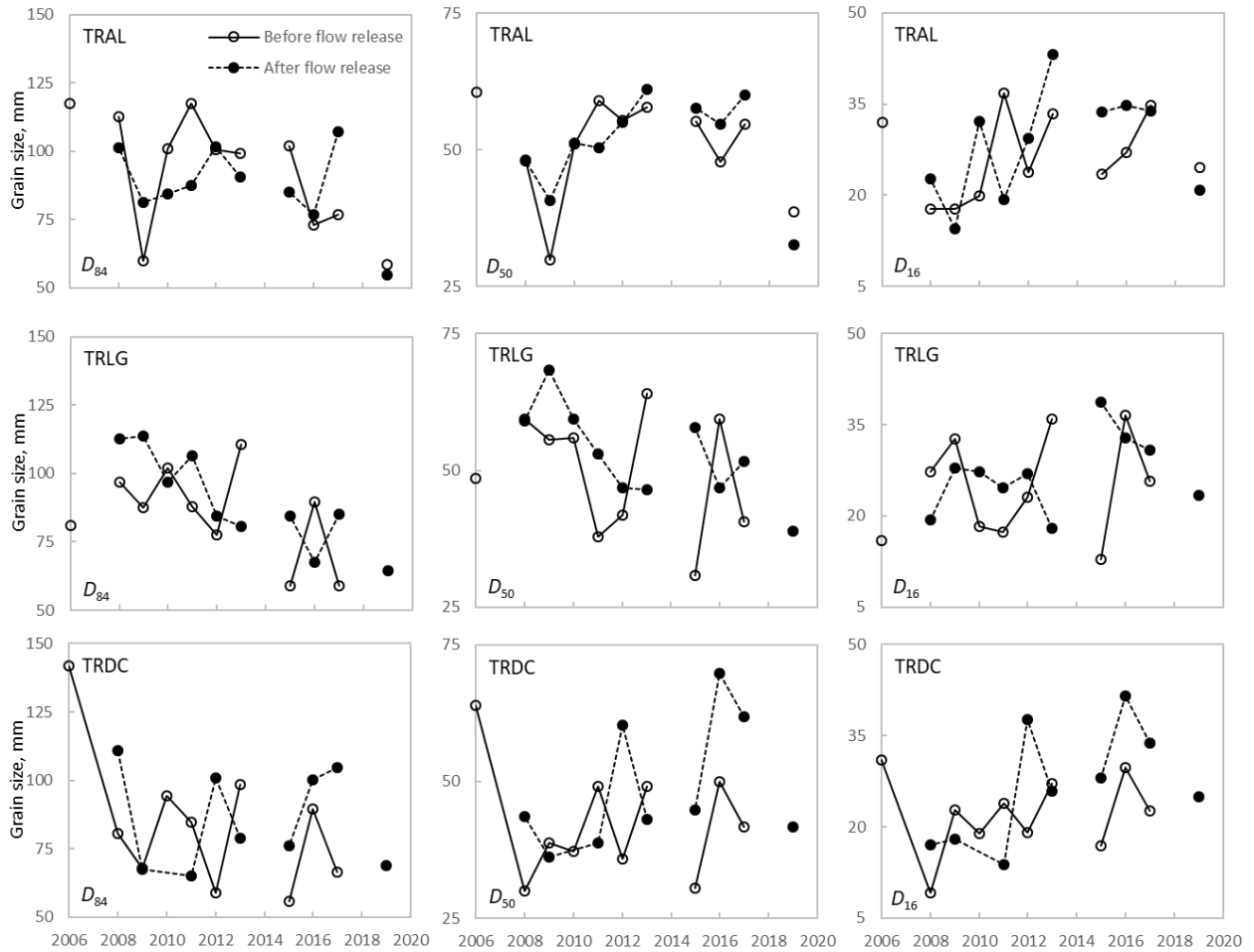


Figure 48. Diameters of framework particles ( $D_{84}$ ), median grains ( $D_{50}$ ) and the 16th percentile of grain-size distributions ( $D_{16}$ ) from Wolman (1954) samples taken before and after spring flow releases at TRAL, TRLG, and TRDC from WY 2006–2019. Lines connect grain sizes for contiguous years.

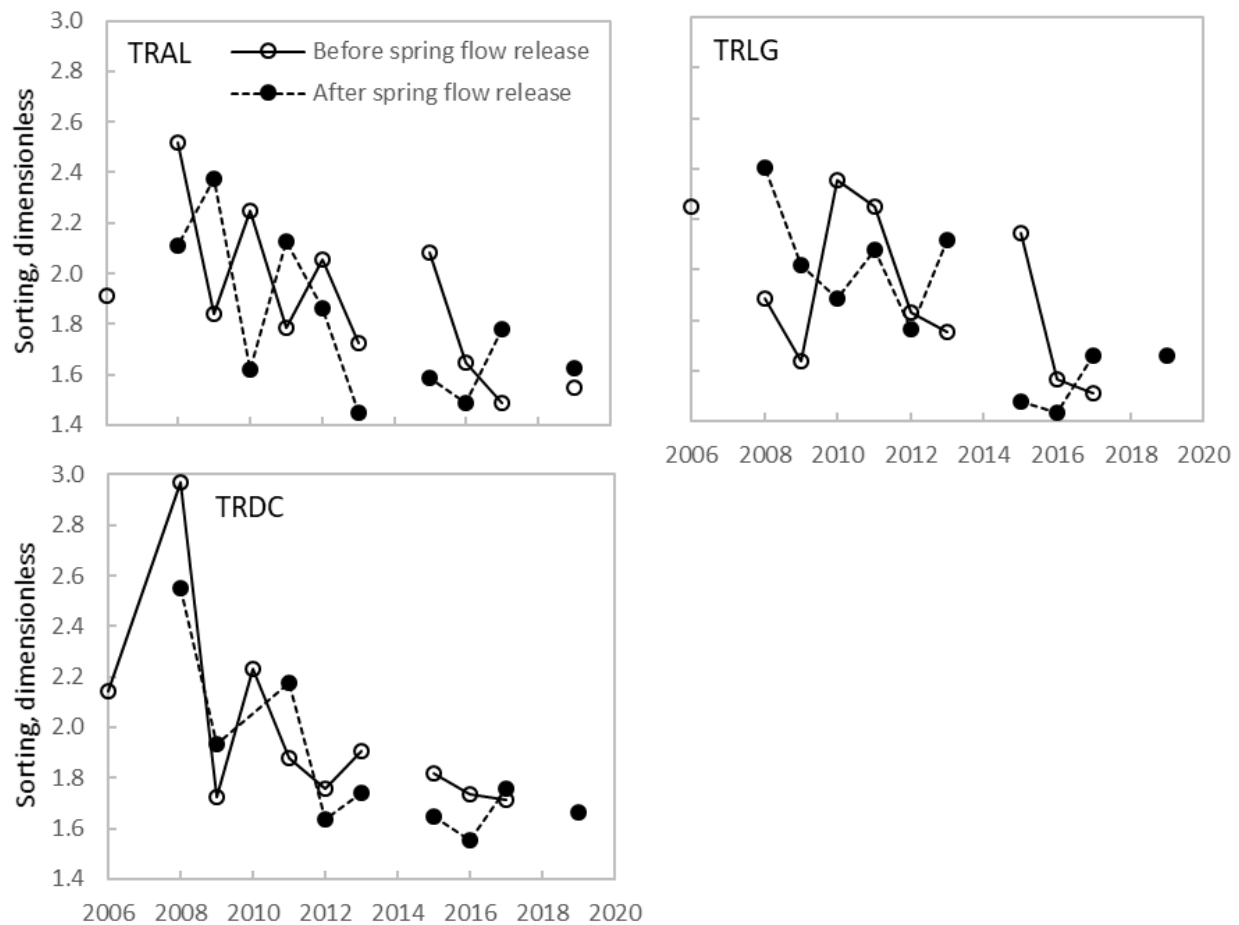


Figure 49. Sorting coefficients computed as  $(D_{84}/D_{16})^{0.5}$  for Wolman (1954) samples were taken at TRAL, TRLG, and TRDC in 2006–2019. Lower values indicate improved sorting. Lines connect sorting values for contiguous years.

Bulk sampling indicates the percentage of fines in the active layer and subsurface domain have notably decreased at most stations since as early as 1991 or 2001 (Figure 50; also GMA, 2010 and 2020b). The largest decrease in percent fines occurred at Poker Bar (RM 102.7), where fines in the active layer lowered from 17% to 11% and subsurface fines from 69% to 25%. The improvement is certainly most attributed to restoration flow releases and sediment capture by Hamilton Ponds on Grass Valley Creek (Sections 3.3.7 and 5.3.1). Notable decreases in fines also occurred at Steel Bridge (RM 99.0; subsurface 58% to 27%; active layer 22% to 6%), Evans Bar (RM 84.1; 40% to 23%; 6% to 4%), near Indian Creek (RM 95.3; 48% to 35%; 5% to 6%), and at Rush Creek (RM 107.4; 34% to 33%; 25% to 8%). However, percent fines only moderately lowered at Junction City (RM 80.3; 30% to 29%; 2% to 3%) and increased between sampling locations at Lewiston (RM 110.2) and Rush Creek, the first major tributary below Lewiston Dam. Sample locations at Steel Bridge and upper Steiner Flat are respectively within 0.1 river miles of sediment transport monitoring at TRLG and TRDC, and decreased fines indicated by bulk samples (Figure 50) generally reflect the same in Wolman (1954) samples taken before and after transport monitoring at these stations (see Figure 47). Variation in percent fines in the active layer and subsurface domains between samples was notable at Junction City and Upper Steiner Flat, and in the subsurface domain at Lewiston. The relatively high percentage

in 2008 at Lewiston resulted from channel reconstruction projects that occurred on 132 acres of the river corridor upstream of this location. The high value in 2019 resulted from an influx of fines from Deadwood Creek after the Carr fire.

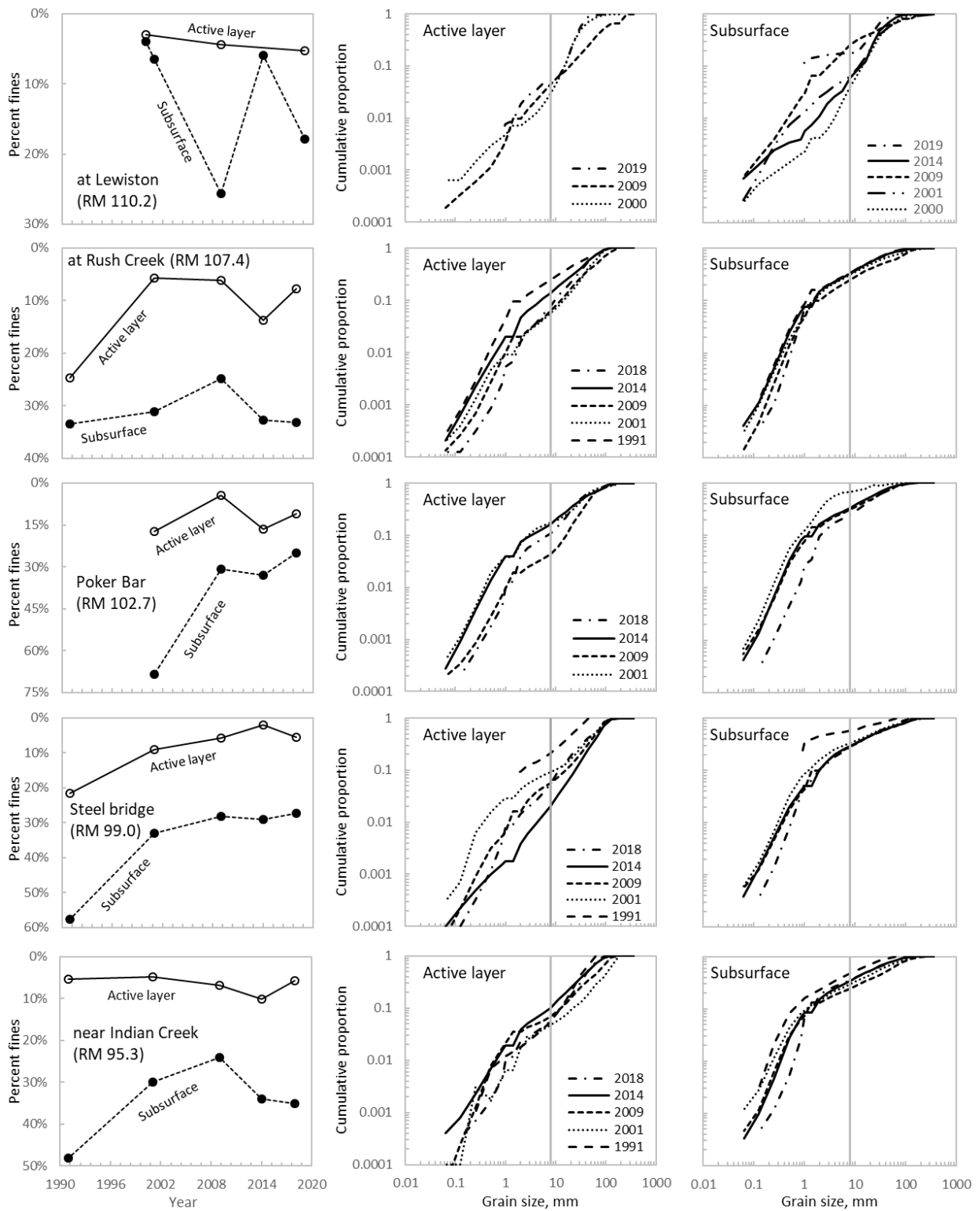


Figure 50. (continued)

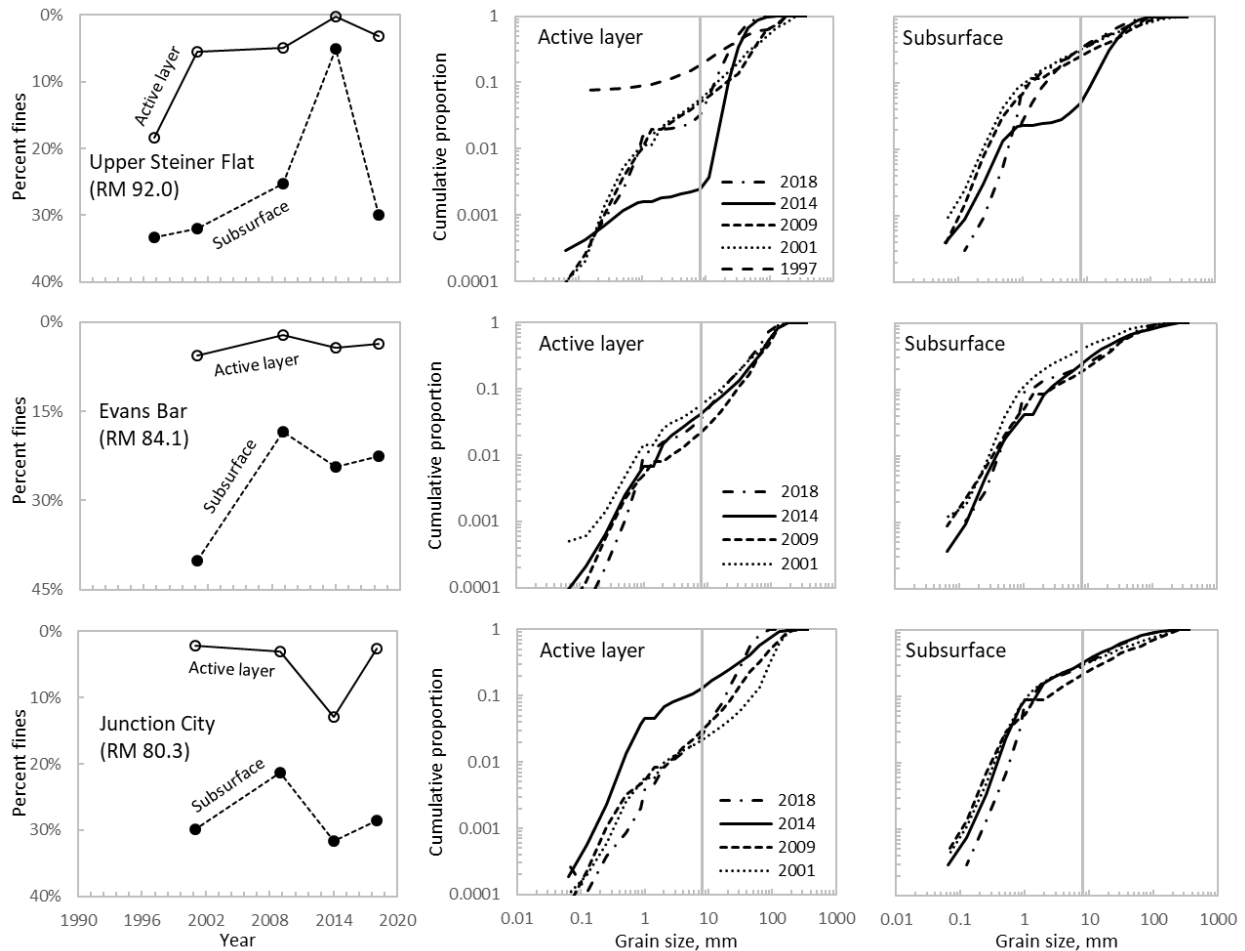


Figure 50. Percent fines and grain-size distributions from bulk samples of the streambed surface and subsurface domain at stations on the Trinity River. River miles (RM) are the distance upstream from the confluence of the Trinity and Klamath Rivers, and Lewiston.

## 6.2 Sediment transport

Suspended sediment and bed load transport have been measured at stations on the Trinity River at Lewiston (TRAL), above Grass Valley Creek (TRGV), TRLG, and TRDC during spring flow releases in WY 2004–2019 (Appendix D-H). An exception is that sediment transport was not monitored in 2014 and 2018 because flows were too low to significantly mobilize the bed in these critically dry water years. Data from TRGV are not considered in the current paper because loads at this station are directly affected by gravel augmentations that occur most years at a location 250 ft upstream of this monitoring station. At all other sites, daily suspended and bed loads are summarized as computed by Graham Mathews and Associates (e.g., GMA, 2020a) for the April 1–July 31 period (Appendix F and H; Section 6.2.5.1). Total annual load estimates for 2006–2019 are then computed in Section 6.2.5.3 by adding the GMA loads to daily loads that result when thresholds for grain mobility (Section 6.2.1) are exceeded outside the aforementioned period (Section 6.2.5.2). Total loads are not estimated for 2004 and 2005 because data for stress partitioning needed for the threshold analysis were not measured these years. Thresholds analyses enables the influence of fine sediment availability on grain mobility

and hiding function exponents to be evaluated. Source domains for bed load were evaluated with ratios of the median surface grain size on the bed surface to the median bed load particle size. Finally, ratios of the fine sediment load to coarse bed loads for spring flow releases are used to assess how the relative contribution of these size classes to the total sediment load changed through time at TRAL, TRLG, and TRDC.

A note regarding fine bed load estimates by GMA is that grains <0.5 mm are not sampled in proportion to their availability for capture because mesh openings for sample bags used with the TR-11 samplers on the Trinity River are 0.5 mm. Therefore, until the sample bag's mesh partially clogs with fines and detritus, an unknown proportion of grains <0.5 mm that are transported in the bed load domain is not collected. Bed loads are therefore somewhat underestimated on the Trinity River.

### 6.2.1 Thresholds of mobility

Critical conditions for sediment mobility were estimated with the reference transport rate method as the discharge or basal shear stress that produces a low but measurable transport rate (Parker et al., 1982). The reference transport method involves extrapolating mass transport rates for grain-size fractions to a low dimensionless value,  $W_i^*$ , at which the critical condition is estimated

$$W_i^* = \frac{(\rho_s/\rho - 1)gq_{si}}{\rho_s u_*^3} \quad \text{Eqn. 5}$$

where  $u_*$  is shear velocity ( $\equiv(\tau_{\text{grain}}/\rho)^{0.5}$ ),  $\tau_{\text{grain}}$  is the shear stress that acts on the granular bed,  $\rho_s$  is the density of sediment (2,650 kg/m<sup>3</sup>),  $\rho$  is the density of water (1,000 kg/m<sup>3</sup>),  $g$  is gravitational acceleration (9.81 m/s<sup>2</sup>), and  $q_{si}$  is the mass transport rate for size fraction  $i$ . Numbers of bed load samples used in the threshold analyses were 408 at TRAL, 490 at TRLG, and 487 at TRDC. Calculating shear velocity requires partitioning  $\tau_{\text{grain}}$  from other forms of roughness in the flow, including stream banks, wood and vegetation, bedforms, and mobile grains. After Whiting and Dietrich (1990), we neglect stress borne by mobile sediment and use a formulation by Wilcock (2001) to estimate  $\tau_{\text{grain}}$  as

$$\tau_{\text{grain}} = 0.052\rho(gSD_{65})^{0.25}U^{1.5} \quad \text{Eqn. 6}$$

where  $S$  is the energy slope,  $D_{65}$  is the grain size that is coarser than 65% of particles on the bed, and  $U$  is the average cross-sectional flow velocity. Separate plots of  $W_i^*$  versus discharge and  $\tau_{\text{grain}}$  were extrapolated to  $W_i^* = 0.002$  (Parker et al., 1982) with power functions or lines of best fit drawn by eye to estimate critical discharges ( $Q_{ci}$ ) and shear stress ( $\tau_{ci}$ ) for size fraction  $i$ .

Energy slopes ( $S$ ) in equation (6) were measured during spring flow releases as the water surface slope through each sediment monitoring transect. The slopes were defined by water surface elevations measured from the top of metal fenceposts surveyed into a local benchmark at each site. Three to six fenceposts were located over a span of 362 to 2,278 ft (2.4–22.7 channel widths) with the monitoring transects located generally in the middle of these distances. Energy slopes through the transects were estimated with linear regressions of water surface elevation and channel distance using all points available (average  $r^2=0.94$ ). The resulting slopes were linearly regressed with their associated discharge published in the 15-minute flow record by the U.S. Geological Survey for TRAL, TRLG, and TRDC. An exception was the time of day that slope

measurements were taken in 2006 and 2007 was not recorded, so daily average flows were used instead. The  $r^2$  between discharge and slope averaged 0.72 for all stations and years.

A linear regression of water surface elevations measured at the nearest up- and downstream side of each monitoring transect was used to estimate the flow stage at the monitoring transect for each transport sample (an exception was stages were measured directly at the monitoring transect at TRLG in WYs 2010–2019). Stages were related by time to discharges in the 15-minute flow record to provide stage-discharge rating curves. These curves were used with a cross section survey of the channel performed shortly before each spring flow release, and flow areas were computed as a function of discharge for each transport measurement. Flow areas were divided by the associated discharges to determine the average cross-sectional flow velocity with the continuity equation. Flow velocities between channel banks are most appropriate for  $U$  in equation (6), and an option was to divide discharges by the flow area in the active portion of the channel, which neglects flow conveyance in vegetated floodplain areas. At TRLG, these calculations yielded flow velocities that were on average 8% higher (range 0-22% higher) than what results when the total cross section area of flow is used. A decision was therefore made to conservatively estimate values of  $\tau_{\text{grain}}$  with velocities computed with the total flow area. Flows were conveyed in the surveyed portion of the channel cross section all years at all stations except at TRLG in 2011, 2016, and 2017 and at TRDC in 2013 and 2017. In these years at TRLG, the cross sections were extended with elevations measured by LIDAR in 2011 to enable flow areas to be computed for all discharges (see Appendix E for cross section surveys for all stations). At TRDC, the affected cross sections were extended with the 2012 survey because the upper portion of the channel exhibited almost no elevation change between 2012 and 2016.

Values of  $D_{65}$  were estimated with Wolman (1954) pebble counts made prior to the spring flow releases for use in  $\tau_{\text{grain}}$  estimates in all years except 2006 at all stations and 2019 at TRLG and TRDC. In these cases, the  $D_{65}$  was set as the grain size measured after the spring flow release multiplied by the average ratio of the  $D_{65}$  sampled before and after the spring flows.

Representing bed roughness with the grain size measured at the start of the flow release neglects changes in grain roughness that occur during sediment transport events. This simplification was unavoidable lacking a method to estimate grain sizes for roughness calculations during high flows. This omission likely had little effect on the thresholds because grain size is only raised to the quarter power in equation (6).

Separate analyses were used to respectively determine  $Q_{ci}$  and  $\tau_{ci}$  for load computations outside spring flow releases on the Trinity River (Section 6.2.5.2) and for hiding function analyses (section 6.2.2). For annual estimates of  $Q_{ci}$ , fractional bed load samples were summed for fine ( $\leq 8$  mm) and coarse sediment ( $> 8$  mm) to estimate critical conditions for each size bin using all transport measurements for a particular year. Hiding function analyses considered bed load fractions ranging from 0.5 to 180 mm in half-phi increments ( $\text{phi} = -\log_2 D$ ). The largest sampled particles all years at all stations was in the 180 mm size class, so the upper size range of the bed load sampler (152 mm tall by 305 mm wide) was not limiting. The lower caliber of bed load was set by the 0.5 mm mesh size of the TR-2 sample bag, as previously mentioned. Collection of bed load particles in the 180 mm size bin was too infrequent to enable entrainment thresholds to be estimated for these sized grains, so analyses were limited to grains in the 0.5 to 128 mm size bins. For estimating fine sediment loads outside the spring flow release period on the Trinity River (April 1–July 31), critical conditions for suspended sediment ( $< 0.063$  mm and 0.063 to

<0.5 mm) and bed load ( $\geq 0.5$  to  $\leq 8$  mm) were considered. Particles  $\geq 5$  mm were excluded from the suspended loads to avoid double sampling that occurs for this grain size in the suspended and bed load domains that overlap within the height the TR-2 sampler extends above the bed.

Linear regressions of critical discharges for fine bed load ( $\leq 8$  mm) during spring flow releases trended strongly upward at TRDC, were largely flat at TRLG, and trended slightly downward at TRAL (Figure 50; Appendix G). A downward trend in critical flow indicates fines are increasingly available for transport and an upward trend (i.e., higher critical flows) shows fines are less available for transport through time. Both trends are sensitive to individual values. For example, prior to WY 2019 at TRAL, fine sediments were relatively scarce (Figure 51) and the slope ( $m$ ) of the trend in critical flow was upward ( $m=15.5$ ) before a large input of fine sediment from Deadwood Creek in WY 2019 (see Figure 25) elevated the availability of fines and reversed the trend to  $m=-21.3$ . The increased availability of fines at TRAL in WY 2009 from channel reconstruction and in 2019 from the Carr Fire was apparently enough to also significantly lower critical flows for coarse grains in the reach (Figure 51), in agreement with observations of fine sediment effects on coarse grain mobility by Wilcock and Kenworthy (2002) and others. These results suggest augmentations of fine sediment in the Lewiston reach that are on the order of the contribution of fines by the forementioned sources may be necessary to aide disbursement of gravel additions made in the reach (Gaeuman, 2020). The results also suggest that adding fine sediment to the channel could help restore coarse grain mobility to levels observed at Douglas City, where the coarse sediment budget is assumed unaffected by Trinity and Lewiston Dams and thus natural for the contemporary Trinity River. Such restorative actions are warranted in part from consideration that even with the increased supply of fine sediment in WY 2019, linear regressions indicate that median particle sizes and skewness of bed load size distributions increased and percentages of fine sediment substantially lowered in the period of record (Figure 52), reflecting the decrease in fines in the Trinity River restoration reach since implementation of the ROD (2000). Indeed, the average critical discharge for fines at TRAL (3,554 cfs) between WY 2006 and 2019 is more than 12-times higher than the critical discharge (<300 cfs; Denton, 1980) observed near this location in 1979.

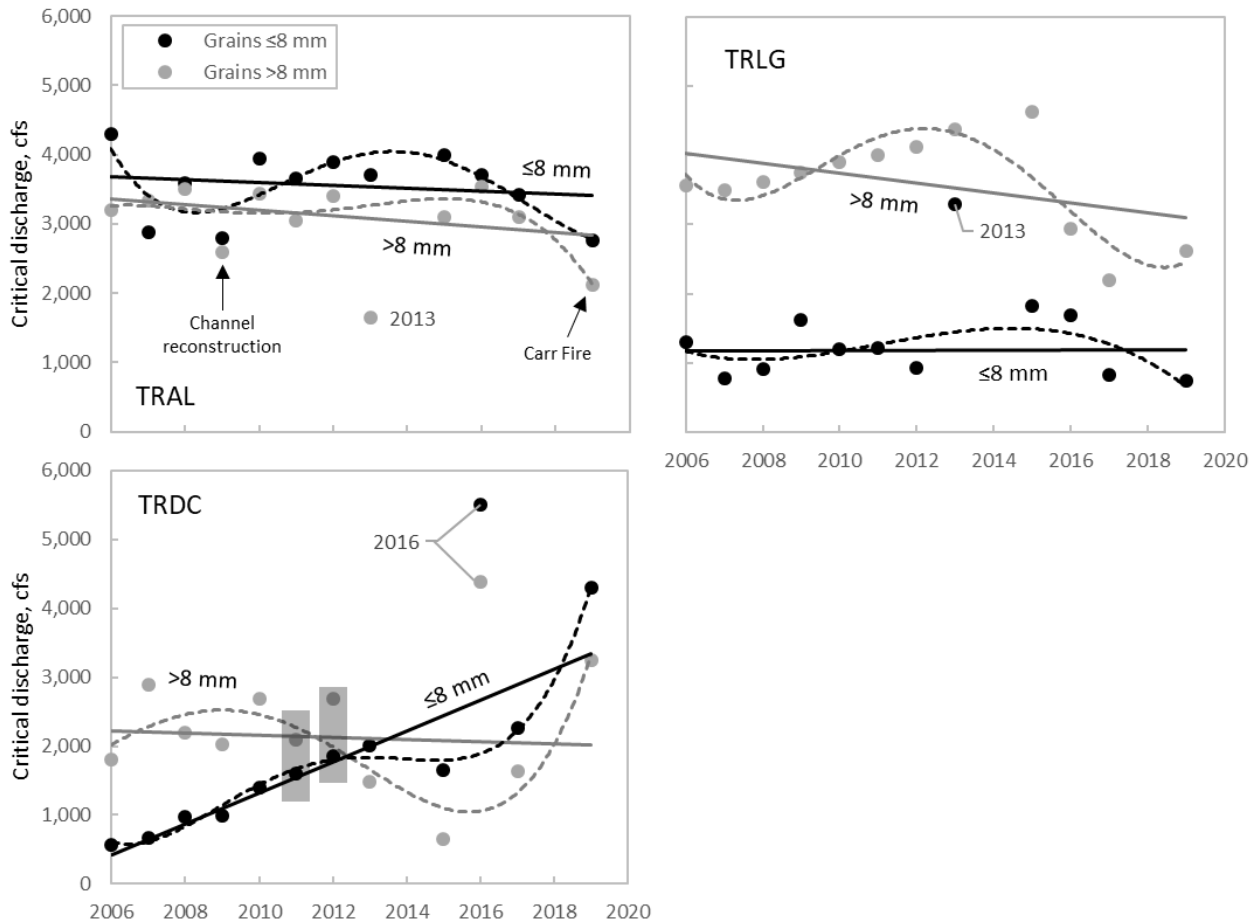


Figure 51. Critical discharges for fine and coarse bed load in WY 2006–2019. Dotted lines are 4<sup>th</sup> order polynomials that generalize temporal variations in critical discharge and solid lines are linear functions fit by least squares to show overall trends in the data. Outliers not included in either curve are labeled by water year as are critical values for TRAL affected by channel reconstruction and the Carr Fire. Boxes at TRDC indicate years the station location was changed.

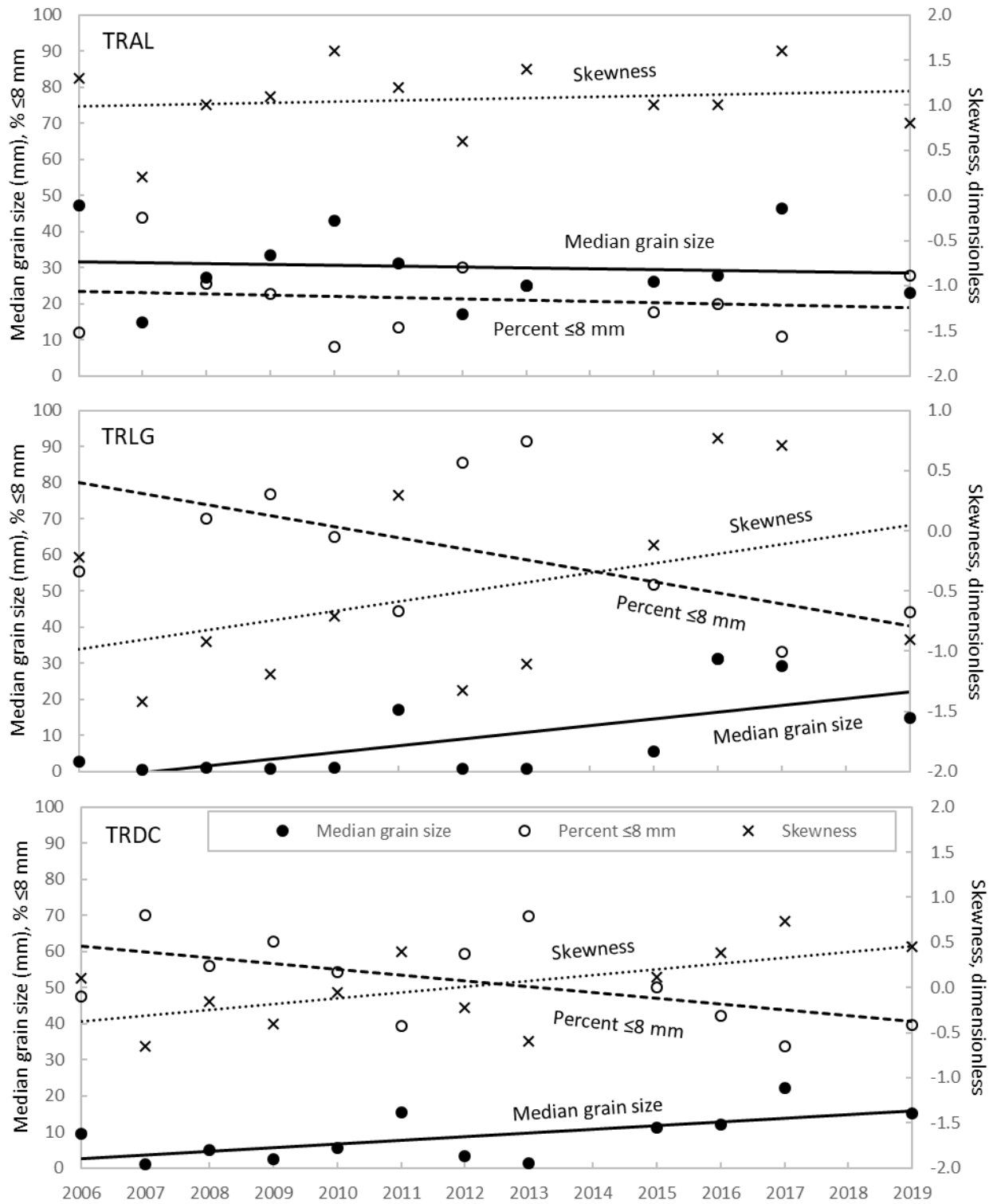


Figure 52. Median grain size, skewness, and percentage of fine sediment ( $\leq 8$  mm) in bed load sampled at TRAL, TRLG, and TRDC. Higher skewness indicates a coarser distribution of particle sizes. The straight lines are least squares regressions of each parameter.

Tributary input of sediment to the Trinity River increases the availability of fines with distance from Lewiston Dam, which causes the average  $Q_{ci}$  for fines in the period of record to decrease from 3,554 cfs at TRAL to 1,187 cfs at TRLG and 1,661 cfs at TRDC (Figure 51). In WY 2019, the critical discharge for fine sediment at TRDC (4,309 cfs) exceeded that for TRAL (2,754 cfs) for the first time. Lessened mobility of fines (i.e., higher critical flows) at TRDC and predominantly also at TRAL has resulted from a reduced supply limiting their availability for transport. A hypothesis is that supply limitations have resulted from restoration activities in tributary watersheds, Hamilton ponds reducing delivery of fines to the Trinity River, and the effectiveness of spring flow releases transporting fine sediment at rates that exceed the supply from tributaries, as mentioned before. Under supply limitations, fine sediments winnow from interstitial spaces between coarse grains, which promotes armor layer development (increased surface coarseness and active layer depth; Figure 53) and increases grain protrusion (Kirchner et al., 1990). As coarse grains extend further into the flow, turbulence and shear stress acting on the bed between them declines because the mixing layer does not reach the high friction areas where fine sediments are stored in interstitial spaces (Raus et al., 2019). Alternatively, where fines are transport limited and abundant, interstitial spaces are filled by them and the bed is smoothed, which leads to increased shear stress and turbulence intensity because the lowered roughness promotes higher flow velocities to interact with the bed. With spheres in a flume, Grams and Wilcock (2014) measured a transition between when a coarse bed is starved of fines versus supplied abundant fines occurred when ~40% of the radius of spheres ( $R$ ) protruded ( $k$ ) into the flow, as opposed to the respective 60% and 20% protrusion states ( $P=k/R \times 100\%$ ) for the supply limited versus transport limited conditions described above (Grams and Wilcock, 2014). For comparison, I measured  $P$  for 487 randomly selected grains on a lateral bar near TRDC between discharge peaks in the WY 2019 spring flow release. The non-spherical particles were typically aligned with their short axis normal to the bed, so  $R$  was the shortest axis of the grain and  $k$  was measured following Yager et al. (2018) from the grain top to the average bed elevation immediately downstream of each grain. The average  $P$  was 39% suggesting armor layer development near TRDC reflects a supply limitation in fine sediment, which helps explain why critical discharges are higher for smaller sediments than coarse grains at this station.



Figure 53. Lateral bar 0.3 miles upstream of TRDC with the armor layer removed in a patch (circled) to show fine sediment that is sheltered in the subsurface domain. Photograph dated March 10, 2020.

Numerous interannual shifts in trends in fine and coarse sediment mobility thresholds have occurred at TRAL, TRLG, and TRDC (see Figure 50). In addition to the stochasticity of sediment transport and variations in sediment supply, a reason for the shifts may be tributary driven flow events that occur between high spring flow releases from Lewiston Dam. In fact, changes in trends in critical flows estimated for fine and coarse sediment correlate with discharges outside spring flow releases exceeding annual thresholds in respectively all, most, or almost no events at TRDC (6 for fine sediment, 2 for coarse sediment), TRLG (4 of 4, 1 of 2), and TRAL (0 for 7, 1 for 4) for 2007–2019 (2006 is excluded because critical flows are not available in a prior year for comparison). The exceedance for coarse sediment was greatest in terms of percentage that critical flows were exceeded outside the spring flow period at TRDC in WY 2015 (413%; peak flow 3,370 cfs v. critical flow 657 cfs) and at TRLG for fine sediment in WY 2019 (403%; peak flow 3,760 cfs v. critical flow 747 cfs). The largest exceedance occurred at TRDC in WY 2019 (Figure 54), which apparently caused transport in the main channel to exceed the supply of fine sediment delivered by the tributary-driven flows, causing thresholds for coarse and fine in spring to dramatically increase this year. The record-high entrainment thresholds estimated at TRDC in WY 2019 were corroborated by the sediment sampling crew at this site noting that mobile sediment was not available for transport until around the critical discharges estimated in this paper (see Figure 51).

An additional reason for some of the shifts could be channel reconstruction work that occurred near the sediment transport monitoring sites. For example, threshold estimates for fine and coarse sediment the first year after work in the Lewiston reach (2009) decreased to the second lowest in the period of record at 2,800 cfs for fine and 2,590 cfs for coarse sediment, with the lowest occurring in WY 2019 (2,754 cfs for fines, 2,119 cfs for coarse sediment; see Figure 50).

Relative to TRLG and TRLG, entrainment thresholds for fine and coarse sediments are in a relatively narrow range at TRAL likely due to the consistent low availability of fine sediment and gravel augmentations that generally match the volume of coarse material exported from the reach. The augmentations have largely maintained the exposed area of bars at levels that formed the first year after construction in 2008 (Figure 55). At Limekiln Gulch in 2015, channel reconstruction work mostly involved side-channel construction and floodplain lowering. The following spring, critical flow for coarse sediment significantly decreased for an unknown reason given the work would likely have resulted in sediment storage rather than recruitment to the channel. Finally, at Douglas City, work in 2013 and 2015 involved mid-channel bar construction, meander building, and floodplain lowering at locations 4,600 ft and 7,600 ft upstream of TRDC. This almost certainly influenced local transport conditions that may have been mitigated by sediment from Weaver and Reading creeks, making it unclear whether the decrease in thresholds in 2015 (the first year that transport was monitored at this station after 2013) and extreme outliers in 2016 were affected by this work. Changes in the location of TRDC could have also influenced threshold estimates at this station. Relocation of TRDC from its position in WY 2004–2010 to a new site 1,245 ft upstream occurred in WY 2011, and then another move 200 ft downstream to the current site the following year is reflected in changes in cross sectional geometry where samples were taken and therefore also hydraulics affecting transport through the stations (Appendix D and E). However, no discernible effect of these relocations is apparent in the critical discharge estimates (see Figure 50).

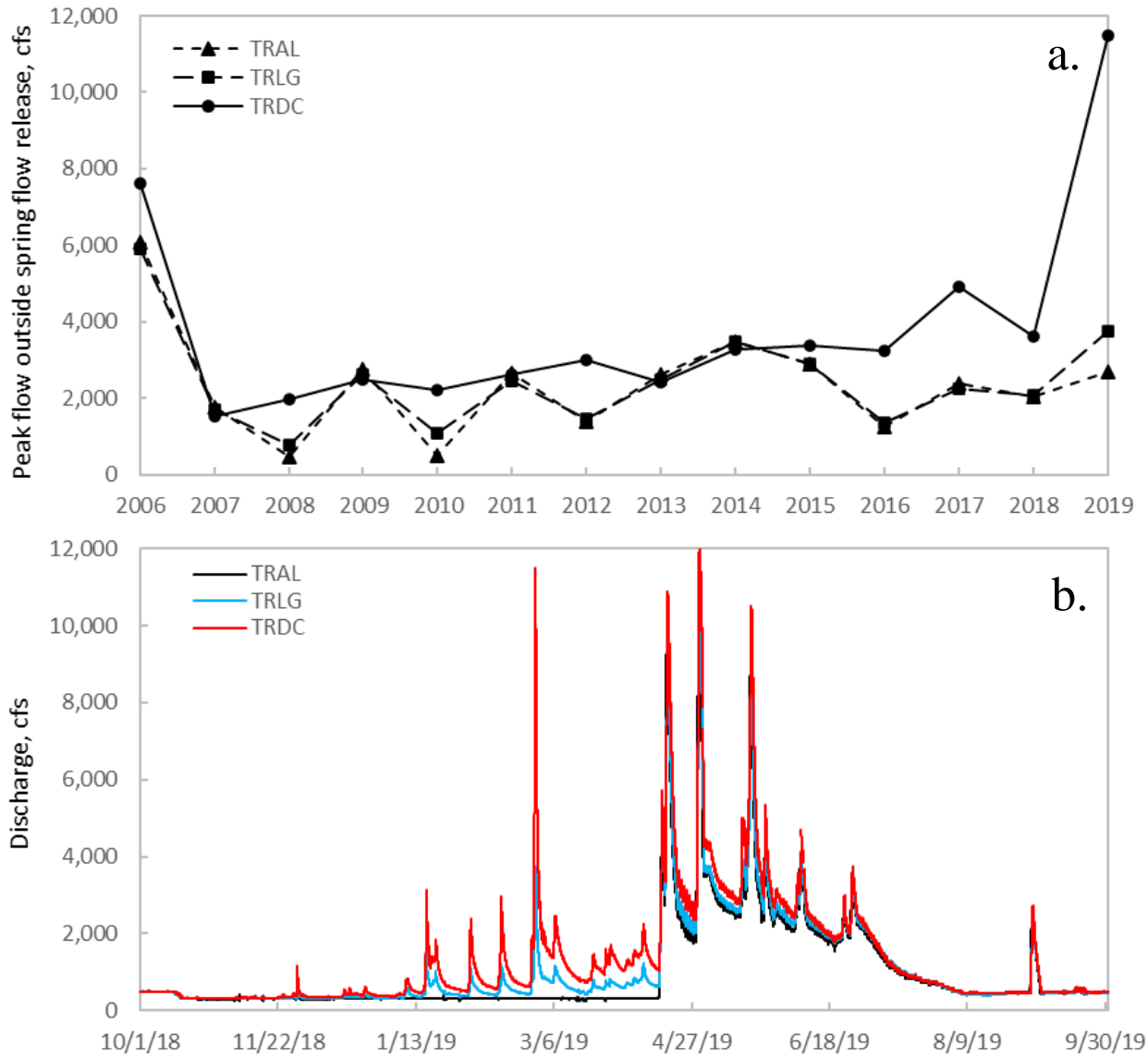


Figure 54. Peak discharges that occurred outside the spring flow season at TRAL, TRLG, and TRDC (a.) and WY 2019 discharges showing winter flows experienced at these stations this year (b.).

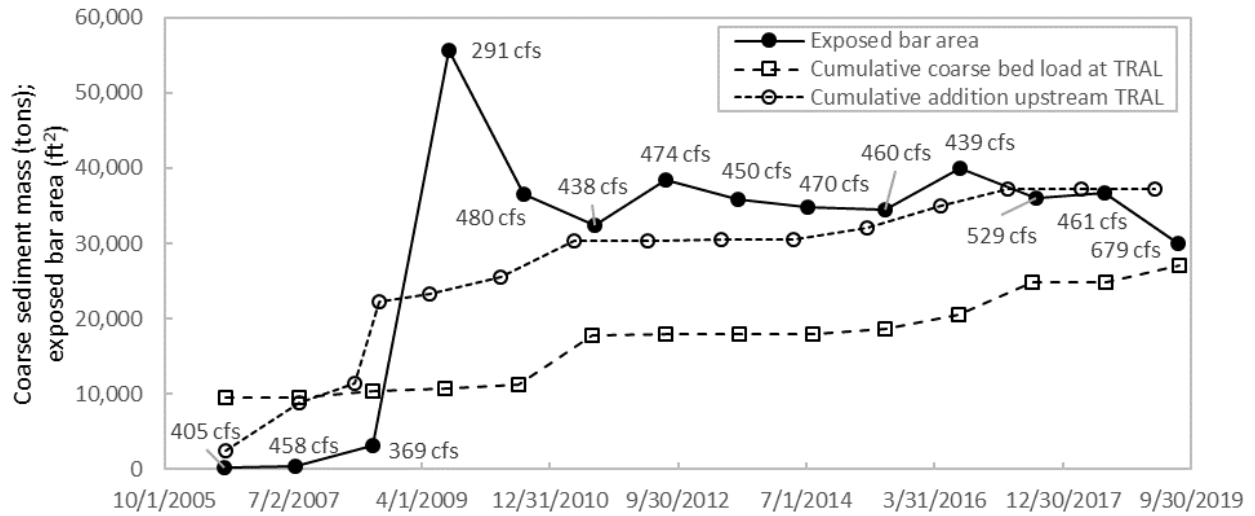


Figure 55. Cumulative addition of coarse sediment to the channel upstream of TRAL and transported from the reach by spring flow releases. Exposed bar areas are shown labeled with flows at which they were measured from aerial photographs within 17 channel widths (2,300 ft) upstream of TRAL.

### 6.2.2. Hiding effects and Shields stresses

A hiding function (Parker et al., 1982) was used to evaluate the combined effects of grain resistance and projection (Kirchner et al., 1990) on the relative mobility of grain-size fractions in the Trinity River

$$\tau_{ci}^* = \tau_{c50}^* \left( \frac{D_i}{D_{50}} \right)^b \quad \text{Eqn. 7}$$

where  $\tau_{c50}^*$  is the critical Shields stresses for the median grain size ( $D_{50}$ ) and  $\tau_{ci}^*$  is the critical dimensionless Shields stress, given by

$$\tau_{ci}^* = \frac{\tau_{ci}}{(\rho_s - \rho)gD_i} \quad \text{Eqn. 8}$$

with  $D_i$  defined as the lower size limit of size fraction  $i$  (Shields, 1936). As demonstrated by Shields (1936) and many others since, values of  $\tau_{c50}^*$  vary with the critical boundary Reynolds number, given by

$$Re_c^* = \frac{u_c^* D_{50}}{\nu} \quad \text{Eqn. 9}$$

where  $u_c^*$  is the critical shear velocity for  $\tau_{c50}^*$  ( $\equiv \sqrt{\tau_c/\rho}$ ) and  $\nu$  is the kinematic viscosity of water. Plotted values of  $\tau_{c50}^*$  versus  $Re_c^*$  follow the well-known Shields curve, albeit with substantially variability around the curve that results from several factors that are discussed further below. The exponent ( $b$ ) in equation (7) typically ranges between 0 and -1. A value of 0 represents purely weight-driven transport in which fine grains move before coarse sediment (i.e.,

size-selective transport). An exponent of -1 occurs when all grain sizes move at the same critical shear stress (i.e., equal mobility; Parker et al., 1982) because differences in grain weight are offset by hiding and resistance effects (Einstein, 1950; Egiazaroff, 1965; Yager and Schott, 2013). Values less than -1 indicate coarse grains mobilize before fine grains because hiding and resistance exceed the effect of particle weight on transport thresholds. Hiding effects describe the tendency for small particles to be sheltered from flow in pockets on the bed, which cause them to experience lower fluid drag and lift forces than large, exposed grains (Fenton and Abbott, 1977). Resistance to motion is can be greater for fines when they rest in pockets that are deep relative to their diameter, which results in higher friction angles that decrease their mobility relative to coarse grains and lowers the  $b$ -exponent (Kirchner et al., 1990).

For 2006–2019, the trend in  $b$ -exponents for TRAL increased slightly (Figure 56) and the mean exponent was -0.97 and varied from -0.88 (2015) to -1.04 (2012). These values indicate approximate equal mobility for coarse and fine grains, which agrees with the similar values of  $Q_{ci}$  for fine and coarse sediment at this station (see Figure 51). This result indicates a paucity of fines at TRAL, such that hiding and resistance for smaller grains offsets their lower weight so they mobilize at approximately the same discharge as larger, heavier, and more exposed particles. This outcome is strongly influenced by coarse gravel augmentations in the reach that mitigate for sediment captured by Trinity and Lewiston Dams. The augmented gravels are screened to remove fines before placement so the only notable supply of fine sediment supply is contributed by Deadwood Creek, since bank collapse is minimal due to the lack of channel meandering in the reach. Given the gravel augmentations are the primary source of mobile bed material at TRAL, bed load size distributions at this station are coarser and lacking fines in comparison to TRLG and TRDC (see Figures 47 and 52).

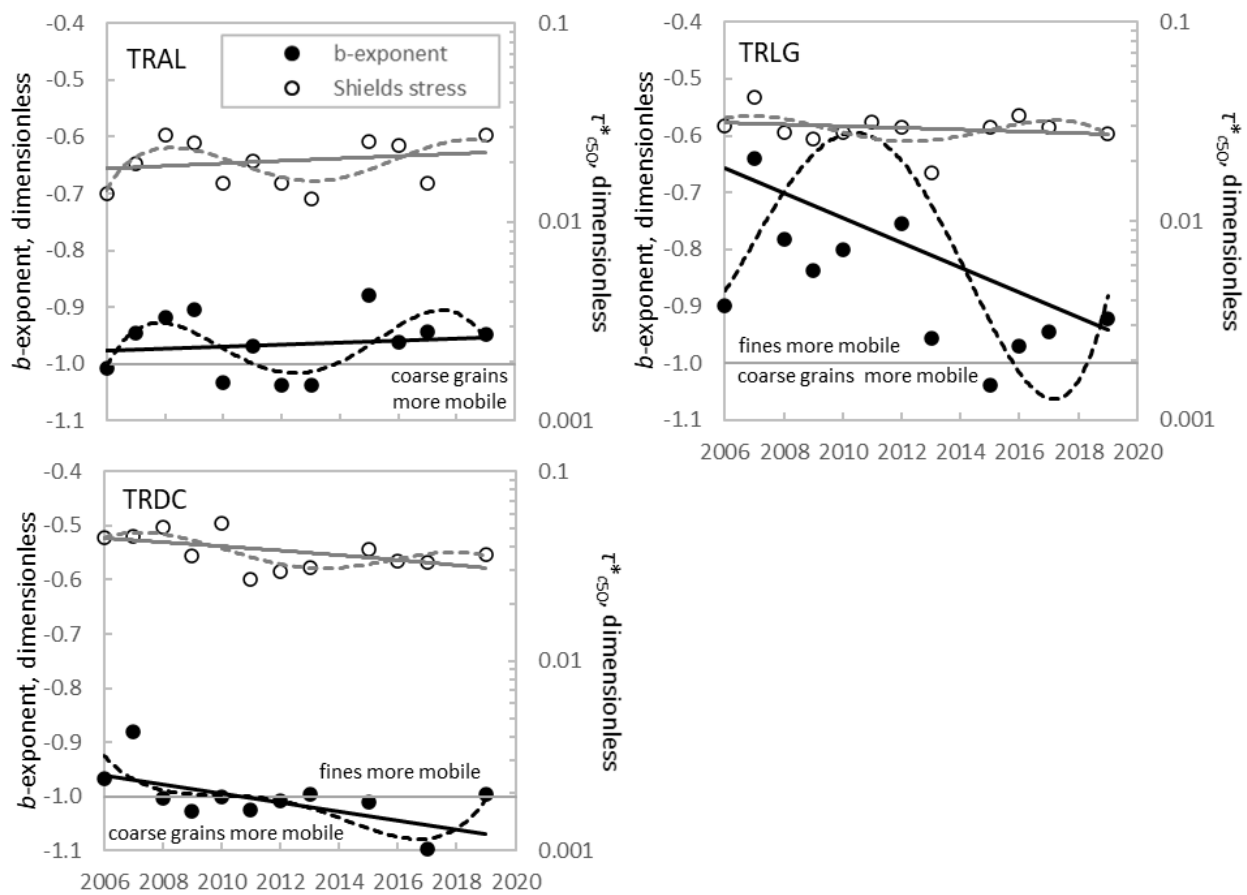


Figure 56. Hiding exponents ( $b$ ) and Shields stresses for the median grain size ( $\tau^*_{c50}$ ) estimated with the hiding function of Parker et al. (1982) for WY 2006–2019. The solid lines are linear regressions that show the trend in values and the dotted lines are 4<sup>th</sup> order polynomials that generalize temporal variation in the results.

In contrast to TRAL, hiding exponents exhibit strongly negative trends at TRLG and TRDC. At TRLG, the average (-0.86) and range of exponents (-0.64 to -1.04) indicate weight-driven transport (ie., fine grains mobilize before coarse grains) predominates, which is supported by  $Q_{ci}$  for fines being substantially lower than for coarse grains at this station (see Figures 51 and 56). However, exponents at TRLG have trended toward equal mobility since 2013, which agrees with threshold discharge results trending toward equal mobility and reflects the progressive decrease in fine sediments on the bed at this station (see Figure 47) and in the surface and subsurface domain nearby at Steel Bridge (see Figure 50). Results for TRDC were somewhat intermediate to those at TRAL and TRLG, with exponents averaging -1.01 (range -0.88 to -1.11) likely due to particle sheltering by an increasingly coarse, sorted, and stable armor layer (see Figures 47-50 and 52-53). Progressively negative trends in exponents at TRDC results from the lower availability of fine sediment for transport and development of a coarse surface layer at this station.

Values of  $\tau^*_{c50}$  for a given  $Re^*_c$  vary with a number of factors, including the definition of incipient motion, technique for partitioning shear stress, methodology to extrapolate shear stresses to a critical value, procedure for characterizing the grain-size distribution of the bed, and

material properties of the bed itself, including grain shape, sorting, skewness, and packing (Buffington and Montgomery, 1997). Research has additionally shown that critical conditions exhibit stochastic behavior based on the probabilities of turbulence and shear stress and intergranular resistance between particles on the bed. Due to these factors, values of  $\tau_{c50}^*$  for rough turbulent flow ( $Re_c^* > 350$ ) summarized by Miller et al. (1977) and Yalin and Karahan (1979) range more than 3-fold, from 0.02 to 0.065 (Buffington and Montgomery, 1997). Further research on sediment incipient motion has shown that  $\tau_{c50}^*$  exhibits a characteristic range (dashed lines in Figure 57) that varies with  $Re_c^*$ . Values of  $\tau_{c50}^*$  for TRDC and TRLG fall within the range in all years except WY 2009 and 2013 at TRLG. In these dry water years, record or near record low sediment loads (all size fractions) and their flow normalized values were measured at this station during spring high flow releases from the dams (Section 6.2.5.1). Conversely, at TRAL, all values of  $\tau_{c50}^*$  were outside the ordinary range except in WY 2008 (normal WY) and 2019 (wet WY). The cause for the higher than normal value of  $\tau_{c50}^*$  at TRAL in WY 2008 is unclear, but may have resulted in WY 2019 from the large amount of fine sediments delivered to the reach by Deadwood Creek stabilizing the bed through partial burial of coarse grains and increased packing and cementation of framework particles (e.g., Yager et al., 2018). This explanation aligns with the possibility that relatively low values of  $\tau_{c50}^*$  at TRLG resulted, in part, from fine sediment being relatively unavailable for stabilizing the bed in comparison to years when values were within the common range.

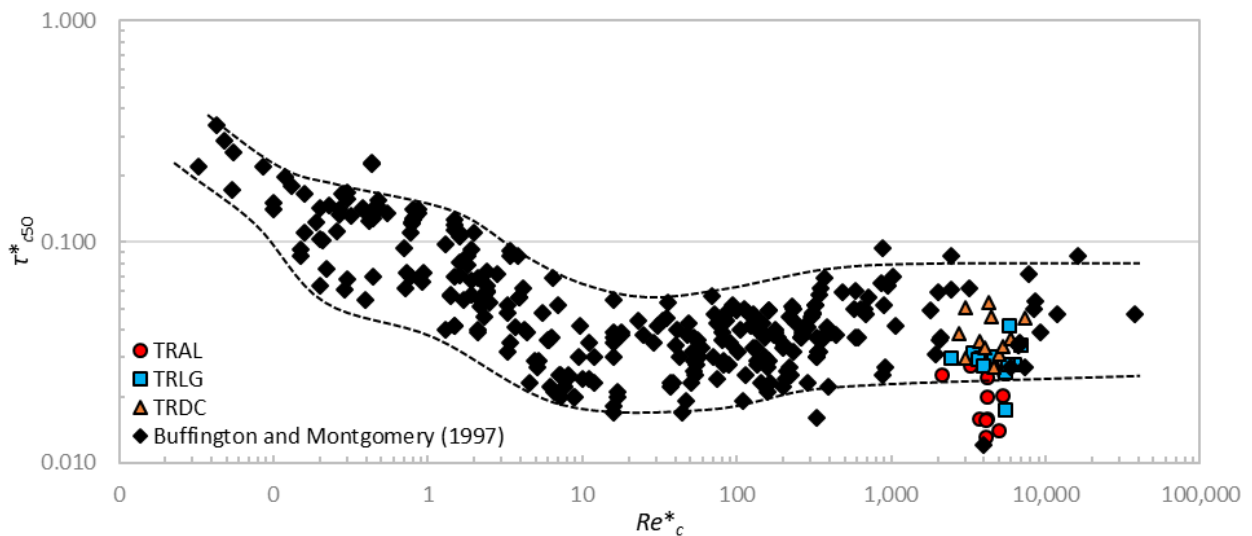


Figure 57. Shields stresses for the median grain size ( $\tau_{c50}^*$ ) and associated Reynolds particle numbers ( $Re_c^*$ ) from Plate 1 in Buffington and Montgomery (1997) and for TRAL, TRLG, and TRDC, which occurred in rough turbulent flow ( $Re_c^* > 350$ ). The dotted lines designate the characteristic range of values at a given  $Re_c^*$ . These data are for conditions where relative roughness ( $D_{50}/h_c$ ) was  $\leq 0.2$  with  $h_c$  as critical depth. Form drag and  $\tau_{c50}^*$  increase with relative roughness so restricting the comparison to this range of  $D_{50}/h_c$  helps maintain comparability of  $\tau_{c50}^*$  with values in the literature.

Higher values of  $\tau_{c50}^*$  occur on more stable beds, so the relatively low  $\tau_{c50}^*$  at TRAL compared to TRLG and TRDC may appear to disagree with estimates of critical flow for bed load at TRAL commonly exceeding values for the other stations (see Figure 50). The disparity results from  $\tau_{\text{grain}}$  tending to be higher at a given discharge and increase at a faster rate with flow at TRDC, then TRLG, and finally TRAL, which exhibited the lowest values (Figure 58). The different relationships of  $\tau_{\text{grain}}$  to discharge at these stations results from energy slopes and flow velocities tending to be higher at comparable discharges with downstream distance (Figure 59). The only other variable in  $\tau_{\text{grain}}$ ,  $D_{65}$ , exhibited unsystematic variation between stations and years (Figure 60). Consequently, the higher energy slopes and flow velocities at a given discharge at the more downstream stations results in larger magnitude flows being required to generate critical values of shear stress at TRAL.

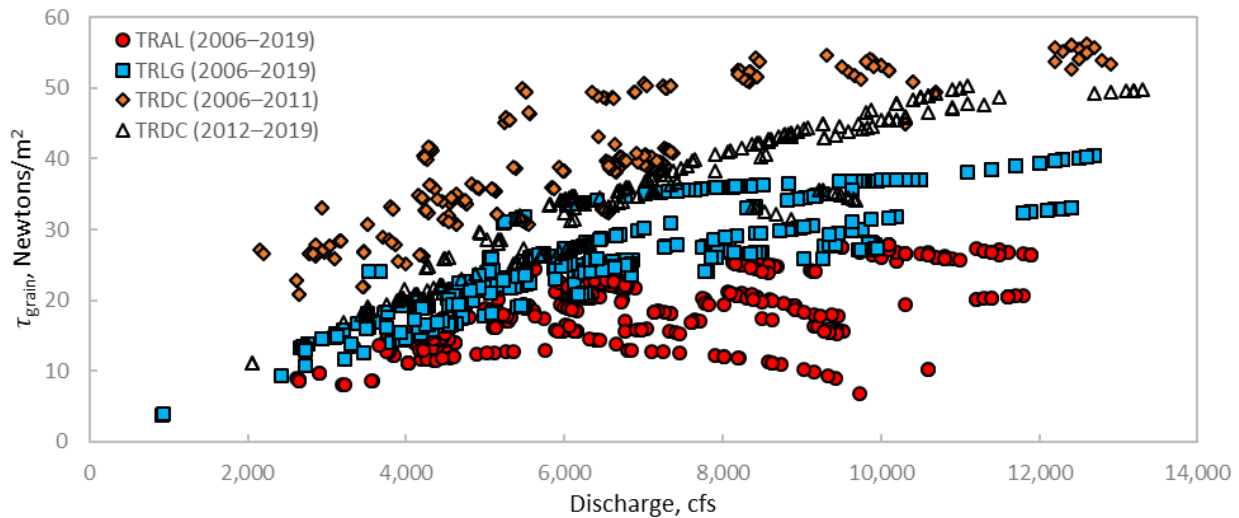


Figure 58. Shear stress partitioned for the granular bed ( $\tau_{\text{grain}}$ ) at discharges that bed load transport was measured at TRAL, TRLG, and TRDC. The two sets of values for TRDC show how  $\tau_{\text{grain}}$  varied between stations that transport was respectively measured in 2006–2011 and 2012–2019.

### 6.2.3 Median bed material to bed load ratios

Evidence for the dominant source of bed load at TRAL, TRLG, and TRDC is provided by the ratio of the median surface grain diameter before spring flow releases ( $D_{\text{surface}}^*$ ) and the average subsurface median grain size ( $D_{\text{subsurface}}^*$ ) each to the median bed load diameter (Figure 61). Ratios  $\leq 1$  infer bed load is dominated by surface particles and bar and riffle material and ratios  $> 1$  indicate dominance of fine sediment entrained by local scour exposing subsurface sediments and mobilization of fines from channel banks, lee areas, and patches in the channel (e.g., Paola and Seal, 1995). Values of  $D_{\text{surface}}^*$  and  $D_{\text{subsurface}}^*$  markedly exceeded 1.0 at TRLG and TRDC, inferring transport of fines over a coarse and relatively stable bed surface, with fines predominantly originating from other than subsurface areas of the bed (e.g., Lisle, 1995). These transport conditions are most common at TRLG (mean  $D_{\text{surface}}^*$  36.1, mean  $D_{\text{subsurface}}^*$  17.8), where bed loads are strongly dominated by fine grains (Figure 61). Note that in Figure 61, values of  $D^*$  are not shown for 2006 and 2007 because Wolman (1954) pebble counts were not taken before the spring flow release. Data are also not shown for 2014 and 2018 because sediment

transport was not measured these years. Evidence for transport of fine material over a stable surface layer also occurs at TRDC (mean  $D^*_{\text{surface}}=10.0$ , mean  $D^*_{\text{subsurface}}=7.6$ ). At TRAL,  $D^*_{\text{surface}}$  and  $D^*_{\text{subsurface}}$  respectively averaged 1.8 and 1.2, which suggests near equal mobility of coarse surface grains and relatively fine grains in subsurface areas and surface deposits on the bed. Linear slopes of  $D^*_{\text{surface}}$  and  $D^*_{\text{subsurface}}$  decreased at TRLG and TRDC because values were generally high through 2013 before markedly decreasing in 2015–19 due to increases in the median bed load diameter at these stations (3.1 to 20.2 mm and 5.4 to 15.2 mm respectively at TRLG and TRDC for 2006–2013 and 2015–2019; also see Figure 52). In WY 2019 at TRAL,  $D^*$  equaled the historic average (1.7) because both the surface  $D_{50}$  before the flow release and the bed load  $D_{50}$  decreased by the same percentage in comparison to average values from previous years (74%). Decreases in both particle sizes resulted from the large influx of fine sediment from Deadwood Creek and Hoadley Gulch in water year 2019.

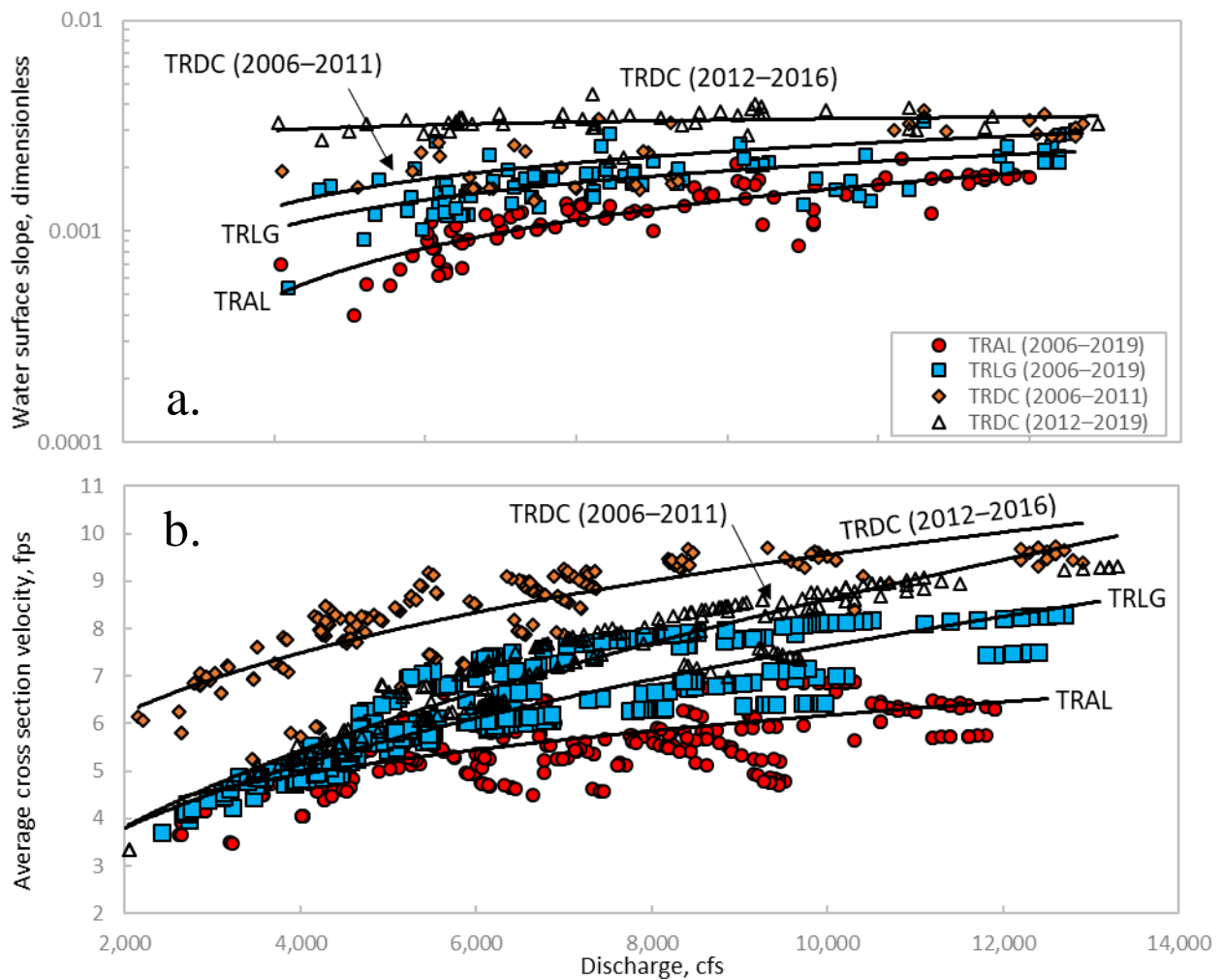


Figure 59. Energy slopes (a.) and cross section average flow velocity for discharges that bed load transport was measured at TRAL, TRLG, and TRDC (b.). The solid lines are power equations of the respective data for each station.

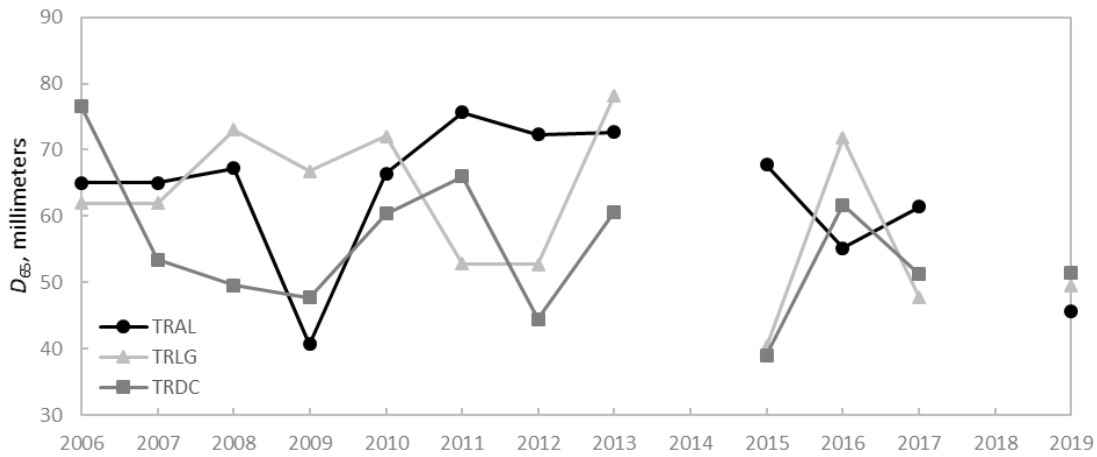


Figure 60. Diameters of the  $D_{65}$  particle in Wolman (1954) samples taken prior to spring flow releases and used in estimates of  $\tau_{\text{grain}}$  at TRAL, TRLG, and TRDC.

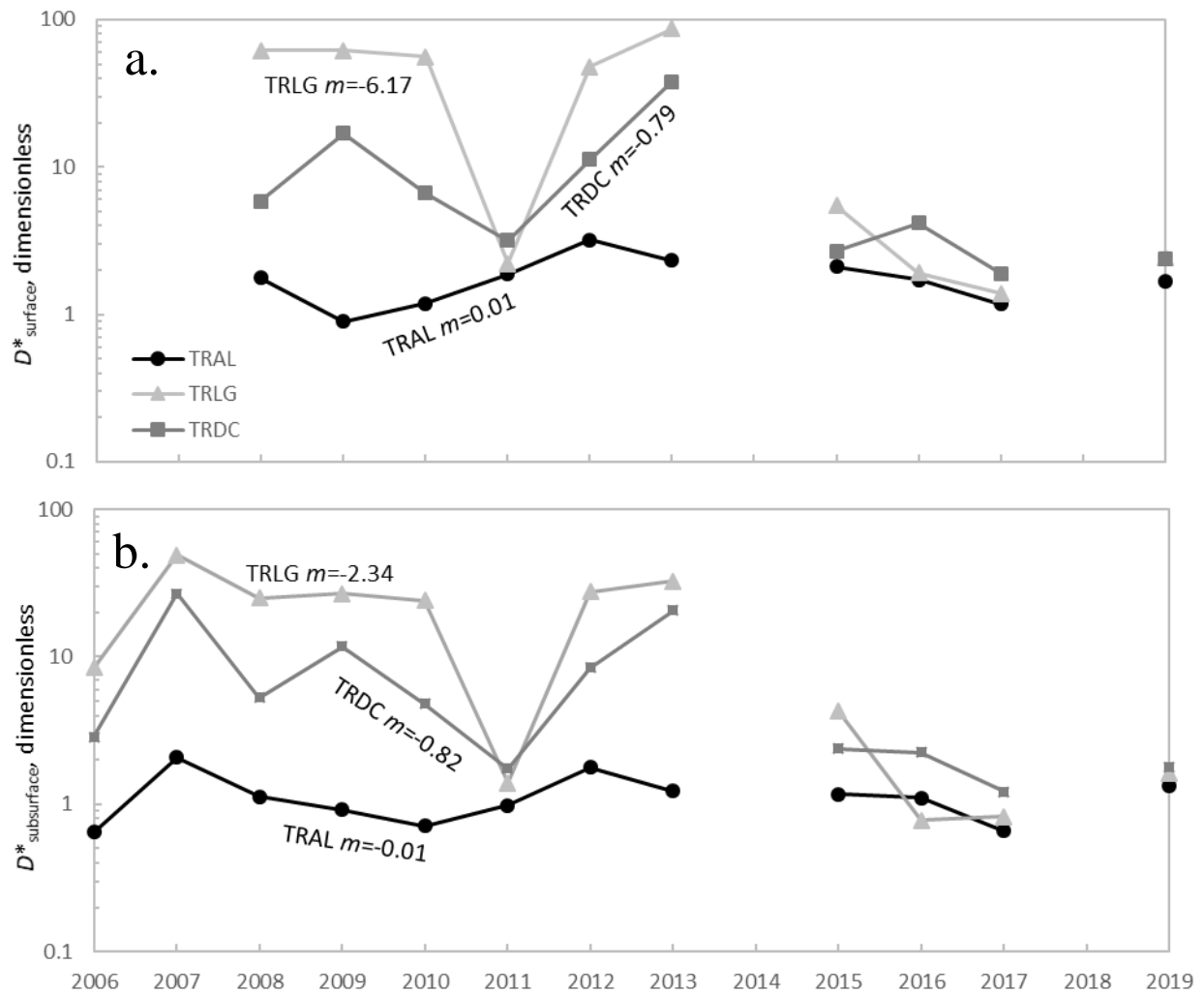


Figure 61. Values of  $D^*_{\text{surface}}$  by year for 2008–2019 ( $D^*_{\text{surface}}$ ; a.) and  $D^*_{\text{subsurface}}$  for 2006–2019 (b.). The labels are slopes ( $m$ ) of linear regressions of the data for each station. Lines connect values for contiguous years.

$D^*_{\text{surface}}$  and  $D^*_{\text{subsurface}}$  inversely relate to the peak discharge for spring flow releases at TRLG and TRDC but were largely consistent with variations in peak flow at respectively around 1.8 and 1.1 at TRAL (Figure 62). Furthermore, power estimates of discharges at unity in  $D^*_{\text{subsurface}}$  indicating complete bed mobility at 8,650, 13,200, and 15,060 cfs at TRAL, TRLG, and TRDC, respectively. These figures indicate flow magnitudes that are typical for wet and extremely wet water years at TRAL added to tributary accretions at TRLG and TRDC are required to transport fine sediments delivered to the channel over winter and coarsen the bed load to bed material sizes at these stations. Further increases in flow are then required to deplete the fine sediment supply or perhaps reform the armor layer and coarsen bed load to near the size distribution of particles on the bed surface at the start of the flow release, as indicated by unity in  $D^*_{\text{surface}}$  occurring at 14,000 cfs at TRLG and 16,900 cfs at TRDC. A discharge at unity for  $D^*_{\text{surface}}$  at TRAL is not reported because values did not trend toward unity with increased flow. These findings indicate that high spring flow releases are able to reduce the amount of fine sediment that is available for transport in the channel downstream of Lewiston and generate somewhat of a depletion of fines until recharge reoccurs the following winter. Conversely in the Lewiston reach, results indicate that fines exhibit a perennial depletion, as shown by values of  $D^*_{\text{surface}}$  and  $D^*_{\text{subsurface}}$  near unity at all discharges (Figure 62).

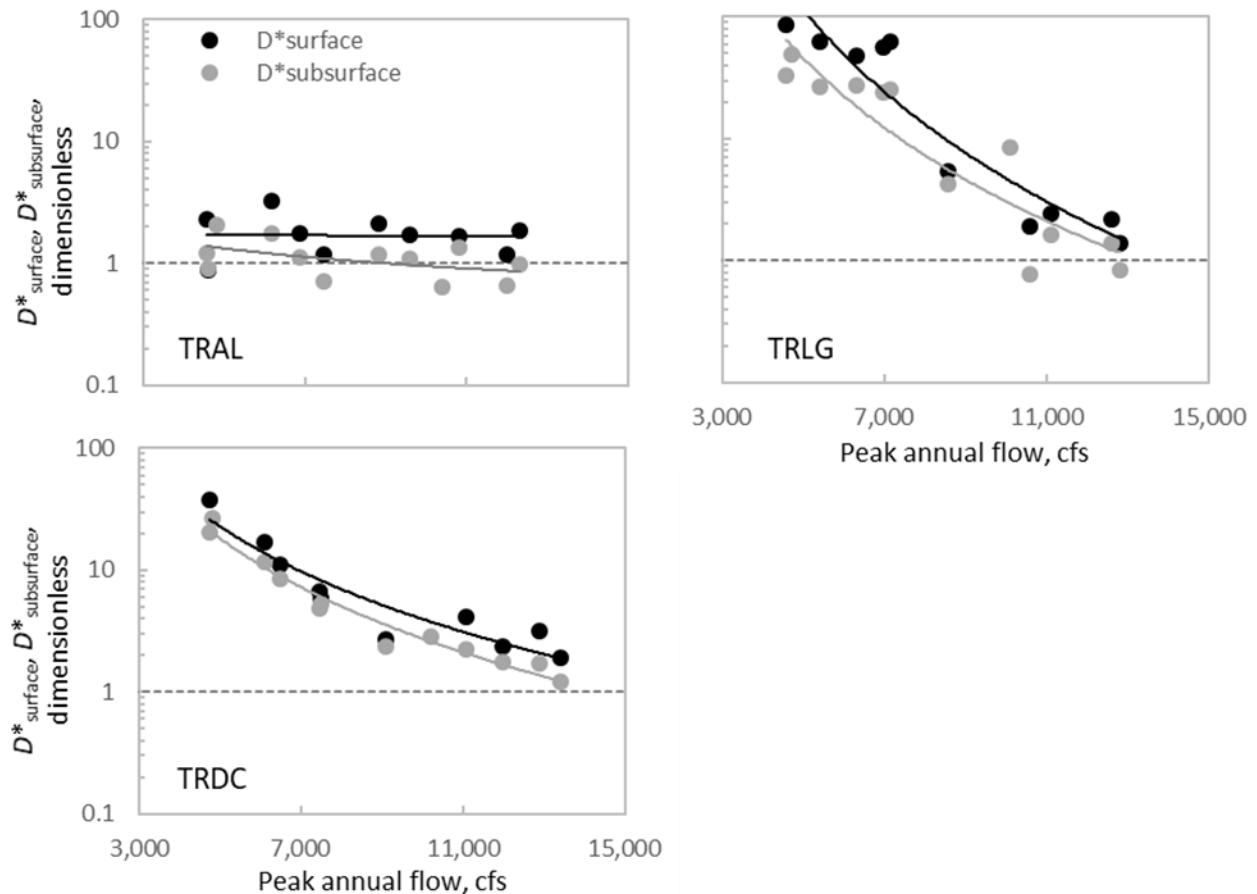


Figure 62. Values of  $D^*_{\text{surface}}$  and  $D^*_{\text{subsurface}}$  versus discharge at TRAL, TRLG, and TRDC. The solid lines are power functions of the data for WY 2004–2019 and the dotted line indicates unity in the ratios.

#### 6.2.4 Fine sediment to coarse bed load ratios ( $S^*$ )

Values of  $S^*$  for the spring flow release period (April 1–July 31) in WY 2006–2019 indicate fine sediment loads (suspended sediment + fine bed load) exceed coarse bed loads for the period of record at TRLG and TRDC and for half the time at TRAL (Figure 63; Appendix I). Values of  $S^*$  ranged widely and averaged 1.4 (range 0.5-3.4) at TRAL, 38.0 (range 2.3-206.5) at TRLG, and 7.7 (range 1.3-34.6) at TRDC and generally increase with downstream distance because tributaries increase the fine sediment supply to the river with distance from Lewiston Dam. Additional factors are flows increase with downstream distance and widen the active channel of the Trinity River through bank erosion (see Section 3.1.7). Trends in  $S^*$  are negative at all stations except TRAL where coarse bed loads exceeded fine sediment loads in 5 of 12 years due to the paucity of fines available for transport in the Lewiston area and coarse gravel augmentation that often occurs at diversion pool, located one mile upstream of the monitoring station.  $S^*$  was highest at TRLG because fine sediments are relatively plentiful at this station and coarse bed load is thought to be in deficit (Gaeuman and Stewart, 2017) due to this station being located 5.6 miles downstream of the nearest gravel augmentation location and 9.1 miles downstream of Rush Creek, the only major upstream tributary. Gravel augmentation proposals for remedying the potential deficit in coarse sediment are currently being developed by the physical workgroup of the TRRP. In comparison to TRLG, TRDC exhibited substantially lower  $S^*$  because potentially due to fine sediments becoming increasingly scarce at this station. This possibility is indicated by Wolman (1954) samples at TRDC (Figures 47-48), bulk sampling for the active layer at nearby Upper Steiner Flat (0.7 miles downstream; Figure 50), protrusion measurements near TRDC (Section 6.2.1), and increasingly higher critical flows for fine than coarse sediment at this station (Figure 51, Appendix G). However, several lines of evidence counter this possibility, as summarized in Section 9.3.

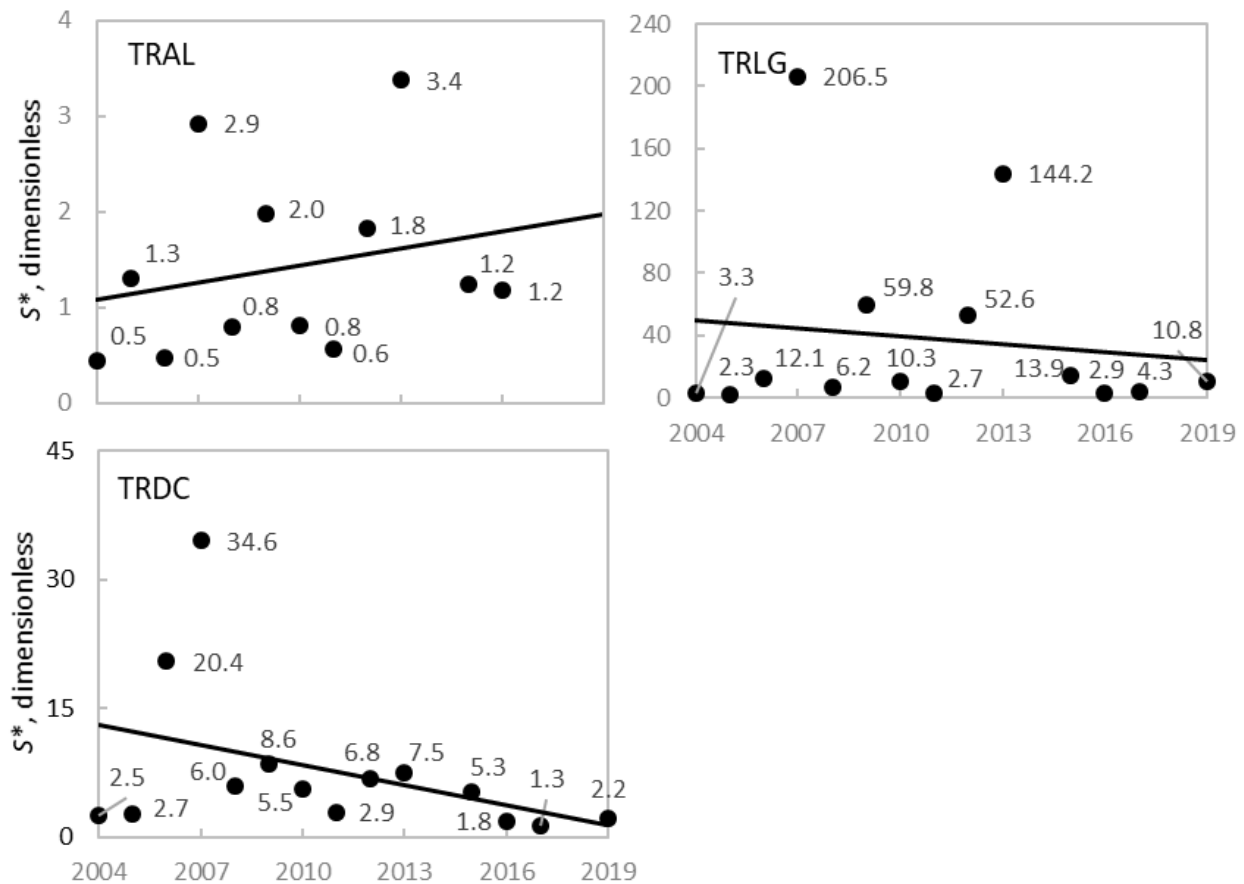


Figure 63. Ratios of the total fine sediment loads to coarse bed loads ( $S^*$ ) measured during spring flow releases at TRAL, TRLG, and TRDC. The solid lines are linear regressions fit by least squares to ratios for WY 2004–2019, which show a decreasing trend at TRLG and TRDC and an increasing trend at TRAL.

### 6.2.5 Suspended load and bed load estimates

#### 6.2.5.1 Spring flows

Sediment loads were estimated for the spring flow release period (April 1–July 31) for WY 2004–2019 at TRAL, TRLG, and TRDC by GMA (2020a; Figure 64). Exceptions were that sediment transport monitoring and associated load estimates were not made in WY 2014 or 2018 because the peak flow releases (respectively 3,370 cfs and 1,860 cfs) were too low to substantially mobilize the bed in these critically dry water years. Suspended sediment has also not been measured at TRAL since 2016 because loads were considered too low to justify monitoring. For water year's and stations that sediment transport was measured, suspended loads (in tons) were measured as the dry weight of particles  $<0.5$  mm sampled from the water column and bed load was sampled within 152 mm of the bed with TR-2 samplers and reported in half-phi increments and in bins corresponding to fine bed load ( $\geq 0.5$  mm to  $\leq 8$  mm) and coarse bed load ( $>8$  mm). Total and fractional loads (in tons) and their flow normalized values for the spring flow period are tabulated in Appendix I and shown in Figures 64 and 65. Discharges for normalizations included the sum of daily average flows for the spring flow period that transport

was computed (April 1–July 31) for each station (i.e., total discharge) and the volume of flow that exceeded critical discharges in the computational period (Appendix J).

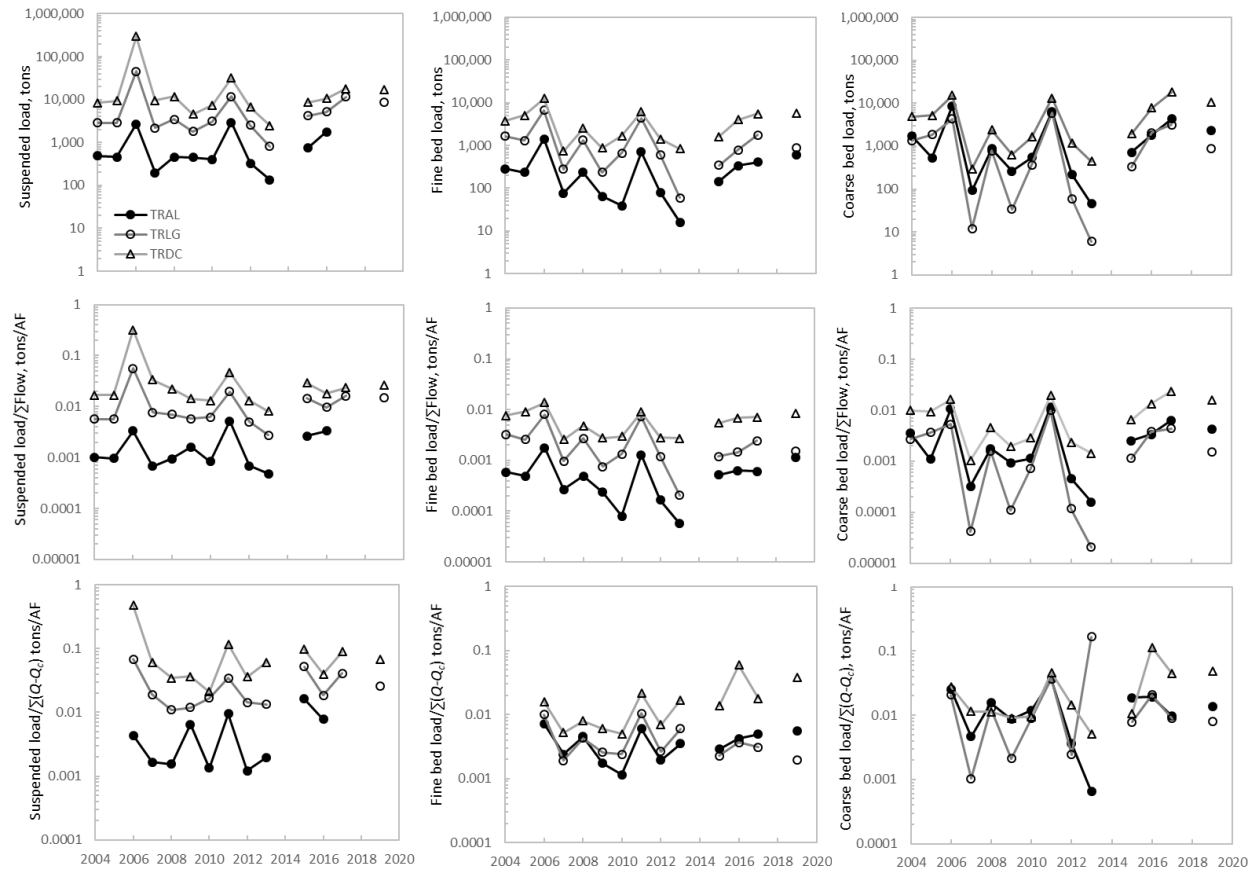


Figure 64. Suspended loads and fine and coarse bed loads estimated for the spring flow period (April 1–July 31) in 2004 through 2019 by GMA (e.g., GMA, 2014). Loads are also shown normalized by the total flow volume in the spring flow period and the volume of flow during spring that exceeded critical discharges in 2006–2019. Loads for 2014 and 2018 are absent because sediment transport was not monitored in these critically dry water years. Lines connect loads for contiguous years.

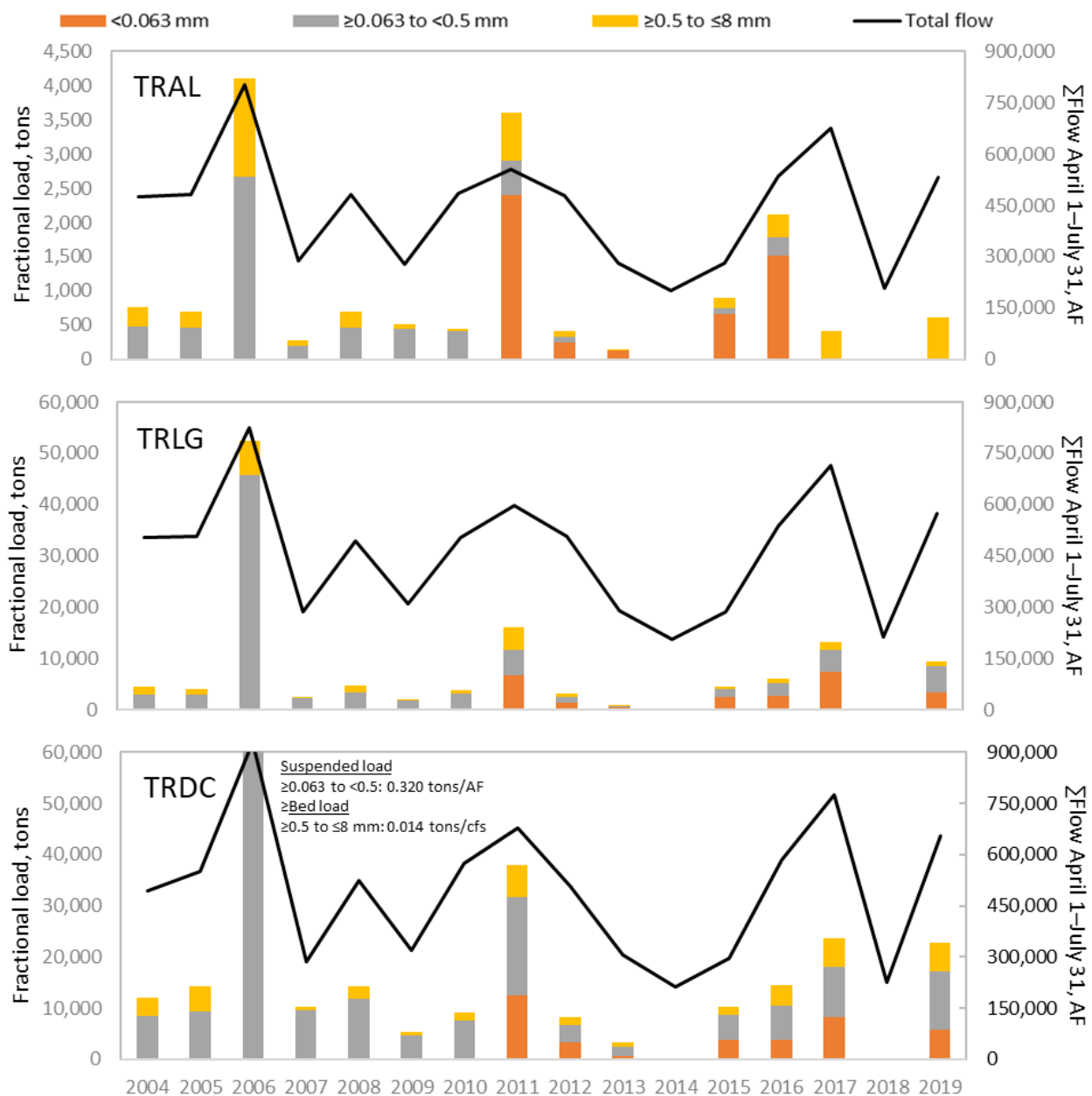


Figure 65. Fractional loads of fine sediment estimated for spring flow releases on the Trinity River and associated flow volumes that occurred during the computational period (April 1–July 31) for water years 2004–2019. Missing data include suspended sediment that has not been measured at TRAL since WY 2016, and transport monitoring for all size fractions did not occur in the critically dry water years of 2014 and 2018.

Loads and their normalized values displayed substantial variability due to different magnitude flows and total annual water volumes acting on the channel bed, variation in entrainment thresholds (see Figure 51), and changes in bed texture (see Figures 47-50) and sediment supply between years (Section 5). All loads increased with distance from Lewiston Dam and total fine sediment loads (suspended sediment + fine bed load) at Lewiston averaged 18% (range 8-35%) of those at TRLG for 2004–2016 and 6% (1-15%) of loads at TRDC for 2004-2019 (Figures 64-65).

Record high annual loads of fine sediment in spring occurred at TRLG and TRDC in WY 2006, the first extremely wet water year following implementation of ROD (2000) flows in WY 2005 and the first Lewiston Dam release to exceed 10,000 cfs in the 32 years since 1974 (peak flow was 10,400 cfs on May 24, 2006; Figure 64). The high flows mobilized large volumes of fines that were presumably stored in the channel over this period and caused active channel widening and associated bank collapse to elevate fine sediment loads to values not measured since WY 1986 at TRLG (Figure 66; Curtis et al., 2015). Additional explanation for the fine sediment load in WY 2006 is that winter respectively involved record (in italics) or near record high flows in the admittedly short period of record (2004–present) on Rush Creek (*1,940 cfs*; 1,470 cfs) and Indian Creek (*1,860 cfs*). Grass Valley Creek likely had little influence on the fine sediment supply in the Trinity River in 2006 because Hamilton Ponds were operational this year and did not over fill, so trapped most fines delivered to them (Table 5). The next highest fine sediment load for the spring flow period of record on the Trinity River occurred in WY 2011 (Figures 64–65). In this year, fine sediment loads were likely higher at TRAL than the other stations due to adjustments following channel rehabilitation work that occurred in 2008 at several locations upstream of this station. In all cases, the highest loads in the period of record at all stations are associated with flow releases from Lewiston Dam that are around 10,000 cfs and above.

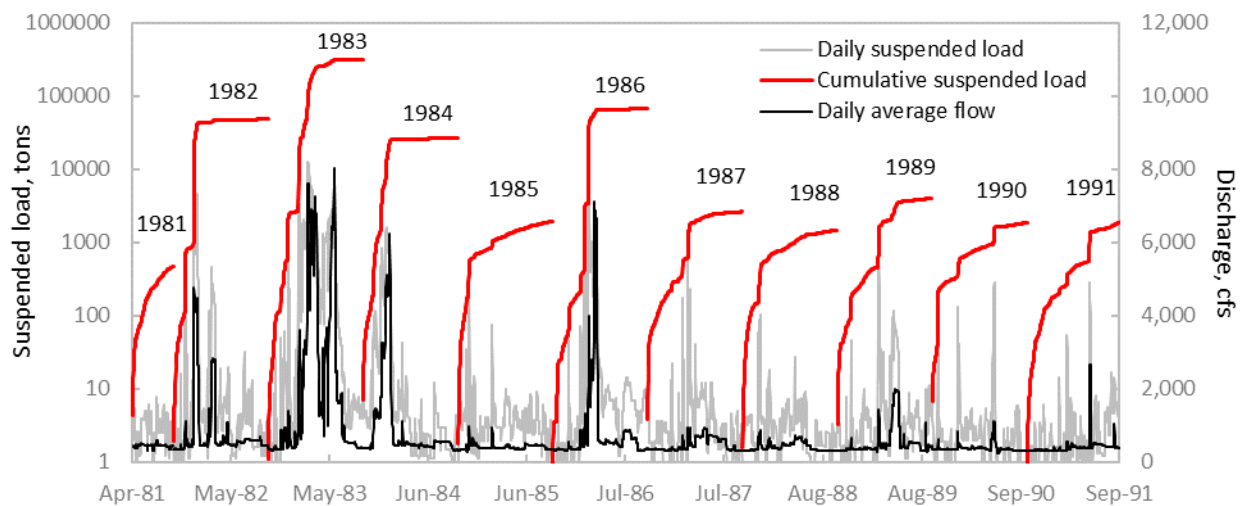


Figure 66. Suspended sediment loads and daily average flows at TRLG for April 1981–September 1991.

Bed loads collapsed more tightly when normalized by discharges that exceeded critical thresholds than total discharges during the spring flow period, but the opposite was true for suspended loads (see Figure 64). This probably reflects the higher sampling effort for bed loads than suspended loads that results in greater inaccuracy in estimates of critical flow for suspended sediment. Estimates of error in critical thresholds and loads are not presented in this document because inaccuracy in measurements used to partition stress and measure loads were not quantified. Linear regressions indicated suspended loads normalized by total flow volumes decreased at an average annual rate of 0.005 tons/AF at TRDC for 2004–2019 and were essentially flat at TRAL (2004–2017) and TRLG (2004–2019). The same was true for fine and coarse bed loads normalized by exceedance flows at TRAL and TRLG, but these size fractions both increased at TRDC at a rate of 0.003 and 0.004 tons/AF, respectively.

Fractional suspended loads estimated for spring flows on the Trinity River indicate the average percent that suspended sediment is of the total fine sediment load varies from 77% at TRAL (range 63-91%) to 82% (64-93%) and 80% (65-96%) at TRLG and TRDC, respectively. Furthermore, wash load (<0.063 mm) dominated the fine sediment load at all stations except TRDC in years it was partitioned from suspended sediment samples (2011–2016 at TRAL and 2011–present at TRLG and TRDC; Figure 65). Though perhaps surprising, this result at TRAL was not unexpected because turbidity can result at Lewiston from reservoir bank erosion by rain when water levels in Trinity Lake are significantly below capacity (CWQC, 2004). Also, because wash load does not tend to settle in the channel, but rather accumulate from stream banks and other sources as flow transits downstream, it is expected to increase with downstream distance. This held true through TRLG, but coarse suspended sediment dominated the fine sediment load at TRDC for reasons that are not clear.

### 6.2.5.2 Fall and winter flows

For water years 2006–2019, bed loads were estimated for intervals outside the spring flow period (10/1–3/31 and 8/1–9/30) with equations of the form

$$Q_{bi} = \alpha_{bi}(Q - Q_{ci})^{\beta_{bi}} \quad \text{Eqn. 10}$$

where  $Q_{bi}$  is the bed load transport rate in tons/day for size fraction  $i$ ,  $Q_{ci}$  is the critical flow for size  $i$ , and  $\alpha$  and  $\beta$  are parameters fitted by least squares to power functions. With equation (10), bed load transport occurs when  $Q$  exceeds  $Q_{ci}$ , which was determined with the reference transport method for the rising and falling limb of spring flow hydrographs when hysteresis was observed. When hysteresis did not occur,  $Q_{ci}$  was determined with all bed load measurements available for that year. Total loads in the fall and winter flow periods were determined by summing the daily loads. Suspended sediment loads outside the spring flow periods were estimated with exponential equations of the form

$$Q_{sc} = \alpha_s e^{\beta_s(Q - Q_{cs})} \quad \text{Eqn. 11}$$

where  $Q_{sc}$  is the suspended sediment concentration in mg/L for particles <0.5 mm,  $Q_{cs}$  is the critical flow for suspended sediment, and  $\alpha_s$  and  $\beta_s$  are parameters fitted by least squares to exponential functions of the suspended sediment data. Exponential functions were used instead of power equations because they provided better fits to the data. Suspended concentrations were estimated with equation (11) as done for bed load using equation (10) when hysteresis was observed.

Hysteresis occurs when sediment transport rates vary in a pattern with discharge in a hydrograph. When transport is higher on the increasing limb than other portions of a hydrograph, clockwise hysteresis is said to occur because a trace of transport rate on the abscissa versus discharge is in this direction with respect to time (Appendix G). Alternatively, counterclockwise hysteresis occurs when transport rates are higher on the decreasing limb of the hydrograph. Clockwise hysteresis is commonly attributed to depletion of sediment derived from the channel bed and banks early in a flow event, and counterclockwise hysteresis from recruitment and transport of material from tributaries, terraces, and floodplains (Martin et al., 2014). Other hysteresis traces can also occur, such as figure-eight, and the variety of traces can result from interaction of factors that include depletion of material available for transport (Hassan and Church, 2001),

formation of bedforms decreasing shear stress on the granular bed around the hydrograph peak (Lee et al., 2004), protracted flows near critical that destroy the armor layer (Kuhnle, 1992), and depletion of relatively mobile patches early or late in a flow event (e.g., Paulo and Seal, 1995). Due to the multiple factors that interact and influence sediment transport rates, hysteresis, when it occurs, rarely follows a given trace perfectly. This was often the case with fine bed load ( $0.5 \text{ mm} \leq i \leq 8 \text{ mm}$ ) and coarse bed load ( $i > 8 \text{ mm}$ ) measured during spring hydrographs. Even so, evaluation for hysteresis of these sized grains here largely agree with those for 2004–2015 by Gaeuman and Stewart (2017) at TRAL, TRLG, and TRDC. In both examinations, hysteresis occurred in most years, and clockwise hysteresis was most prevalent (Table 6, Appendix F-G). Given the banks of the Trinity River are largely stable through time outside channel rehabilitation areas (Section 3.1.7) and that tributaries rarely transport sediment during spring flow releases (Section 4.1.4), the predominance of clockwise hysteresis suggests rapid depletion of delta sediments and bed material that is available for transport.

Table 6. Percentages of years<sup>1</sup> that hysteresis was or not observed in suspended sediment and bed load transport at TRAL, TRLG, and TRDC from WY 2006–2019.

Station	Clockwise	Counter-clockwise	Figure-eight	None	Unknown <sup>2</sup>
TRAL	83%	0%	8%	8%	0%
TRLG	42%	17%	8%	25%	8%
TRDC	50%	8%	8%	25%	8%
Fine bed load ( $0.5 \text{ mm} \leq i \leq 8 \text{ mm}$ )					
TRAL	75%	8%	8%	8%	0%
TRLG	75%	0%	17%	8%	0%
TRDC	50%	25%	0%	17%	8%
Suspended load ( $< 0.5 \text{ mm}$ )					
TRAL	80%	10%	0%	0%	10%
TRLG	83%	8%	0%	0%	8%
TRDC	83%	8%	0%	0%	8%

<sup>1</sup> The number of years with suspended sediment samples at TRAL was 10 and the number of sample years for all other size fractions and stations is 12.

<sup>2</sup> Unknown determinations occurred when too few sediment samples were taken to estimate the occurrence or lack of hysteresis.

Evidence for hysteresis in suspended sediment also occurred in 90% or more years that transport was monitored on both the rising and falling limbs of hydrographs and here again clockwise hysteresis dominated (Table 6, Appendix G and H). In 16 of 32 years that sampling occurred at TRAL, TRLG, and TRDC, too few transport samples were taken to indicate  $Q_{cs}$ . In these cases, an exponential equation fit to the historic data (WY 2006–2017) for each respective station was adjusted to provide a best fit to the year's data (Appendix K) or  $Q_{cs}$  was taken as reported by GMA (e.g., GMA, 2020a) when suspended sediment concentrations for a particular year did not show a clear relationship to discharge. In years the relationship was evident and gave a realistic approximation based on turbidity values, critical flows were estimated at 1 mg/L with power equations of concentration versus discharge. The concentrations were then converted to daily loads in tons by multiplying by the daily average flow and 0.0027.

Suspended loads in winter were adjusted to account for tributary contributions of fines outside the spring flow period. The need for such adjustment was indicated by sediment transport samples taken at TRLG between 1981 and 1991 that show suspended loads are notably higher during tributary flow events in winter than during high flow releases from Lewiston Dam (Figures 67-69). However, a possibility is the differences may arise from winter loads being estimated from samples taken during the rising limb of hydrographs when transport rates are often higher due to clockwise hysteresis. To evaluate this possibility, suspended loads estimated from samples taken during the rising limb, falling limb or steady flows, and peak discharge of hydrographs were compared at TRLG (Figure 67). Most suspended sediment samples were taken during the falling limb or steady flows ( $n=30$ ), followed by peak discharges ( $n=19$ ), and the rising limb of hydrographs ( $n=13$ ). In this order, power equations relating suspended loads to discharge respectfully displayed increasing exponents ( $n=62$ ; Figure 68), indicating relatively high loads estimated for winter flows are unlikely to be an artifact of sample timing.

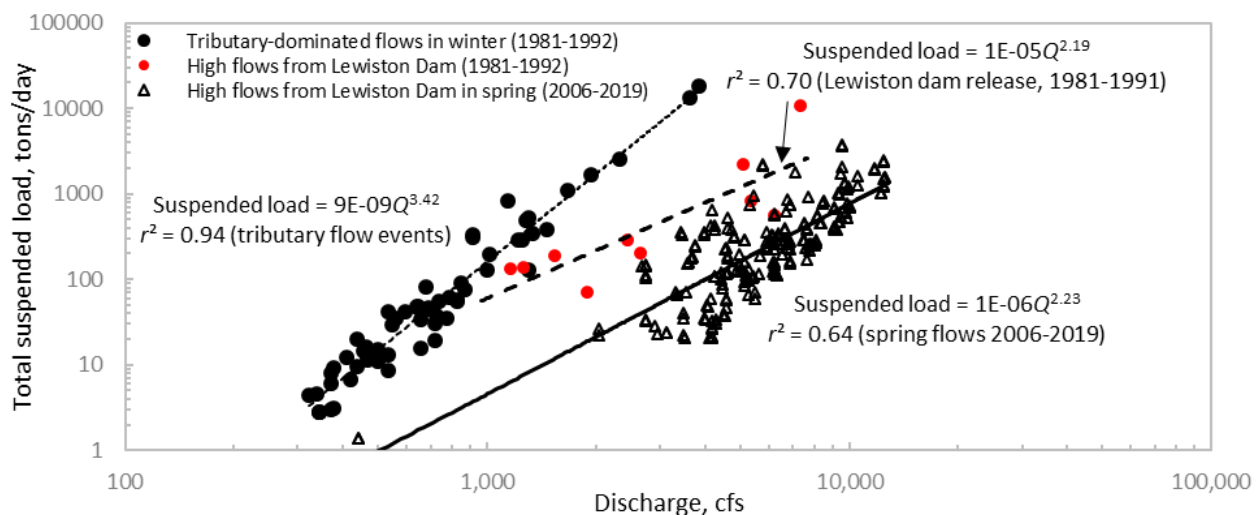


Figure 67. Total suspended sediment loads measured at TRLG during tributary flow events and late winter or early spring high flow releases from Lewiston Dam for 1981–1992. Daily average load estimates for spring flow releases from Lewiston Dam in 2006–2019 are shown for comparison.

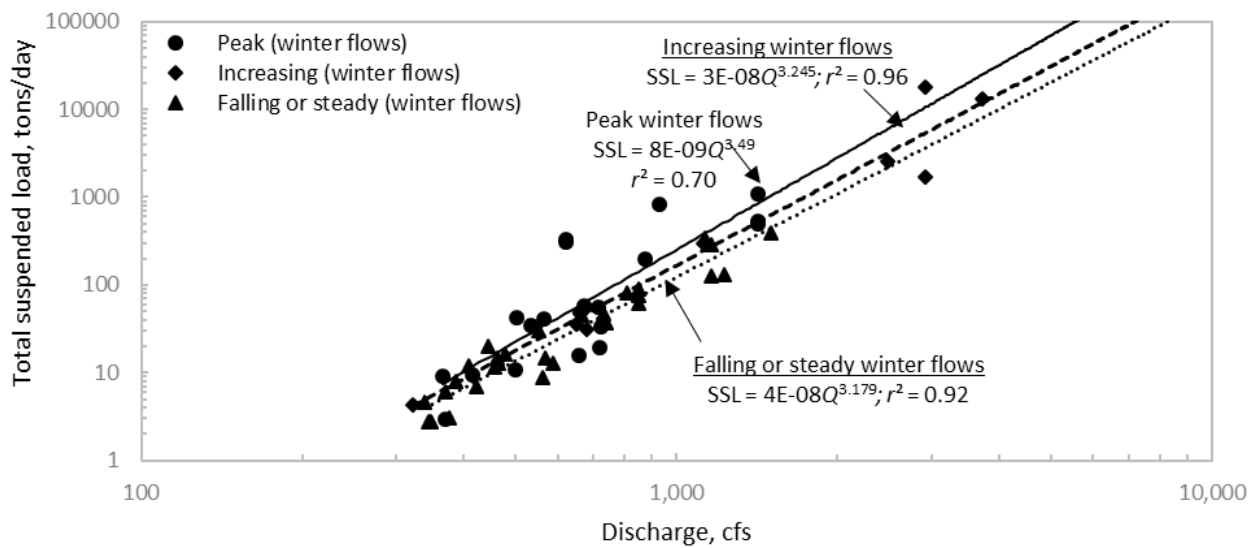


Figure 68. Power estimates of loads estimated for around the peak discharge, increasing limb of the hydrograph, or decreasing limb and steady flows at TRLG in winter in WY 1981–1991.

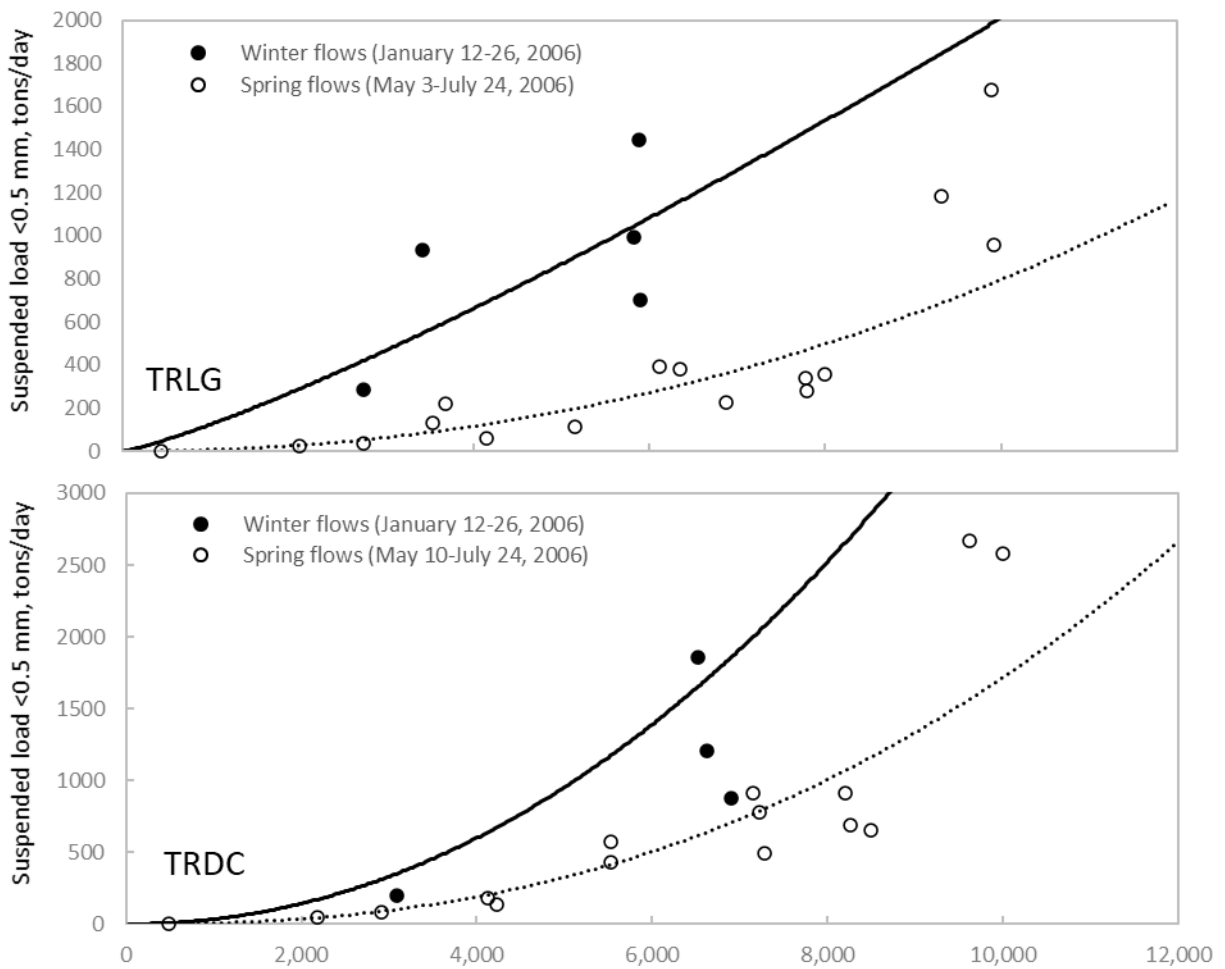


Figure 69. Suspended loads (<0.5 mm) measured during winter and spring flows in WY 2006 at TRLG and TRDC. The solid and dotted lines in the upper two panels are power functions of the data shown as closed and open circles, respectively.

The applicability of this finding to more recent flow events was assessed by comparing suspended loads measured in the winter and spring periods of WY 2006 at TRLG and TRDC (Figure 69). In agreement with the 1981–1991 data, power equations of the respective data applied at the same discharges between 500 and 14,500 cfs indicated that at comparable discharges, winter loads of suspended sediment exceeded spring loads by an average factor of 2.4 at TRLG and 2.2 at TRDC in 2006. These factors were used to adjust  $Q_{sc}$  estimated with equation (10) at TRLG and TRDC for the period when high flows typically commence on tributary streams (January 1) and lasting until the start of the computation period for spring flow releases from Lewiston Dam (April 1) when tributary hydrographs are on their declining limb. An adjustment factor was not used at TRAL due to the low suspended load at this station due to its proximity of this station to Lewiston Dam and because suspended loads on which to derive a factor have not been measured in winter at this station. Adjustment factors for fine bed load ( $\leq 8$  mm) were also not applied because loads measured in winter at TRLG were not significantly different than spring loads and too few data were available to compute a factor at TRDC (Figure 70).

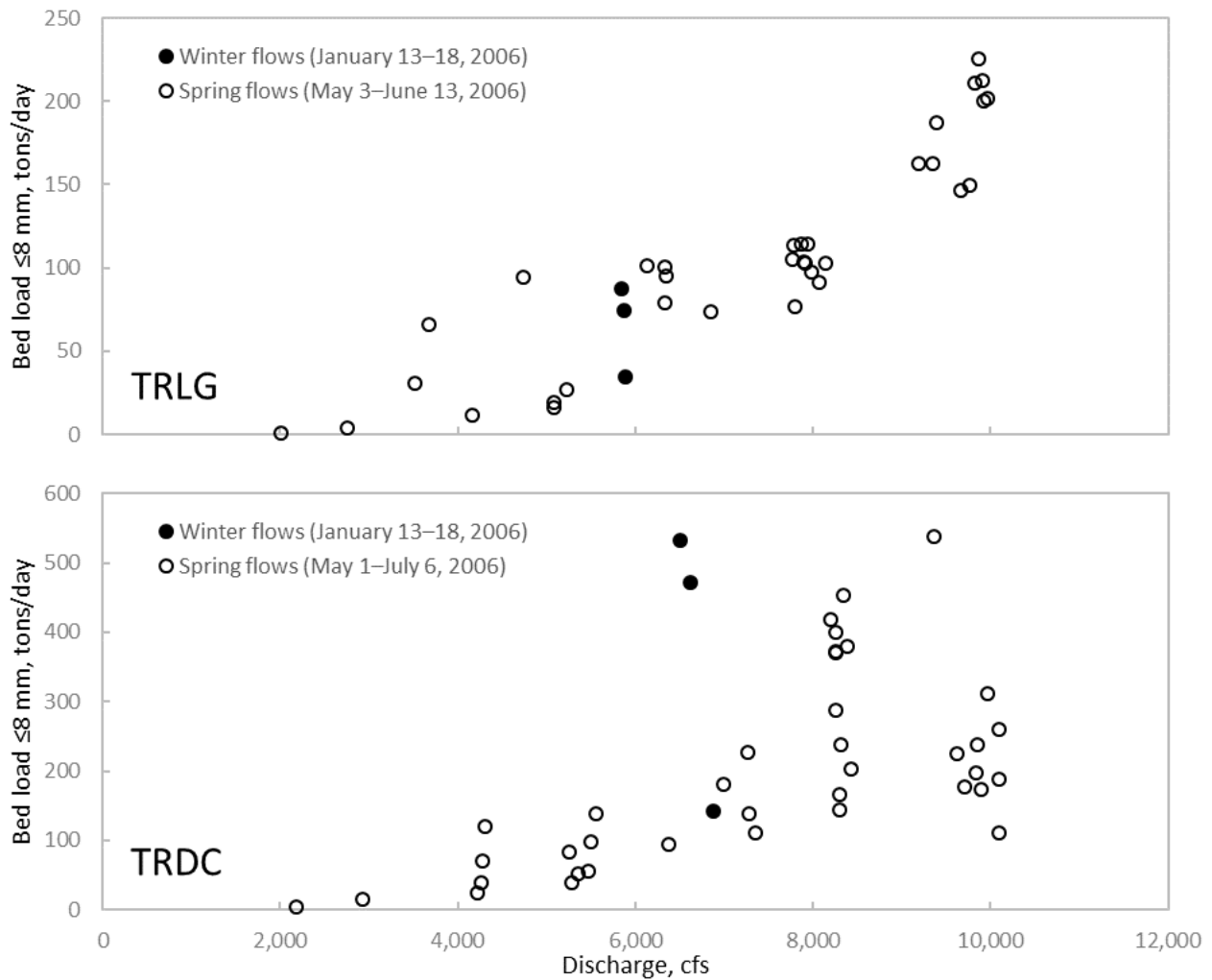


Figure 70. Fine bed load measured during winter and spring flows in WY 2006 at TRLG and TRDC.

Outside the spring flow period, critical discharges were exceeded more frequently with distance from TRAL in WYs 2006–2019. This resulted primarily because critical values tend to be lower at TRLG and TRDC than TRAL and tributary inputs increase flow on the Trinity River with distance from Lewiston Dam (Appendix G and J). Excepting a safety of dam release in February 2006, peak exceedances outside the spring release period at TRAL paradoxically occurred during the natural low flow period on the Trinity River in summer. These occurrences resulted from Lewiston Dam releases in late August to early September for augmentation of Klamath River flows ( $\leq 2,900$  cfs) that have occurred annually since 2012 (except 2017) and the Hoopa Boat Dance flows ( $\leq 2,750$  cfs) that are released in odd-numbered years. The rarity of sediment transport in winter at TRAL extends to at least Rush Creek, upstream of which around 80% of the Trinity River escapement of Chinook salmon spawn (see Rupert et al., 2017). Therefore, when fine sediments from Deadwood Creek and Hoadley Gulch accumulate in the Trinity River (see below), survival to emergence of salmonids eggs upstream of Rush Creek is low. This potential impact to salmon reproduction is not captured in bulk samples of the armor layer or subsurface bed material (see Figure 50) because sampling occurs in summer after spring high flow releases reduce or eliminate these conditions.

At all stations, suspended loads were generated more often than fine and coarse bed loads and increased with distance from Lewiston Dam due to tributary contribution of fine sediments and flow in winter much more than in fall (Figure 71, Appendix J). At TRAL, suspended loads were limited to spring flow periods except during Klamath augmentation flows, Hoopa Boat Dance flows, and safety of dam releases; frequencies of suspended sediment discharges then increased dramatically at TRLG and TRDC as flow variability increased from tributary accretions. These trends also occurred with fine and coarse bed load, but the relative paucity of bed load transport outside the spring flow period made load comparisons between stations difficult, so differences in suspended load estimates are the focus here. Most years, suspended loads were around an order of magnitude higher at TRLG than TRDC, but the loads were similar at these stations in 2006, 2007, 2012, and 2017. Conversely, suspended loads at TRAL were more than an order of magnitude lower than at TRLG in all years. Suspended loads normalized by flow volumes in excess of threshold discharges collapsed load values for TRLG and TRDC, but the normalized loads at TRAL remained substantially below values for these stations, again suggesting grains  $< 0.5$  mm are in relatively short supply in the Lewiston reach.

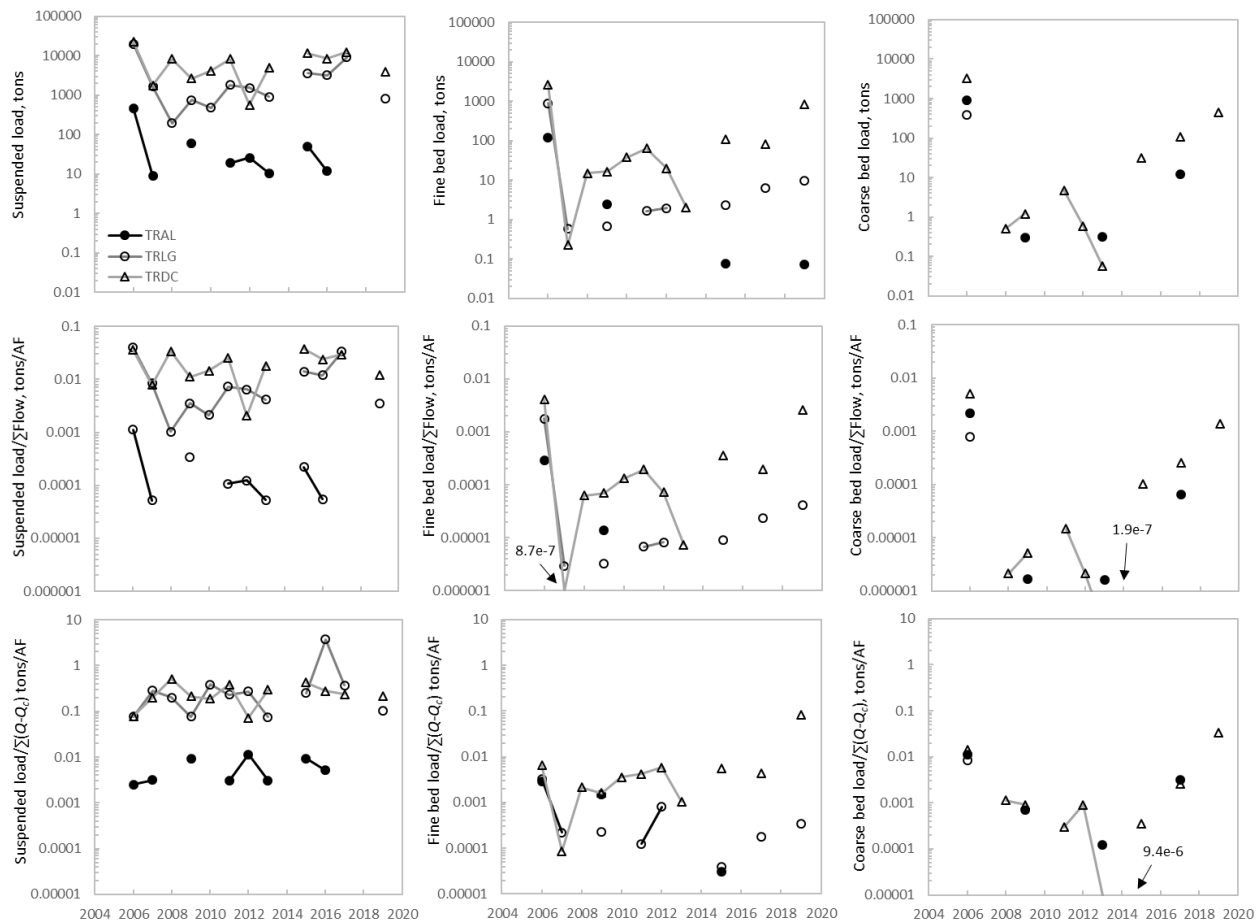


Figure 71. Suspended loads and fine and coarse bed loads estimated for times of year outside the computational period for spring flow releases (October 1–March 31, August 1–September 30) in WYs 2006–2019 using equations (10) and (11). Only non-zero loads are displayed. Lines connect loads for contiguous years.

### 6.2.5.3 Annual load estimates

Annual estimates of suspended sediment and fine and coarse bed loads increased with downstream distance from TRAL to TRLG and TRDC, and disparities in loads between stations inversely related to particle size (Figure 72). Using loads at TRAL as a baseline, coarse bed loads at this station were on average 111% (range 32-370%) and 31% (10-52%) of estimates for TRLG and TRDC, respectively. The percent difference between TRAL and TRLG further supports Gaeuman and Stewart’s (2017) contention that coarse sediments are in deficit in the Limekiln Gulch area for reasons explained above. Differences between loads at TRAL and the other stations were even greater for total fine sediment (suspended sediment + fine bed load), which at TRAL respectively averaged 13% (2-31%) of loads at TRLG and 4% (1-9%) of loads at TRDC. These percentages reflect suspended loads at TRAL that averaged only 15% of those at TRLG (6-27%) and 4% of those at TRDC (1-12%), and fine bed loads at TRAL that averaged 27% of those at TRLG (3-70%) and 8% in comparison to TRDC (2-12%). Disparities in coarse bed load and total fine sediment between stations occurs despite daily flows for the period of record (2006–2019) at TRAL being only 8% lower on average than at TRLG and 20% lower than at TRDC, with most differences in flow occurring at discharges below 1,000 cfs in fall and

winter (Figure 73). Altogether, these results indicate the largest disparity in loads between stations is in the size range of fine sediment. This is based on the channel distance and watershed area (in parenthesis) for contributing fines to the channel upstream of TRAL are respectively only 2.0 miles (10.2 mi<sup>2</sup>), as compared to 13.1 miles (91.6 mi<sup>2</sup>) at TRLG and 19.4 miles (212.6 mi<sup>2</sup>) at TRDC. Nonetheless, if size fractions were available for transport in proportion to the flow available to mobilize them, fractional loads scaled by flow volumes above critical discharges would collapse the data to similar trends between stations, but this only occurred for coarse bed load (Figure 71). Once again, the magnitude of disparity in scaled loads was highest for suspended sediment followed by fine bed load, providing yet additional evidence for the relative absence of fines in the Trinity River.

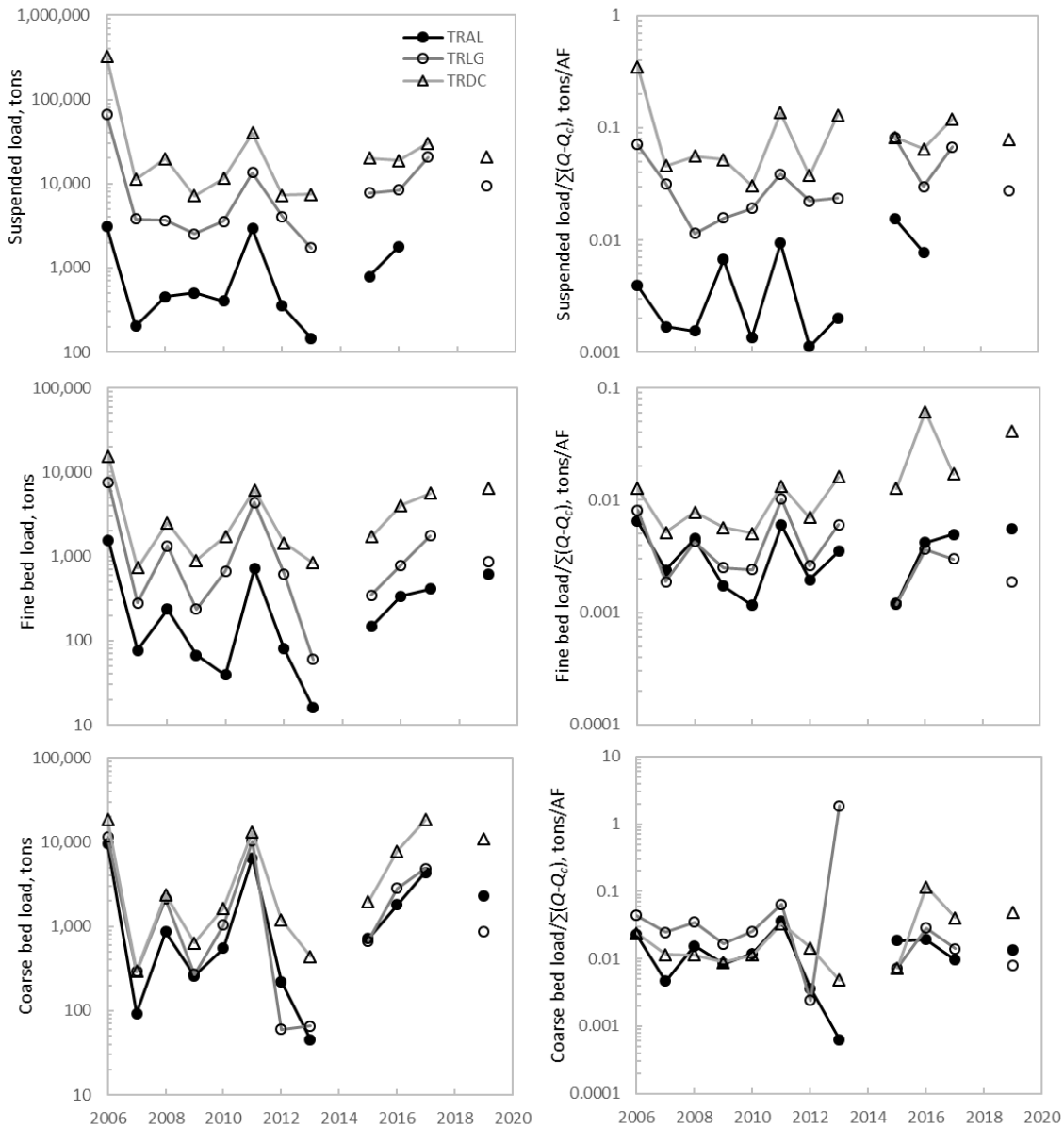


Figure 72. Annual (left panels) and flow-normalized loads (right panels) of suspended sediment and fine and coarse bed load at TRAL, TRLG, and TRDC (left panels). The normalizations were made with the volume of flow above critical discharges at each station. Lines connect loads for contiguous years.

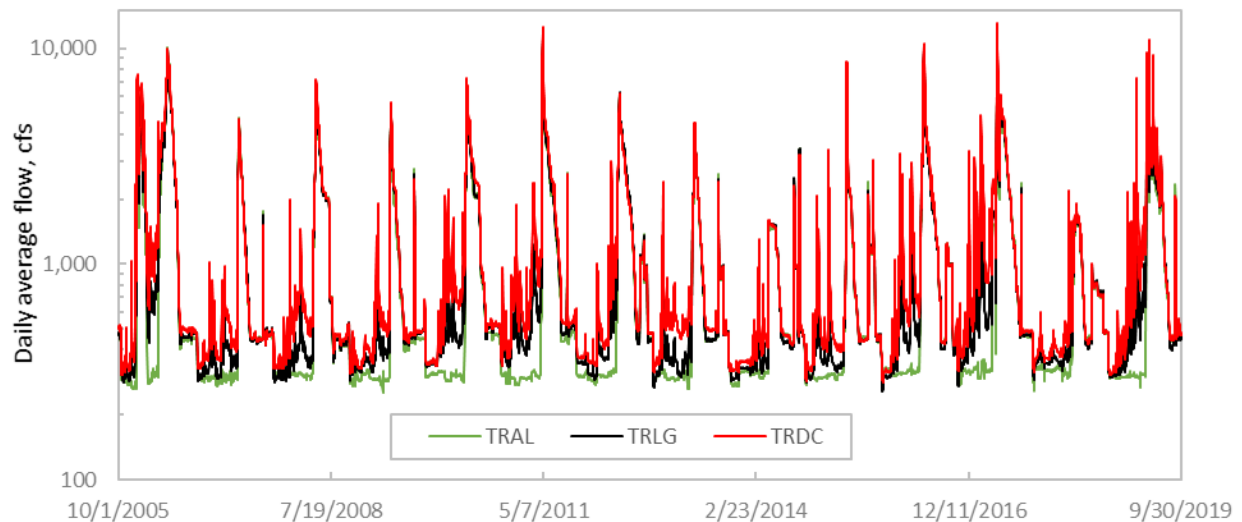


Figure 73. Daily average flows for the period of record that sediment loads were calculated at TRAL, TRLG, and TRDC (WY 2006–2019).

Except in 2012–2015,  $\geq 60\%$  of the total annual loads at TRAL, TRLG, and TRDC and nearly all fine and coarse bed load transport occurred during spring flows (Figure 74). Conversely, suspended loads during spring flows were typically only 40% or more of the total annual load for these sized particles because they are delivered by tributaries for transport in the Trinity River outside spring flow periods when their relatively low thresholds for mobility are commonly exceeded (Figure 73 and Appendix J). The percentage of annual suspended loads that occur during spring flows decreases with upstream distance from TRDC, which reflects that river flows are relatively unaffected by tributaries and a comparative paucity of fines are available for transport with proximity to Lewiston Dam. The delayed transport of most the annual loads until spring flow releases from Lewiston Dam results in temporal storage of sediment delivered by tributaries in deltas and the mainstem channel (Figures 73–75). The interruption in sediment routing can result in fine sediments depositing on the bed surface, which, as mentioned above, has negative implications for salmonid eggs that rely on intergravel flows through redds and bed forms to deliver oxygenated water for respiration during incubation in the fall through winter period (Tonina and Buffington, 2009). Reductions in intergravel flow also impede intergravel storage and hyporheic cycling of marine-derived nutrients delivered to the river by salmonid spawners (Buxton et al., 2015b). These effects of mainstem flows being out-of-sync with tributary flows would be avoided by scheduling higher than baseflow releases from Lewiston Dam in winter when sediment transport occurs on tributary channels. This paper is not the first to highlight benefits of synchrony in mainstem and tributary flows; the advantages were published two decades prior in the Trinity River flow study (USFWS and HVT, 1999).

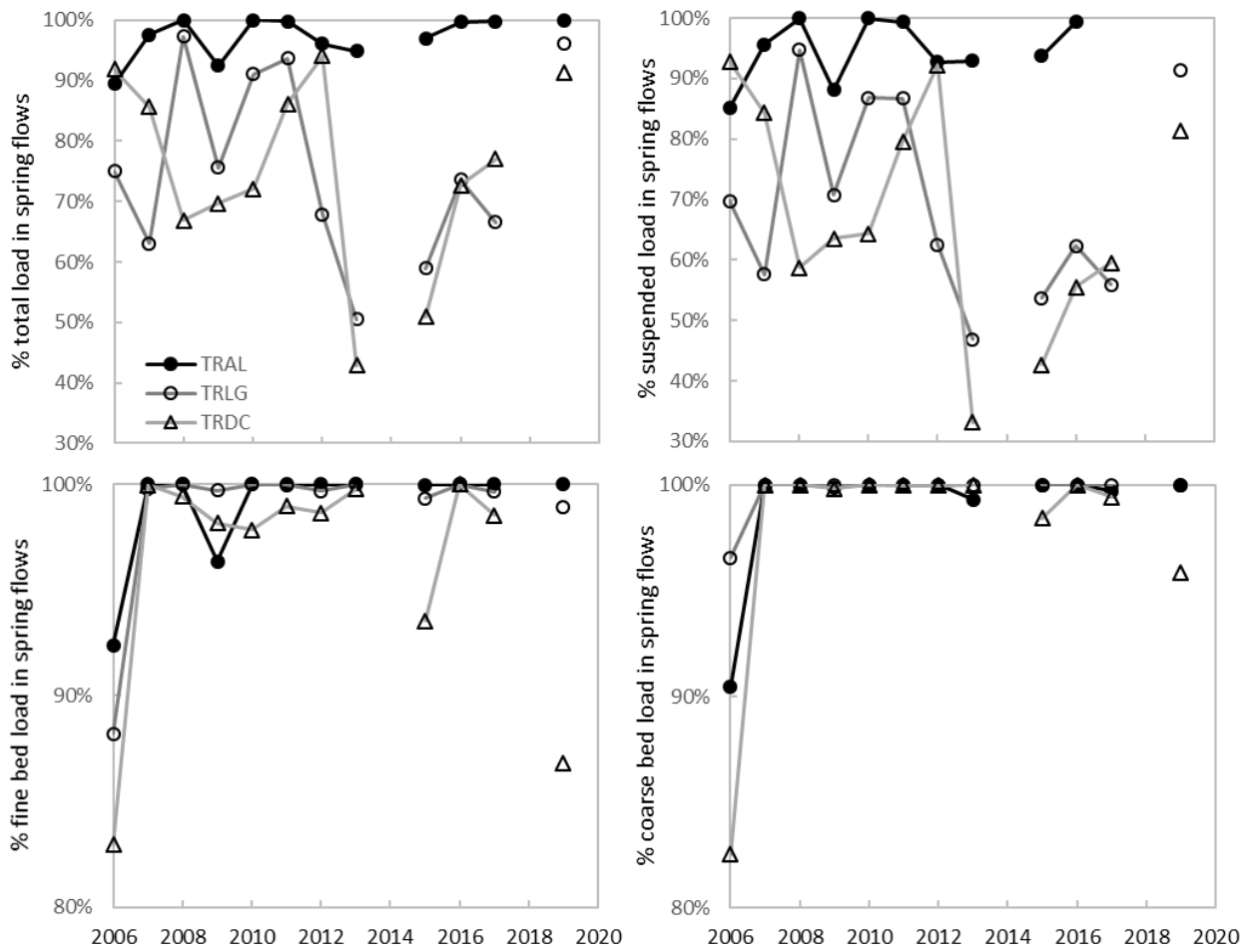


Figure 74. Percentages of the total annual load and fractional loads transported during spring flow releases (4/1–7/31) at TRAL, TRLG, and TRDC. Lines connect percentages for contiguous years.



Figure 75. Deltas in March 2019 (left panels) where Deadwood Creek (a.) Hoadley Gulch (b.), and Indian Creek (c.) confluence with the Trinity River. The right panels show the same areas in August 2019 after the spring flow release evacuated the deltas. Fines from turbidity plumes that were coincident with formation of the Deadwood Creek delta deposited on the channel bed in the Lewiston reach in winter when Lewiston Dam releases are 300 cfs (lower panels, photos taken March 2019). This resulted in several inches of organic soil and silt mud capping the winter baseflow channel at TRAL.

Decreases in suspended sediment transport on the Trinity River following dam closure were large, as total suspended loads at TRAL declined from between 65,765 and 420,000 tons in WYs 1956–1960 (before Trinity Dam closure) to 1,800 tons in WY 1961 after closure (Hawley and Jones, 1969; Knott, 1974). A comparison of the total suspended load (all suspended particles, regardless of size) in WY 1961 to those in WYs 2006–2019 after normalizing by annual flow indicates that even wet and extremely wet water years in the post-ROD period do not reach the normalized suspended sediment load for the critically dry WY 1961 (Figure 76). Restricting the comparison to dry water years post-ROD (transport is not monitored in critically dry years) indicates the average load ( $9.3 \times 10^{-4}$  tons/AF) is almost a magnitude-of-order lower than the load in WY 1961 ( $8.1 \times 10^{-3}$  tons/AF) despite peak discharges being 4 to 7 times greater in the dry water years (Figure 77).

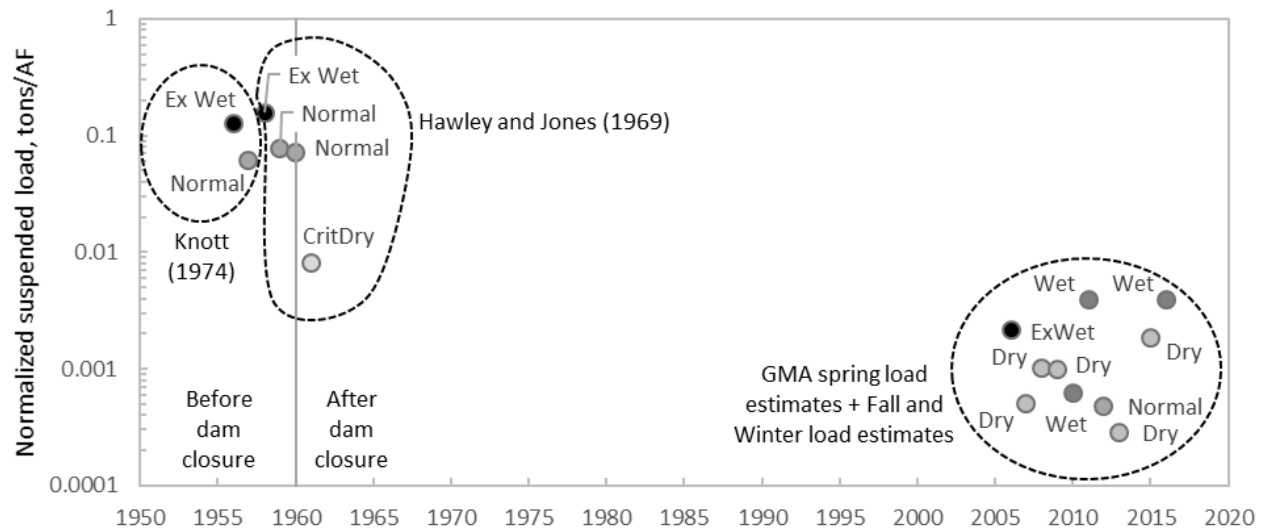


Figure 76. Flow normalized suspended sediment loads at TRAL before and after Trinity Dam closure in November 1960. a.

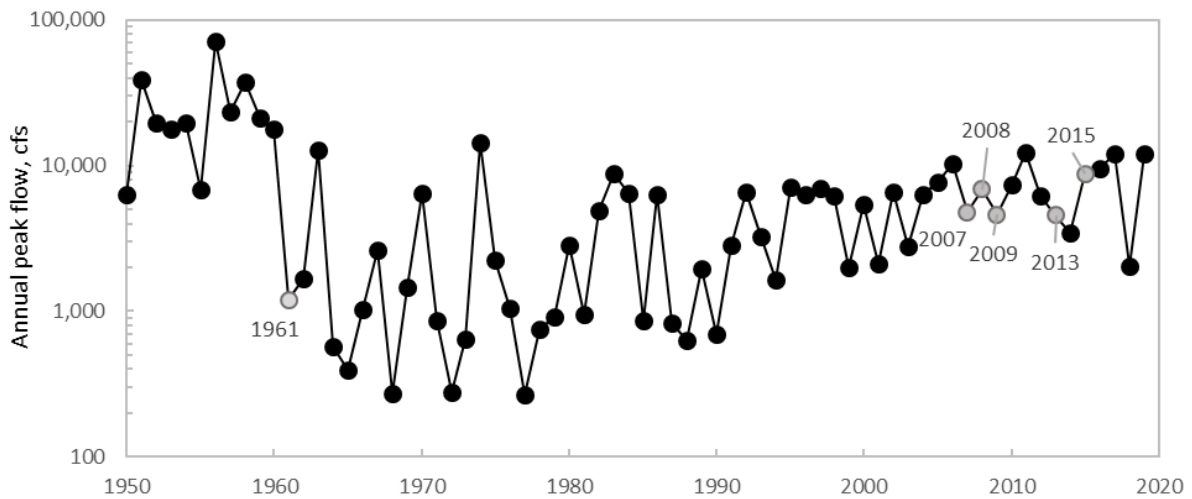


Figure 77. Peak annual discharges at TRAL for WY 1950–2018. Data labels indicate annual floods that occurred the first year after Trinity Dam closure (WY 1961) and dry water years after 2006 with suspended load estimates that are compared to the critically dry WY in 1961.

Whereas reductions in total suspended loads at TRAL primarily resulted from Trinity Dam closure and flow diversions via Carr Tunnel, suspended loads at TRLG have likely been reduced most by fine sediment abatements on Grass Valley Creek, including watershed restoration, construction of Buckhorn Dam, and operation of Wellock and Hamilton ponds (Section 5.3). Evidence for Grass Valley Creek being the principal contributor of suspended sediment at TRLG is that annual loads at this station tracked loads at Fawn Lodge on Grass Valley Creek from 1982–1991, according to USGS data in Milhouse (1994; Figure 78). The correlation in loads between these stations continued past 1984 and 1989, the respective years that operation of Wellock and Hamilton ponds began, likely from transport of fines stored in the mainstem channel and floodplain areas. Annual suspended loads at TRLG have since decreased from an average of 47,035 tons (range 1,476 to 315,916 tons) in 1982–1991 to 9,942 tons (1,185 to 54,075 tons) in 2006–2019 as a gravel-bed channel was progressively restored on the Trinity River (see Section 3.3.7). The post-ROD decrease in suspended sediment is also evident in normalized loads (by annual flow volume) for the respective periods notably decreasing through time for normal and wetter water years and slightly lowering for dry and critically dry water years (Figure 79), indicating that loads decreased in proportion to the flow available to transport them. The decrease in normalized loads reflects the reduced availability of fine sediment in the Trinity River, which occurred despite the average annual peak flow respectively doubling from 3,500 to 7,033 cfs between 1982–1991 and 2006–2019.

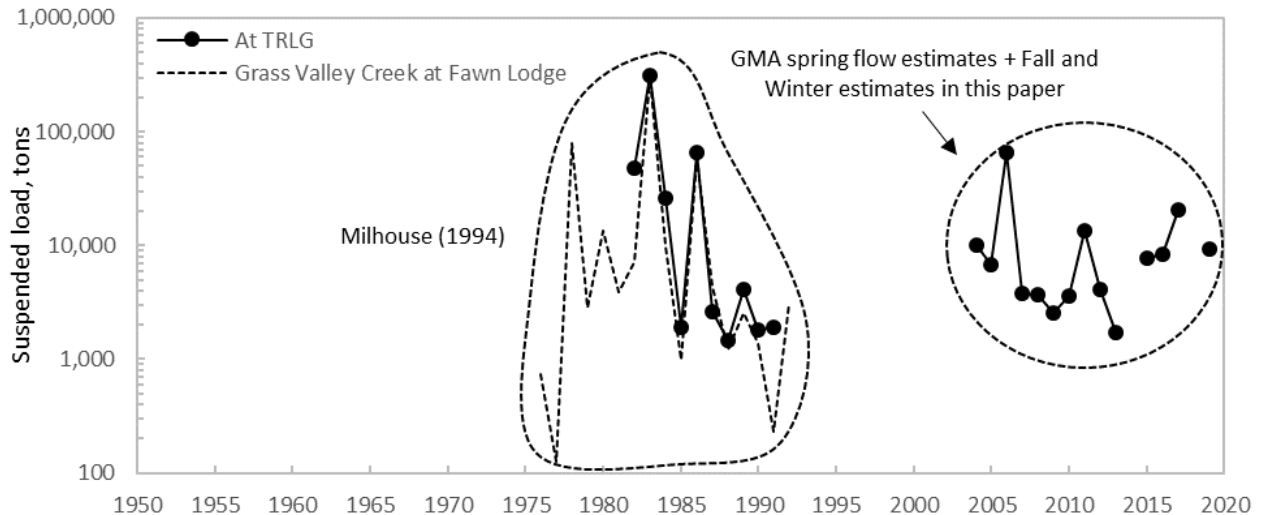


Figure 78. Suspended sediment loads at TRLG and Grass Valley Creek at Fawn Lodge. For the period that data were available, Grass Valley Creek was the primary contributor of suspended material to TRLG.

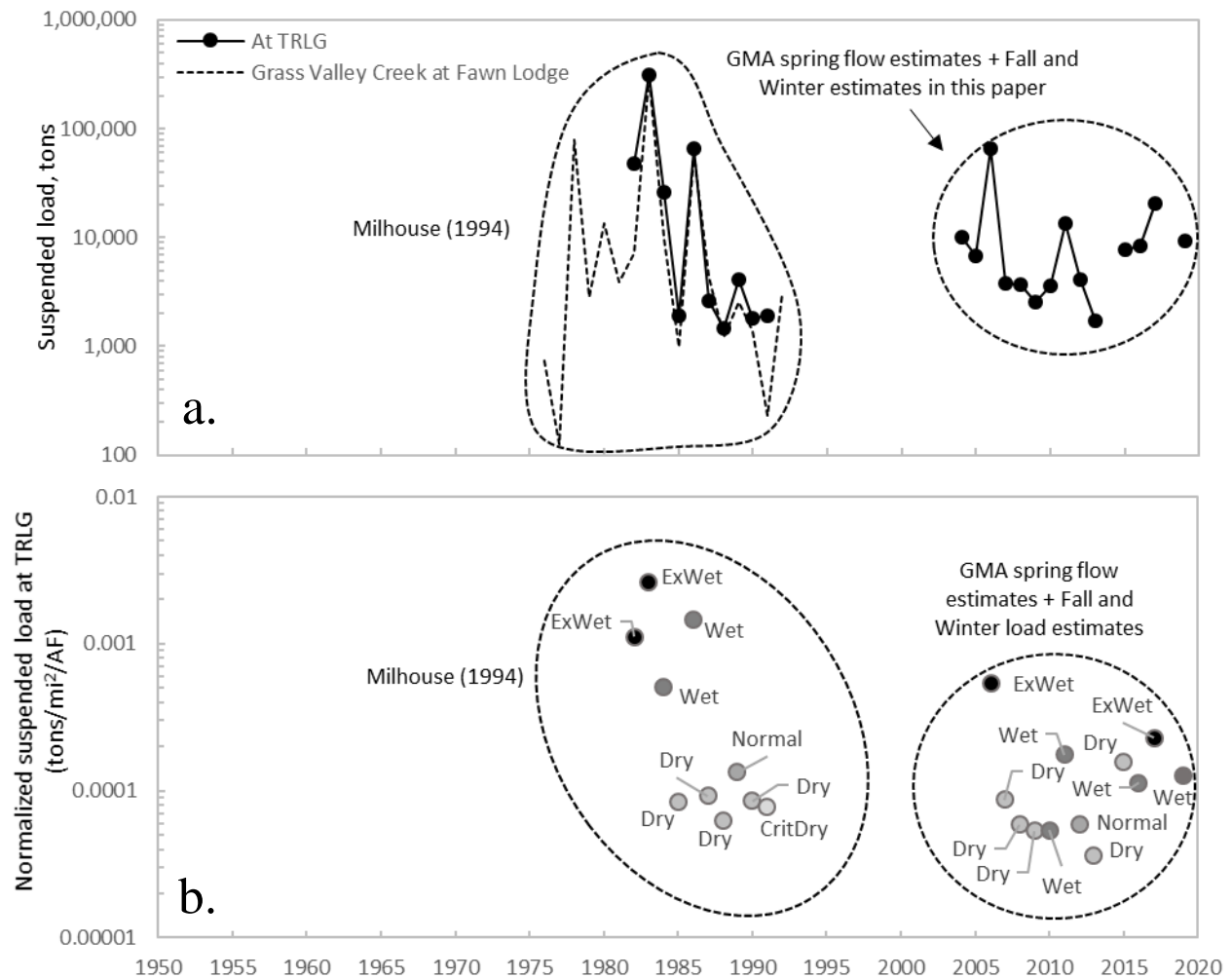


Figure 79. Annual suspended loads at TRLG and Grass Valley Creek at Fawn Lodge (a.) with values standardized by drainage area and annual flow volumes at TRLG (b.). Points in the lower panel are colored respective to their water year designation.

### 6.2.6 Turbidity

Turbidity is a measure of light that is scattered in water due to the presence of impurities, including fine sediments. Suspended sediment-laden flows exhibit turbidity that can be on the order of 100 to several thousand units, but perfectly solute-free water does not exhibit zero turbidity because even water molecules scatter light. Other impurities that cause turbidity in lotic waters include dissolved organic matter, algae, plankton, and diatoms. The USGS measures turbidity year-round in hourly time steps at TRLG and on the Trinity River above North Fork Trinity River (TRNF) in NTUs. Turbidity has also been measured during spring flow releases at TRLG and TRDC by GMA in FNU. NTUs and FNUs are not equivalent because of differences in how each measures the scattering properties of impurities in water (see Section 4.1.4). Only turbidity measured in NTU at TRLG and TRNF is considered in this section because turbidity measurements in FNU during spring flow releases do not provide a consistent record for evaluation (Appendix L).

The average of the median daily values of turbidity at TRLG from 2003–2019 during high spring flow releases from Trinity and Lewiston Dams (4.1 NTU) is more than double the average that occurs other times of year (1.8 NTU; Figure 80). The median values for spring flows are dominated by large spikes in turbidity that occurred during spring flows in 2005, 2006, 2015, 2016, and 2019 (Figure 79). Nonetheless, annual median values of turbidity at TRLG when winter and summer baseflows are released from the dams exceed median values for the spring flows in six of 13 years, or about half the time. Moreover, annual average turbidity normalized by daily average flows outside the spring flow release periods (0.0046 NTU/cfs) more than doubled the average normalized value for spring flows (0.0020 NTU/cfs). The elevated turbidity during relatively low flows in fall and winter results from tributaries delivering most of the annual suspended loads to the channel in these periods (Appendix M). What then results in a stepwise process of delivery and storage of turbidity-inducing materials in fall and winter followed by resuspension and mobilization of this material during high mainstem flows in spring (Figures 80 and 81). Fall and winter storage of these materials occurs when salmonid embryos are incubating in the bed, so that negative impacts to egg development may result. Storage of turbidity-inducing materials outside spring flow periods at TRNF is much less than at TRLG (Figures 82 and 83, Appendix N), according to average turbidity and normalized turbidity during spring flows (3.3 NTU, 0.0028 NTU/cfs) in the period of record for TRNF (10/1/2011–9/30/2019) being only slightly higher than the average for other times of year (3.0 NTU, 0.0017 NTU/cfs). The relative lack of storage of turbidity inducing materials in the vicinity of TRNF likely results from an increasingly natural flow regime as tributary flows accrete with distance from Lewiston Dam. For example, at TRNF, the average ratio of peak discharges during spring flow releases and periods outside spring releases is 1.17, indicating similar high flows in these periods (Figure 82).

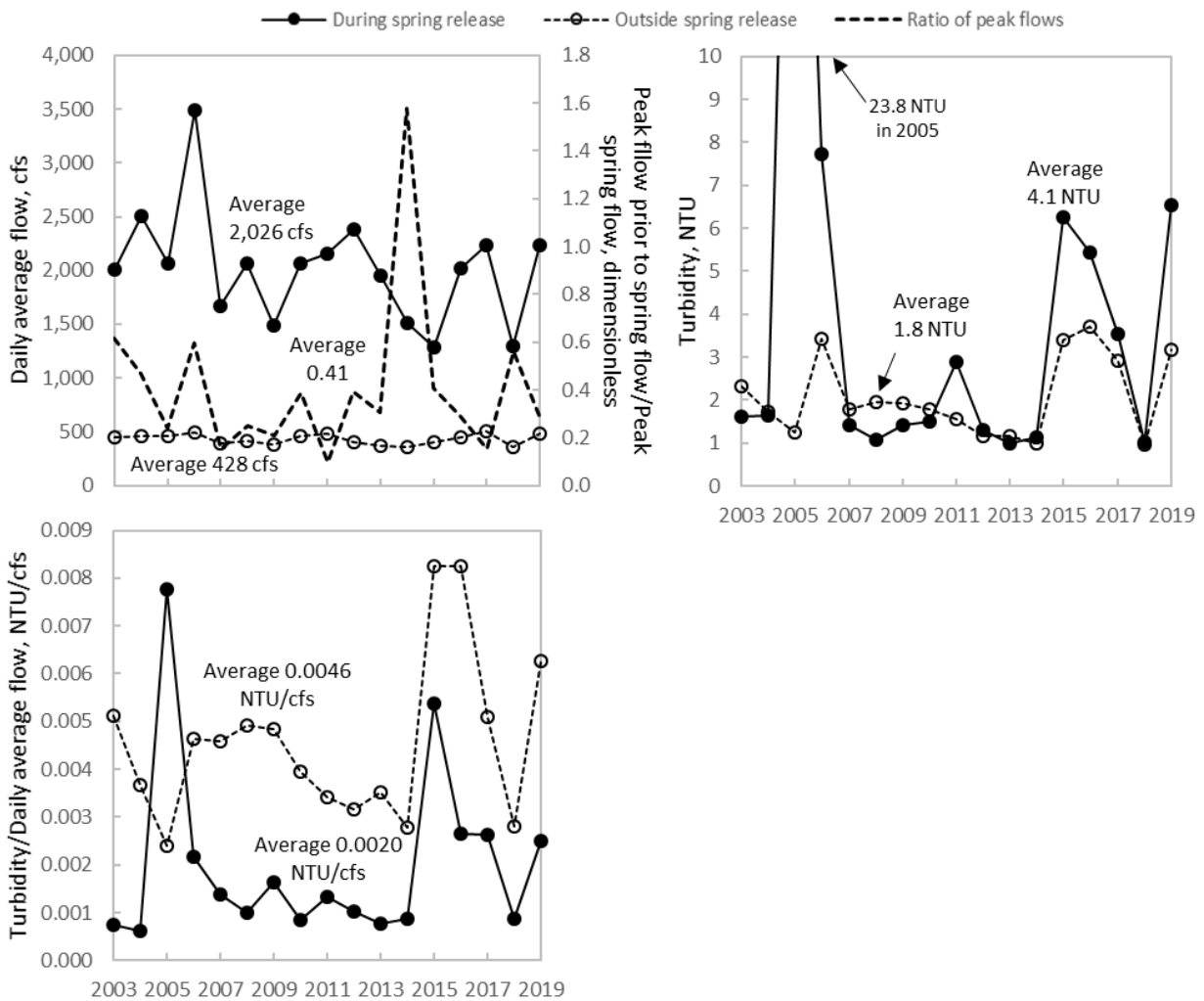


Figure 80. Median daily average flow and turbidity at TRLG during high spring flow releases from Trinity and Lewiston Dams and for periods outside the high flow releases. Ratios of peak flow in each time frame are indicated in the top right panel.

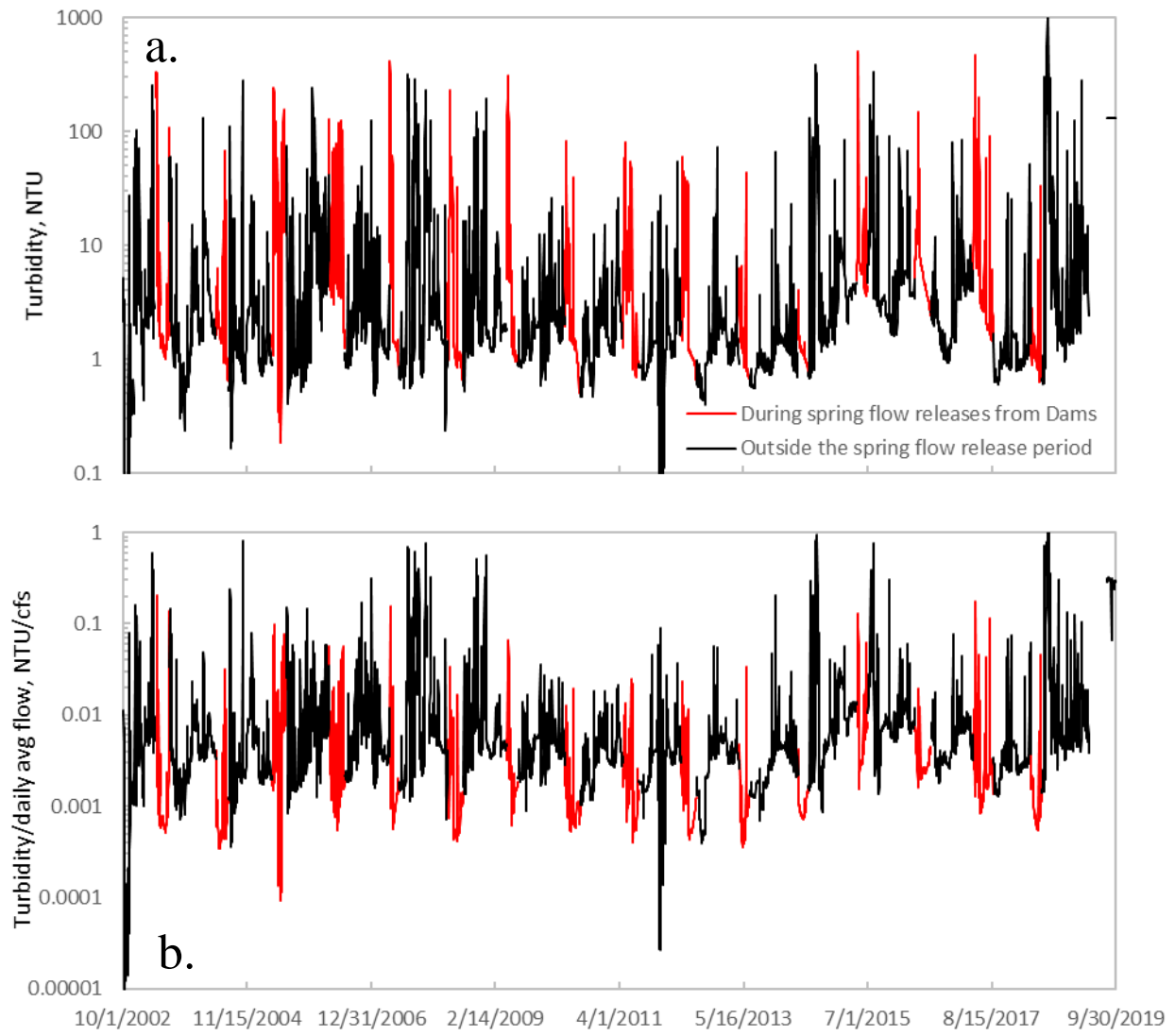


Figure 81. Daily average turbidity (a.) and flow normalized turbidity at TRLG (b.).

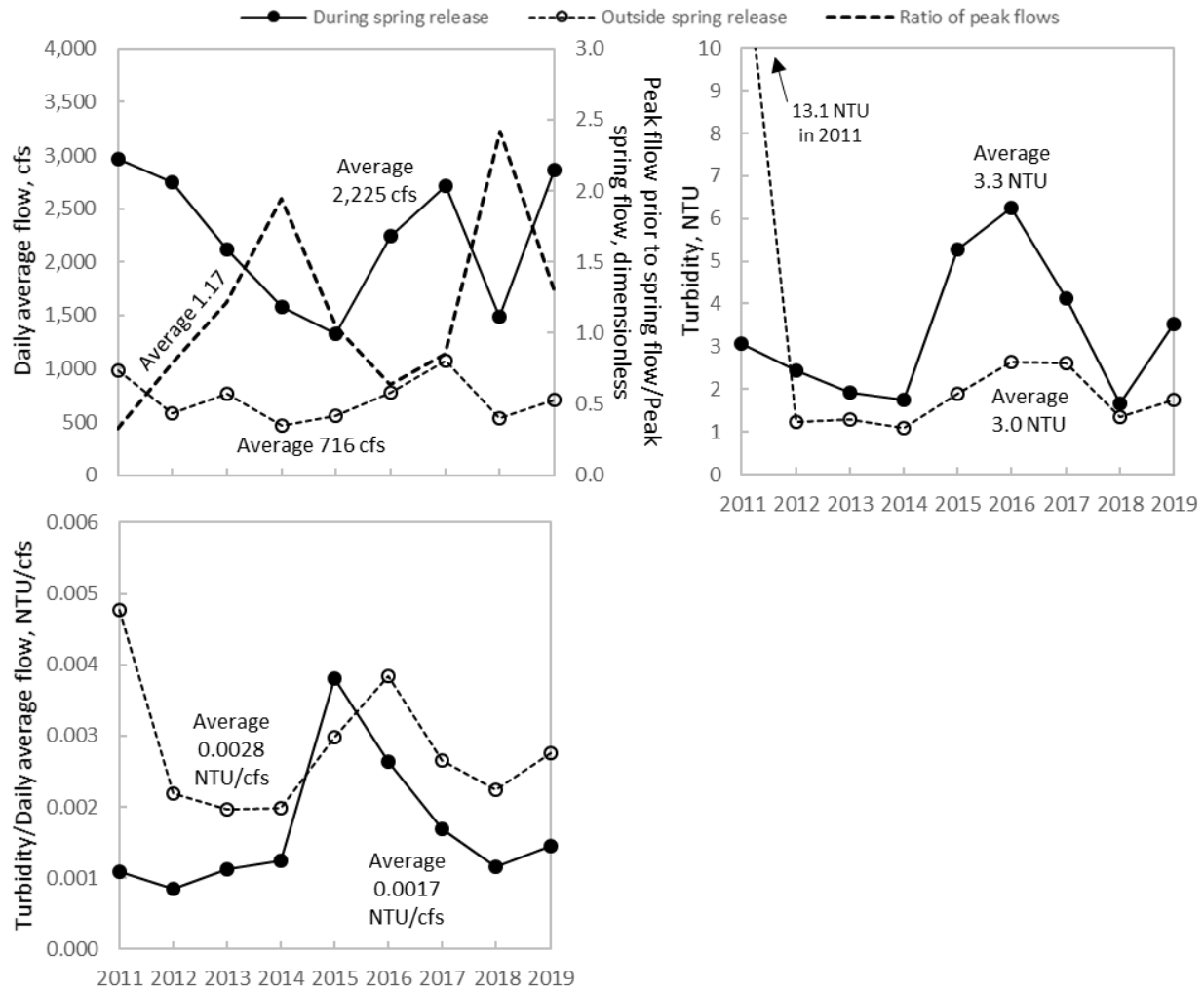


Figure 82. Median daily average flow and turbidity at TRNF during high spring flow releases from Trinity and Lewiston dams and for periods outside the high flow releases. Ratios of peak flow in each time frame are indicated in the top right panel.

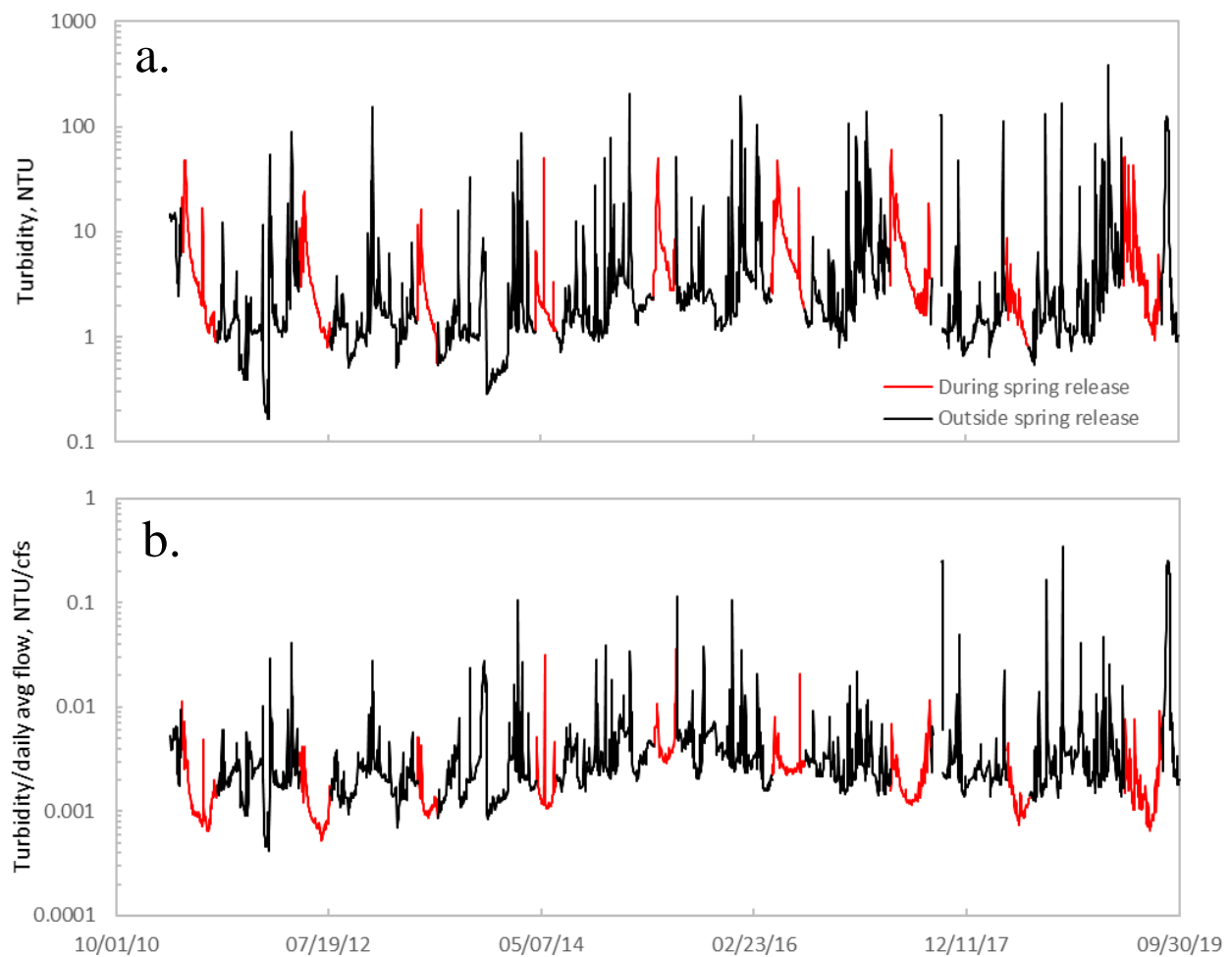


Figure 83. Daily average turbidity (a.) and flow normalized turbidity at TRNF (b.).

## 7. Application of fine sediment targets

Bulk subsurface sediment samples taken in the 1990s (see Figure 50) and photographic evidence from as early as the mid-1970s shows the Trinity River heavily impacted by fines (see Figures 14 and 20-23). In following years, remediation of these conditions was primarily accomplished through decreased logging and improved logging practices (Section 3.1.4), watershed restoration (Section 3.3.2), operation of Buckhorn Dam and Hamilton Ponds on Grass Valley Creek (Section 5.3), and flushing flows that were released on the Trinity River starting in the mid-1990s (Wilcock et al., 1995). Fine sediments were also reduced in the Trinity River by ROD flow releases that began in spring 2004 and mechanical channel rehabilitation projects that began in summer 2005 (USFWS and HVT, 1999). As a result of these actions, the availability of fine sediment in the Trinity River has been dramatically lowered and targets are now overwhelmingly met, as demonstrated below. However, fine sediment abatements have been overly successful in some areas of the river as determined by assessment of targets listed in Table 2. The deficit is particularly strong at and upstream of TRAL (RM 110.2) and extends to Rush Creek confluence, and indications from several targets are that deficits exist as far downstream as Junction City (RM 80.3).

The target for spawning gravel quality and incubation success that fines  $\leq 2$  mm compose  $<15\%$  in subsurface bulk samples in spawning areas was surpassed at all stations that bulk samples were collected in 1991, with the peak exceedance being 30.8% at Steel Bridge. Ten years later in 2001, targets were met at Lewiston and near Rush and Indian Creeks but exceeded at all other stations downstream to Junction City (Table 7). Storage of fine sediments  $\leq 2$  mm in the subsurface portion of the channel then rapidly decreased so that targets were met at all stations in 2009. Since then, percentages have varied between 1.1% and 19.1% at all stations, with overages averaging only 1.5%, and targets have been met at the majority, but not all stations from 2014 to present. Notably, targets have been met upstream of Steel Bridge since 2009, excepting Poker bar in 2014 (16.4%) and Lewiston in 2019 (15.5%). Results for Lewiston are particularly informative, as they show the large contribution of fine sediment to the Trinity River that resulted from the Carr Fire in Deadwood Creek (Section 5.1.3; also see Figure 75) only exceeded the target by 0.5%. Prior to the fire,  $\leq 2$  mm grains ranged 0.4 to 6.6% at Lewiston (average 2.7%) from 2000–2014, with the peak value in 2009 resulting from channel reconstruction work that was undertaken in the upper portion of the reach in 2008. These fines quickly evacuated, as the percentage of fines  $\leq 2$  mm decreased within 6 years to 1.1%. Rapid storage and evacuation of fine sediment pulses in the Lewiston area is indicative of open pore space in the bed for rapid storage and the lack of a consistent upstream supply for storage maintenance. This combined with chronically low percentages of fines at TRAL indicate a deficit of fine sediment in this area that likely extends downstream to Rush Creek.

Table 7. Percent of sediment  $\leq 2$  mm in bulk subsurface samples used to evaluate substrate quality targets for salmonid egg incubation ( $<15\%$ ) and benthic macroinvertebrates ( $<30\%$ ). Cells shaded light or dark grey respectively indicate values that exceed targets for incubation and macroinvertebrates.

Station	Water year							
	2019	2018	2014	2009	2001	2000	1997	1991
Lewiston (RM 111.5)	15.5%	—	1.1%	6.6%	2.5%	0.4%	---	—
at Rush Creek (RM 107.4)	—	14.7%	14.9%	9.9%	13.1%	—	---	16.0%
Poker Bar (RM 102.7)	—	9.5%	16.4%	14.5%	30.0%	—	---	—
Steel Bridge (RM 99.0)	—	10.1%	10.1%	10.0%	15.7%	—	---	45.8%
Indian Creek (RM 95.3)	—	19.1%	15.8%	13.0%	14.7%	—	---	23.1%
Upper Steiner Flat (RM 92.0)	—	15.1%	2.5%	11.6%	15.7%	—	8.6%	—
Evans Bar (RM 84.1)	—	13.8%	8.3%	8.6%	20.1%	—	---	—
Junction City (RM 80.3)	—	17.3%	16.0%	8.8%	16.6%	—	---	—

Benthic macroinvertebrates are the primary food for juvenile salmonids in the early rearing period, and interstitial spaces in streambeds are habitat for macroinvertebrates in most of their lifecycle. Macroinvertebrate habitat decreases as interstitial spaces in the bed fill with fine sediment, and Relyea et al. (2000) reports that peak macroinvertebrate abundance occurs when fines  $\leq 2$  mm are  $<30\%$  of subsurface bulk grain-size distributions, which is the target applied to areas that substrate sampling occurs on the Trinity River (i.e., riffle, glide, and run habitats). The available data indicate this target was only exceeded in two years and stations on the Trinity River (30% at Poker Bar in 2001; 45.8% at Steel Bridge in 1991). Percentages that met the target for macroinvertebrates are as summarized for spawning gravel quality above. Embeddedness of grains exposed on the bed surface (see Figure 25) is an additional measure of habitat availability for benthic macroinvertebrates, and photographic evidence suggests that embeddedness on the

Trinity River is commonly above the target value of  $\leq 33\%$  outside of pools (see Figures 2, 20-22, and 53). However, embeddedness has not been measured on the Trinity River so quantitative evaluation of this target cannot be made here.

Observed levels of fine sediment in subsurface areas of the Trinity River resulted in the targeted Chinook egg-to-fry survival ( $\geq 80\%$ ) estimated with equation (1) to be met at all stations in 2018–2019 and in 78% of samples in the period of record (Table 8). Estimates of survival ranged from 0% at Steel Bridge in 1991 to 100% at Lewiston in 2019 and averages for the 2001 to 2019 data were highest at Lewiston (96%) and lowest at Poker Bar (64%). Relatively low survival at Poker Bar likely reflects continued storage of sediments originating from Grass Valley Creek, which is located directly upstream of this site. Egg-to-fry survival also decreased slightly at Rush and Indian Creeks compared to the next upstream stations due to contributions of fine sediments by these streams. This result and percent fines  $\leq 2$  mm and  $\leq 8$  mm in subsurface area at the sampling stations (see Table 7 and Figure 50) indicate that tributaries function as point source inputs of fines that are dispersed and stored in downstream areas, and that inputs of fines from floodplains, bank collapse, and other mainstem sources on the Trinity River are relatively lacking. Consider that if these inputs were significant and fine sediments were transport limited, their proportions would be largely unchanged in the vicinity of tributary junctions because the added supply would be stored on instead of in the bed and simply add to the transport limitation. Instead, the Trinity River exhibits a supply limitation as tributary fines are rapidly assimilated to cause only a brief (in time (e.g., at Lewiston) and channel distance) increase in storage near tributary delta areas. Limitations in the supply of fine sediment is further supported by the target for suspended sediment loads normalized by the cumulative discharge in the period when salmon eggs are incubating in redds (October 1–March 31;  $\leq 0.05$  tons/cfs) being met in all years at TRAL and the majority of years that transport was measured at TRLG and TRDC (Table 9). Altogether, these results indicate the incubation environment for salmonid eggs in the Trinity River strongly support successful development and emergence of fry.

Table 8. Percent egg-to-fry survival estimated for Chinook with equation (1) by Tappel and Bjornn (1983). The target is  $\geq 80\%$ ; shaded cells indicate years when the target was not met.

Station	Water year								
	2001-2019 average	2019	2018	2014	2009	2001	2000	1997	1991
Lewiston (RM 111.5)	96%	100%	—	95%	92%	97%	94%	—	---
at Rush Creek (RM 107.4)	90%	—	84%	99%	90%	85%	—	—	76%
Poker Bar (RM 102.7)	64%	—	92%	75%	81%	7%	—	—	—
Steel Bridge (RM 99.0)	86%	—	89%	87%	88%	78%	—	—	0%
Indian Creek (RM 95.3)	83%	—	87%	75%	90%	80%	—	—	85%
Upper Steiner Flat (RM 92.0)	87%	—	89%	100%	84%	73%	—	90%	—
Evans Bar (RM 84.1)	84%	—	92%	90%	95%	59%	—	—	—
Junction City (RM 80.3)	85%	—	88%	78%	93%	82%	—	—	—

Table 9. Suspended loads normalized by the sum of discharges (tons/cfs) during the egg incubation period (October-March) on the Trinity River. The target is  $\leq 0.05$  tons/cfs; shaded cells indicate years when the target was not met.

Water year	Station		
	TRAL	TRLG	TRDC
2006	0.003	0.089	0.078
2007	<0.001	0.018	0.016
2008	<0.001	0.007	0.080
2009	<0.001	0.006	0.021
2010	<0.001	0.006	0.037
2011	<0.001	0.014	0.056
2012	<0.001	0.011	0.006
2013	<0.001	0.007	0.037
2014	—	—	—
2015	<0.001	0.024	0.069
2016	<0.001	0.033	0.061
2017	<0.001	0.084	0.068
2018	—	—	—
2019	<0.001	0.007	0.029
Average	<0.001	0.025	0.046
High value	0.003	0.089	0.080

Upon exiting the streambed, juvenile salmonids begin feeding to gain weight and fitness to increase their chances of survival. Salmonids feed by locating prey by eye and require a certain level of water clarity to feed by sight, which makes turbidity levels during the rearing period an important consideration regarding fine sediment in the Trinity River. As such, a somewhat low turbidity target (<30 NTU) was set for the majority (>85%) of the rearing period (January–July). With turbidity >30 NTU, fish may be displaced from their preferred location for feeding and setting the targeted duration of such displacement to <15% of the rearing period limits this impact. The turbidity target was assessed for spring flow releases with data measured by GMA at TRAL, TRLG, and TRDC and for the entire rearing period with data measured by the U.S. Bureau of Reclamation (USBR) at TRLG and TRNF (Table 10). Equipment failures and the limited period of spring flows compared to the duration of the rearing period caused GMA data to only cover 8–89% percent of the rearing period, as opposed to 61–100% of the rearing period covered by USBR data. Nonetheless, results indicate the turbidity target was met in all years at all stations except in 2002–2003 and 2005–2006 at TRLG, according to USBR data. In these years, the duration that turbidity exceeded 30 NTU was <0.1% to 8% of the rearing period. Otherwise, turbidity targets were overwhelmingly met as durations of exceedance indicated low to no impacts to juvenile fish rearing from suspended sediment transport on the Trinity River. Furthermore, the occurrence of turbid flow at TRLG, TRDC, and TRNF in all years that such measurements were taken indicates an availability of fines for nutrient binding, which satisfies the target for nutrient storage.

Table 10. Percent of time in the juvenile rearing period (January–July) that daily average turbidity was measured at stations on the Trinity River<sup>1</sup> and percent of the available data that values were <30 NTU for >85% of the rearing period<sup>2</sup>. The target was met in all years except those indicated by shaded cells.

Water year	TRLG (GMA <sup>3</sup> )		TRLG (USBR <sup>4</sup> )		TRDC (GMA <sup>3</sup> )		TRNF (USBR <sup>5</sup> )	
	% time <sup>1</sup>	% data <sup>2</sup>	% time <sup>1</sup>	% data <sup>2</sup>	% time <sup>1</sup>	% data <sup>2</sup>	% time <sup>1</sup>	% data <sup>2</sup>
2001	—	—	61%	90%	—	—	—	—
2002	—	—	100%	83%	—	—	—	—
2003	—	—	95%	85%	—	—	—	—
2004	13%	100%	100%	98%	—	—	—	—
2005	8%	100%	99%	80%	—	—	—	—
2006	30%	100%	100%	77%	89%	94%	—	—
2007	43%	100%	100%	95%	43%	100%	—	—
2008	48%	100%	99%	91%	26%	100%	—	—
2009	57%	100%	99%	95%	20%	100%	—	—
2010	27%	100%	100%	98%	45%	100%	—	—
2011	45%	100%	100%	92%	44%	94%	64%	97%
2012	40%	100%	100%	94%	33%	100%	100%	98%
2013	48%	100%	100%	100%	25%	100%	100%	100%
2014	32%	100%	100%	98%	20%	100%	100%	98%
2015	31%	100%	100%	94%	15%	100%	100%	98%
2016	53%	100%	100%	96%	42%	100%	100%	96%
2017	52%	100%	100%	89%	56%	100%	100%	95%
2018	—	—	100%	92%	—	—	100%	100%
2019	53%	99%	84%	93%	22%	96%	100%	94%

<sup>3</sup>Turbidity measured by GMA during spring flow releases (Appendix L).

<sup>4</sup>Turbidity measured year-round by the U.S. Bureau of Reclamation (Appendix M).

<sup>5</sup>Turbidity measured year-round by the U.S. Bureau of Reclamation (Appendix N).

Severity-of-ill ( $z$ ; equation 4) impacts to salmonids were targeted as  $z \leq 5$  for  $\geq 80\%$  of the rearing (January–July) and spawning period (September–January) for adult and juvenile salmonids, respectively (USFWS and HVT, 1999). As explained above, a value of 5 is associated with “minor physiological stress and increased rates of coughing and respiration”, but the actual impact to fish resulting from suspended sediments  $\leq 0.25$  mm (the size range used to derive equation 1) on the Trinity River would be lower because suspended loads in this size range are less than loads for grains  $< 0.5$  mm that are measured on the Trinity River and used in the calculations. The actual impacts to fish are therefore expected to fall under at most the next lower  $z$ -value of 4 that is associated with a “short term reduction in feeding success”. Results indicate the target for the juvenile rearing (January–July) was met in all years that suspended sediment samples were taken on the Trinity River since 2006 at TRAL and TRLG, and the target was only missed in this period at TRDC in 2006 (58% of time) and 2017 (81% of time; Table 11). Evaluation of the target  $z$ -value for adult spawning yielded slightly better results, as the only exceedance occurred at TRDC in 2006 (78% of time). In the upstream direction from TRDC, the average percent and the high and low percentages of time that  $z$  was  $\leq 5$  increased for both juvenile rearing and adult spawning periods, which indicates an increasing paucity of fines with proximity to Lewiston Dam.

Table 11. Percentages of time that daily average values of severity-of-ill ( $z$ , equation 4) were  $\leq 5$  in the juvenile rearing (January–July) and adult spawning (September–January) periods for salmonids in the Trinity River. The target is  $\geq 80\%$ ; shaded cells indicate years when the target was not met.

Water year	Juvenile Chinook (January – July)			Adult Chinook (September – January)		
	TRAL	TRLG	TRDC	TRAL	TRLG	TRDC
2006	100%	81%	58%	100%	89%	78%
2007	100%	92%	92%	100%	94%	97%
2008	100%	93%	83%	100%	99%	90%
2009	100%	96%	91%	100%	100%	100%
2010	100%	97%	85%	100%	99%	94%
2011	100%	91%	85%	100%	99%	94%
2012	100%	95%	96%	100%	98%	100%
2013	100%	97%	90%	100%	99%	91%
2014	—	—	—	—	—	—
2015	100%	92%	93%	100%	93%	95%
2016	100%	86%	82%	100%	99%	95%
2017	—	81%	71%	—	93%	93%
2018	—	—	—	—	—	—
2019	—	91%	90%	—	100%	100%
Average	100%	91%	85%	100%	97%	94%
High value	100%	97%	96%	100%	100%	100%
Low value	100%	81%	58%	100%	89%	78%

Fine sediment moderates the stability of streambed surfaces to benefit the river biome. If a bed is over-stabilized, biomatter can accumulate and reduce intergravel flow to the subsurface environment while under-stabilized beds may threaten salmonid eggs with scour. The moderating influence of fines on bed stability was clearly shown by Wilcock and Kenworthy (2002). In this work, critical Shields (1936) stresses for experimental beds that lacked fines ranged 0.024 (0.010 to 0.034) while critical values ranged only 0.010 (0.015 to 0.024) for matrix supported beds that exhibited 10% to 30% sand in the subsurface domain. To promote such mediation, targets for fines  $\leq 2$  mm are set as 5-12% in Wolman (1954) or bulk surface samples and 16-24% of subsurface bulk samples. Wolman (1954) samples taken before and after spring flow releases at TRAL, TRLG, and TRDC indicate the minimum target value of 5% fines  $\leq 2$  mm was only met before the spring flow release at TRDC in 2008 (Table 12). In all other years at these stations, fine sediment was in deficit on the bed surface according to the Wolman (1954) samples. Bulk surface samples taken at repeat sites indicated slightly more surface fines than the Wolman (1954) samples as would be expected based on the latter typically under-sampling small grains, but the target was still only met in 5 of 35 samples, with the only exceedance at Steel Bridge in 1991 (Table 13). Otherwise, fine sediments have not been sufficiently available at the sample sites to meet the target range, except for Poker Bar (7.5%) and Junction City (6.9%) in 2001. Similarly, bulk subsurface samples indicate the target percentages of fines was only met in 8 of 35 samples, with exceedances occurring at Poker bar in 2001 (30%) and Steel Bridge in 1991 (45.8%; Table 14). In total, these results again indicate that fine sediments  $\leq 2$  mm are in deficit at most sampling locations in the restoration reach of the Trinity River.

Table 12. Percentage of grains  $\leq 2$  mm in Wolman (1954) samples taken at sediment monitoring stations before and after spring flow releases on the Trinity River. Bold values are below the target range (5-12%) for gravel mobility. Dashes indicate values that were not measured.

Water year	TRAL	TRLG	TRDC
2006	—/0%	—/0%	—/4%
2007	—	—	—
2008	<b>1%/1%</b>	<b>2%/4%</b>	8%/4%
2009	<b>0%/0%</b>	<b>0%/0%</b>	<b>1%/0%</b>
2010	<b>0%/0%</b>	<b>1%/2%</b>	<b>0%/—</b>
2011	<b>0%/1%</b>	<b>1%/4%</b>	<b>2%/0%</b>
2012	<b>0%/1%</b>	<b>3%/3%</b>	<b>2%/1%</b>
2013	<b>0%/0%</b>	<b>0%/0%</b>	<b>4%/0%</b>
2014	—	—	—
2015	<b>0%/0%</b>	<b>0%/0%</b>	<b>0%/0%</b>
2016	<b>0%/0%</b>	<b>0%/0%</b>	<b>0%/0%</b>
2017	<b>0%/0%</b>	<b>0%/0%</b>	<b>0%/0%</b>
2018	—	—	—
2019	<b>0%/0%</b>	<b>0%/0%</b>	<b>0%/0%</b>

Table 13. Percentages of grains  $\leq 2$  mm in bulk surface samples at stations on the Trinity River. Bold values are below the target range and shaded cells indicate values that are above the target range (5-12%) for gravel mobility. Underlined values are within range. Dashes indicate unmeasured values.

Station	Water year							
	2019	2018	2014	2009	2001	2000	1997	1991
Lewiston (RM 111.5)	<b>1.8%</b>	—	—	<b>1.0%</b>	—	<b>0.7%</b>	—	—
at Rush Creek (RM 107.4)	—	<b>1.7%</b>	<b>4.6%</b>	<b>2.0%</b>	<b>1.8%</b>	—	—	<u>9.5%</u>
Poker Bar (RM 102.7)	—	<b>4.1%</b>	<u>7.5%</u>	<b>1.9%</b>	<u>6.9%</u>	—	—	—
Steel Bridge (RM 99.0)	—	<b>1.5%</b>	<b>0.4%</b>	<b>1.6%</b>	<b>4.3%</b>	—	—	21.7%
Indian Creek (RM 95.3)	—	<b>2.3%</b>	<b>3.9%</b>	<b>3.6%</b>	<b>1.8%</b>	—	—	<b>1.8%</b>
Upper Steiner Flat (RM 92.0)	—	<b>1.9%</b>	<b>0.2%</b>	<b>2.0%</b>	<b>2.1%</b>	—	<u>10.3%</u>	—
Evans Bar (RM 84.1)	—	<b>1.6%</b>	<b>1.5%</b>	<b>0.8%</b>	<b>2.5%</b>	—	—	—
Junction City (RM 80.3)	—	<b>0.9%</b>	<u>6.9%</u>	<b>0.8%</b>	<b>1.0%</b>	—	—	—

Table 14. Percentages of sediment  $\leq 2$  mm in bulk subsurface samples used to evaluate the target range for gravel mobility (16-24%). Bold values are below the target range and shaded cells indicate values that are above the target range for gravel mobility. Underlined values are within range. Dashes indicate unmeasured values.

Station	Water year							
	2019	2018	2014	2009	2001	2000	1997	1991
Lewiston (RM 111.5)	<b>15.5%</b>	—	<b>1.1%</b>	<b>6.6%</b>	<b>2.5%</b>	<b>0.4%</b>	—	—
at Rush Creek (RM 107.4)	—	<b>14.7%</b>	<b>14.9%</b>	<b>9.9%</b>	<b>13.1%</b>	—	—	<u>16.0%</u>
Poker Bar (RM 102.7)	—	<b>9.5%</b>	<u>16.4%</u>	<b>14.5%</b>	30.0%	—	—	—
Steel Bridge (RM 99.0)	—	<b>10.1%</b>	<b>10.1%</b>	<b>10.0%</b>	<b>15.7%</b>	—	—	45.8%
Indian Creek (RM 95.3)	—	<u>19.1%</u>	<b>15.8%</b>	<b>13.0%</b>	<b>14.7%</b>	—	—	<u>23.1%</u>
Upper Steiner Flat (RM 92.0)	—	<b>15.1%</b>	<b>2.5%</b>	<b>11.6%</b>	<b>15.7%</b>	—	<b>8.6%</b>	—
Evans Bar (RM 84.1)	—	<b>13.8%</b>	<b>8.3%</b>	<b>8.6%</b>	<u>20.1%</u>	—	—	—
Junction City (RM 80.3)	—	<u>17.3%</u>	<u>16.0%</u>	<b>8.8%</b>	<u>16.6%</u>	—	—	—

High percentages (>28%) of sediment  $\leq 2$  mm in composite bulk samples in slack water areas enables ammocoetes to burrow into the sediment where they will rear for 4 to 7 years before migrating to the Pacific Ocean for the adult phase of their lifecycle (Torgerson and Close, 2004). Ammocoetes will also rear in lee areas of the channel where fine sediment deposits are present. Unfortunately, surveys of the Trinity River channel have not been conducted to map areas where these sediment conditions exist, but Alvarez et al. (2015) mapped the presence and abundance of ammocoetes between RM 83.7 and 81.4 (near Sheridan) and RM 86.8 and 84.8 (near Dutch Creek) in January 2015 (Figure 84). The maps indicate that ammocoete rearing occurs throughout these reaches and so provide anecdotal evidence of substrate conditions that satisfy the fine sediment target for ammocoetes. Consequently, the fine sediment target for ammocoete rearing is considered met in reaches where surveys have been performed.

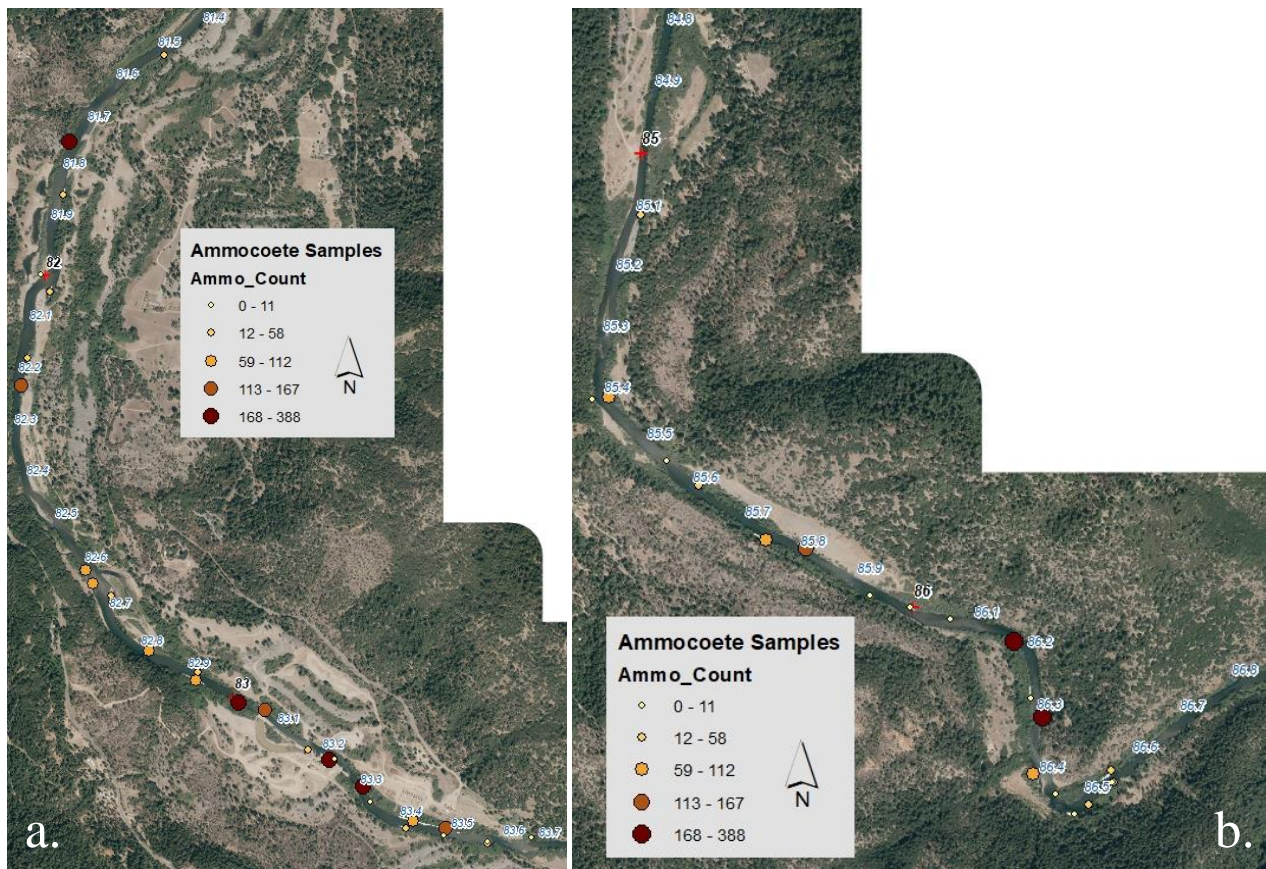


Figure 84. Ammocoete survey results on the Trinity River between RM 86.8-84.8 and RM 83.7-81.4 (from Alvarez et al., 2015). Numbers with white background indicate river miles on the Trinity River upstream from the confluence with the Klamath River.

Fine sediment targets addressed above are the only targets with data for evaluation on the Trinity River. The parameter  $V^*$  has not been quantified for pools on the river and fine sediment for colonization by riparian plants and channel meandering has not been measured on bars and floodplains (see Table 2). A recommendation is made in Section 9 for a pilot study to assess the feasibility of monitoring  $V^*$  in selected pools on the Trinity River and for systematic assessments of fine sediment storage on bars and floodplains for riparian establishment and channel meandering.

## 8. Summary of findings

Fine sediment contributions from Deadwood, Indian, and Rush creeks have varied through time and either decreased or remained stable in the period that data are available (WY 1997-2006) on these creeks and been near wholly eliminated by sediment capture in Hamilton Ponds on Grass Valley Creek (Figure 23 and 38, Table 5, Appendix C). This and ROD (2000) flow releases have therefore reduced fine sediments in the Trinity River over the past two decades to a degree that a deficit now occurs in some. This finding is supported by Wolman (1954) and bulk sediment samples showing strong declines in fine sediment and progressive armoring and sorting of bed surface sediments at stations throughout the restoration reach of the Trinity River (Figures 47-50). Diminished availability of fine sediments is also documented in bed load samples taken during spring flow releases that show increased skewness of grain-size distributions (lower skew=fewer fines), larger median bed load diameters, and lower proportions of fine sediment in the total loads (Figure 52). These changes are most apparent at TRLG and TRDC, and lesser at TRAL, where fines have been in deficit since at least 2006, excepting pulse inputs from channel reconstruction in 2008 (Figure 55) and wildfire in 2019 (see Figure 75). Further evidence of fine sediment reductions is provided by biological targets that require minimization of fines stored in the channel being met with only few exceptions upstream of Junction City (Tables 4, 6-7). Suspended sediment transport and turbidity targets for salmonid egg incubation and juvenile rearing have also been met throughout the restoration reach with only one exception since 2014 (Tables 4, 8-10). Surveys have nonetheless indicated that fine sediments are sufficiently present in lee areas of the channel to enable ammocoete rearing to occur in what appear to be good numbers in the middle portion of the restoration reach (Table 5, Figure 84). However, levels of fine sediment storage on and in active channel areas of the stream bed are well short of meeting targets for particle mobility (Tables 4, 11-13) and geomorphic processes, including bar mobility and scour, may be suppressed as a result.

Fractional loads have varied between years depending on their supply and discharges available for transport. After normalizing spring loads by the volume of spring flow releases and discharges in excess of mobility thresholds to isolate the effect of supply, linear regressions indicate that coarse bed load increased at TRDC, fine bed load decreased at TRLG, and suspended loads decreased at TRDC and increased slightly at TRAL (Figure 64). The latter result is due to reservoir bank erosion in 2015–2016 and not contemporary supplies of fine sediment since turbidity and suspended loads were not measured at this station in 2017–2019 (Appendix I). Normalized loads have otherwise remained approximately constant on average through time. Excluding 2012–2015, >60% of the total annual load (spring load + winter and fall loads) and nearly all bed load transport occurred during spring flows at TRAL, TRLG, and TRDC (Figure 74). Outside high flow releases from Trinity and Lewiston dams in spring, suspended sediments are the primary load constituent due to their low entrainment thresholds and the relative frequency of tributary flow events, safety of dam releases, Klamath augmentation flows, and Hoopa Boat Dance flows that exceed them (Appendix J).

Threshold analyses indicate the average critical discharge for fines at TRAL (3,554 cfs) in WY 2006–2019 is more than 12-times higher than the critical discharge (<300 cfs; Denton, 1980) observed near this location in 1979. The analyses also indicate that fine bed load has required higher discharges for entrainment than coarse bed load at TRAL in all years since 2006 (except 2007) and in all years since 2013 at TRDC (Figure 50, Appendix G). The result at TRAL further indicates a chronic shortage of fine sediment in the Lewiston reach and data for TRDC indicates

a more recent scarcity of fines in the Douglas City area (Figures 47-50). The relative mobility of grain-size fractions analyzed with a hiding function by Parker et al. (1982) supports these results and indicates higher mobility has alternated between fine and coarse grains through time, with average hiding exponents indicating approximately equal mobility at TRAL and TRDC since 2006 (Figure 56). Threshold analysis and the hiding function analyses further indicate that fine sediment is substantially more mobile than coarse particles at TRLG, where critical discharges for fines average 33% of those for coarse grains (Figures 51 and 56, Appendix G).

Critical Shields stresses for the median grain size ( $\tau_{c50}^*$ ) plotted within the published range of variation in  $Re_c^*$  at TRDC and TRLG, excepting WY 2009 and 2013 results for TRLG (Figure 57). At TRAL, all values of  $\tau_{c50}^*$  were below the expected range except in WY 2008 and 2019. Higher  $\tau_{c50}^*$  occurs on more stable beds, so relatively low  $\tau_{c50}^*$  at TRAL may seem to disagree with critical flows at this station commonly exceeding values for the other stations (Figure 51 and 57). Rather, low  $\tau_{c50}^*$  and high critical discharges occur at TRAL because the bed requires comparatively low shear stress for entrainment but relatively high discharges to increase energy slopes and flow velocities to levels that generate critical shear stresses (Figures 58-59). At both TRAL and TRLG, low values of  $\tau_{c50}^*$  correlate with lessened availability of fines on the bed for partially burying and packing coarse surface grains, and the higher than normal  $\tau_{c50}^*$  for TRAL in WY 2019 occurred when fines were relatively plentiful from contributions by Deadwood Creek (Figure 31 and 70). These correlations support research indicating grain stability increases with the availability of fine sediments (Yager et al., 2018; Buxton, 2014; Barzilai et al., 2013), but counter flume research by Wilcock et al. (2001) and others that measured the opposite effect.

Evidence for dominant sources of bed load captured in transport sampling were provided by values of  $D_{\text{surface}}^*$  and  $D_{\text{subsurface}}^*$ . At TRLG and TRDC, these ratios inferred transport of fines over a coarse and relatively stable bed surface, with fines mostly originating outside subsurface areas of the bed (Figure 62). At TRAL, values suggested near equal contributions to bed load by coarse surface grains and relatively fine grains from subsurface areas and surface deposits on the bed. Linear trends in  $D_{\text{surface}}^*$  and  $D_{\text{subsurface}}^*$  decreased toward unity through time at TRLG and TRDC due primarily to increases in median bed load diameters that could result from depletion of fines in surface deposits, progressive armoring of the bed protecting grains in subsurface areas from transport, or reduced supply of fine sediment from upstream sources, or all of these. At TRLG and TRDC,  $D_{\text{surface}}^*$  and  $D_{\text{subsurface}}^*$  inversely related to the peak discharge during spring flow releases from Trinity and Lewiston Dams but values were largely constant with increase in peak flow at TRAL (Figure 62). Power estimates of discharges at unity in  $D_{\text{subsurface}}^*$  that indicate peak flows needed to generally exhaust surface deposits of fines and produce a median bed load diameter equal to that for subsurface areas of the bed are 8,650, 13,200, and 15,060 cfs at TRAL, TRLG, and TRDC, respectively. Further increases in flow are then required to deplete the fine sediment supply in the subsurface domain or perhaps reform the armor layer and coarsen bed load to near the size distribution of particles on the bed surface at the start of the flow release, as indicated by unity in  $D_{\text{surface}}^*$  occurring at 14,000 cfs at TRLG and 16,900 cfs at TRDC. These figures may indicate that spring flow releases can reduce the amount of fine sediment that is available for transport at TRLG and TRDC and cause a depletion of fines until recharge reoccurs either in the declining limb of the hydrograph or the following winter. Conversely for TRAL, results indicate fines exhibit a perennial depletion, as shown by values of  $D_{\text{surface}}^*$  and  $D_{\text{subsurface}}^*$  near unity at all discharges (Figure 62).

Ratios of fine sediment loads to coarse bed loads ( $S^*$ ) for spring flow releases exceeded unity in the period of record at TRLG and TRDC and just under half the time at TRAL (Figure 63; Appendix I). Values of  $S^*$  averaged 1.4 (range 0.5–3.4) at TRAL, 38.0 (range 2.3–206.5) at TRLG, and 7.7 (range 1.3–34.6) at TRDC. Trends in  $S^*$  were negative except at TRAL where coarse bed loads exceeded fine sediment loads in 5 of 12 years due to the scarcity of fines in the Lewiston area and coarse gravel augmentation that occurs most years at a location one mile upstream of TRAL.  $S^*$  was highest at TRLG because coarse bed load is thought to be in deficit and fines are relatively plentiful at this station. In comparison, TRDC exhibited substantially lower  $S^*$  because it probably receives an ample supply of coarse bedload by its location downstream of several large tributaries and because fine sediment has been increasingly scarce at and in the vicinity of this station (see Figure 47 and Upper Steiner Flat in Figure 50), protrusion measurements near TRDC in Section 6.2.1, and increasingly higher critical flows for fine than coarse sediment at this station in Figure 50 and Appendix G).

A comparison of total suspended loads at TRAL in WY 1961 to values for WYs 2006–2019 after normalizing by total annual flow indicates that loads in wet and extremely wet water years in the post-ROD period do not reach that for the critically dry WY 1961 (Figure 76). Restricting the comparison to dry water years post-ROD and the average load ( $9.3 \times 10^{-4}$  tons/AF) is still almost an order-of-magnitude lower than the load in WY 1961 ( $8.1 \times 10^{-3}$  tons/AF) despite peak discharges being 4 to 7 times greater in the dry water years (Figure 77). Reductions in total suspended loads at TRAL primarily resulted from Trinity Dam closure and flow diversions from Lewiston Reservoir via Carr Tunnel while suspended loads at TRLG have probably been lowered most by fine sediment abatements on Grass Valley Creek. Supporting evidence is that annual loads at TRLG closely tracked loads at Fawn Lodge on Grass Valley Creek from 1982–1991, according to data in Milhouse (1994; Figure 78). The correlation in loads between stations continued past 1984 and 1989 when Wellock and Hamilton ponds respectively began operations likely resulted from transport of fines stored in the mainstem channel and floodplain areas. Annual suspended loads at TRLG have since decreased from an average of 47,035 tons in 1982–1991 to 9,942 tons in 2006–2019. The post-ROD decrease in suspended sediment at TRLG is also evident in normalized loads (by drainage area and total annual flow) in the aforementioned periods notably decreasing through time for normal and wetter water years and slightly lowering for dry and critically dry water years (Figure 79). The decrease in normalized loads reflects the reduced availability of fine sediment in the Trinity River, which occurred despite the average annual peak flow respectively doubling from 3,500 to 7,033 cfs between 1982–1991 and 2006–2017.

## 9. Recommendations

### 9.1 Release flows for sediment routing and salmonid protection

Most tributary sediments delivered to the Trinity River in winter are stored in deltas and the mainstem channel until mobilization in spring (Figure 74). The delta deposits can increase greatly in size as a result and potentially limit adult salmon and steelhead access to spawning grounds in the creeks and juvenile salmonid migration between rearing areas in the mainstem and tributaries (e.g., CA DWR, 1979). Tributary sediments can also deposit in the Trinity River channel and degrade the quality of stream bed sediments for salmonid egg incubation, macroinvertebrate production, and intergravel flow. In unregulated rivers, elevated discharges coincide with high tributary flows and contributed sediments are dispersed and routed downstream rather than allowed to accumulate and imperil salmonid populations. Winter flow

releases from Lewiston Dam are therefore recommended to simulate this natural process on the Trinity River to benefit adult and juvenile salmonid access to tributary channels and promote high egg to fry survival rates and macroinvertebrates in the mainstem channel.

An additional recommendation is to release high flows as required to route unnaturally high contributions of sediment from landslides, wildfire, or other natural processes to the Trinity River when they occur in fall and winter when salmonid eggs are incubating in the stream bed. The most recent need for emergency flows occurred in winter 2019 when marginal areas of the channel upstream of Rush Creek were capped with silt from Deadwood Creek that undoubtedly impacted egg incubation in this reach where ~80% of Chinook salmon spawn in the Trinity River. In this case, increasing flow from Lewiston Dam would have mobilized and dispersed the fine sediment downstream and avoided significant mortality at the early life stage in winter in the Lewiston reach. This type of action is not without precedence, as emergency flow releases in late summer are commonly used to protect the adult life stage in the lower Trinity and Klamath Rivers (ROD, 2017).

## 9.2 Add fine sediment to the channel between Lewiston Dam and Rush Creek

Despite the lack of elevated flows in winter to disburse fine sediment delivered to the Trinity River by tributaries this time of year, a deficit of fine sediments has resulted at and upstream of TRAL since around 2006, with exceptions in 2008 and 2019 when fines were respectively supplied by upstream channel reconstruction projects and Deadwood Creek after the Carr Fire (Figure 55 and 75). Several indications also suggest that a deficit in fine sediment may be developing in the Douglas City reach (Section 6.2.4), but the shortage has not yet reached a level requiring the addition of fines to the channel. This conclusion is based on normalized suspended and fine bed loads in spring at TRDC approximating those for TRLG (Figure 64), discharge normalized mass transport of suspended sediments during the egg incubation period at TRDC exceeding values for TRLG (Table 9), and  $\tau^*_{c50}$  plotting within the expected range of  $Re_c^*$  at TRDC (Figure 57), suggesting an absence of the overly-mobile bed conditions that occur at TRAL (Section 8; also see Figure 57). One way to reverse deficits in fine sediment is to end spring high flow releases from Lewiston Dam. This is not recommended because the high flows impart significant benefits to the physical (e.g., bar construction and bed scour), riparian (e.g., plant recruitment on upper floodplains), and biological (e.g., fish access to off-channel food sources) functioning of the Trinity River ecosystem. Instead, a recommendation is made to add fine sediment to the Trinity River in the reach that fines are in the strongest deficit between Lewiston Dam and Rush Creek.

Fine sediment additions will be designed to restore the beneficial effects of fines without violating targets for salmonids and macroinvertebrates in the Lewiston reach (Table 2). The benefits are expected to include increased floodplain development, ammocoete habitat, nutrient storage, channel dynamics, and the potential for increased mobility of coarse sediment in the reach. The preferred site for adding fines is across from Trinity Hatchery (RM 111.8), which is the furthest upstream location with river access (Figure 85). A second location is the coarse gravel augmentation site at Weir Hole (RM 111.2). Adding fine sediments to these sites should address the deficit that extends to TRAL and likely downstream to Rush Creek and beyond due to the long travel distance of fine grains in rivers (e.g., Madej and Ozaki, 1996). Both proposed sites are on land owned by the U.S. Forest Service and provide around 6,000 ft<sup>2</sup> for stockpiling material outside the area inundated by 11,000 cfs (the maximum allowable restoration flow

release from Lewiston Dam). Material for addition to the channel could include fine sediments screened from coarse gravel at the Sawmill processing site (at RM 109.0) and fines dredged from Hamilton Ponds at Grass Valley Creek (RM 104.4; Section 5.3.1). These locations are respectively about 3.2 and 6.5 miles from the preferred location for fine sediment additions. All but the last 0.5 miles of these distances to the Trinity River is on paved road to facilitate trucking. Enough fine sediment would be added to the channel just before or during spring flow releases to restore beneficial roles of stored fines in the reach and maintain a dynamic equilibrium in the annual supply and transport of fine sediment. Several options for determining the timing and volume of additions and adding material to the channel are available (e.g., Bunte, 2004). For example, coarse grains may be included with the fine sediment additions as needed to further restoration goals, including increasing channel complexity through bar development and habitat for salmonid spawning. With programmatic support for this recommendation, a comprehensive proposal will be developed with a monitoring plan and adaptive management loops for applying the monitoring data to modify the sediment augmentation volumes and methods to meet the objectives for this action.

### 9.3 Undertake analyses to remove Trinity River listing as sediment impaired

In 2001, the Trinity River was listed under section 303(d) of the Clean Water Act for a sediment TMDL (US EPA, 2001). Water quality standards of concern listed in the TMDL were turbidity and suspended material, and the generic identifier “sediment” without a defined behavior or size definition. Beneficial uses impacted by these sediments were cold water fish habitat for spawning, rearing, and migration, and environmental indicators for these beneficial uses were listed as spawning gravel quality and permeability, turbidity, pool depth. These beneficial uses have been restored, as respectively demonstrated in Section 7 and by Gaeuman (2020) for pool depths. Additional beneficial uses listed in the TMDL were geomorphic indicators of a healthy alluvial river, including attributes 1 and 3-6 in USFWS and HVT (1999) and TREIR (1999). The attributes and evidence for their restoration in the Trinity River (in parenthesis) include

Attribute 1: Channel morphology is spatially complex (Gaeuman et al., 2017);

Attribute 3: Channel-bed surfaces are frequently mobilized (Appendix J);

Attribute 4: Channel-bed surfaces are frequently scoured and filled (Hales et al., 2020);

Attribute 5: Fine and coarse sediment supplies are approximately balanced (Gaeuman and Stewart (2017) for coarse sediment); and

Attribute 6: The channel location periodically migrates (Curtis et al., 2015).

Given these restoration accomplishments and considering that a deficit of fine sediments has developed at and upstream of TRAL with likely extension to Rush Creek and at Douglas City with possible extension to Junction City, a recommendation is to undertake analysis to formally delist the Trinity River from Lewiston Dam to the confluence with the Klamath River as sediment impaired. Undertaking this action is timely in consideration that Trinity County instituted a grading ordinance in April 2019, which replaces the TMDL as the first defense against elevated sediment contributions to streams from anthropogenic activities. Delisting will benefit restoration of the Trinity River by potentially enabling turbidity limits for channel reconstruction projects and gravel augmentations to be relaxed from the current standard of <20 NTU within 500 ft downstream of these activities. Removal of the TMDL will additionally be

necessary to justify changes to TRRP water quality permits that currently only allow augmentations of sediment to the channel to be made with coarse material that is screened to remove fine sediments.

#### 9.4 Monitor sediment transport and storage

Sediment transport measurements should be undertaken on the Trinity River to enable coarse and fine sediment management actions to adapt to changing conditions on the river and lessons learned in the TRRP. Specifically, bed load transport monitoring should occur at TRAL, TRLG, and TRDC as done in the past for dry and wetter water years (see GMA, 2020a). Sediment transport monitoring at TRGV should be curtailed because loads, particle size distributions, and threshold estimates made at this station are directly affected by gravel augmentations that occur most years immediately upstream. Additionally, suspended sediment and turbidity measurements should be restarted at TRAL and TRLG in units of NTU beginning at least the spring release before and continuing for all spring releases after the start of fine sediment additions, including critically dry water years. The bed load and suspended sediment transport measurements will enable sediment budgeting, provide contemporary transport rates for designing fine and coarse sediment additions, enable computations of the relative mobility of grain-size fractions to assist detection of supply-transport imbalances, and provide data to evaluate the effect of fine sediment additions near Lewiston on sediment availability and transport dynamics that govern salmonid populations in gravel bed channels (Lisle and Lewis, 1992).

Sediment storage should also be periodically evaluated in the restoration reach to enable management actions to be modified through time to reflect changing mainstem channel conditions from natural (e.g., landscape disturbance, tributary flow events) and imposed (e.g., restoration flow releases, channel rehabilitation, watershed restoration) conditions. At a minimum, storage measurements should include bulk sampling at the repeat sites in Figure 50 every 5 years and after spring flow releases from Lewiston Dam exceed 8,500 cfs and bathymetry surveys of the mainstem channel in the vicinity of sediment augmentation locations to evaluate the effects of this management action on sediment storage and channel conditions when it is taken. Repeat, paired Wolman (1954) samples should be measured along with embeddedness and resisting forces (see Buxton et al. (2015a)) for coarse grains in the samples on select bars to track sediment conditions for macroinvertebrates and grain mobility through time. Hereto, these recommendations can be expanded if programmatic interest exists for their implementation. A pilot study is also recommended to assess the feasibility of monitoring  $V^*$  in selected pools on the Trinity River to compliment bulk samples in quantifying temporal and spatial variability in fine sediment storage and for systematic assessments of fine sediment storage on bars and floodplains.

#### 9.5 Cease dredging Hamilton Ponds

Hamilton Ponds were originally constructed to prevent fine sediments from entering the Trinity River while restoration work proceeded to stabilize the watershed. With revegetation of formerly denuded areas, an upgraded and storm-proofed road system, and a strong decrease in sediment production from the watershed (Table 5), restoration goals in the watershed have been met and this function is no longer needed or desired. A current, broad estimate is the ponds will continue to prevent the majority of fine sediments from Grass Valley Creek from entering the Trinity River for another 20 years when their storage capacity is reached. Dredging to increase the

duration for pond filling is not recommended because fine sediment targets in the nearest downstream reaches where data is available for their application have been overwhelmingly met in the past decade (Section 7). Also, in consideration that the average decrease in annual fine bed load at TRLG for the period of record is -198 tons/yr, an expectation is that targets will be increasingly met through time in the downstream vicinity of Grass Valley Creek. Indeed, evidence suggests a deficit in fine sediment has formed in the Limekiln Gulch area (Section 6.2.5.3), where annual total fine sediment loads at TRLG are 36% of those at TRDC despite daily average flows at TRLG being only 13% lower on average. Therefore, a further recommendation is to evaluate the feasibility and benefits of decreasing the elevation of the hydraulic control on lower Hamilton Pond to reduce its storage capacity and enable fines to be contributed to the Trinity River from Grass Valley Creek sooner than is projected to occur from pond filling (Section 5.3.1). This action could be taken along with reimagining the purpose of the ponds to function as cold-water habitat for ammocoetes and juvenile salmonids rather than a sediment trap. Such repurposing of the pond features could also include re-routing Grass Valley Creek from the lower Hamilton Pond outlet to meander in Lowden Meadows, where high-quality coho rearing habitat could be provided.



Figure 85. Aerial view showing the preferred location for adding fine sediment to the Trinity River across from Trinity Hatchery (red arrow) and the weir hole site for additions (black arrow). Potential locations for storing fine sediment outside the area inundated by 11,000 cfs near the hatchery are outlined red.

## 10. Conclusions

Restoration actions have reduced fine sediments in the Trinity River to levels that are no longer detrimental to ecosystem functioning and salmonid populations. However, the reductions have been at a level in some areas of the Trinity River between Lewiston Dam and the North Fork Trinity River that a deficit in fines currently exists or is developing through time. Despite their effect of transporting fine sediment at higher rates than tributary contributions, spring high flow releases from Lewiston Dam should continue for their critical roles in Trinity River restoration. The releases along should be implemented along with actions recommended herein to remedy fine sediment imbalances that have developed in the river. Proposals are also made to release flows in winter to avoid negative impacts of sediment from tributaries on salmonids and to monitor sediment transport and storage in the Trinity River channel to adapt the recommended actions for maximizing benefits to the tribal, sport, and commercial fisheries.

## References

- Abernathy, B. and I.D. Rutherford (2001), The distribution and strength of riparian tree roots in relation to riverbank reinforcement. *Hydrol. Proc.*, 15: 63-79.
- Allan A.F. and L.E. Frostick (1999), Framework dilation, winnowing and matrix particle size: the behaviour of some sand–gravel mixtures in a laboratory flume. *J. Sed. Res.*, 69: 21-26.
- Alvarez, J., D. Goodman, K. DeJulio, and A. Martin (2015), Ammocoete Sample Locations. Trinity River Restoration Program Data Package. Hoopa Tribal Fisheries, U.S. Fish and Wildlife Service, and Yurok Tribal Fisheries, Arcata, CA. <http://odp.trrp.net/>.
- Bailey, J. (2008). The other California gold: Trinity county placer mining, 1848–1962. Bureau of Reclamation. Denver: 103.
- Bair, J.H. (2001), Riparian woody plant initiation, establishment, and mortality on rehabilitated banks of the Trinity River, California. Masters thesis, Humboldt State University, Arcata, CA.
- Barnes, E.J. (1978). Trinity River Pool construction for fishery enhancement: Initial study and environmental determination. <http://www.trrp.net/library/document/?id=1355>.
- Barry, J.J., J.M. Buffington, and J.G. King (2004), A general power equation for predicting bed load transport rates in gravel bed rivers. *Wat. Res. Resour.*, 40: doi:10.1029/2004WR003190.
- Barzilai, R. J.B. Laronne, and I. Reid (2013), Effect of changes in fine-grained matrix on bedload sediment transport in a gravel-bed river. *Earth Surf. Proc. Landforms*, 38: doi:10.1002/esp.3288.
- Bash, J, C. Berman, and S. Bolton (2001), Effects of turbidity and suspended solids on salmonids. Final Research Report, project T1803, task 42. Prepared for the Washington State Transportation Commission and U.S. Department of Transportation, November 2001.
- Battin, T.J., K. Besemer, M.M. Bengtsson, A.M. Romani, and A.I. Packman (2016), The ecology and biochemistry of stream biofilms. *Nat. Rev. Microbiol.*, 14: 251-263.
- Benda, L., D. Miller, P. Bigelow, and K. Andras (2003), Effects of post-wildfire erosion on channel environments, Boise River, Idaho. *For. Ecol. Manage.*, 178: 105-119.
- Berg, L. (1982), The effect of exposure to short-term pulses of suspended sediment on the behavior of juvenile salmonids. IN G.F. Hartman et al. [eds.], *Proc. of the Carnation Creek workshop: a ten-year review*. Department of Fisheries and Oceans, Pacific Biological Station, Nanaimo, Canada.
- Berg, L. and T.G. Northcote (1985), Changes in territorial, gill-flaring, and feeding behaviour in juvenile coho salmon (*Oncorhynchus kisutch*) following short-term pulses of suspended sediment. *Can. J. Fish. Aq. Sci.*, 42: 1410-1417.
- Biedenharn, D.S., C.R. Thorne, and C.C. Watson (2006), Wash load/Bed load material load concept in regional sediment management. Proc. Eight Federal Interagency Sedimentation Conference, April 2-6, Reno, NV.
- Bjornn, T.C., and D.W. Reiser (1991), Habitat requirements of salmonids in streams, in Influences of Forest and Rangeland Management on Salmonid Fishes and Their Habitat, *Am. Fish. Soc. Spec. Pub.* 19, edited by W.R. Meehan, pp. 83-138, *Am. Fish. Soc.*, Bethesda, Md.

- Bjorn, T.C., and seven coauthors (1974), Sediment in streams and its effect on aquatic life. University of Idaho, Water Resources Research Institute, Research Technical Completion Report Project B-025-IDA, Moscow, ID.
- Bjorn, T.C., and seven coauthors (1977), Transport of Granitic Sediment in Streams and its Effects on Insects and Fish. University of Idaho, College of Forestry, Wildlife and Range Science, Bulletin 17, Moscow, ID.
- Braudrick, C.A., W.E. Dietrich, G.T. Leverich, and L.S. Sklar (2009), Experimental evidence for the conditions necessary to sustain meandering in coarse-bedded rivers. *Proc. Natl. Acad. Sci.*, 106: doi:10.1073/pnas.0909417106, 16936-16941.
- Bridgewater, J., N.W. Sharpe, and D.C. Stocker (1969), Particle mixing by percolation. *Trans. Inst. Chem. Eng.*, 47: 114-119.
- Buffington, J.M. and D.R. Montgomery (1997), A systematic analysis of eight decades of incipient motion studies, with special reference to gravel-bedded rivers. *Wat. Resour. Res.*, 33: 1993-2029.
- Buffington, J.M. and D.R. Montgomery (1999), Effects of hydraulic roughness on surface textures of gravel-bed rivers. *Wat. Res. Resour.*, 35: 3507-3521.
- Buffington, J.M., W.E. Dietrich, and J.W. Kirchner (1992), Friction angle measurements on a naturally formed gravel streambed: Implications for critical boundary shear stress. *Wat. Resour. Res.*, 28: 411-425.
- Bunte, K. (2004), Gravel mitigation and augmentation below hydroelectric dams: a geomorphological perspective. Report submitted to the Stream Systems Technology Center, USDA Forest Service, Rocky Mountain Research Station: doi:10.13140/2.1.1094.3361
- Bunte, K. and S.R. Abt (2001), Sampling surface and subsurface particle-size distributions in wadable gravel- and cobble-bed streams for analyses in sediment transport, hydraulics, and streambed monitoring. Gen. Tech. Rep. RMRS-GTR-74. Fort Collins, CO: U.S. Department of Agriculture, Forest Service, Rocky Mountain Research Station. 428 p.
- Buxton, T.H. (2014), Grain packing resistance to particle mobility and the influence of salmon spawning on stream bed stability and storage and exchange of marine nutrients in stream channels. Ph.D. Dissertation, University of Idaho, Boise.
- Buxton, T.H., J.M. Buffington, D. Tonina, A.K. Fremier, and E.M. Yager (2015a), Modeling the influence of salmon spawning on hyporheic exchange of marine-derived nutrients in gravel stream beds. *Can. J. Fish. Aq. Sci.*, 72: doi.org/10.1139/cjfas-2014-0413.
- Buxton, T.H., J.M. Buffington, E.M. Yager, M.A. Hassan, and A.K. Fremier (2015b), The relative stability of salmon redds and unspawned streambeds. *Wat. Resour. Res.*, 51: doi:10.1002/2015WR016908.
- CA DWR (California Department of Water Resources) (1979), Delta formations at mouths of tributary streams. Memorandum to the Trinity River Task Force. <https://www.trrp.net/library/document/?id=1839>

- CDFG (California Dept of Fish and Game) (1977), Potential effects of sediment control operations and structures on Grass Valley Creek and Trinity River fish and wildlife. Memorandum report to the E.C. Fullerton, Director CDFG.
- CDFG-WPCL (Water Pollution Control Laboratory) (1996), California stream bioassessment procedure. Rancho Cordova, CA. [https://www.epa.gov/sites/production/files/2015-06/documents/csbp\\_2003.pdf](https://www.epa.gov/sites/production/files/2015-06/documents/csbp_2003.pdf)
- CRA (California Resources Agency) (1970), Task force findings and recommendations on sediment problems in the Trinity River near Lewiston and a summary of the watershed investigation. <http://www.trrp.net/library/document/?id=1347>.
- CWQC (California Water Quality Control Policy) (2004), Water quality control policy for California's clean water act section 303(d) list. [www.waterboards.ca.gov/water\\_issues/programs/tmdl/docs/ffed\\_303d\\_listingpolicy093004.pdf](http://www.waterboards.ca.gov/water_issues/programs/tmdl/docs/ffed_303d_listingpolicy093004.pdf)
- Carling, P.A. and N.A. Reader (1981), A freeze-sampling technique suitable for coarse river bed material. *Sed. Geol.*, 29: 233-239.
- Camenen, B. and M. Larson (2005), A general formula for non-cohesive bed load sediment transport. *Est. Coastal, and Shelf Sci.*, 63: 249-260.
- Casas-Mulet, R., G. Lakhapal, and M.J. Stewardson (2018), The relative contribution of near-bed vs. intragravel horizontal transport to fine sediment accumulation processes in river gravel beds. *Geomorphology*, 303: doi.org/10.1016/j.geomorph.2017.12.013.
- Casas-Mulet, R., K.T. Alfredsen, A.H. McCluskey, and M.J. Stewardson (2017), Key hydraulic drivers and patterns of fine sediment accumulation in gravel streambeds: A conceptual framework illustrated with a case study from the Kiewa River, Australia. *Geomorphology*, 299: doi.org/10.1016/j.geomorph.2017.08.032.
- Chapman, D.W. (1990), Fines in redds of large salmonids. *Trans. Am. Fish. Soc.*, 119: 156-162.
- Church, M. (1972), Baffin Island sandurs: A study of arctic fluvial processes. *Geol. Surv. Canada Bulletin* 216. 208 pp.
- Clague, J.J., R.J.W. Turner, and A.V. Reyes (2003), Record of recent river channel instability, Cheakamus Valley, British Columbia. *Geomorphology*, 53: 317-332.
- Claire, C.W. (2003), Pacific lamprey larvae life history and habitat utilization in Red River sub-basin, South Fork Clearwater River drainage, Idaho. Draft Master's Thesis, Univ. Idaho, 74 pp.
- Cover, M.R., C.L. May, W.E. Dietrich, and V.H. Rush (2008), Quantitative linkages among sediment supply, streambed fine sediment, and benthic macroinvertebrates in northern California streams. *J. N. Am. Bentho. Soc.*, 27: 135-149.
- Curran, J.C. and P.R. Wilcock (2005), The effect of sand supply on transport rates in a gravel-bed channel. *J. Hydraul. Eng.*, 131: doi:10.1061/(ASCE)0733-429(2005)131:11(961).
- Curtis, J.A., S.A. Wright, J.T. Minear, and L.E. Flint (2015), Assessing geomorphic change along the Trinity River downstream from Lewiston Dam, California, 1980–2011. U.S. Geological Survey Scientific Investigations Report 2015–5046, 69 p., plus appendix, <http://dx.doi.org/10.3133/sir20155046>.

- DeBano, L.F. (2000), The role of fire and soil heating on water repellency in wildland environments: a review. *J. Hydrol.*, 195-206.
- Dietrich, A.L., C. Nilsson, and R. Jansson (2015), Restoration effects on germination and survival of plants in the riparian zone: a phytometer study. *Plant Ecol.* 216: 465-477.
- Diller, J.S. (1910), Gold and Silver: the auriferous gravels of the Trinity River basin, California. U.S. Geological Survey Bulletin 470, Part 1: metals and nonmetals except fuels. Ed. C.W. Hayes and W. Lindgren.
- Dinehart, R.L. (1989), Dune migration in a steep, coarse bedded stream. *Wat. Resour. Res.*, 25: 911-923. doi: 10.1029/wr025i005p00911.
- Dunne, T. and L.B. Leopold (1978), Water in environmental planning. Published by W.H. Freeman and Company, 818 pp.
- Ebasco Environmental (1990), Trinity River basin restoration program Deadwood Creek fish habitat assessment, <http://www.trrp.net/library/document/?id=1652>.
- Egiazaroff, I. V. (1965), Calculation of nonuniform sediment concentrations. *J. Hydraul. Div., Amer. Soc. Civ. Eng.*, 91: 225-247.
- Einstein, H.A. (1950), The bedload function for sediment transport in open channel flows, Rep. Technical Bulletin no. 1026, US Department of Agriculture, Washington DC.
- FKA (Frederiksen, Kamine, and Associates) (1980), Proposed Trinity River basin fish and wildlife management program, Sediment and related analysis. <https://www.trrp.net/library/document/?id=1753>.
- Francis, J.R.D. (1973), Experiments on the motion of solitary grains along the bed of a water-stream, *Proc. R. Soc. Lond. A*, 332: 443-471.
- Furniss, M.J, T.D. Roelofs, and C.S. Yee (1991), Road construction and maintenance, in Influences of Forest and Rangeland Management on Salmonid Fishes and Their Habitat, *Am. Fish. Soc. Spec. Pub.* 19, edited by W. R. Meehan, pp. 297-324, *Am. Fish. Soc.*, Bethesda, Md.
- Gaeuman, D. (2010), Recommendation for Hamilton Ponds Sediment Control Plan. Technical Brief to the Trinity River Restoration Program. <http://www.trrp.net/library/document/?id=447>.
- Gaeuman, D. (2020), WY2016-2017 Trinity River gravel augmentation monitoring report. Yurok Tribal Fisheries Program, Klamath, California. <https://www.trrp.net/library/document?id=2464>.
- Gardner, M.B. (1981), Effects of turbidity on feeding rates and selectivity of bluegills. *Trans. Am. Fish. Soc.*, 110: 446-450.
- Gibson, S., D. Abraham, R. Heath, and D. Schoellhamer (2009), Vertical gradational variability of fines deposited in a gravel framework. *Sedimentology*, 56: 661-676.
- GMA (2001), Sediment source analysis for the mainstem Trinity River, Trinity County, CA. <http://www.trrp.net/library/document/?id=229>.
- GMA (2007), Trinity River comprehensive sediment transport data compilation report. <http://www.trrp.net/library/document?id=335>.

- GMA (2010), Trends in substrate composition of the Trinity River, 1991–2009.  
<http://www.trrp.net/library/document/?id=439>.
- GMA (2019), 2018 Trinity River Hamilton Ponds and Buckhorn reservoir survey report.  
<http://www.trrp.net/library/document/?id=2446>; associated data available at  
<http://www.trrp.net/library/data/?id=122> and <http://www.trrp.net/library/data/?id=123>.
- GMA (2020a), 2019 Trinity River sediment transport monitoring final report. Report for the Trinity River Restoration Program. GMA Hydrology, Arcata, California.  
<https://www.trrp.net/library/document/?id=2477>
- GMA (2020b), 2018 substrate investigation of the Trinity River, Lewiston Dam to Junction City. Report for the Trinity River Restoration Program. GMA Hydrology, Arcata, California.  
<https://www.trrp.net/library/document/?id=2482>
- Gradall, K.S. and W.A. Swenson (1982), Responses of brook trout and creek cubs to turbidity. *Trans. Am. Fish. Soc.*, 111: 392-395.
- Gregory, R.S. and C.D. Levings (1997), Turbidity reduces predation on migrating juvenile Pacific salmon. *Trans. Am. Fish. Soc.*, 127: 275-285.
- Hafs, A.W., L.R. Harrison, R.M. Utz, and T. Dunne (2014), Quantifying the role of woody debris in providing bioenergetically favorable habitat for juvenile salmon. *Ecol. Modelling*, 285: 30-38.
- Hales, G., A. Hilton, S. McBain, and S. Howlin (2020), Statistical evaluation of Trinity River point bar bed mobility and bed scour during annual spring ROD releases for WY 2009–2013.  
<https://www.trrp.net/library/document?id=2463>.
- Hall, J.D. and R.L. Lantz (1969), Effects of logging on the habitat of coho salmon and cutthroat trout in coastal streams. p. 355-375. IN: T.G. Northcote, ed. Symposium on Salmon and Trout in Streams. Institute of Fisheries, University of British Columbia.
- Hax, C.L. and S.W. Golladay (1993), Macroinvertebrate colonization and biofilm development on leaves and wood in a boreal river. *Fresh. Biol.*, 29, doi:10.1111/j.1365-2427.1993.tb00746.x.
- Haynes, H. and G. Pender (2007), Stress history effects on graded bed stability. *J. Hydraul. Eng.*, 33: 343-349.
- Hassan, M.A. and M. Church (2001), Sensitivity of bed load transport in Harris Creek: Seasonal and spatial variation over a cobble-gravel bar. *Wat. Resour. Res.*, 37: 813-825.  
doi:10.1029/2000WR900346.
- Helfield J.M., J. Engström, J.T. Michel, C. Nilsson, and R. Jansson (2012), Effects of river restoration on riparian biodiversity in secondary channels of the Pite River, Sweden. *Environ Management* 49: 130-141
- Hook, P.B., K.M Salsbury, and J.M. Klausmann (2009), Revegetation of reed canarygrass infested riparian areas: Performance of pre-vegetated coir after 3 to 6 years. IN *Revitalizing the Environment: Proven Solutions and Innovative Approaches*, R.I. Barnhisel (Ed.), ASMR, Lexington, KY.

- Hostetter, N.J., A.F. Evans, D.D. Roby, and K. Collis (2012), Susceptibility of juvenile steelhead to avian predation: the influence of individual fish characteristics and river conditions. *Trans. Am. Fish. Soc.* 141: 1586-1599.
- Hough-Snee, N., R. Pond, and J. Jacobson (2010), The Stillaquamish Big Trees Project: Watershed-scale riparian restoration (Washington). *Ecol. Restoration*, 28: 243-245.
- HVT and McBain Associates (in review), Vegetation encroachment synthesis for the Trinity River, 109 pp.
- Irwin, W.P. (2009), Geologic map of the Weaverville 15' quadrangle, Trinity County, California: U.S. Geological Survey Scientific Investigations Map 3095, scale 1:50,000.
- Isaak, D.J., C.H. Luce, B.E. Rieman, D.E. Nagel, E.E. Peterson, D.L. Horan, S.Parkes, and G.L. Chandler (2010), Effects of climate change and wildfire on stream temperatures and salmonid thermal habitat in a mountain river network. *Ecol. Appl.*, 20: <https://doi.org/10.1890/09-0822.1>
- Jenson, D.W., E.A. Steel, A.H. Fullerton, and G.R. Pess (2009), Impact of fine sediment on egg-to-fry survival of Pacific salmon” a meta-analysis of published studies. *Rev. Fish. Sci.*, 17: 348-359.
- Kirchner, J.W., W.E. Dietrich, F. Iseya, and H. Ikeda (1990), The variability of critical shear stress, friction angle, and grain protrusion in water worked sediments. *Sedimentology*, 37: 647-672.
- Klasz, G., W. Reckendorfer, H. Gabriel, C. Baumgartner, R. Schmalfluss, and D. Gutknecht (2014), Natural levee formation along a large and regulated river: The Danube in the National Park Donau-Auen, Austria. *Geomorphology*, 215: 20-33.
- Klein, R.D., J. Lewis, and M.S. Buffleben (2012), Logging and turbidity in the coastal watersheds of northern California. *Geomorphology*, doi:10.1016/j.geomorph.2011.10.011.
- Komar, P.D. and Z. Li (1988), Applications of grain-pivoting and sliding analyses to selective entrainment of gravel and to flow-competence evaluations, *Sedimentology*, 25: 681-695.
- Kondolf, G.M., and W.V.G. Matthews (1991a), Management of coarse sediment in regulated rivers in California, Technical completion report, Univ. of California Water Resources Center, 126 pp.
- Kondolf, G.M. and W.V.G. Matthews (1991b), Unmeasured residuals in sediment budgets: a cautionary note. *Wat. Resour. Res.*, 27: 2483-2486.
- Koschersberger, J.P. (2008), Linking embeddedness and macroinvertebrate health in two southwest Ohio streams. Masters thesis, School of Systems and Engineering Management, Air Force Institute of Technology, Wright-Patterson Air Force Base, Ohio.
- Krause, A.F. (2010), Legacy effects of Trinity River gold mining. Oral presentation provided at the Trinity River Restoration Program's 2010 Trinity River Science Symposium. Trinity River Restoration Program, Weaverville, California. <http://www.trrp.net/library/document/?id=409>.
- Krause, A.F. (2012), History of mechanical sediment augmentation and extraction on the Trinity River, California, 1912-2011. Technical Report TR-TRRP-2012-2 (Revised). Bureau of Reclamation. Trinity River Restoration Program. Weaverville, California. <http://www.trrp.net/library/document/?id=1807>.
- Kuhnle, R.A. (1992), Bed load transport during rising and falling stages on two small streams, *Earth Surf. Proc. Landforms*, 17: 191-197. doi:10.1002/esp.3290170206.

- LaFauce, D. A. (1968), 1967 Spawning Survey of the Trinity River, Final Report. State of California, Eureka, California. <http://www.trrp.net/library/document/?id=538>.
- Lee, K. T., Y.L. Liu, and K.H. Cheng (2004), Experimental investigation of bedload transport processes under unsteady flow conditions. *Hydrol. Proc.*, 18: 2439–2454. doi:10.1002/hyp.1473.
- Leopold L.B. and M.G. Wolman (1960), River meanders. *Geol. Soc. Amer. Bull.*, 71: 769–794.
- Lind, A.J., H.H. Welsh, and R.A. Wilson (1996), The effects of a dam on breeding habitat and egg survival of the Foothill yellow-legged frog (*Rana boylei*). *Herpetological Review* 27: 62-67.
- Lisle, T.E., Y. Cui, G. Parker, J.E. Pizzuto, and A.M. Dodd (2001), The dominance of dispersion in the evolution of bed material waves in gravel-bed rivers. *Earth Surf. Proc. Landforms*, 26: doi:10.1002/esp.300.
- Lisle, T.E. and S. Hilton (1999), Fine bed material in pools of natural gravel bed channels. *Wat. Resour. Res.*, 35: 1291-1304.
- Lisle, T.E. (1995), Particle size variations between bed load and bed material in natural gravel bed channels. *Wat. Resour. Res.*, 31: 1107-1118.
- Lisle, T.E. and S. Hilton (1992), The volume of fine sediment in pools: an index of sediment supply in gravel-bed streams. *Wat. Resour. Bull.*, 28: 371-383.
- Lisle, T.E. and J. Lewis. (1992), Effects of sediment transport on survival of salmonid embryos in a natural stream: a simulation approach. *Can. J. Fish. Aquat. Sci.*, 49: 2337-2344.
- Lisle, T.E. (1989), Sediment transport and resulting deposition in spawning gravels, North Coastal California. *Water Resour. Res.*, 25: 1303-1319.
- Lorenz, J.M. and J.H. Eiler (1989), Spawning habitat and redd characteristics of sockeye salmon in the glacial Taku River, British Columbia and Alaska. *Trans. Am. Fish. Soc.*, 118: 495-502.
- Madej, M.A. and V. Ozaki (1996), Channel response to sediment wave propagation and movement, Redwood Creek, California, USA. *Earth Surf. Proc. Landforms*, 21: [https://doi.org/10.1002/\(SICI\)1096-9837\(199610\)21:10<911::AID-ESP621>3.0.CO;2-1](https://doi.org/10.1002/(SICI)1096-9837(199610)21:10<911::AID-ESP621>3.0.CO;2-1).
- Madej, M.A. (2007), A Strategy to Reduce Fine Sediment from Tributaries in the Trinity River Basin. A Report in Fulfillment of the Trinity River Restoration Project Agreement # 04AA202062. U.S. Geological Survey Western Ecological Research Center Redwood Field Station. Arcata, CA.
- Martin, S.E., M.H. Conklin, and R.C. Bales (2014), Seasonal accumulation and depletion of local sediment stores in four headwater catchments. *Water*, 6: 2144-2163. <https://doi.org/10.3390/w6072144>.
- Marzadri, A., D. Tonina, and A. Bellin (2012), Morphodynamic controls on redox conditions and on nitrogen dynamics within the hyporheic zone: application to gravel bed rivers with alternate-bar morphology. *J. Geophys. Res.*, 117: doi:10.1029/2012JG001966.
- McBain and Trush (1997), Trinity River Maintenance Flow Study Final Report. Report to the Hoopa Valley Tribal Fisheries Department. McBain and Trush, Inc., Arcata, CA.

- McBain and Trush (2000), Evaluation of 1997 flood impacts on Riparian Berms along the Trinity River, California-Final Report. <http://www.trrp.net/library/document/?id=1905>.
- Meehan, W.R. and W.S. Platts (1978), Livestock grazing and the aquatic environment. *J. Soil Water Cons.*, 33: 274-278.
- Meyer, C.B., M.D. Sparkman, and B.A. Klatte (2005), Sand seals in coho salmon redds: Do they improve egg survival? *N. Am. J. Fish. Mgmt.*, 25: 105-121.
- Milhous, R.T. (1994), Sediment balance and flushing flow analysis: Trinity River case study. Proceedings of the American Geophysical Union, Fourteenth Annual Hydrology Days, Colorado State University. <http://www.trrp.net/library/document/?id=1256>.
- Milhous, R.T. (2001), Specific weight and median size of the bed material of gravel and cobble bed rivers. Proceedings of the Seventh Federal Interagency Sedimentation Conference, March 25-29, 2001, Reno, Nevada.
- Miller, M.C., I.N. McCave, and P.D. Komar (1977), Threshold of sediment motion under unidirectional currents. *Sedimentology*, 24: 507-527.
- Mohammad, A.G. and M.A. Adam (2010), The impact of vegetative cover type on runoff and soil erosion under different land uses. *Catena*, 81: 97-103.
- Montgomery, D.R., J.M. Buffington, N.P. Peterson D. Schuett-Hames, and T.P. Quinn (1996), Stream-bed scour, egg burial depths, and the influence of salmonid spawning on bed surface mobility and embryo survival. *Can. J. Fish. Aq. Sci.*, 53: 1061-1070.
- Moss, A.J. (1990), Rain impact on soil crust. I. Formation on a granite derived soil. *Australian J. Soil Res.*, 29: doi:10.1071/SR9910271.
- Nelson, R.W., J.R. Dwyer, and W.E. Greenberg (1987), Regulated flushing in a grave-bed river for channel maintenance: A Trinity River fisheries case study. *Env. Mgmt.*, 11: 479-493.
- Newcombe, C.P. and J.O.T. Jensen (1996), Channel suspended sediment and fisheries: a synthesis for quantitative assessment of risk and impact. *N. Am. J. Fish. Mgmt.*, 16: 693-727.
- Ock, G., D. Gaeuman, J. McSloy, and G.M. Kondolf (2015), Ecological functions of restored gravel bars, the Trinity River, California. *Ecol. Engin.*, 83: 49-60.
- Ockelford, A.M. and H. Haynes (2013), The impact of stress history on bed structure. *Earth Surf. Proc. Landforms*, 37: 717-727.
- O'Keefe, T.C. and R.T. Edwards (2002), Evidence for hyporheic transfer and removal of marine-derived nutrients in a sockeye stream in southwest Alaska. *Am. Fish. Soc. Symp.*, 33: 99-107.
- Paola, C. and R. Seal (1995), Grain size patchiness as a cause of selective deposition and downstream fining. *Wat. Resour. Res.*, 31: 1395-1407.
- Parker, G., Y. Shimizu, G.V. Wilkerson, and V.R. Voller (2011), A new framework for modeling the migration of meandering rivers. *Earth Surf. Proc. Landforms*, 36: 70-86.
- Perret, E., C. Berni, B Camenen, A. Herrero, and K.E. Abderrezzak (2017), Transport of moderately sorted gravel at low bed shear stresses: the role of fine sediment infiltration. *Riv. Res. Applic.*, doi:10.1002/esp.4322.

- Petticrew, E.L., J.F. Rex, and S.J. Albers (2011), Bidirectional delivery of organic matter between freshwater and marine systems: the role of flocculation in Pacific salmon streams. *J. N. Am. Benthol. Soc.*, 30: 779-786.
- Phillips, R.W., R.L. Lantz, E.W. Claire and J.R. Moring (1975), Some effects of gravel mixtures on emergence of coho salmon and steelhead trout fry. *Trans. Am. Fish. Soc.*, 104: 461-466.
- Platts, W.S., R.J. Torquemada, M.L. McHenry, and C.K. Graham (1989), Changes in salmon spawning and rearing habitat from increased delivery of fine sediment to the South Fork Salmon River, Idaho. *Trans. Am. Fish. Soc.*, 118: 274-283.
- Power, M.E. and W.E. Dietrich (2002), Food webs in river networks. *Ecol. Res.*, 17: 451-471.
- Railsback, S.F., B.C. Harvey, S.J. Kupferberg, M.M. Lang, S. McBain, and H.H. Welsh (2016), Modeling potential river management conflicts between frogs and salmonids. *Can J. Fish. Aquat. Sci.*, 73: 773-784.
- Recking, A., P. Frey, A. Paquier, and P. Belleudy (2009), An experimental investigation of mechanisms involved in bed load sheet production and migration. *J. Geophys. Res.*, 114: doi:10.1029/2008JF000990.
- Reid I., L.E. Frostick, and J.T. Layman (1985), The incidence and nature of bedload transport during flood flows in coarse-grained alluvial channels. *Earth Surf. Proc. Landforms*, 10: 33-44.
- Roberts, R. (1996), Grass Valley Creek sediment basin inventory and evaluation. Natural Resources Conservation Service, Weaverville, CA. 14p
- ROD (Record of Decision) (2000), Record of Decision Trinity River Mainstem Fishery Restoration, Final Environmental Impact Statement/Environmental Impact Report. <http://www.trrp.net/library/document/?id=227>.
- ROD (Record of Decision) (2017), Record of Decision for the lower Klamath River long-term plan. <https://www.trrp.net/library/document/?id=2465>.
- Reid, L.M. and T. Dunne (1996), Rapid evaluation of sediment budgets. *Catena Verl.*, Reiskirchen Germany, 164 pp.
- Relyea, C.D., G.W. Minshull, and R.J. Danehy (2000), Stream insects as bioindicators of fine sediment. Watershed Management 2000 conference, Boise, ID.
- Redding, J.M., C.B. Schreck, and F.H. Everest (1987), Physiological effects on coho salmon and steelhead of exposure to suspended solids. *Trans. Am. Fish. Soc.*, 116: 737-744.
- Rennie, C.D. and R.G. Millar (2000), Spatial variability of stream bed scour and fill: a comparison of scour depth in chum salmon (*Oncorhynchus keta*) redds and adjacent bed. *Can. J. Fish. Aquat. Sci.*, 57: 928-938.
- Rex, J.F., and E.L. Petticrew (2008), Delivery of marine-derived nutrients to streambeds by Pacific salmon. *Nature Geosci.*, 1: 840-843.
- Rinella, D.J., M.S. Wipfli, C.M. Walker, C.A. Stricker, and R.A. Heintz (2013), Seasonal persistence of marine-derived nutrients in south-central Alaskan salmon streams. *Ecosphere*, 4: doi:10.1890/ES13-00112.1.

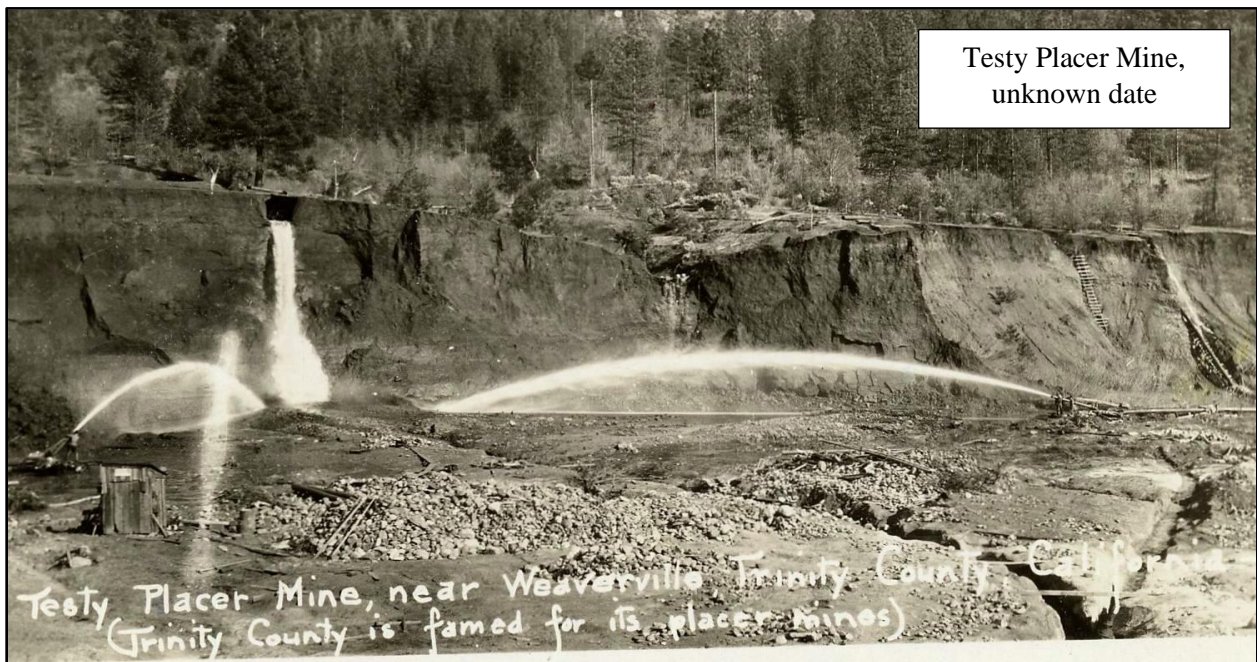
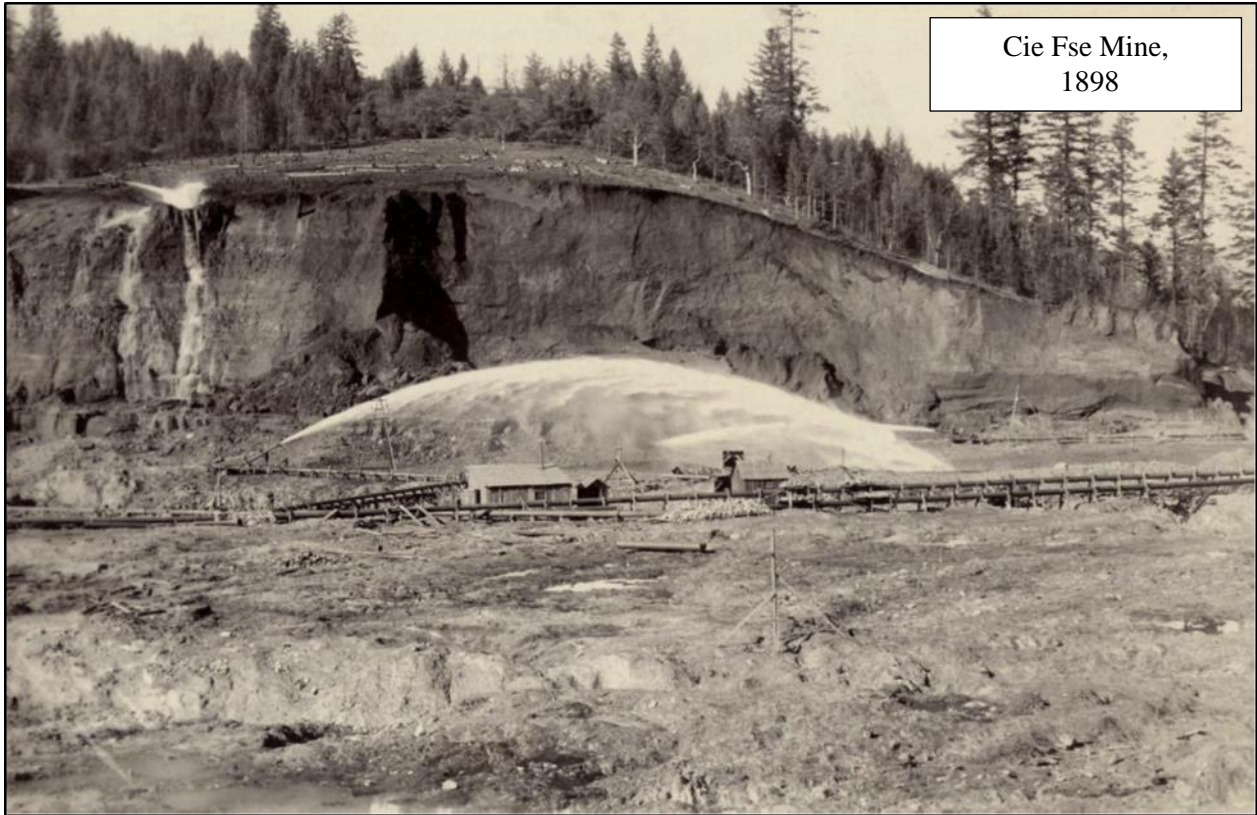
- Ritter, J.R. (1968), Changes in channel morphology of Trinity River and eight tributaries, California 1961-1965. U.S. Geological Survey Open File Report. 60 pp.  
<https://www.trrp.net/library/document/?id=1329>.
- Rupert, D.L., S.A. Gough, N.A. Som, N.J. Davids, W.C. Matilton, A.M. Hill, and J.L. Pabich. 2017. Mainstem Trinity River Chinook Salmon Spawning Survey, 2015 and 2016. U.S. Fish and Wildlife Service. Arcata Fish and Wildlife Office, Arcata Fisheries Data Series Report Number DS 2017-56, Arcata, California.
- Rupp, D. (2019), Landscape level restoration gap and trend analysis for the tributaries of the Trinity River, California. 5C Salmonid Restoration Program document, 187 pp.
- Sedell, J.R., G.H. Reeves, F.R. Hauer, J.A. Stanford, and C.P. Hawkins (1990), Role of refugia in recovery from disturbance: modern fragmented and disconnected river systems. *Env. Management*, 14: 711-724.
- Servizi, J.A. and D.W. Martens (1987), Some effects of suspended Fraser River sediments on sockeye salmon (*Oncorhynchus nerka*), p. 254-264. In H.D. Smith, L. Margolis, and C.C. Wood [ed.] Sockeye salmon population biology and future management. *Can. Spec. Publ. Fish. Aquat. Sci.* 96.
- Servizi, J.A. and D.W. Martens (1992), Sublethal responses of coho salmon (*Oncorhynchus kisutch*) to suspended sediments. *Can. J. Fish. Aquat. Sci.*, 49: 1389-1395.
- Shields, A. (1936), Anwendung der Aehnlichkeitsmechanik und der Turbulenzforschung auf die Geschiebebewegung, *Mitteilungen der Preußischen Versuchsanstalt für Wasserbau und Schiffbau, Berlin*, 26: 1-26.
- Sidle, R.C. (1992), A theoretical model of the effects of timber harvesting on slope stability. *Wat. Resour. Res.*, 28: 1897-1910.
- Sigler, J.W., T.C. Bjornn, and F.H. Everest (1984), Effects of chronic turbidity on density and growth of steelheads and coho salmon. *Trans. Am. Fish. Soc.*, 113: 142-150.
- Slattery, M.C. and T.P. Burt (1998), Particle size characteristics of suspended sediment in hillslope runoff and stream flow. *Earth Surf. Proc. Landforms*, 22: 708-719.
- Stillwater Sciences (2014), A conceptual framework for understanding factors limiting Pacific lamprey production in the Eel River basin. Prepared by Stillwater Sciences, Arcata, California for Wiyot Tribe, Loleta, California.
- Stone, J., J. Pirtle, and S. Barndt (2002), Evaluate habitat use and population dynamics of lampreys in Cedar Creek, WA. BPA contract 200001400.
- Strod, T., I. Izhaki, Z. Arad, and G. Katzir. 2008. Prey detection by great cormorant (*Phalacrocorax carbo sinensis*) in clear and in turbid water. *J. Exp. Biol.* 211: 866-872.
- Suttle, K.B., M.E. Power, J.M. Levine, and C. McNeely (2004), How fine sediment in riverbeds impairs growth and survival of juvenile salmonids. *Ecol. Appl.*, 14: 696-974.
- Sylte, T. and C. Fischenich (2002), Techniques for measuring substrate embeddedness. Techniques for measuring substrate embeddedness,” *EMRRP Technical Notes Collection* (ERDC TN-EMRRP-SR-36), U.S. Army Engineer Research and Development Center, Vicksburg, MS.

- Tappel, P.D. and T.C. Bjornn (1983), A new method of relating size of spawning gravel to salmonid embryo survival. *N. Am. J. Fish. Mgmt*, 3: 123-135.
- Tonina, D., and Buffington, J.M. (2009), A three-dimensional model for analyzing the effects of salmon redds on hyporheic exchange and egg pocket habitat. *Can. J. Fish. Aquat. Sci.*, 66: doi:10.1139/F09-146.
- Torgerson, C.E. and D.A. Close (2004), Influence of habitat heterogeneity on the distribution of larval Pacific lamprey (*Lampetra tridentata*) at two spatial scales. *Freshwater Biol.*, 49: 614-630.
- TRA (Trinity Restoration Associates) (1993). Trinity River maintenance flow report – evaluation of the 6000 cfs flow release. Report prepared for the Hoopa Valley Tribe, 142 p.  
<https://www.trrp.net/library/document/?id=316>.
- TRT (Trinity River Taskforce) (1978), Evaluation Reports FY 1977. Trinity River Basin Fish and Wildlife Taskforce. <https://www.trrp.net/library/document/?id=2052>
- TRRP (Trinity River Restoration Program) and ESSA Technologies Ltd. (2009), Integrated Assessment Plan, Version 1.0 - September 2009. Draft report prepared for the Trinity River Restoration Program, Weaverville, CA, 285 pp.
- Trso, M. (2004), Evaluation of Grass Valley Creek watershed restoration activities. Report to the Trinity River Restoration Program. <http://www.trrp.net/library/document/?id=2323>.
- Turek, S. (1986), Effects of riffle restoration activities in the Trinity River near Poker Bar on the benthic macroinvertebrate community. Department of Water Resources, California.  
<http://www.trrp.net/library/document/?id=1503>.
- Turner, B.G. and M.C. Boner (2004), Watershed monitoring and modelling and USA regulatory compliance. *Water Sci. Technol.*, 50: 7-12.
- USBR (U.S. Bureau of Reclamation) (1965), Hoopa Valley flood rehabilitation program, California, Flood of December 1964 - January 1965.  
<https://www.trrp.net/library/document/?id=2151>.
- USDA (1990), Assessment of Hoadley Gulch, Indian Creek, Deadwood Creek, and Rush Creek watersheds. <http://www.trrp.net/library/document/?id=1961>.
- US DOI (1999), Trinity River Mainstem Fishery Restoration Environmental Impact Report. 2432 pp and appendices.
- US EPA (2001), Trinity River total maximum daily load for sediment.  
<http://www.trrp.net/library/document/?id=228>.
- USFWS (1979), Multi-objective programming in power plant location planning. Federal document FWS/OBS-78/55, 108 pp.
- USFWS (1980a), Trinity River instream flow study, Lewiston Dam to the North Fork, June/July 1978. <http://www.trrp.net/library/document/?id=1500>.
- USFWS (1980b), Environmental impact statement on the management of river flows to mitigate the loss of the anadromous fishery of the Trinity River, California. U.S. Department of the Interior statement number DES 80-54. <http://www.trrp.net/library/document/?id=1413>.

- USFWS and HVT (1999), Trinity River flow evaluation study, final report. A report to the Secretary, US Department of the Interior, Washington D.C.
- USGS (1968), Changes in the channel morphology of the Trinity River and eight tributaries, California, 1961-65. USGS Open File Report, August 1, 1968, Menlo Park, CA.
- Valett, H.M., J.A. Morrice, and C.N. Dahm (1996), Parent lithology, surface groundwater water exchange and nitrate retention in headwater streams. *Limnol. Oceanogr.*, 41: doi:10.4319/lo.1996.41.2.0333.
- Venditti, J.G., W.E. Dietrich, P.A. Nelson, M.A. Wydzga, J. Fadde, and L. Sklar (2010), Mobilization of coarse surface layers in gravel-bedded rivers by finer gravel bed load. *Wat. Resour. Res.*, 46: doi:10.1029/2009WR008329.
- Walling, D.E. (1997), Use of fallout <sup>137</sup>Cs in investigations of overbank sediment deposition on river floodplains. *Catena*, 29: 263-282.
- Walters, D.M., D.S. Leigh, and A.B. Bearden (2003), Urbanization, sedimentation, and the homogenization of fish assemblages in the Etowah River Basin, USA. *Hydrobiologia*, 494: 5-10.
- Westoby, M.J., J. Brasington, N.F. Glasser, M.J. Hambrey, and J.M. Reynolds (2012), Structure from motion photogrammetry: A low-cost, effective tool for geoscience applications. *Geomorphology*, <http://dx.doi.org/10.1016/j.geomorph.2012.08.021>.
- Wilcock, P.R., G.M Kondolf, A.F. Barta, W.V.G Matthews, C.C. Shea (1995), Spawning gravel flushing during trial reservoir releases on the Trinity River: field observations and recommendations for sediment maintenance flushing flows. Univ. of California, Berkeley publication number CEDR-05-95.
- Wilcock, P.R., A.F. Barta, C.C. Shea, G.M Kondolf, W.V.G Matthews, and J. Pitlick (1996), Observations of flow and sediment entrainment on a large gravel-bed river. *Wat. Resour. Res.*, 32: 2897-2909.
- Wilcock, P.R. (2001), Toward a practical method for estimating sediment transport rates in gravel-bed rivers, *Earth Surf. Proc. Landforms*, 26: 1395-1408. doi:10.1002/esp.301.
- Wilcock, P.R. and S.T. Kenworthy (2002), A two-fraction model for the transport of sand/gravel mixtures. *Wat. Res. Research*, 38: 1194. doi:10.1029/2001WR000684.
- Wilcock, P.R. and J.C. Crowe (2003), Surface-based transport model for mixed-size sediment. *J. Hydraul. Engr.*, 129: 120-128.
- Wilcock, P.R. and B.T. DeTemple (2005), Persistence of armor layers in gravel-bed streams. *Geophys. Res. Letters*, 32: doi:10.1029/2004GL021772.
- Wilcock, P.R., S.T. Kenworthy, and J.C. Crowe (2001), Experimental study of the transport of mixed sand and gravel. *Wat. Resour. Res.*, 37: doi:10.1029/2001WR000683.
- Wolman, M.G. (1954), A method for sampling coarse river-bed material. *Trans. Am. Geophys. Union*, 35: 951-956.
- Wood, P.J. and P.D. Armitage (1997), Biological effects of fine sediment in the lotic environment. *Environ. Mgmt.*, 21: 203-217.

- Woods, S.W., A. Birkas, and R. Ahl (2007). Spatial variability of soil hydrophobicity after wildfires in Montana and Colorado. *Geomorphology*, 86: 465-179.
- Woolpert (2010), Report of data development and quality control analysis: Trinity river bathymetry, airborne laser data and photogrammetric DTM merging, verification and certification. Englewood, CO, Woolpert Inc.
- Yager, E.M. and H.E. Schott (2013), The initiation of sediment motion and formation of armor layers, in *Treatise on Geomorphology, Fluvial Geomorphology*, Vol. 9, edited by J. Schroder and E. Wohl, Academic Press, San Diego, pp. 87-102.
- Yager, E.M., M.W. Schmeckle, and A. Badoux (2018), Resistance is not futile: Grain resistance controls on observed critical Shields stress variations. *J. Geophy. Res.*, 123: <https://doi.org/10.1029/2018JF004817>.
- Yalin, M.S. and E. Karahan (1979), Inception of sediment transport. *J. Hydraul. Div. Am. Soc. Civ. Eng.*, 105: 1433-1443.
- Yarnell, S.M. (2000), The influence of sediment supply and transport capacity on Foothill Yellow-Legged frog habitat, South Yuba River, California. Master's thesis, University of California, Davis.

APPENDIX A. Historic photos of hydraulic mining in the Trinity River basin.



APPENDIX A. (continued)



APPENDIX A. (continued)



APPENDIX B. Historic (1964–2018) fire activity in the restoration reach of the Trinity River.

Tributary name	River Mile <sup>1</sup>	Drainage area (mi <sup>2</sup> )	Fire name, start date, area burned (mi <sup>2</sup> ), percent burned
Deadwood Creek	111.0	9.16	Carr fire, 7/23/2018, 7.94, 86% Deadwood fire, 8/9/1997, 0.41, 4%
Hoadley Gulch	110.1	3.61	Carr fire, 7/23/2018, 1.90, 53% Lowden fire, 7/2/1999, 0.34, 9%
Rush Creek	107.9	22.56	Browns fire, 7/12/1994, 0.72, 3%
Grass Valley Creek	104.4	36.85	Carr fire, 7/23/2018, 13.84, 38% Coffin fire, 8/12/2009, 0.86, 2% Lower fire, 6/20/2008, 2.05, 6% Lowden fire, 7/2/1999, 0.26, 1%
Trinity House Gulch	104.0	2.61	Browns fire, 7/12/1994, 1.02, 39%
Tom Lang Gulch	103.3	3.11	No fires reported
McIntyre Gulch	97.2	0.72	No fires reported
Vitzum Gulch	96.7	0.78	No fires reported
Indian Creek	95.6	33.70	Cannonball fire, 8/2/1995, 0.14, <0.01% Hayfork Hwy #2 fire, 8/25/1964, 2.41, 7%
Weaver Creek	94.0	49.66	Helena fire, 8/30/2017, 2.03, 4% Brown fire, 9/8/2015, 0.05, <0.01% Democrat fire, 8/25/2015, 0.06, <0.01% Oregon fire, 8/24/2014, 0.72, 1% Oregon fire, 8/28/2001, 2.29, 5% Browns fire, 7/12/1994, 0.32, <0.01% Unnamed fire, unlisted start date, 1.77, 4% Unnamed fire, unlisted start date, 0.18, <0.01%
Reading Creek	93.1	31.18	Shu Blanch fire, 6/17/2000, 0.03, <0.01% Hayfork Hwy #2 fire, 8/25/1964, 5.04, 16%
Dutton Creek	89.1	4.68	Democrat fire, 8/25/2015, 0.11, 2% Sheill fire, 7/30/2015, 4.63, 6% Deadshot fire, 6/20/2008, 1.63, 2% Deerlick fire, 6/20/2008, 0.36, <0.01%
Browns Creek	88.0	73.70	Hayfork Hwy #2 fire, 8/25/1964, 19.21, 26% Unnamed fire, unlisted start date, 0.51, 1% Unnamed fire, unlisted start date, 0.29, <0.01% Unnamed fire, unlisted start date, 0.14, <0.01% Unnamed fire, unlisted start date, 0.01, <0.01%
Maxwell Creek	86.9	4.98	Barker fire, 8/20/1992, 0.86, 17%
Dutch Creek	86.4	9.58	Dog fire, 7/30/2015, 0.67, 7%
Carr Creek	85.5	1.41	No fires reported
Soldier Creek	84.1	7.07	Eagle fire, 6/21/2008, 1.82, 26%
Deep Gulch	82.3	0.51	No fires reported

<sup>1</sup>River miles for tributary confluences are measured upstream of the confluence with the Klamath River.

APPENDIX B. (continued)

Tributary name	River mile <sup>1</sup>	Drainage area (mi <sup>2</sup> )	Fire name, start date, area burned (mi <sup>2</sup> ), percent burned
Sheridan Creek	82.1	1.60	No fires reported
Mill Creek	81.4	2.42	Eagle fire, 6/21/08, 2.34, 98% Unnamed fire, unlisted start date, 0.05, 2%
Oregon Gulch	81.1	7.44	Helena fire, 8/30/2017, 0.02, <0.01% Democrat fire, 8/25/2015, 0.02, <0.01% Junction fire, 7/29/2006, 3.92, 53% Oregon fire, 8/28/2001, 0.36, 5% Slattery fire, 8/4/1987, 0.17, 0.02% Unnamed fire, unlisted start date, 1.14, 15% Unnamed fire, unlisted start date, 1.07, 14% Unnamed fire, unlisted start date, 0.41, 6%
McKinney Gulch	79.7	1.34	Eagle fire, 6/21/08, 1.29, 96% Helena fire, 8/30/2017, 14.70, 19% Fork fire, 8/7/2017, 5.27, 8% Jones fire, 7/28/2009, 0.06, <0.01% Granite fire, 6/21/2008, 0.86, 1% Little Bar Complex fire, 7/23/2006, 0.33, <0.01% Rush fire, 8/13/1996, 0.19, <0.01%
Canyon Creek	79.2	64.12	Bally fire, 9/2/1987, 17.14, 27% East fire, 8/30/1987, 17.58, 27% Ripstein fire, 8/30/1987, 5.16, 8% Unnamed fire, unlisted start date, 2.66, 4% Unnamed fire, unlisted start date, 2.11, 3% Unnamed fire, unlisted start date, 1.78, 3% Unnamed fire, unlisted start date, 1.02, 2% Unnamed fire, unlisted start date, 0.59, 0.01% Unnamed fire, unlisted start date, 0.50, <0.01%
Conner Creek	77.4	4.83	Eagle fire, 6/21/2008, 4.50, 93%
Hocker Flat	73.8	0.76	Helena fire, 8/30/2017, 0.76, 100% Eagle fire, 6/21/2008, 0.45, 59%

<sup>1</sup>River miles for tributary confluences are measured upstream of the confluence with the Klamath River.

APPENDIX C. Aerial views of Grass Valley Creek delta and Wellock and Hamilton ponds.



August 1944



September 1960



August 1965



May 1971



May 1980



October 1997

APPENDIX C. (continued)



November 2001



July 2007



April 2009



August 2010



August 2011



July 2012

APPENDIX C. (continued)



July 2014



July 2015



July 2016



August 2017

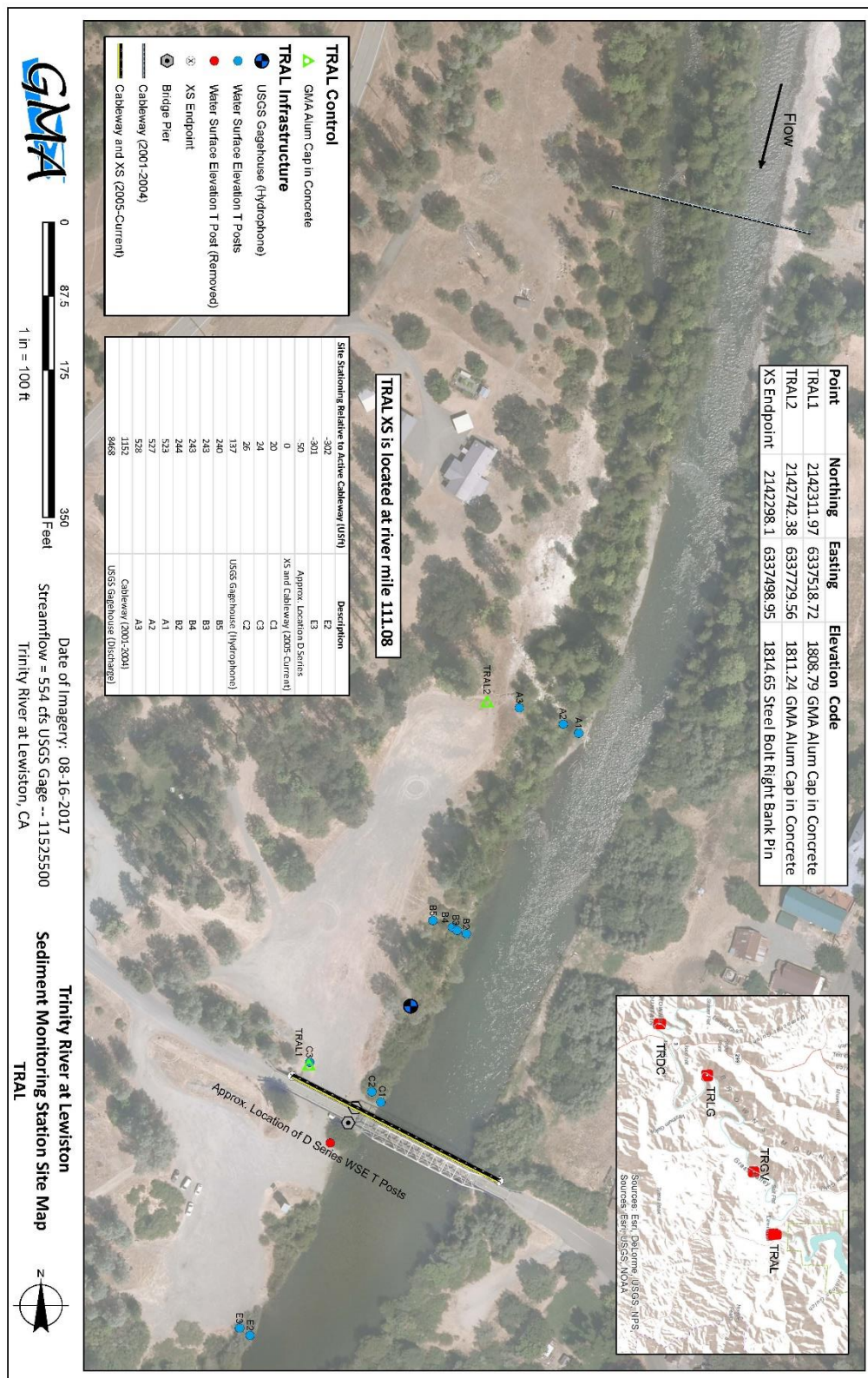


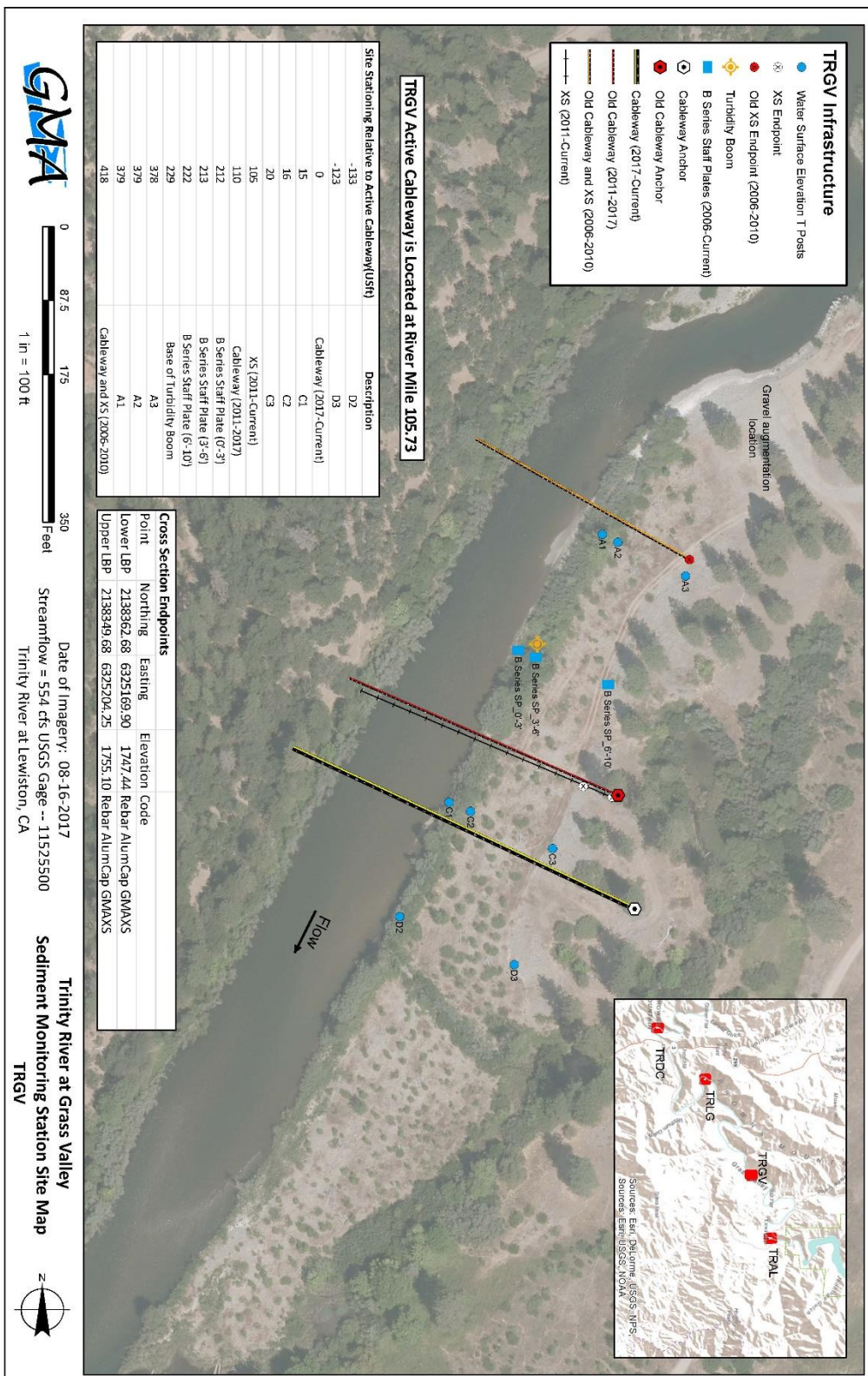
July 2018

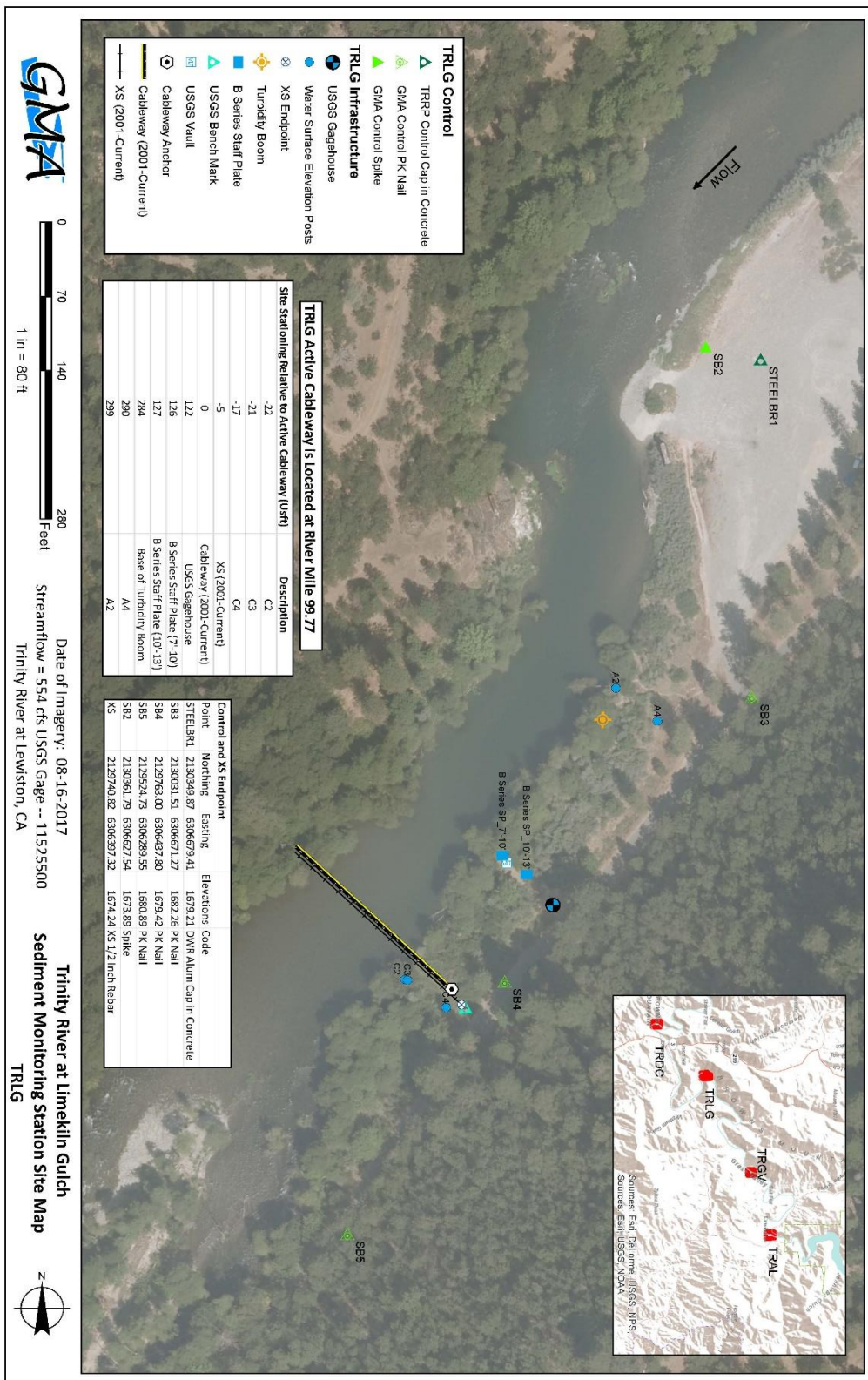


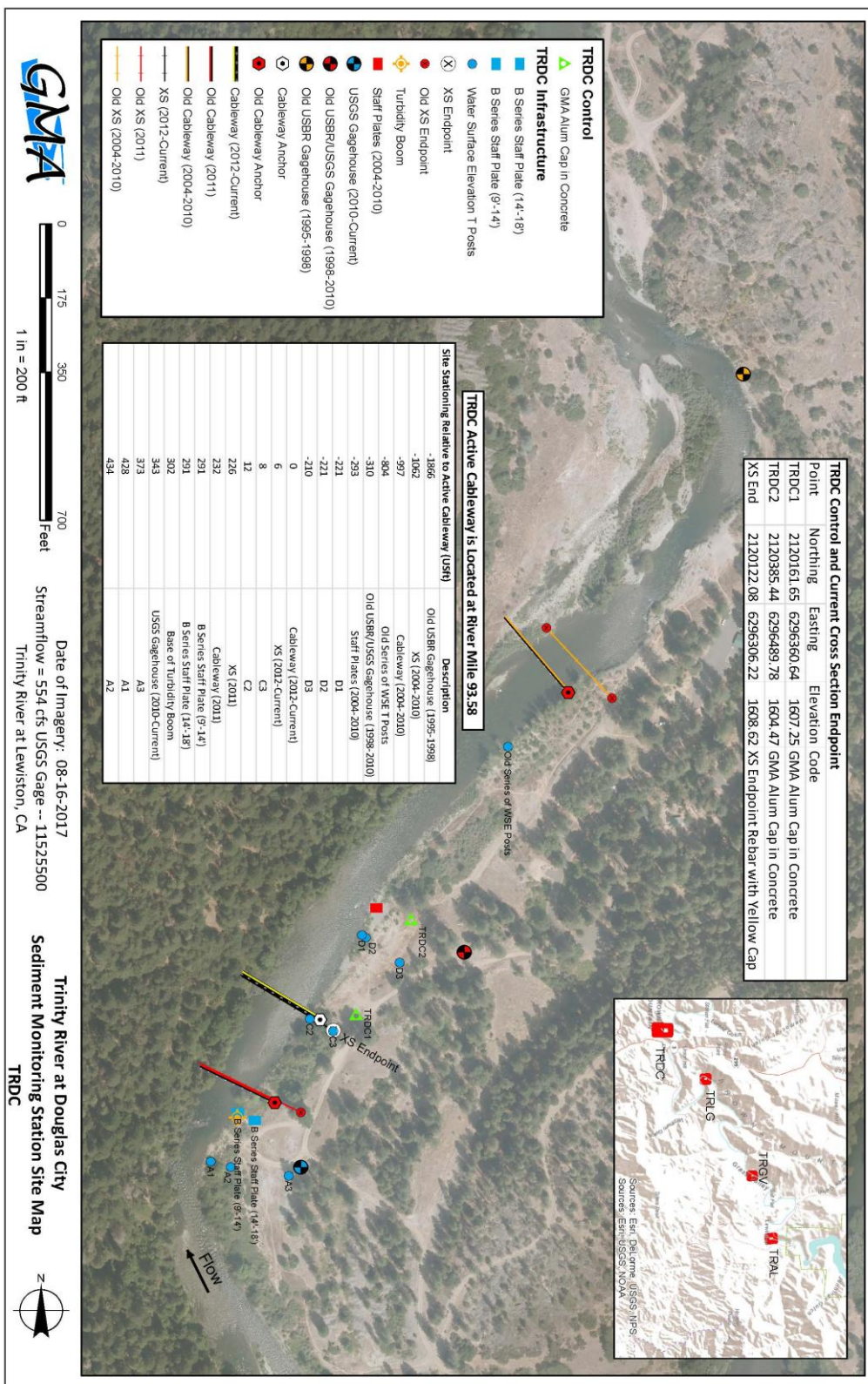
July 2019

APPENDIX D. Planmaps of sediment transport monitoring locations on the Trinity River.

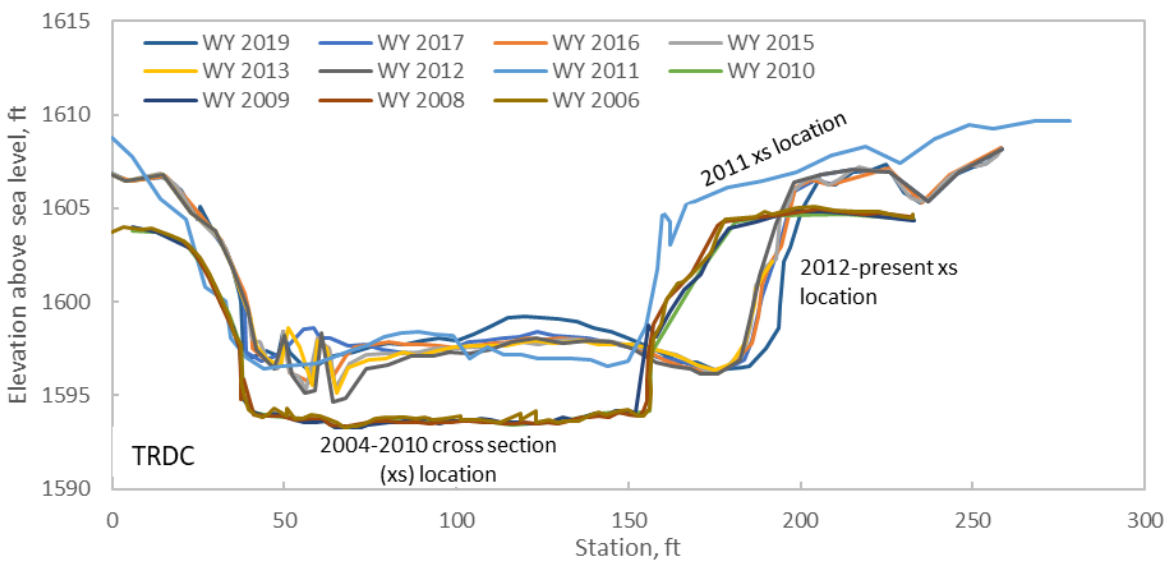
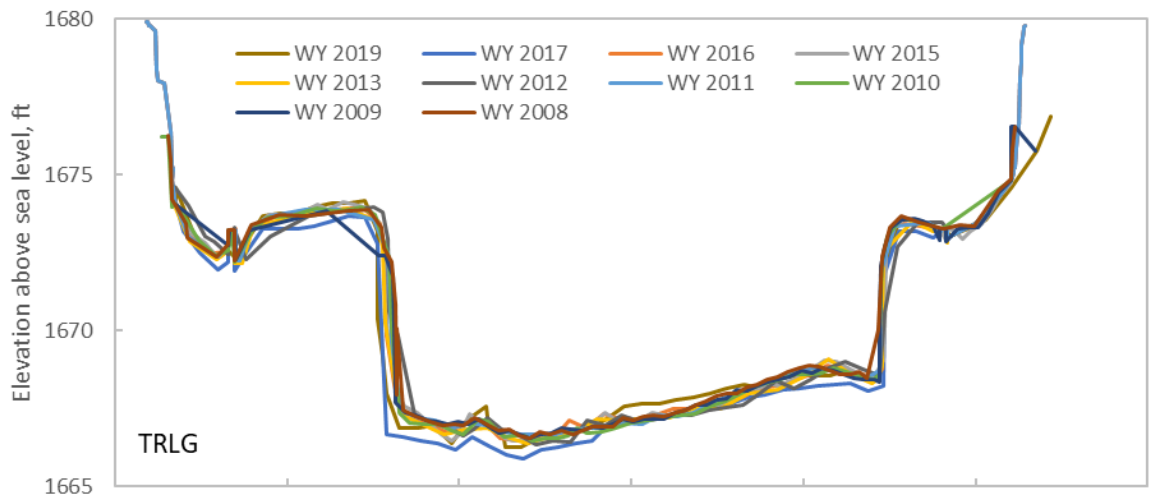
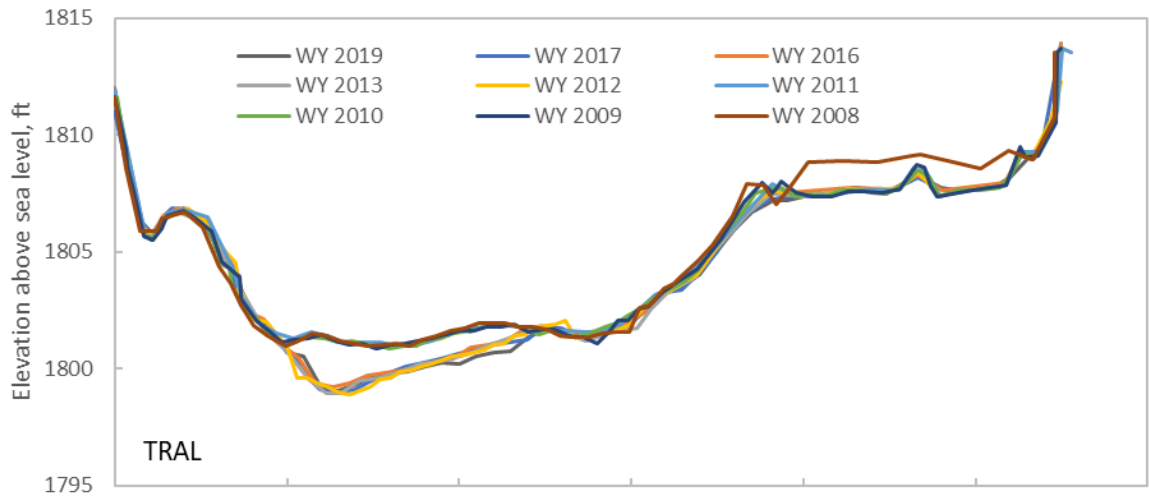




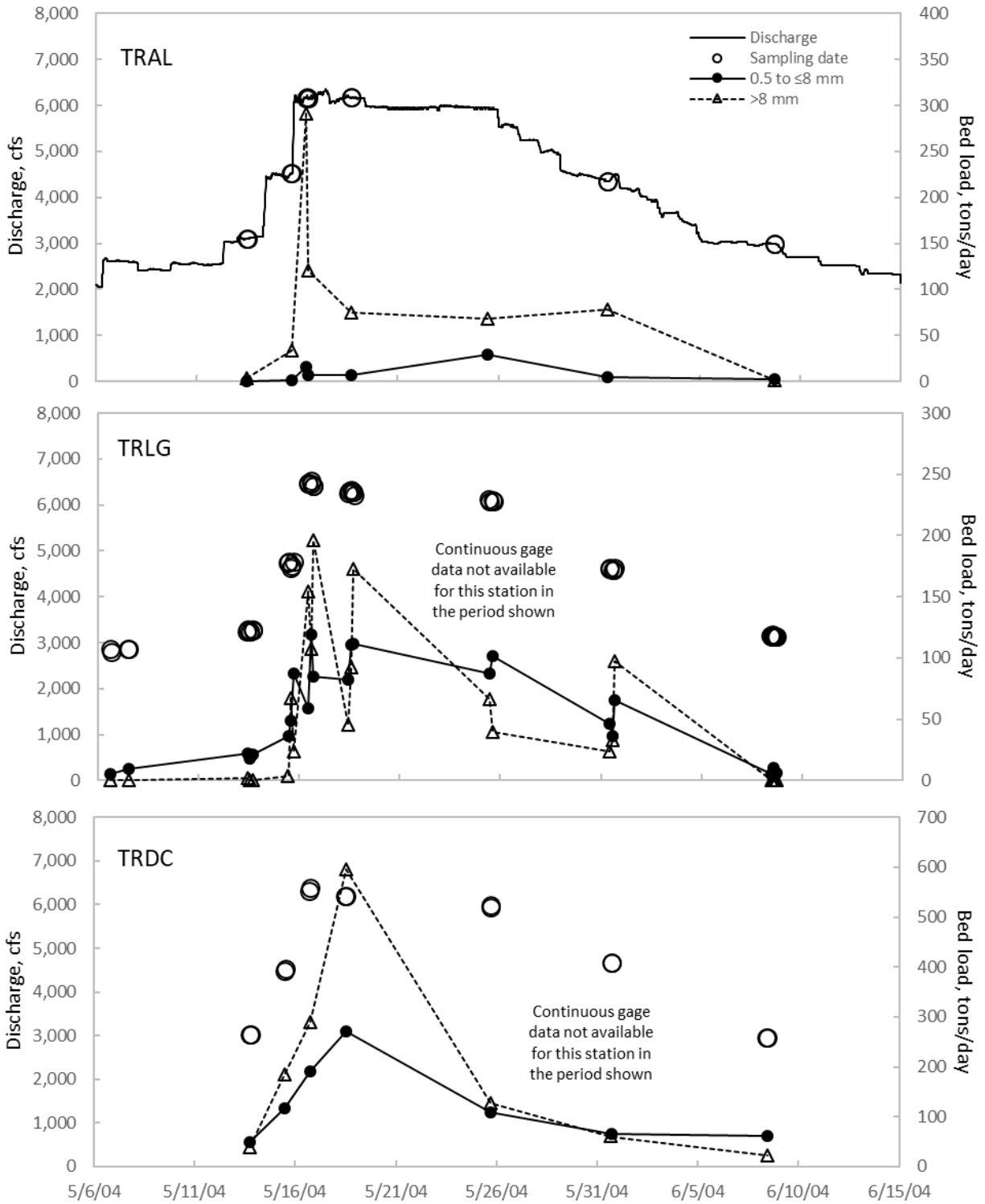




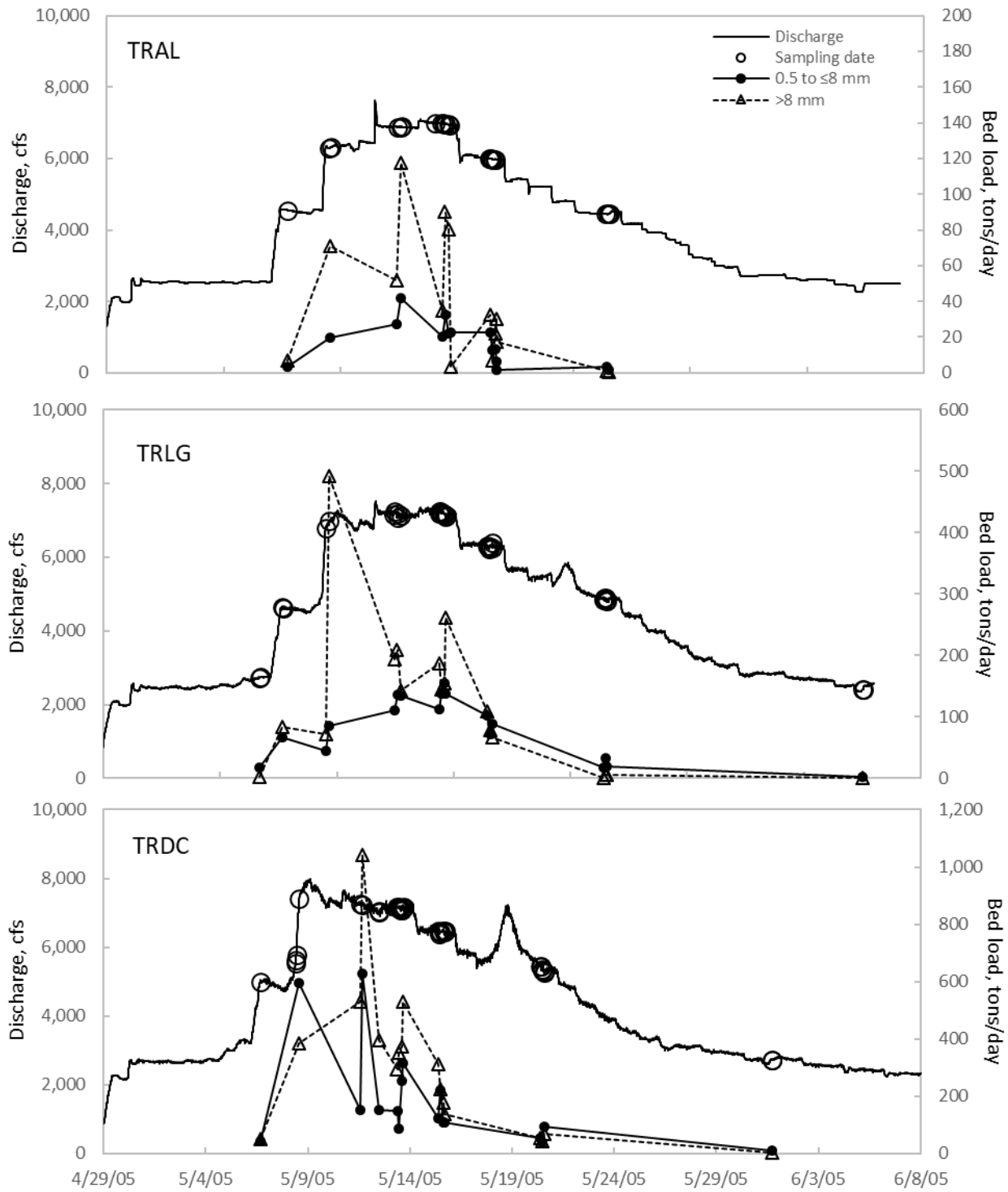
APPENDIX E. Cross sections surveyed prior to spring flow releases at the sediment monitoring stations.



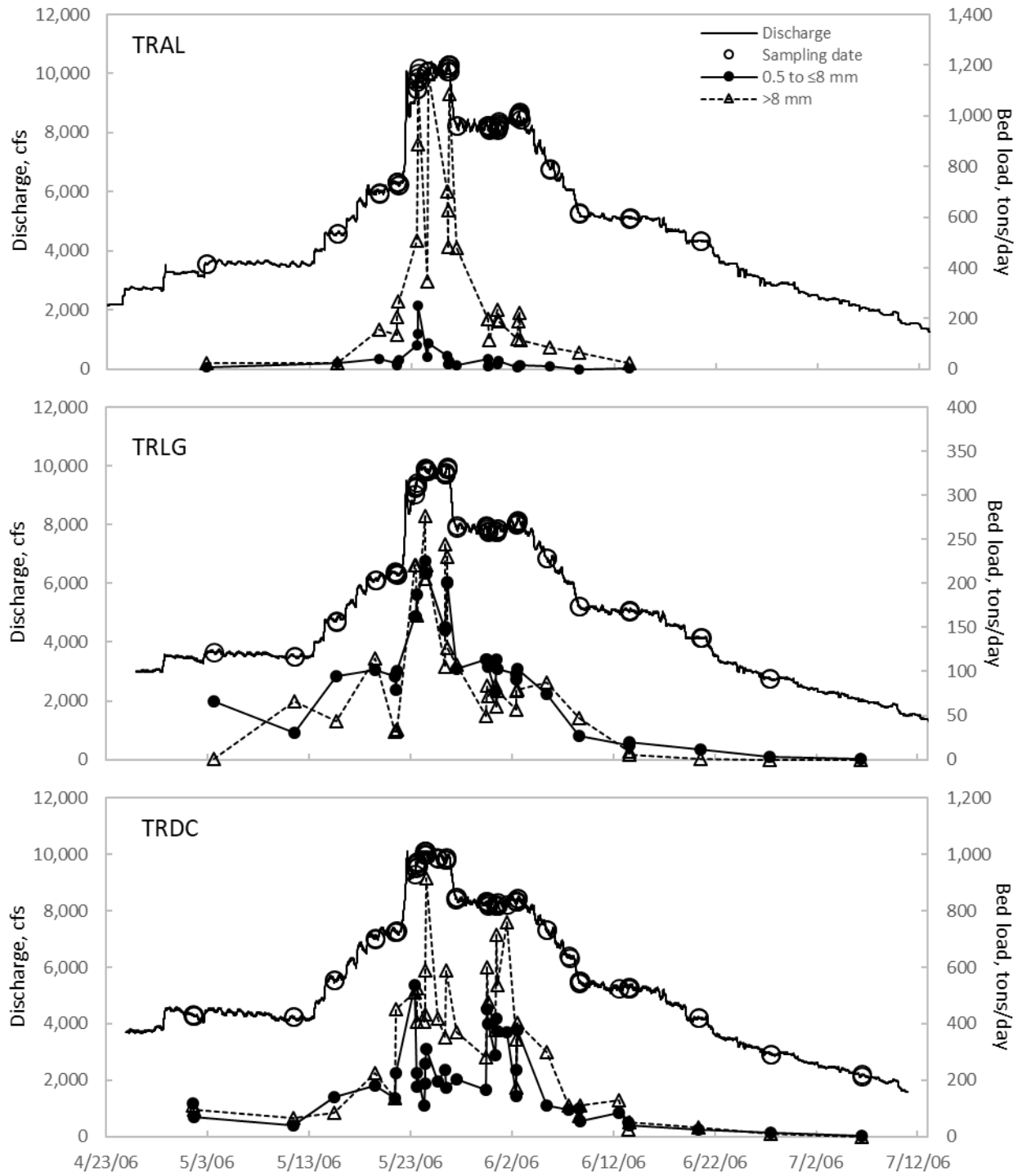
APPENDIX F. Bed loads measured during spring flow releases.



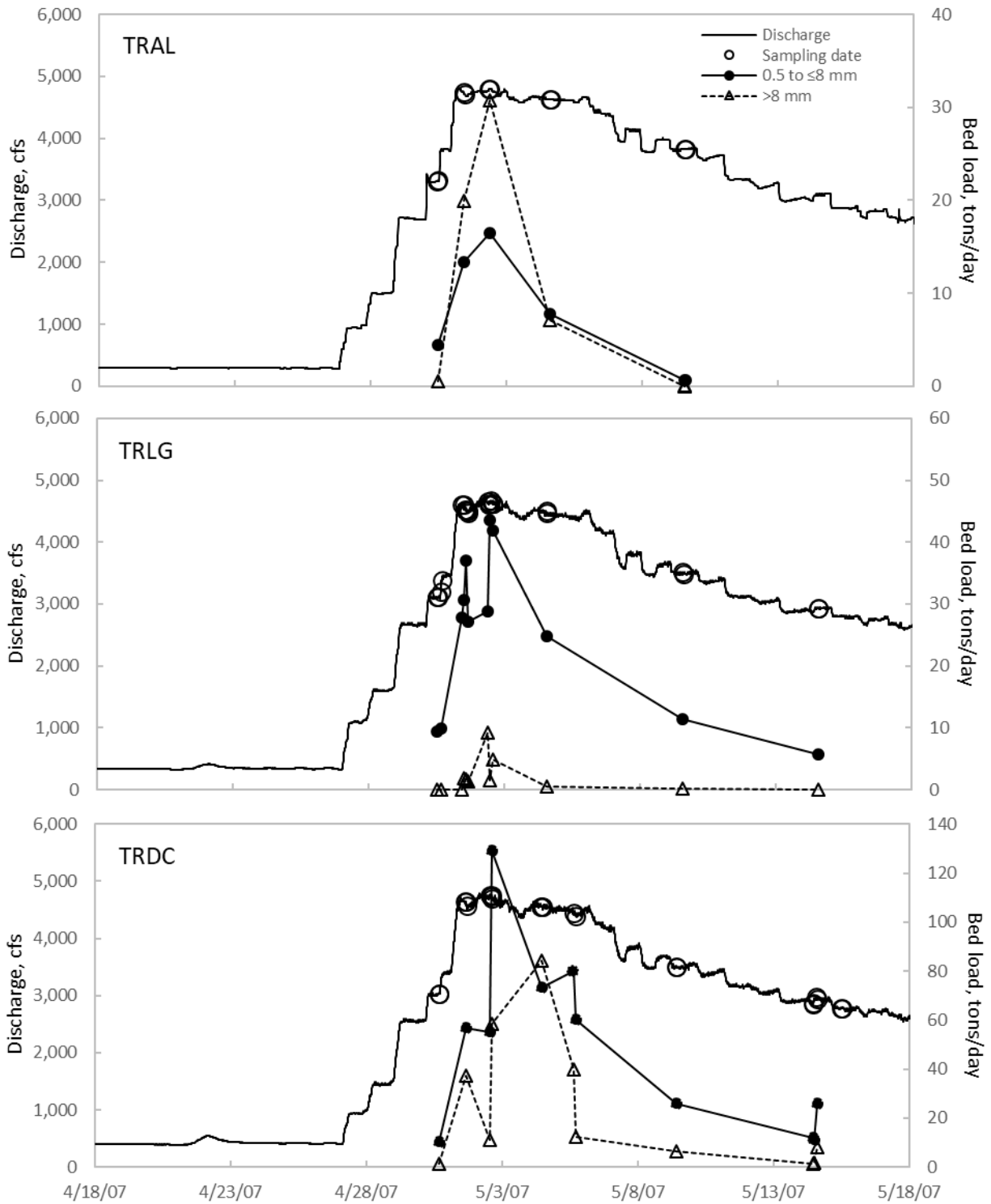
APPENDIX F. (continued)



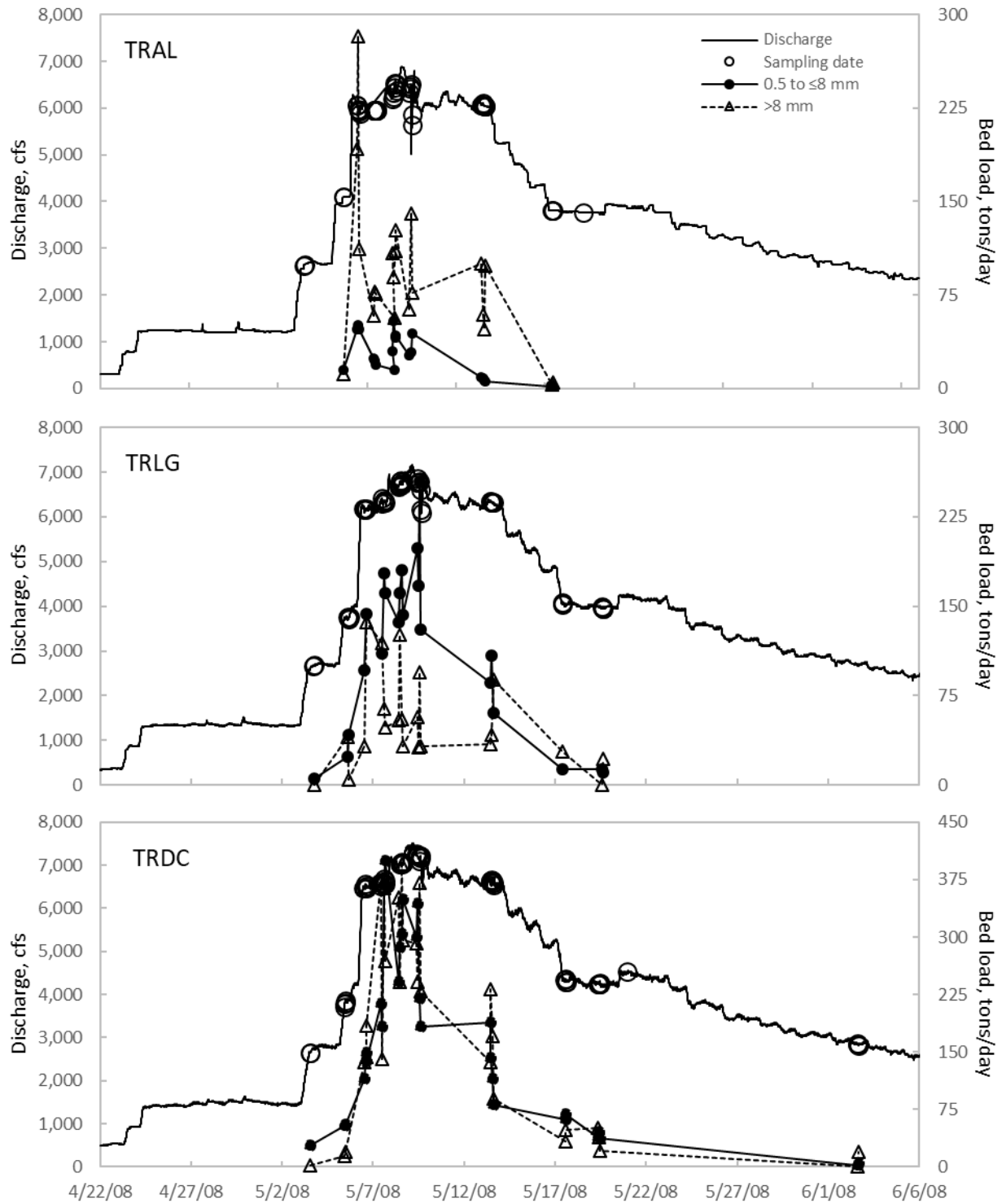
APPENDIX F. (continued)



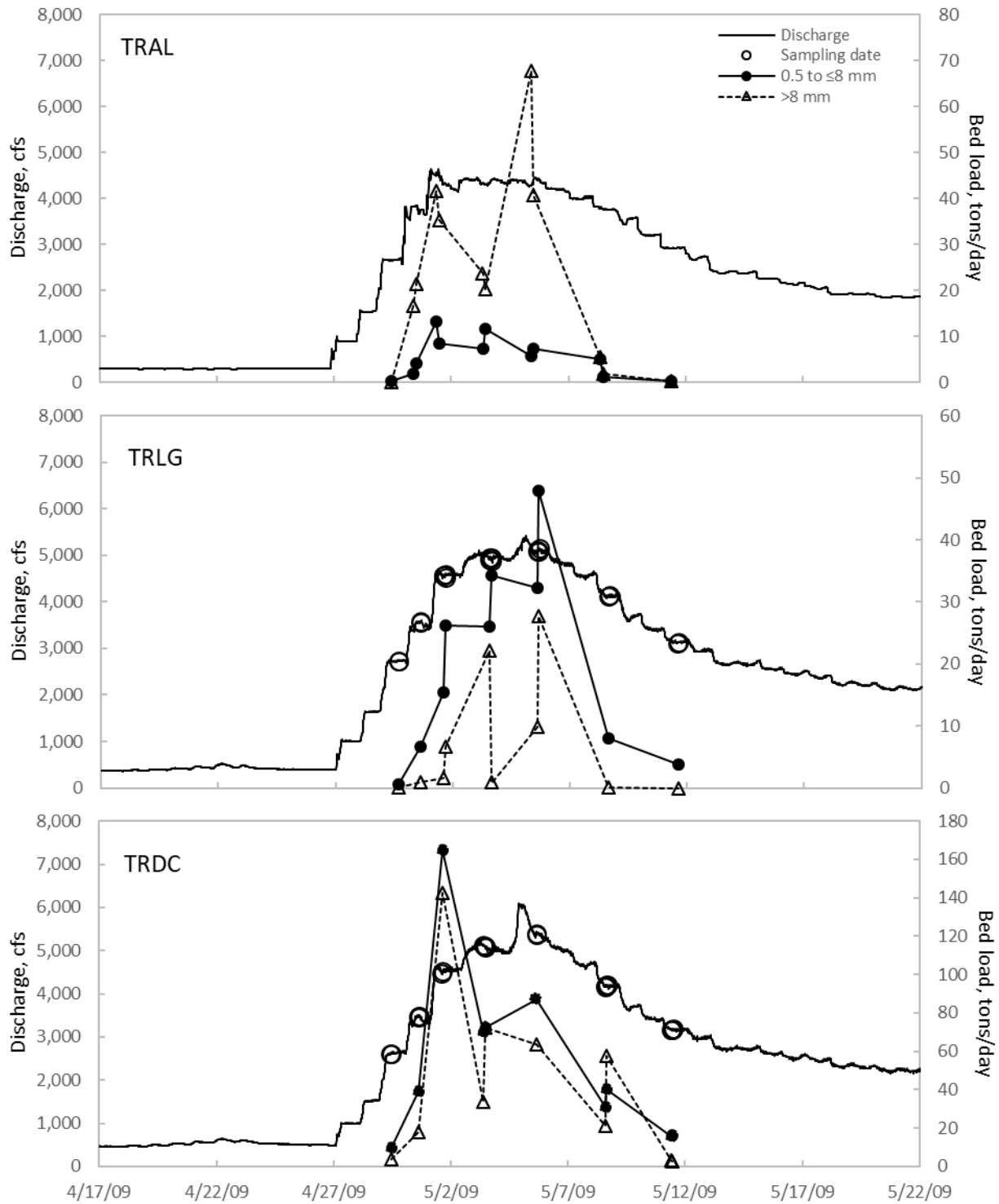
APPENDIX F. (continued)



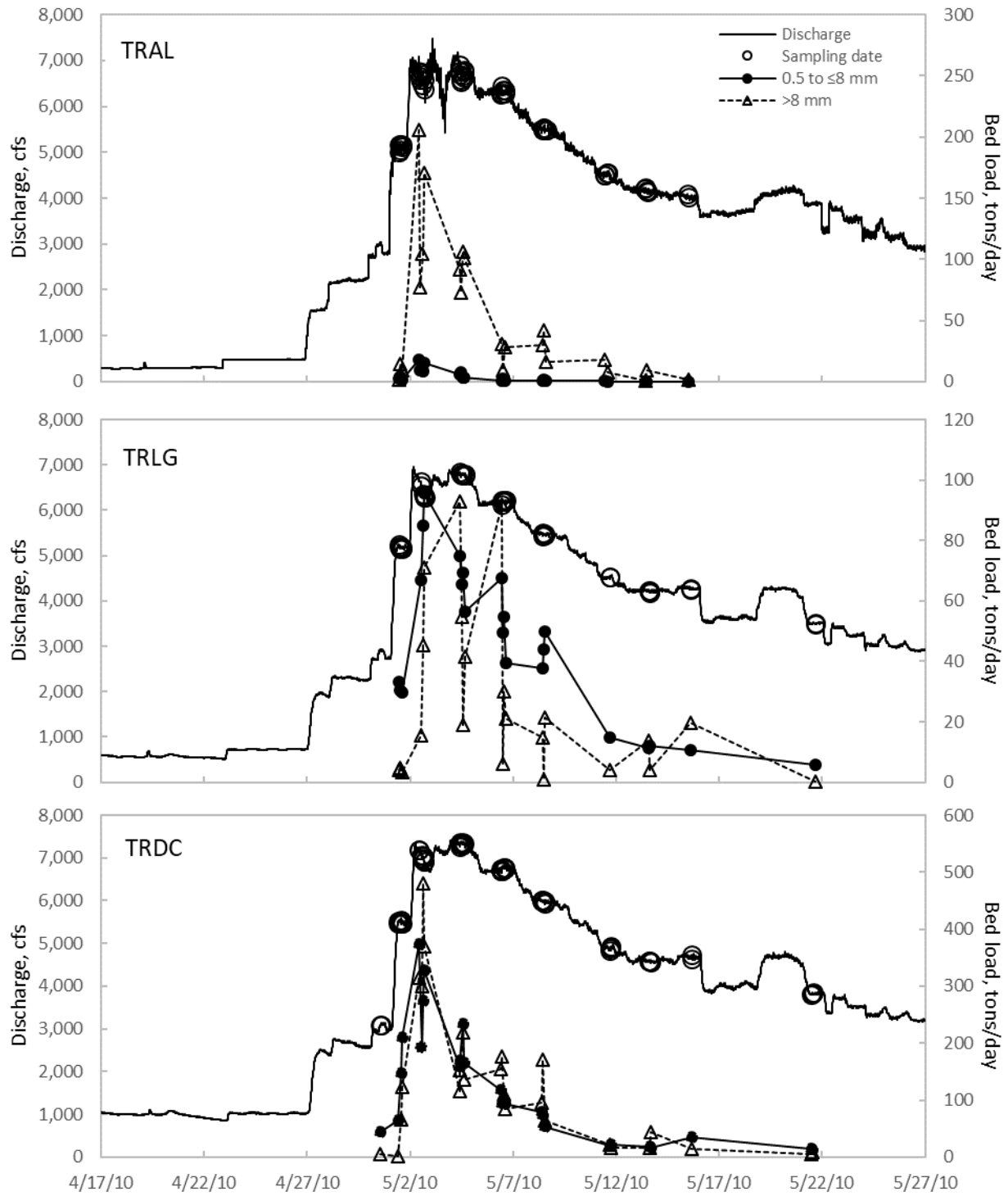
APPENDIX F. (continued)



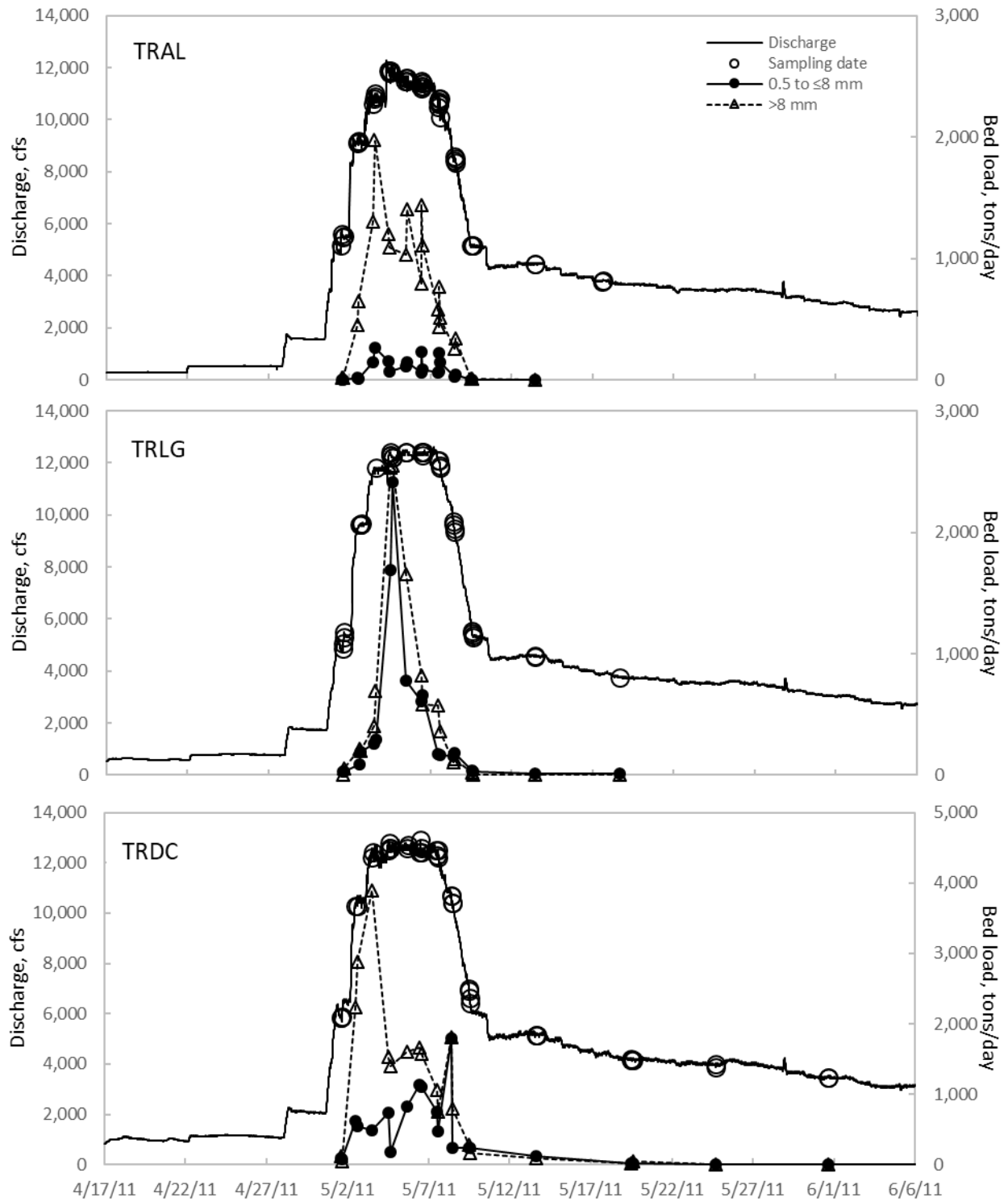
APPENDIX F. (continued)



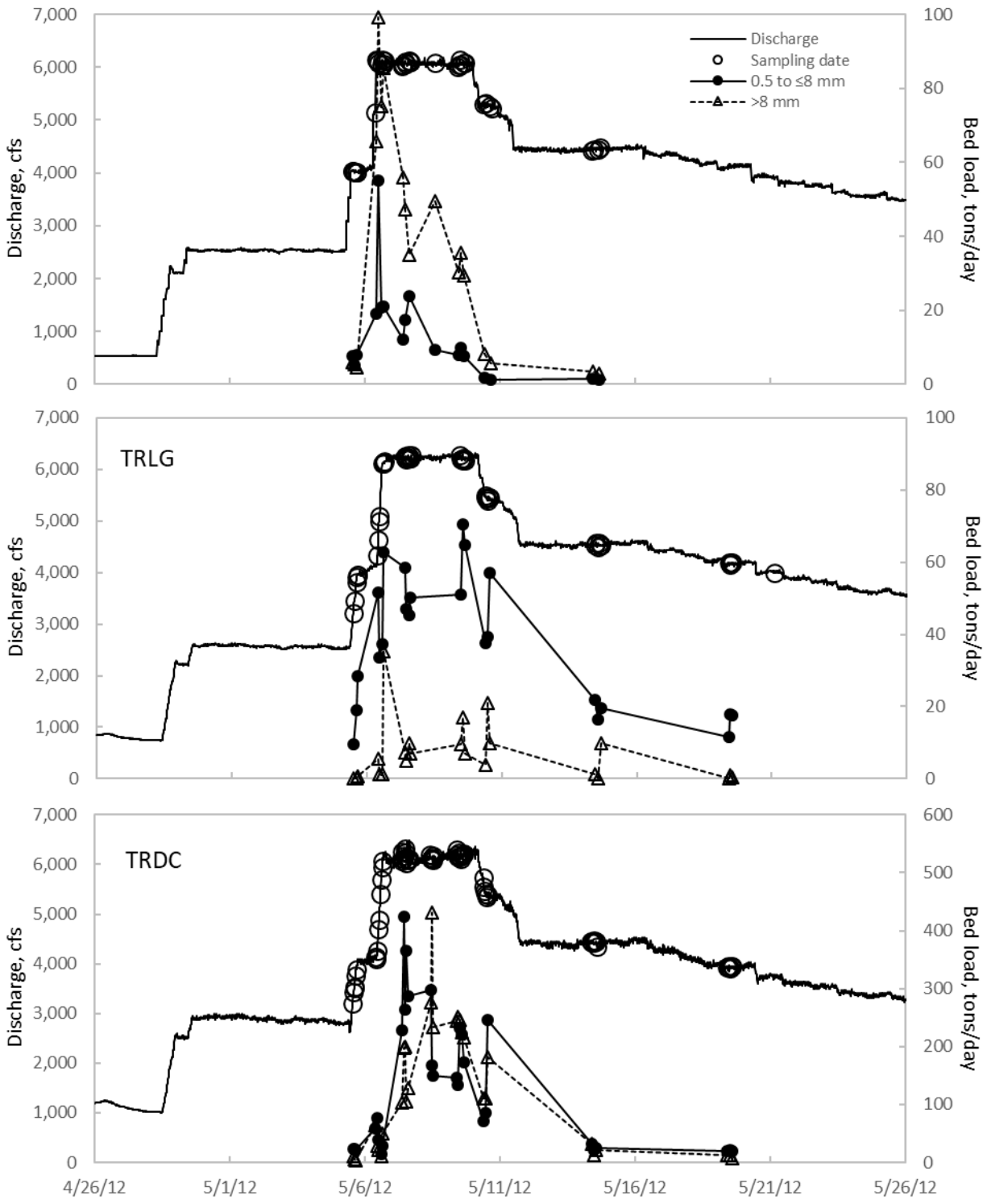
APPENDIX F. (continued)



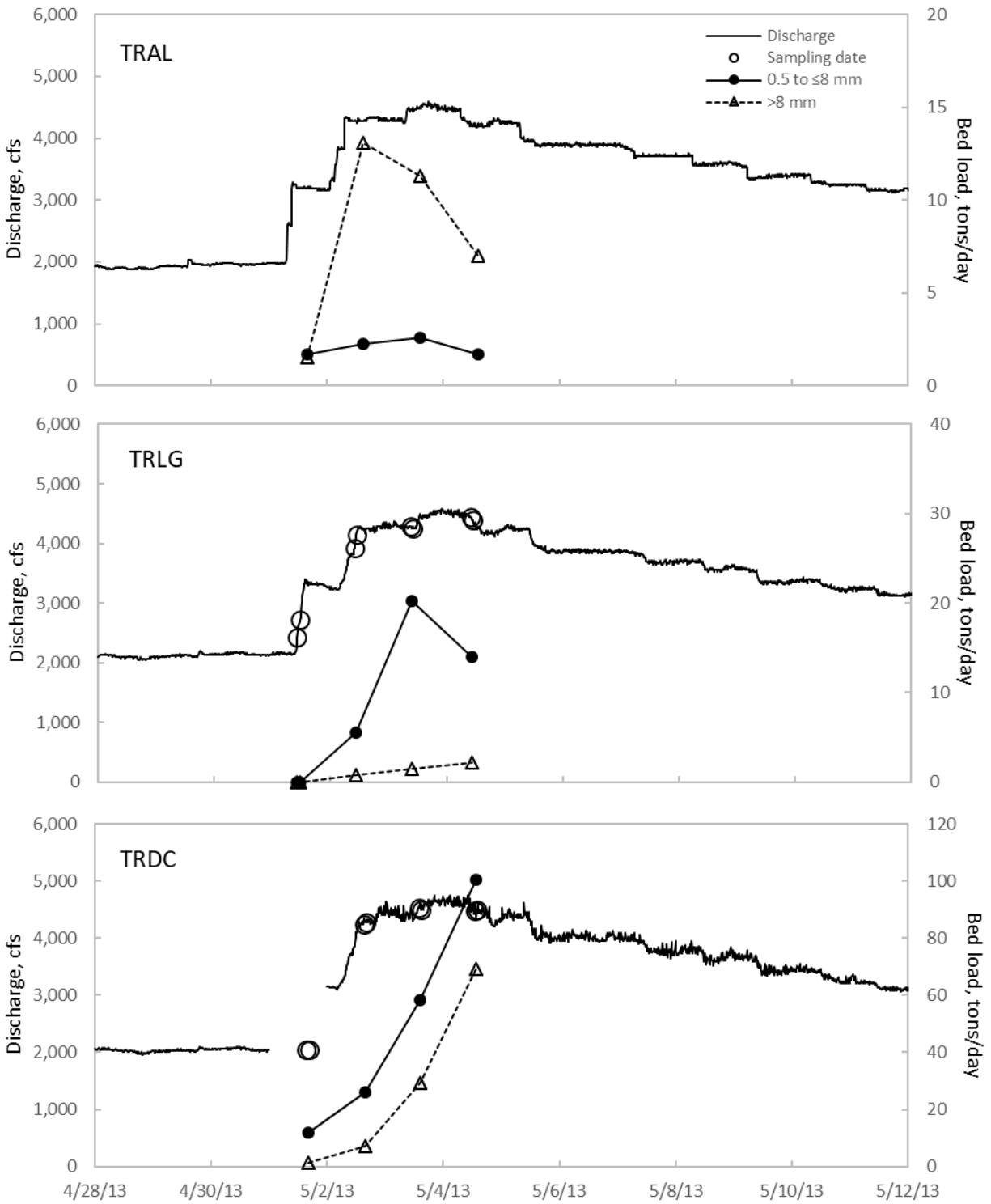
APPENDIX F. (continued)



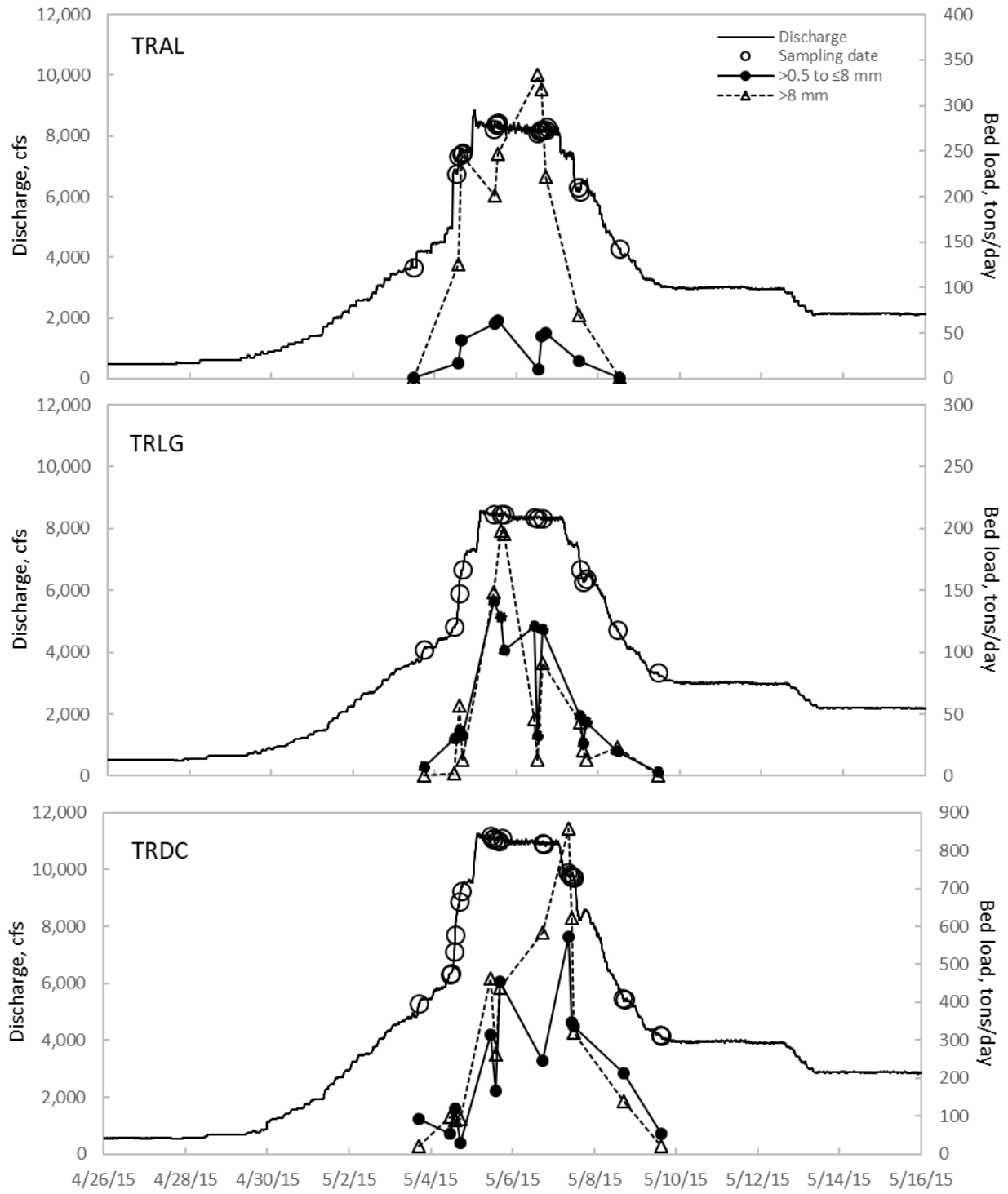
APPENDIX F. (continued)



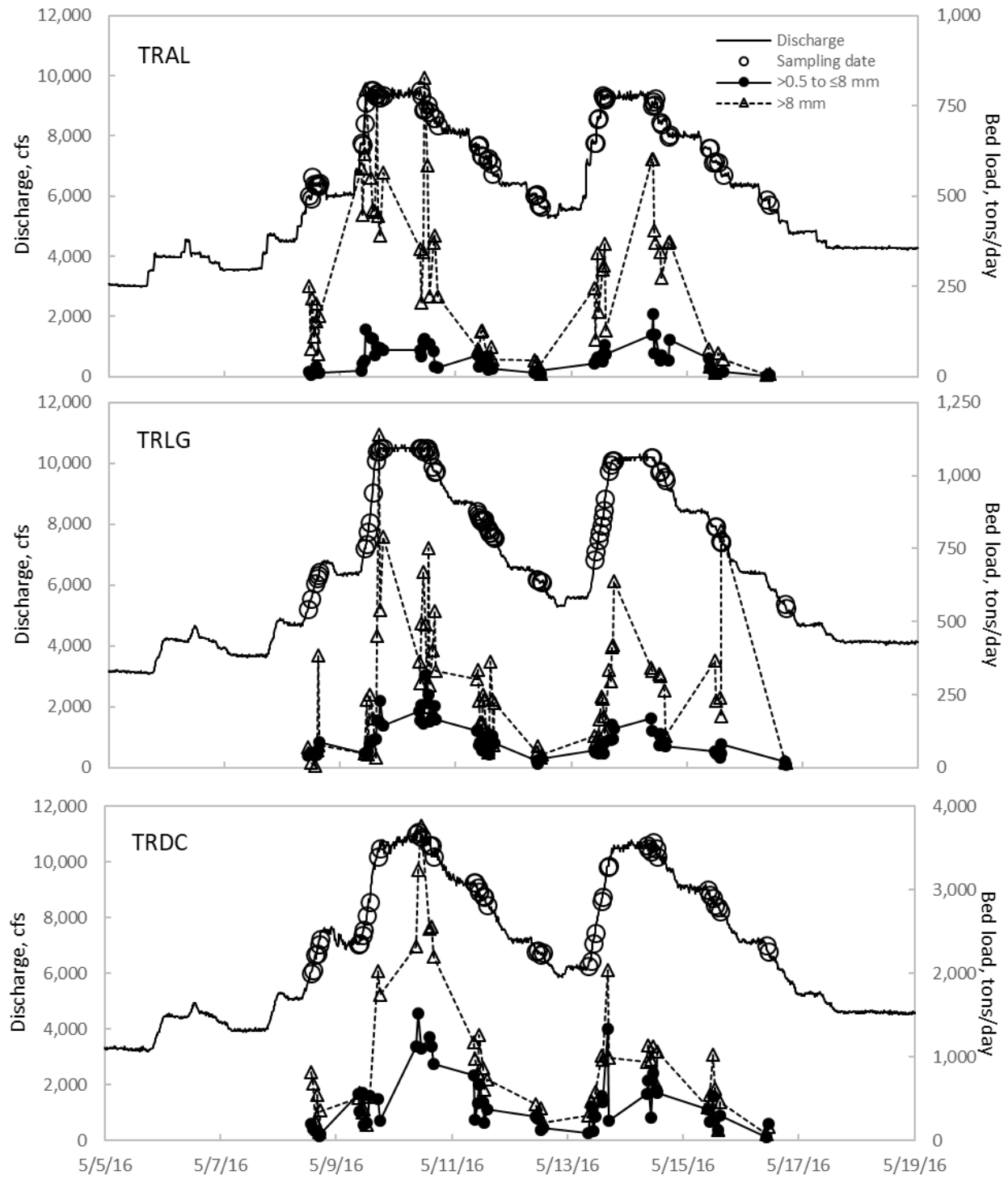
APPENDIX F. (continued)



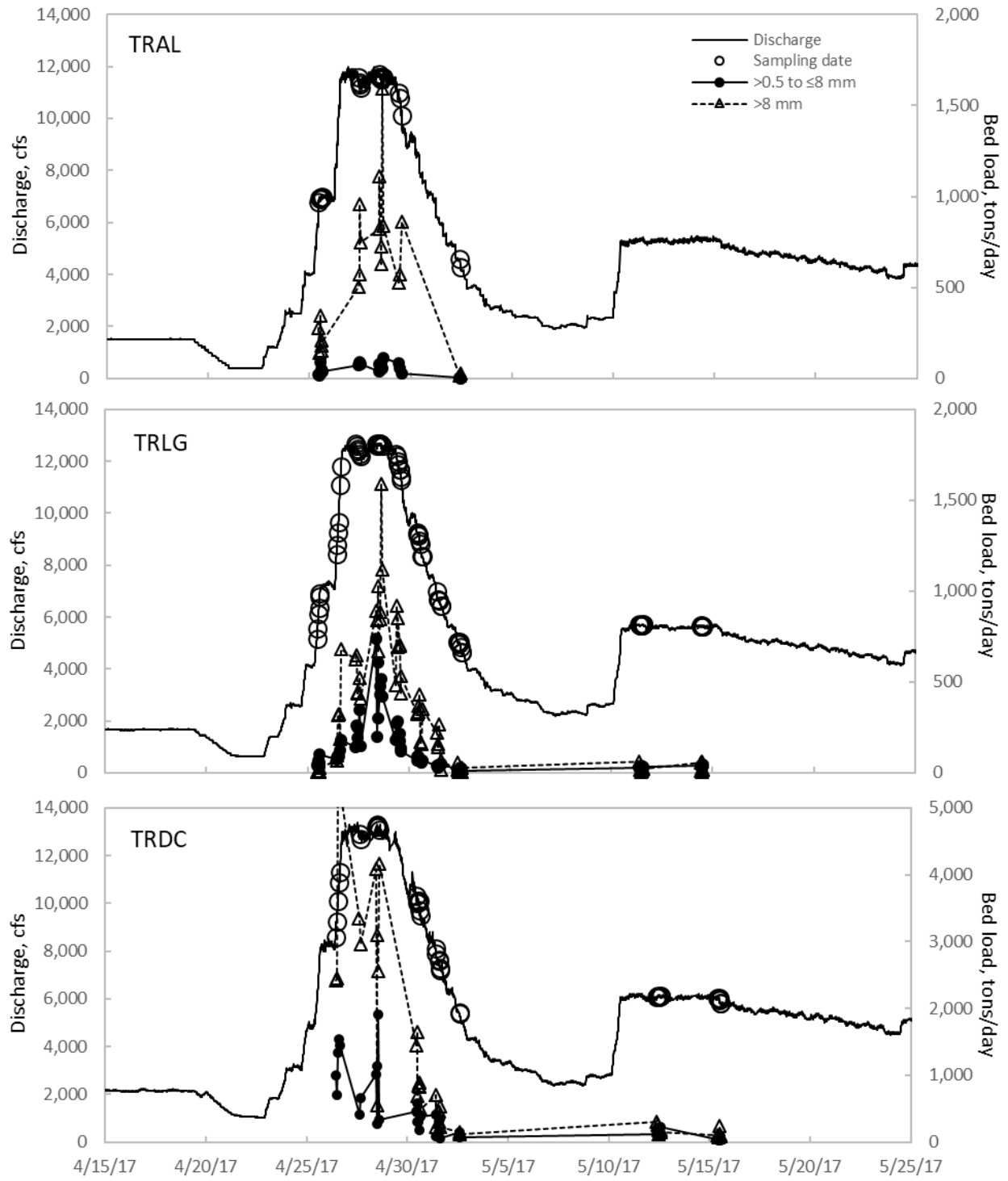
APPENDIX F. (continued)



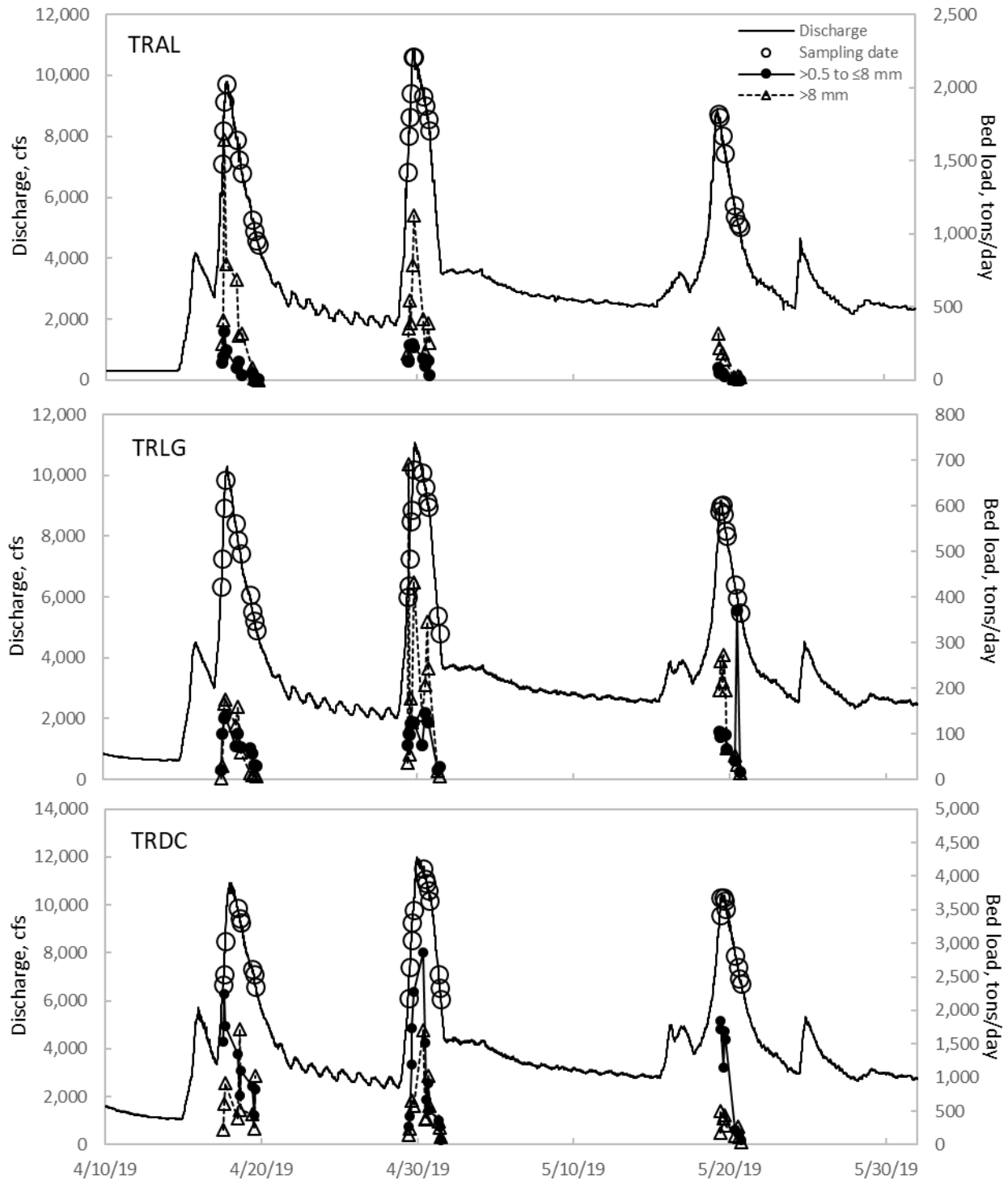
APPENDIX F. (continued)



APPENDIX F. (continued)



APPENDIX F. (continued)

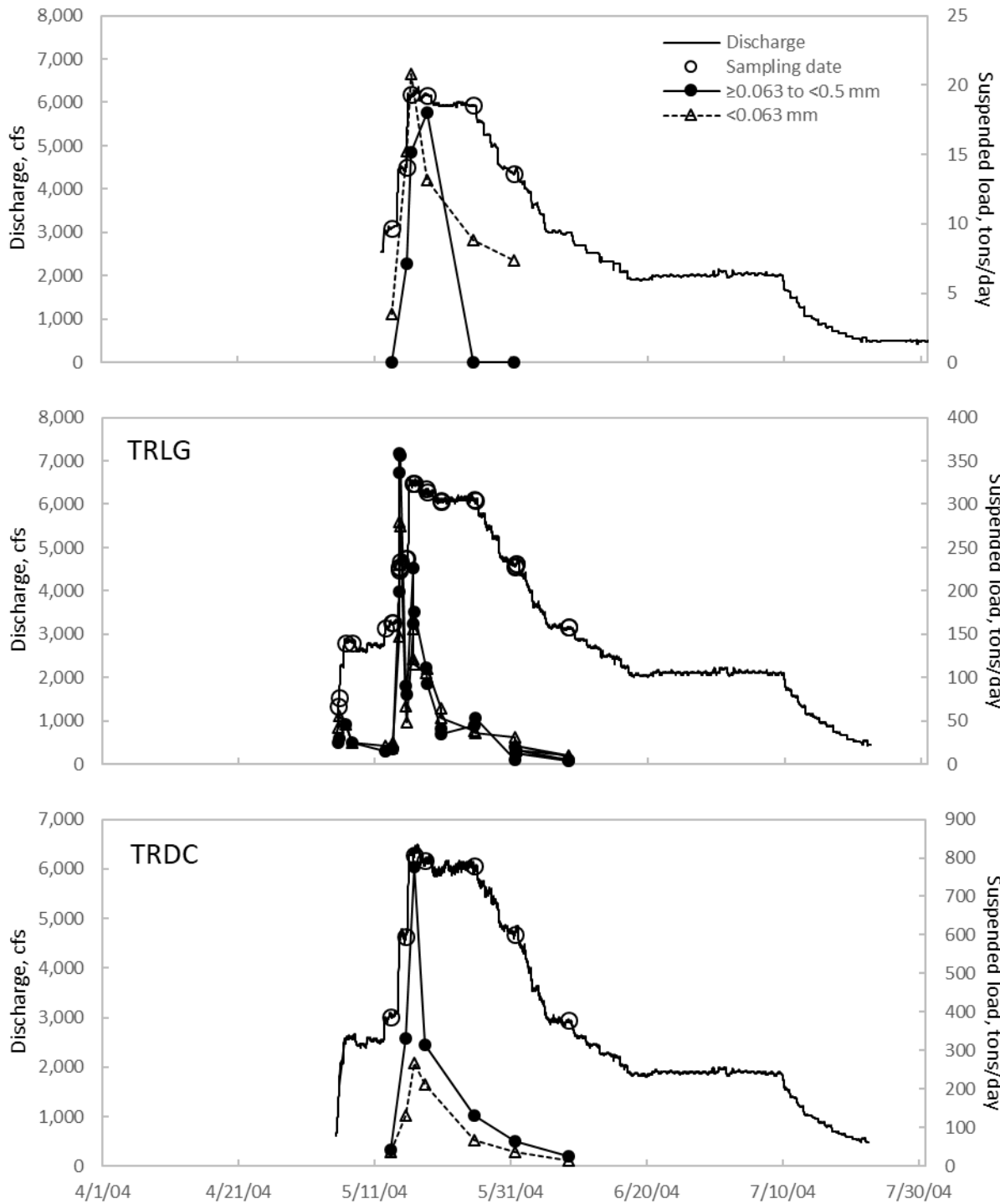


APPENDIX G. Critical discharges and hysteresis for bed loads and suspended loads measured during spring flow releases.

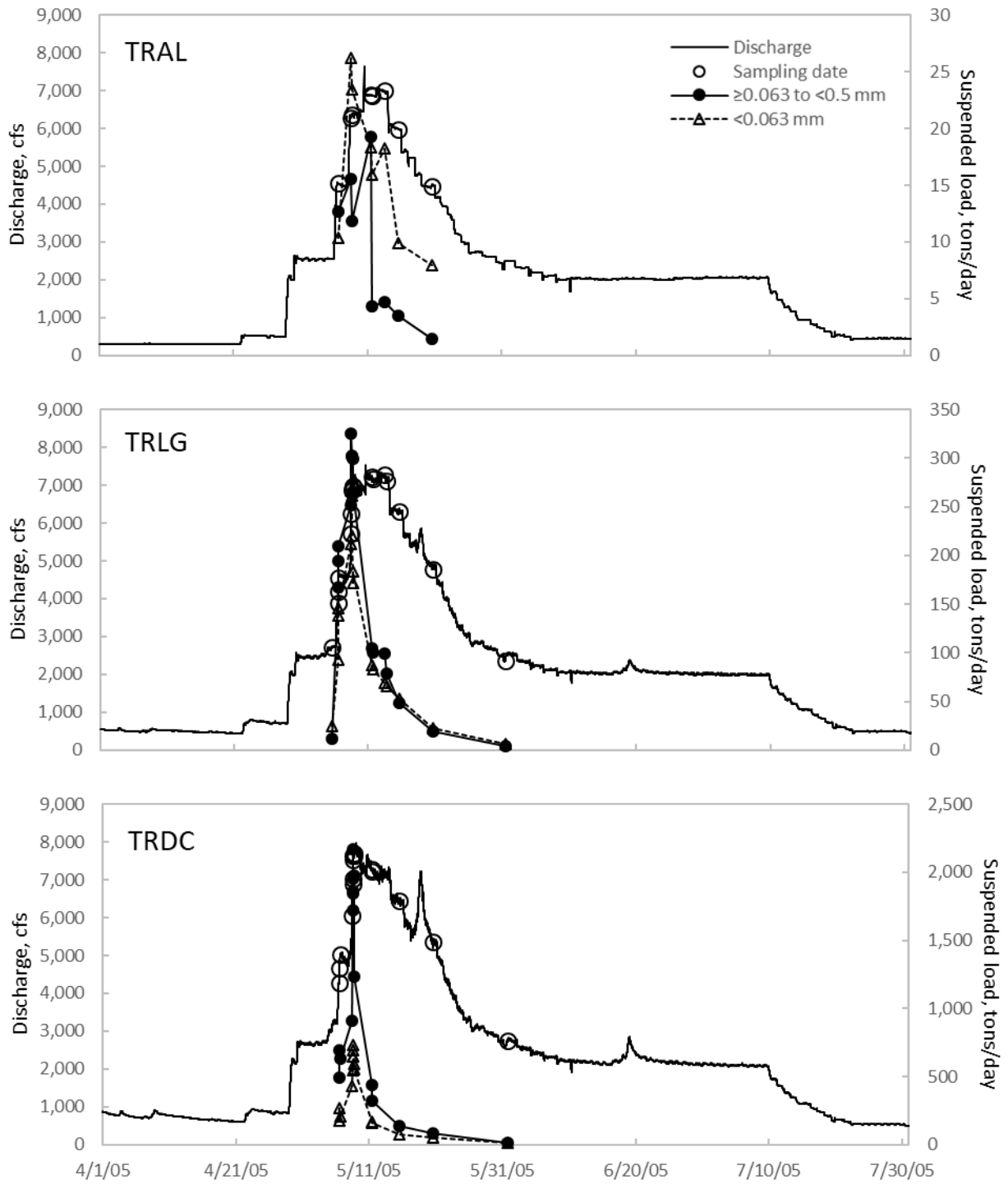
TRAL		Water year	2006	2007	2008	2009	2010	2011	2012	2013	2015	2016	2017	2019
Peak flow (10/1–3/31, 8/1–9/30)			6,090	1,760	472	2,750	512	2,650	1,380	2,630	2,900	1,250	2,380	2,700
Suspended load (<0.5 mm)	Rising stage		560	<b>500</b>	<b>500</b>	397	<b>500</b>	<b>536</b>	<b>720</b>	1,081	1,320	847	NA	NA
	Falling stage		<b>1,000</b>	1,343	<b>1,000</b>	1,997	<b>1,000</b>	1,434	<b>1,000</b>	<b>1,800</b>	<b>4,320</b>	2,356	NA	NA
	Hysteresis (4/1–7/31)?		CW	CW	CW	CW	CW	CCW	CW	<i>i</i>	CW	CW	NA	NA
Bed load	≥0.5 to ≤8 mm	All discharges	4,300	2,885	3,586	2,800	3,950	3,650	3,900	3,700	4,000	3,700	3,422	2,754
		Rising stage	2,948	1,751	5749	1,930	4,481	3,723	2,488	3,650	2,117	2,805	4,391	1,715
		Falling stage	4,490	<i>i</i>	2984	2,579	4,175	3,398	3,783	<i>i</i>	2,649	4,073	4,152	3,066
		Hysteresis (4/1–7/31)?		CW	CW	None	CW	CW	CCW	CW	CW	Fig-8	CW	CW
	>8 mm	All discharges	3,200	3,340	3,500	2,590	3,436	3,050	3,400	1,649	3,100	3,534	3,100	2,119
		Rising stage	2,400	2,595	3790	2,532	3,870	2,324	2,253	1,455	<i>i</i>	2,317	1,746	2,162
Falling stage		2,671	<i>i</i>	2258	2,718	3,846	2,539	3,279	<i>i</i>	2,929	4,165	880	1,818	
	Hysteresis (4/1–7/31)?		CW	CW	None	CW	CW	CW	CW	CW	Fig-8	CCW	CW	
TRLG		Water year	2006	2007	2008	2009	2010	2011	2012	2013	2015	2016	2017	2019
Peak flow (10/1–3/31, 8/1–9/30)			5,900	1,690	777	2,610	1,080	2,460	1,470	2,480	2,890	1,350	2,240	3,760
Suspended load (<0.5 mm)	Rising stage		850	<b>360</b>	496	<b>500</b>	<b>750</b>	<b>750</b>	758	<b>400</b>	<b>800</b>	1200	<b>500</b>	992
	Falling stage		609	<b>1300</b>	920	<b>1000</b>	<b>2000</b>	1330	1963	<b>2200</b>	<b>2000</b>	1358	2760	1121
	Hysteresis (4/1–7/31)?		CW	CW	CW	CW	CW	CW	CW	<i>i</i>	CW	CW	CW	CCW
Bed load	≥0.5 to ≤8 mm	All discharges	1,300	789	908	1,625	1,198	1,214	929	3,298	1,827	1,685	837	747
		Rising stage	1,500	688	700	1,564	1,746	1,421	971	3,182	3,428	1,400	1,100	837
		Falling stage	454	<i>i</i>	1,299	<i>i</i>	959	700	1,465	<i>i</i>	568	2,092	574	491
		Hysteresis (4/1–7/31)?		CW	CW	None	CW	CW	CW	CW	CW	Fig-8	CW	Fig-8
	>8 mm	All discharges	3,569	3,504	3,619	3,745	3,910	4,000	4,121	4,372	4,620	2,946	2,192	2,617
		Rising stage	3,030	3,676	3,285	3,703	4,174	2,579	4,134	<i>i</i>	4,920	3,203	2,459	3,031
Falling stage		4,128	<i>i</i>	3,981	<i>i</i>	3,912	3,093	4,095	<i>i</i>	2,451	3,204	1,572	1,881	
	Hysteresis (4/1–7/31)?		CW	CW	None	None	CW	CCW	CW	<i>i</i>	Fig-8	CCW	None	
TRDC		Water year	2006	2007	2008	2009	2010	2011	2012	2013	2015	2016	2017	2019
Peak flow (10/1–3/31, 8/1–9/30)			7,620	1,510	1,980	2,490	2,210	2,630	3,010	2,420	3,370	3,230	4,900	11,500
Suspended load (<0.5 mm)	Rising stage		425	<b>475</b>	<b>350</b>	<b>525</b>	<b>600</b>	<b>800</b>	1131	<b>525</b>	929	<b>1000</b>	<b>1000</b>	2660
	Falling stage		<b>1800</b>	674	979	1410	<b>1000</b>	<b>2500</b>	<b>1700</b>	<b>3000</b>	1872	<b>2100</b>	<b>4500</b>	1748
	Hysteresis (4/1–7/31)?		CW	CW	CW	CW	CW	CW	CW	<i>i</i>	CW	CW	CW	CCW
Bed load	≥0.5 to ≤8 mm	All discharges	560	661	974	993	1,400	1,600	1,851	2,003	1,655	5,499	2,269	4,309
		Rising stage	1,700	1,004	600	704	1,219	1,002	2,029	3,300	2,029	5,570	2,000	3,328
		Falling stage	622	770	1,092	464	1,030	2,300	1,433	<i>i</i>	1,100	5,628	3,138	2,626
		Hysteresis (4/1–7/31)?		None	CCW	CW	None	CW	CW	CCW	<i>i</i>	CCW	CW	CW
	>8 mm	All discharges	1,813	2,894	2,200	2,024	2,682	2,100	2,684	1,477	657	4,383	1,629	3,256
		Rising stage	2,421	4,124	1,750	1,915	3,208	956	2,895	1,152	643	4,897	4,800	2,885
Falling stage		1,507	2,457	1,726	2,281	2,095	2,300	1,869	<i>i</i>	500	3,879	769	2,016	
	Hysteresis (4/1–7/31)?		None	CW	CW	None	CW	CW	None	<i>i</i>	CCW	CW	Fig-8	

*i*= insufficient data for determination of hysteresis; None=hysteresis did not occur; hysteresis shapes are CW=clockwise, CCW=counter-clockwise, and Fig-8=figure eight; Discharges are in cubic feet per second; Peak flows indicate whether critical conditions were exceeded outside the spring flow release period; Bold values estimated by Graham Mathews and Associates.

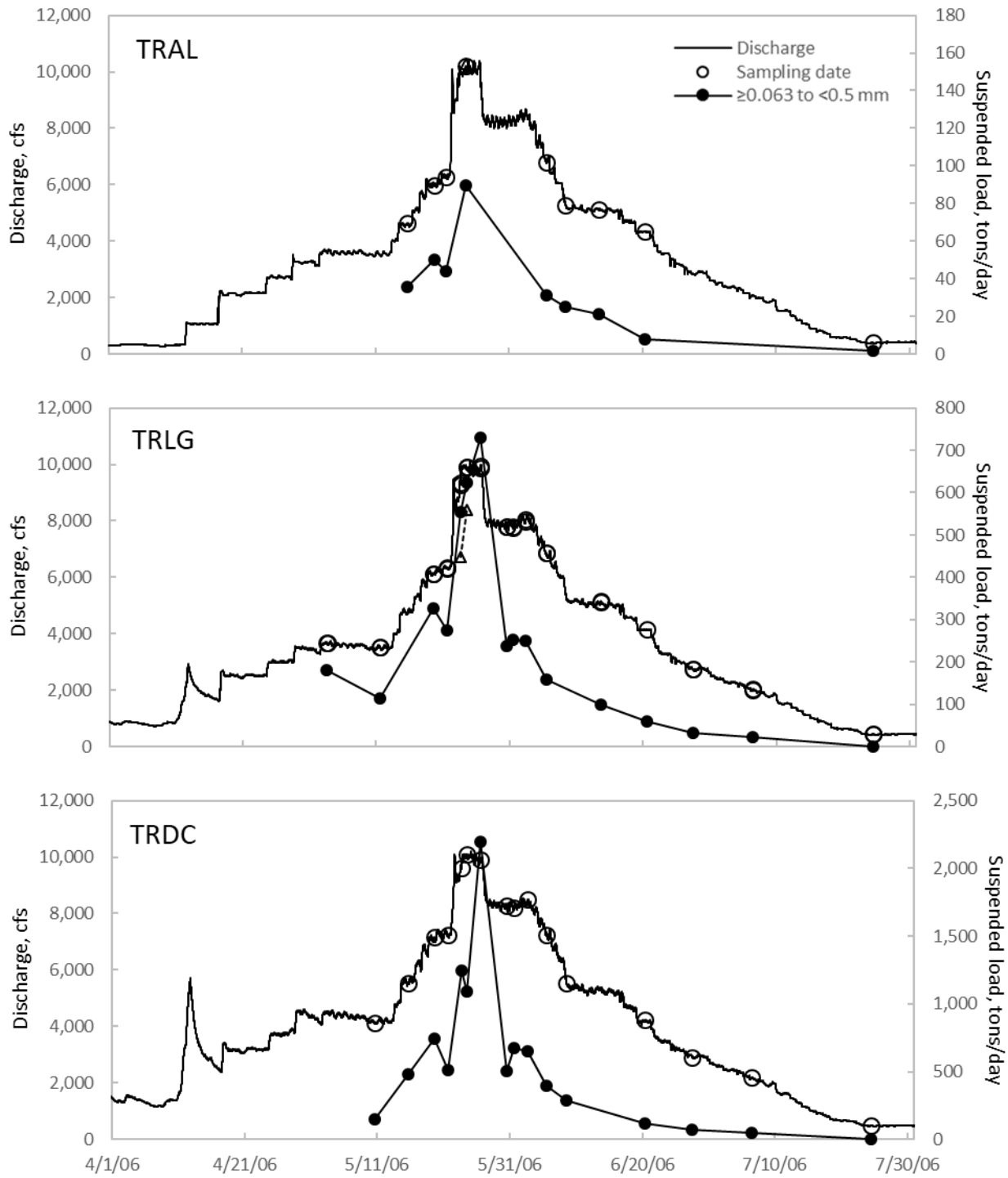
APPENDIX H. Suspended sediment loads measured during spring flow releases.



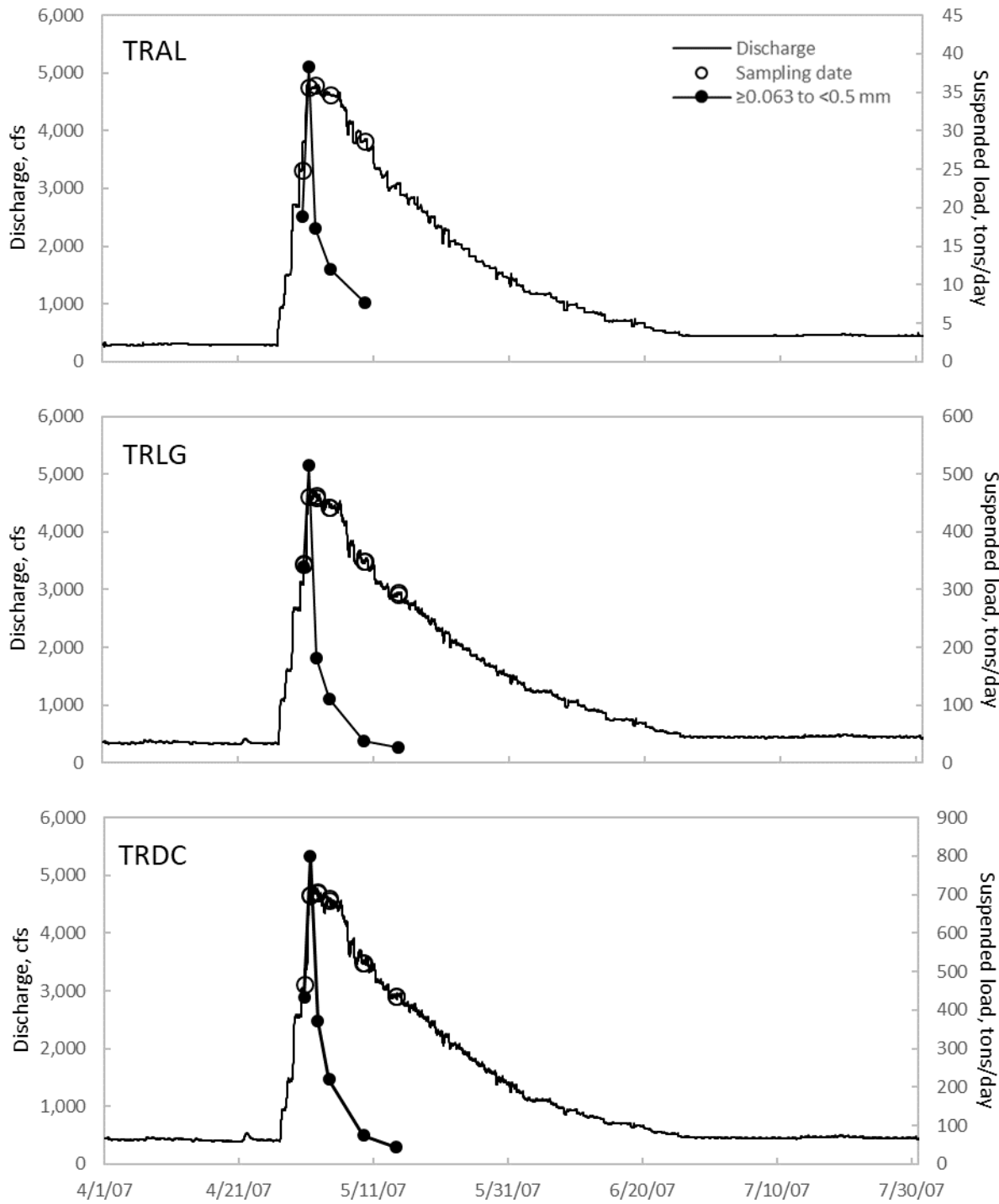
APPENDIX H. (continued)



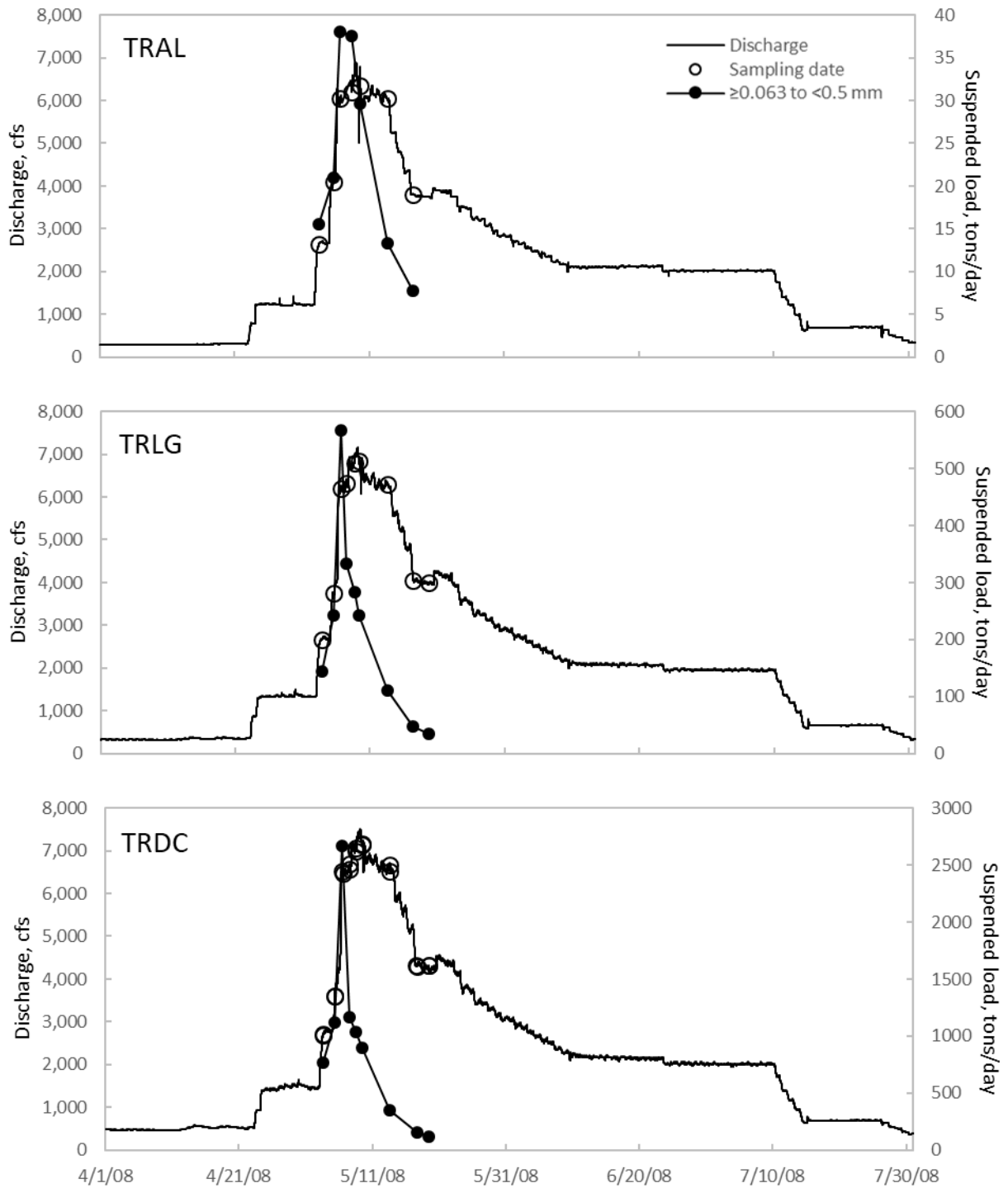
APPENDIX H. (continued)



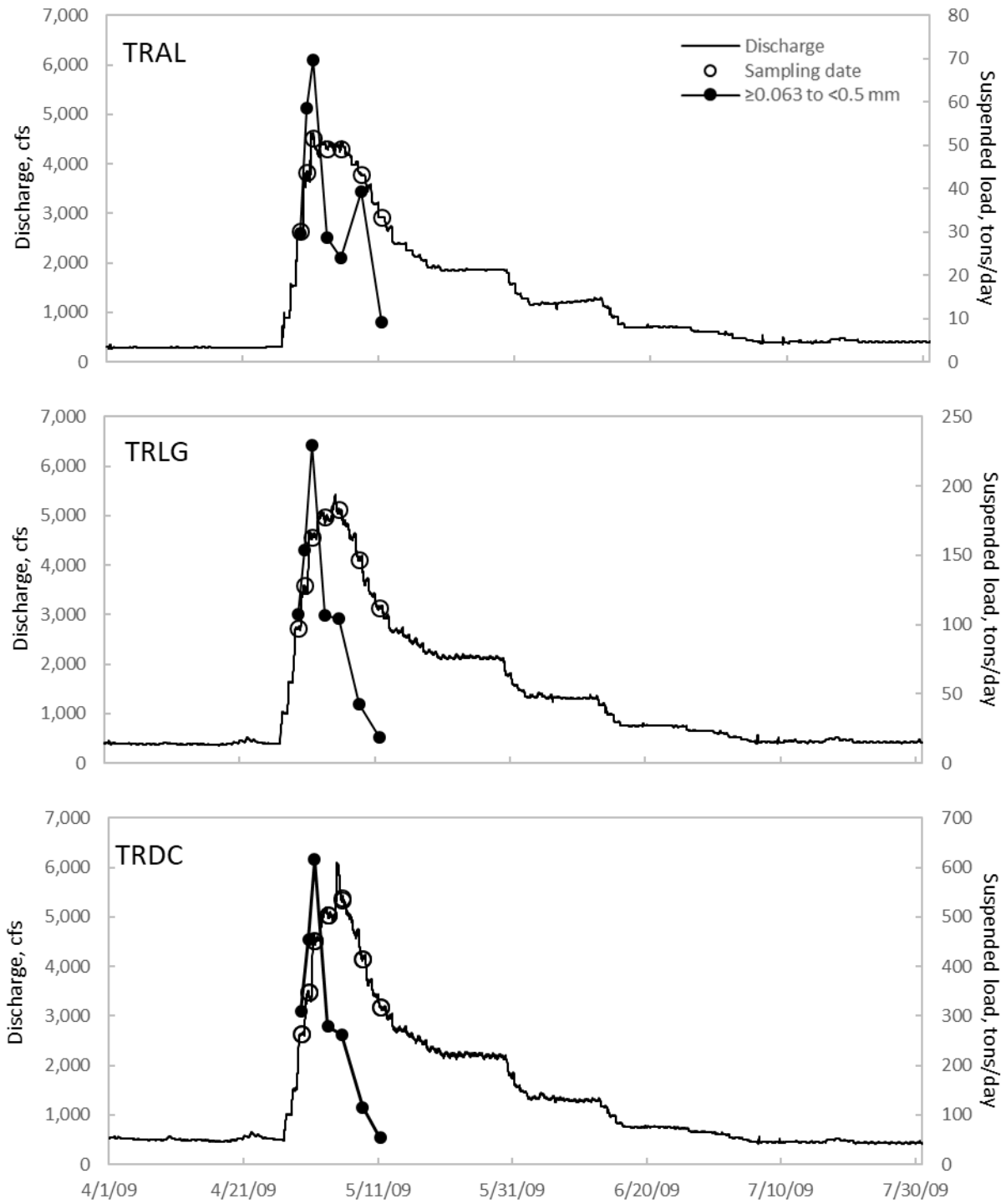
APPENDIX H. (continued)



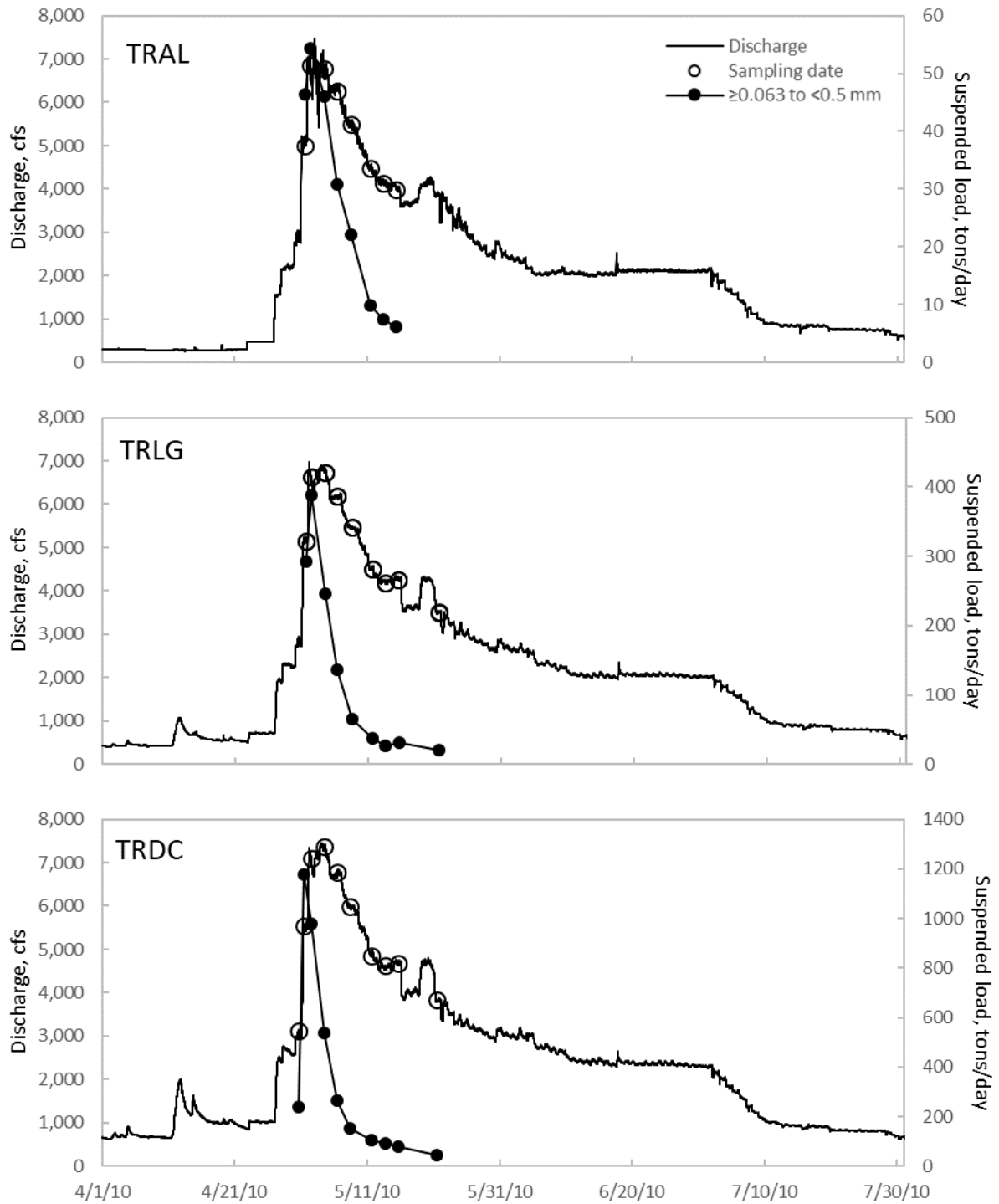
APPENDIX H. (continued)



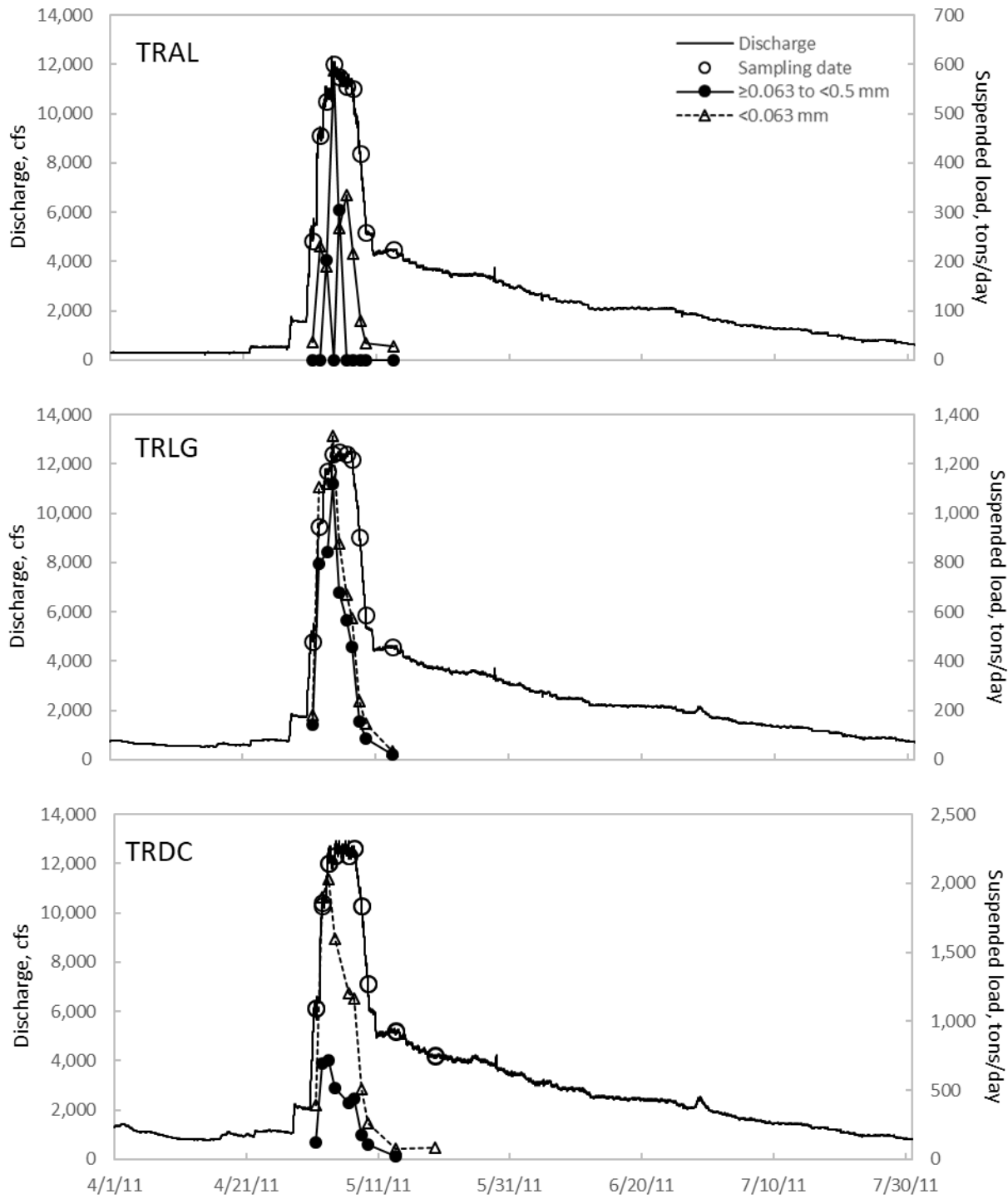
APPENDIX H. (continued)



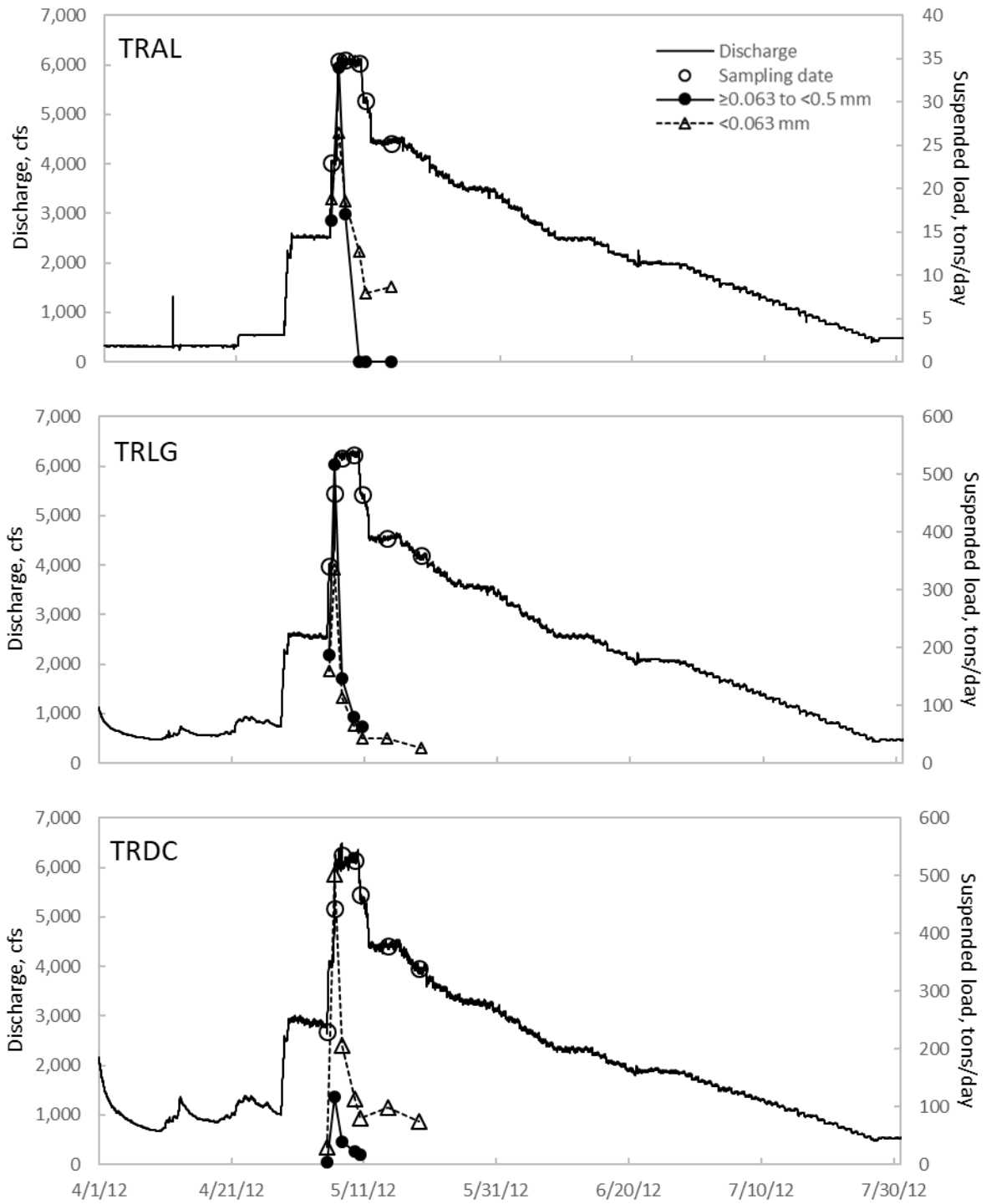
APPENDIX H. (continued)



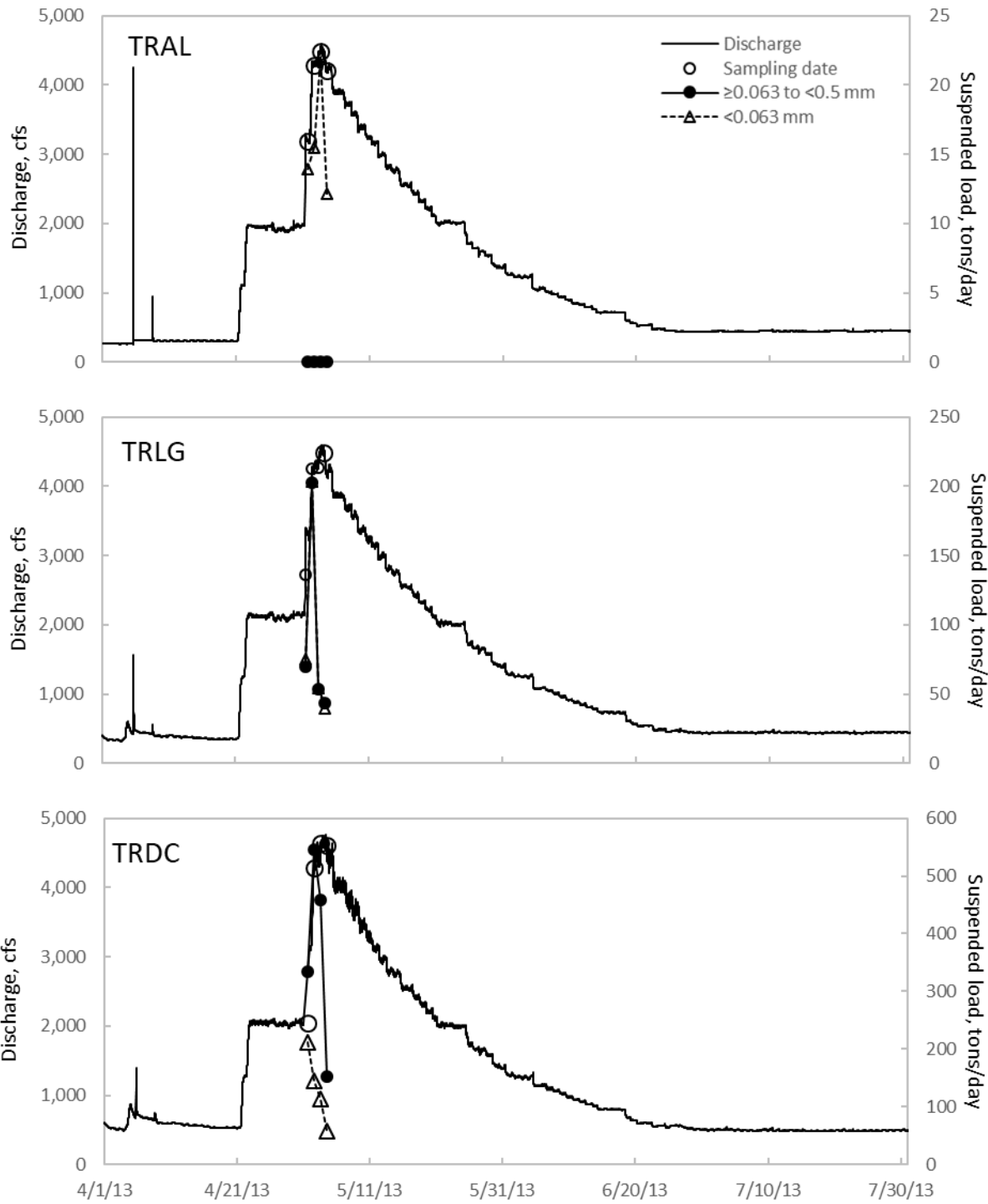
APPENDIX H. (continued)



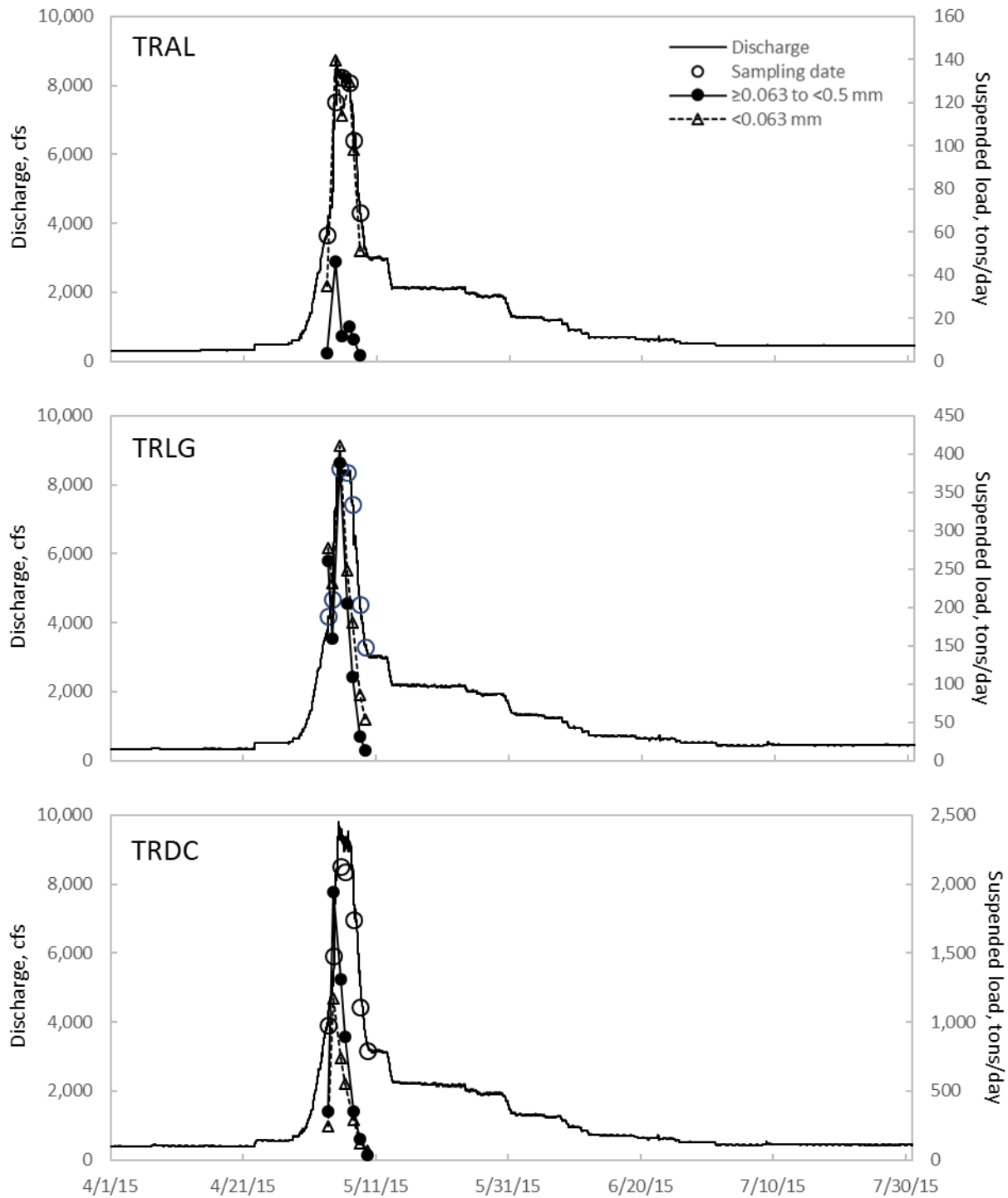
APPENDIX H. (continued)



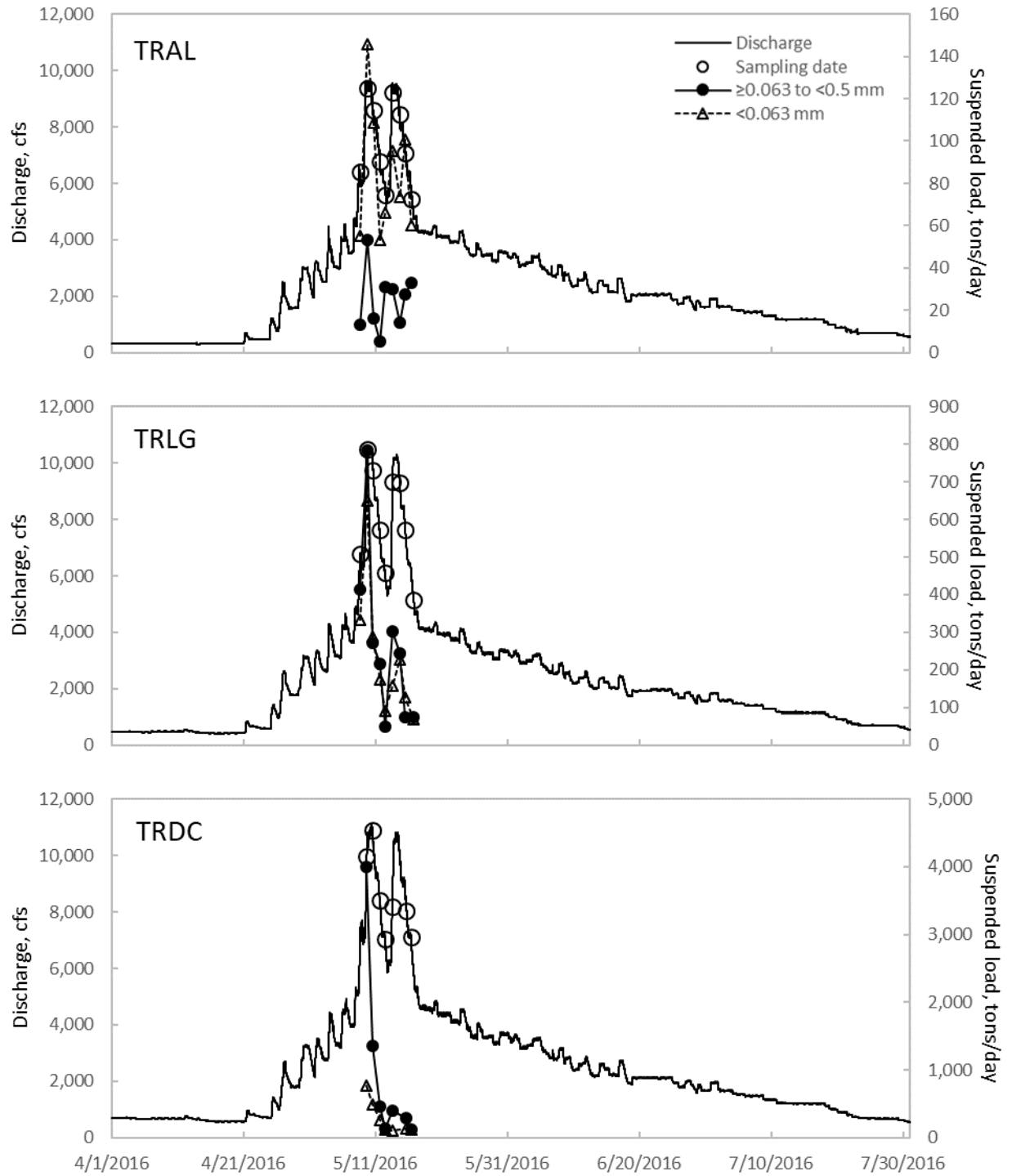
APPENDIX H. (continued)



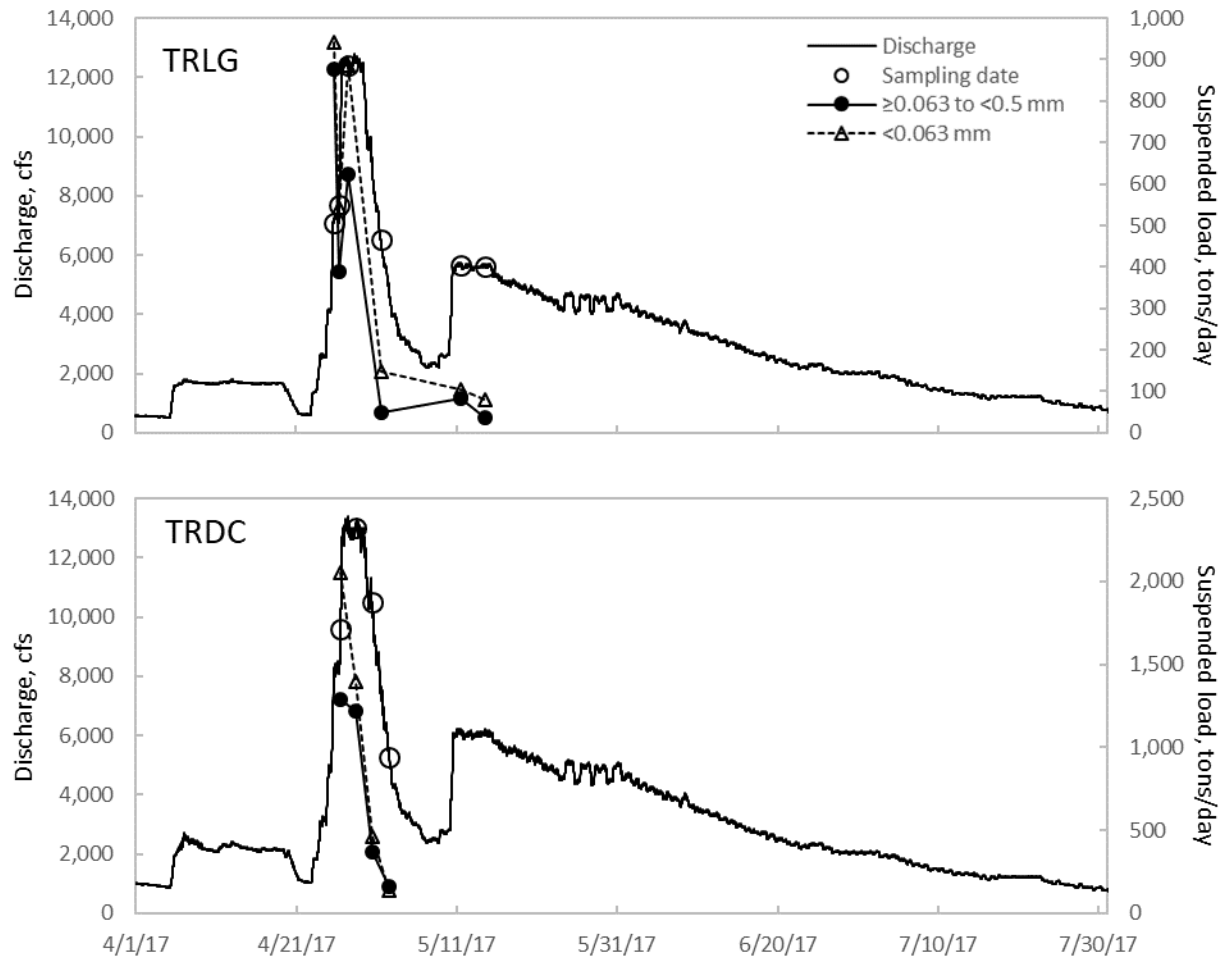
APPENDIX H. (continued)



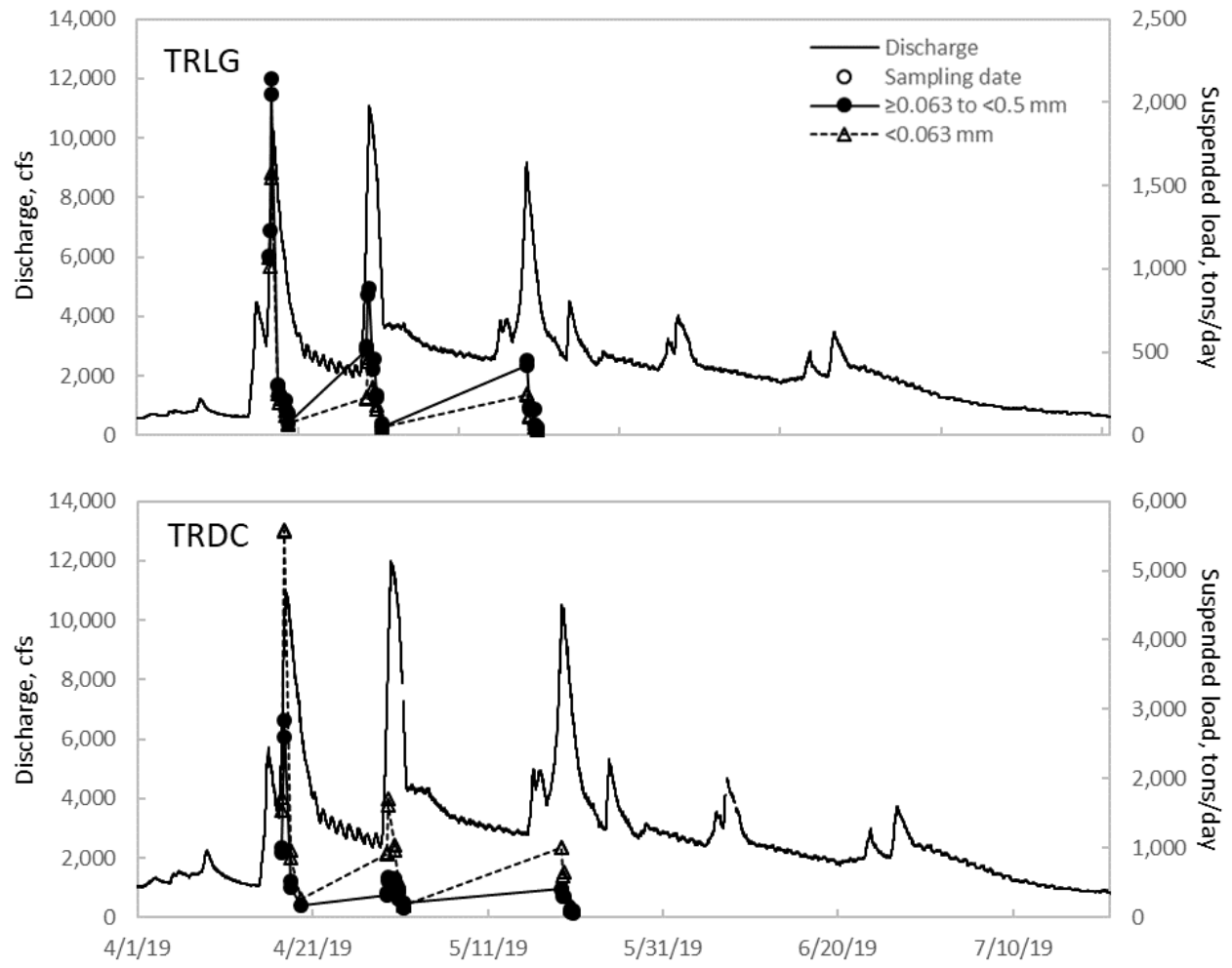
APPENDIX H. (continued)



APPENDIX H. (continued)



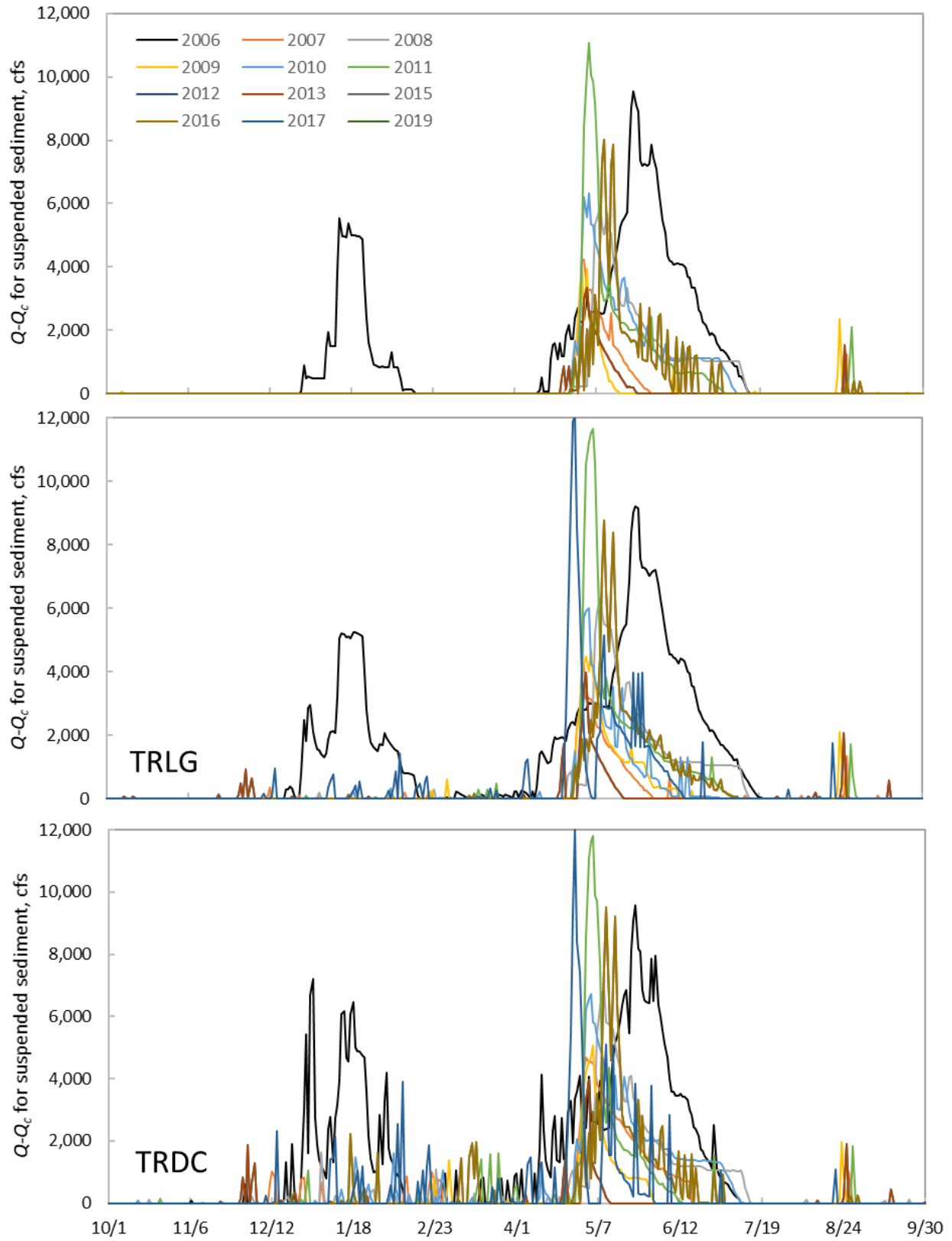
APPENDIX H. (continued)



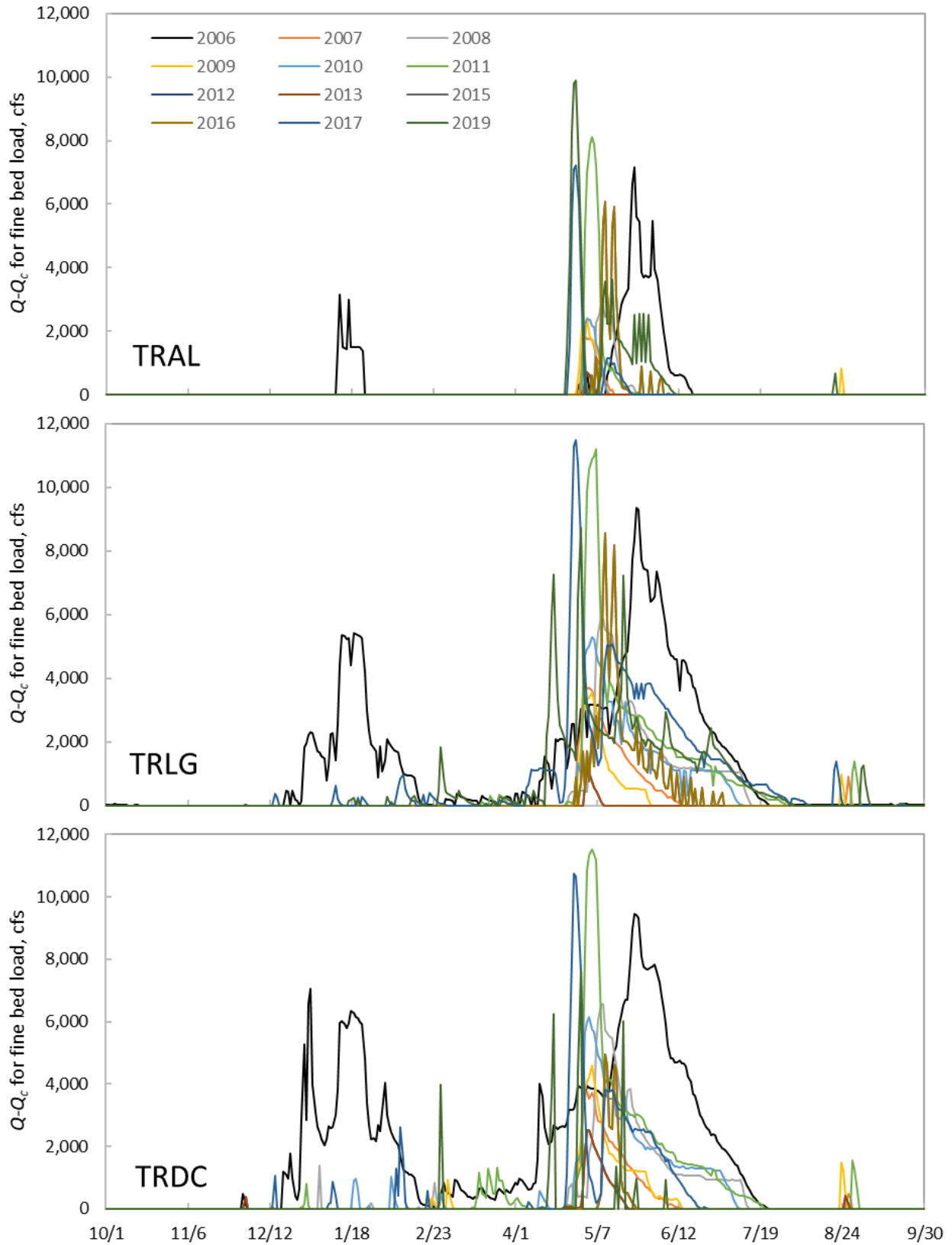
APPENDIX I. Fractional suspended sediment and bed loads measured during spring flow releases.

Water year	Location	Spring flow release (AF)	Suspended sediment (SS)			Bedload			Total fines <sup>1</sup>	Total fines/ >8mm bedload	Total fines/ flow
			<0.063 mm	≥0.063 to <0.5 mm	Total SS	≥0.5 to ≤8 mm	>8 mm	Total bedload			
2019	TRAL	531,840	Suspended sediment transport not measured			614	2,300	<b>2,914</b>	614	0.3	0.00115
2017	TRAL	677,165	Suspended sediment transport not measured			412	4,330	4,740	412	0.1	0.00061
2016	TRAL	535,137	1,510	271	1,781	338	1,800	2,140	2,119	1.2	0.00396
2015	TRAL	282,488	662	83	745	146	715	861	891	1.2	0.00315
2013	TRAL	282,899	136	0	136	16	45	61	152	3.4	0.00054
2012	TRAL	479,982	249	78	327	80	222	302	407	1.8	0.00085
2011	TRAL	556,816	2,400	497	2,897	714	6,460	7,170	3,611	0.6	0.00649
2010	TRAL	486,282		406	406	39	550	589	445	0.8	0.00092
2009	TRAL	276,803		448	448	65	260	325	513	2.0	0.00185
2008	TRAL	482,287		456	456	236	863	1,100	692	0.8	0.00143
2007	TRAL	287,482		195	195	77	93	170	272	2.9	0.00095
2006	TRAL	803,800		2,670	2,670	1,430	8,610	10,000	4,100	0.5	0.00510
2005	TRAL	480,639		459	459	235	531	766	694	1.3	0.00144
2004	TRAL	476,359		483	483	282	1,700	1,982	765	0.5	0.00161
2019	TRLG	573,628	3,450	5,100	8,550	868	870	1,738	9,418	10.8	0.01642
2017	TRLG	714,010	7,340	4,210	11,550	1,740	3,110	4,850	13,290	4.3	0.01861
2016	TRLG	538,931	2,800	2,410	5,210	781	2,040	2,820	5,991	2.9	0.01112
2015	TRLG	287,304	2,580	1,600	4,180	344	326	670	4,524	13.9	0.01575
2013	TRLG	291,592	438	367	805	60	6	66	865	144.2	0.00297
2012	TRLG	508,756	1,470	1,070	2,540	614	60	674	3,154	52.6	0.00620
2011	TRLG	597,890	6,770	4,950	11,720	4,340	5,930	10,300	16,060	2.7	0.02686
2010	TRLG	503,201		3,110	3,110	666	367	1,030	3,776	10.3	0.00750
2009	TRLG	310,681		1,797	1,797	236	34	270	2,033	59.8	0.00654
2008	TRLG	493,918		3,480	3,480	1,330	775	2,100	4,810	6.2	0.00974
2007	TRLG	286,251		2,200	2,200	278	12	290	2,478	206.5	0.00866
2006	TRLG	823,974		45,800	45,800	6,660	4,350	11,000	52,460	12.1	0.06367
2005	TRLG	507,086		2,868	2,868	1,314	1,853	3,167	4,182	2.3	0.00825
2004	TRLG	504,908		2,871	2,871	1,649	1,359	3,008	4,520	3.3	0.00895
2019	TRDC	654,817	5,770	11,300	17,070	5,580	10,410	15,990	22,650	2.2	0.03459
2017	TRDC	775,347	8,300	9,750	18,050	5,510	18,200	23,700	23,560	1.3	0.03039
2016	TRDC	585,380	3,780	6,710	10,490	4,010	7,850	11,900	14,500	1.8	0.02477
2015	TRDC	295,226	3,730	4,880	8,610	1,600	1,920	3,520	10,210	5.3	0.03458
2013	TRDC	306,571	690	1,790	2,480	834	439	1,270	3,314	7.5	0.01081
2012	TRDC	508,423	3,360	3,340	6,700	1,430	1,200	2,630	8,130	6.8	0.01599
2011	TRDC	677,685	12,500	19,300	31,800	6,110	13,200	19,300	37,910	2.9	0.05594
2010	TRDC	574,040		7,460	7,460	1,690	1,650	3,340	9,150	5.5	0.01594
2009	TRDC	320,940		4,554	4,554	882	634	1,515	5,436	8.6	0.01694
2008	TRDC	525,606		11,700	11,700	2,510	2,380	4,900	14,210	6.0	0.02704
2007	TRDC	285,697		9,530	9,530	733	297	1,030	10,263	34.6	0.03592
2006	TRDC	930,575		298,000	298,000	12,700	15,200	27,900	310,700	20.4	0.33388
2005	TRDC	552,129		9,271	9,271	5,067	5,229	10,500	14,338	2.7	0.02597
2004	TRDC	495,074		8,359	8,359	3,754	4,869	8,623	12,113	2.5	0.02447

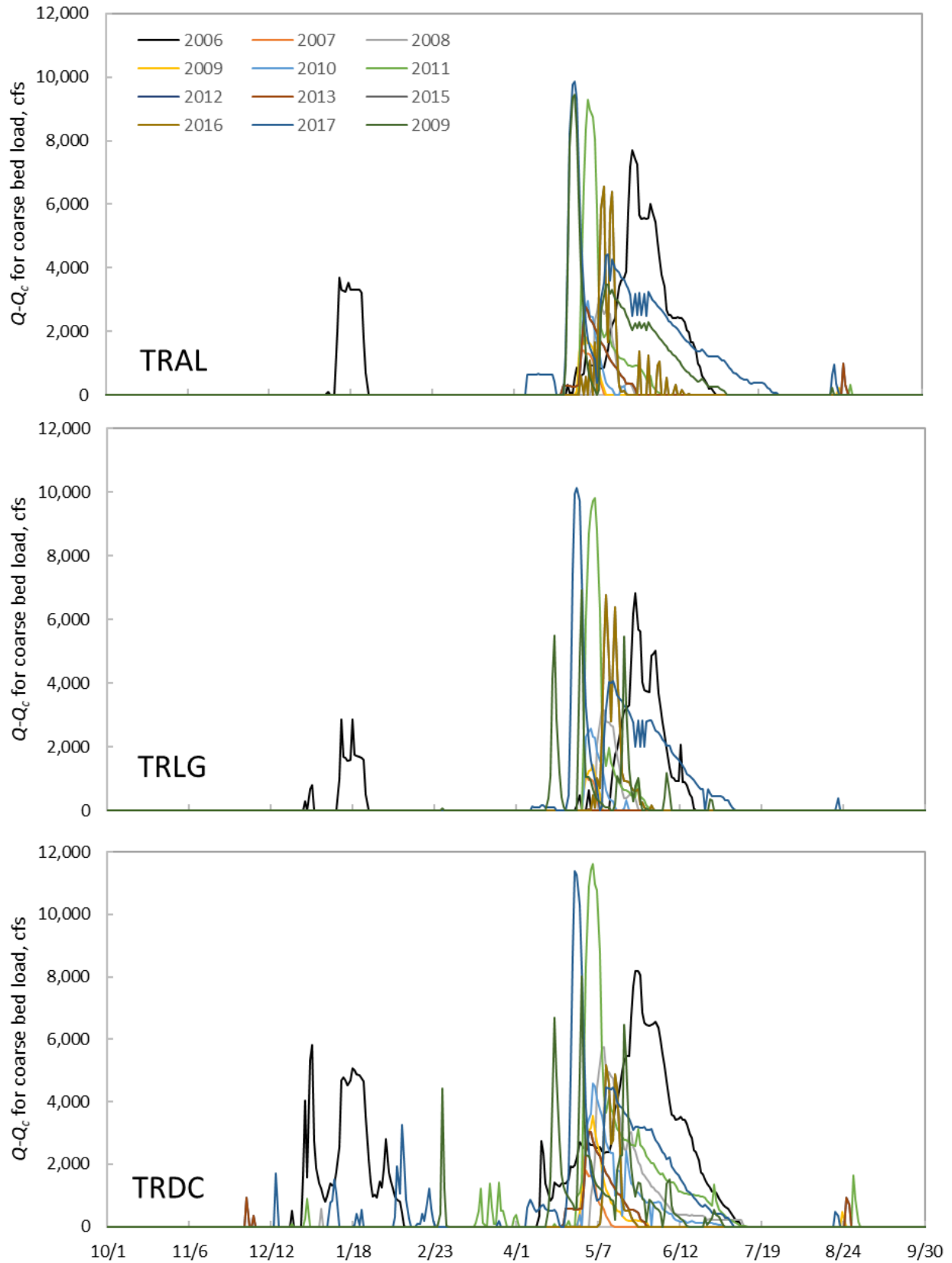
APPENDIX J. Discharges above thresholds for sediment transport at TRAL, TRLG, and TRDC.



APPENDIX J. (continued)

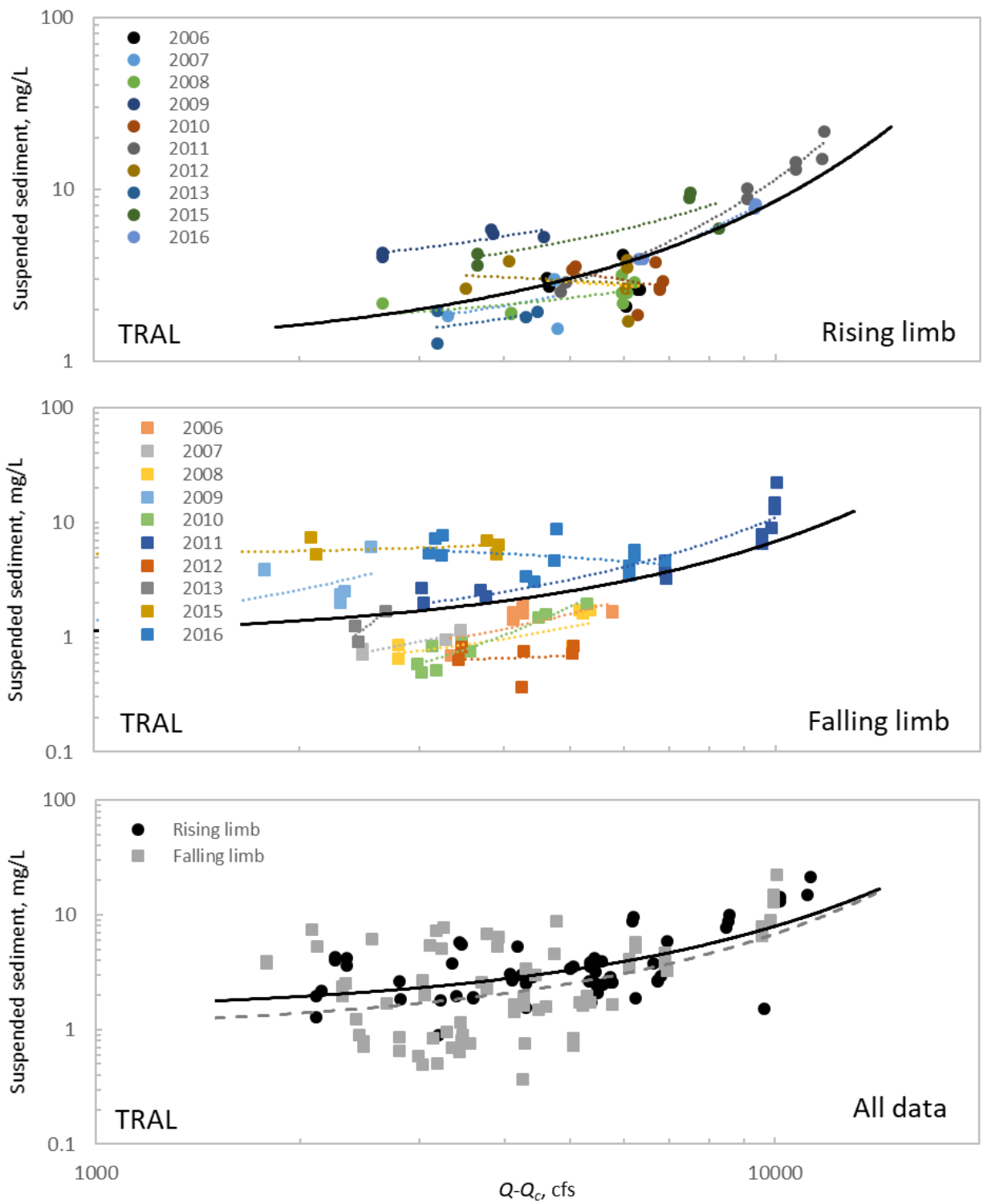


APPENDIX J. (continued)

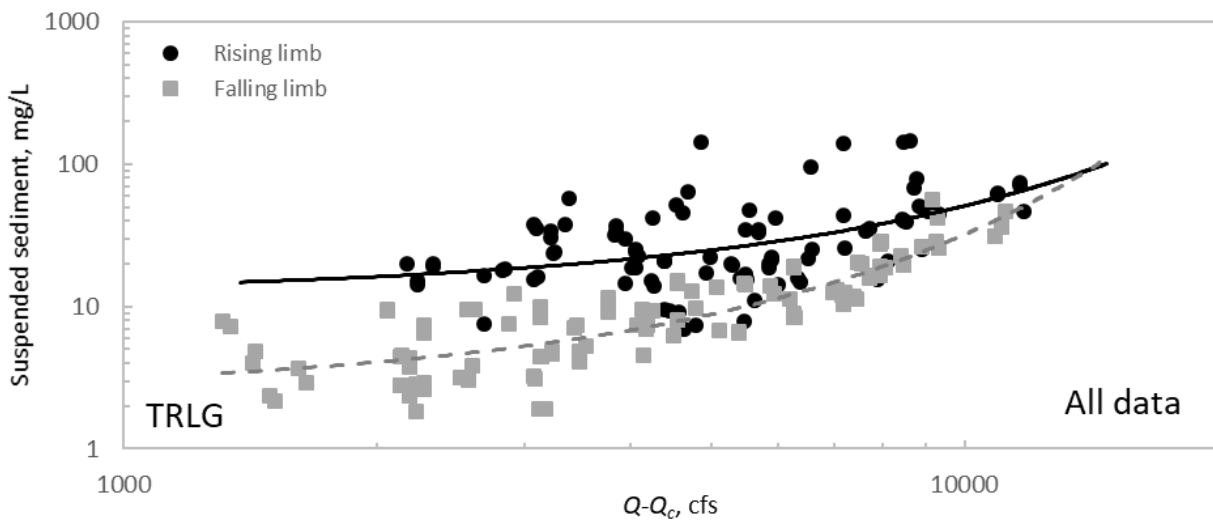
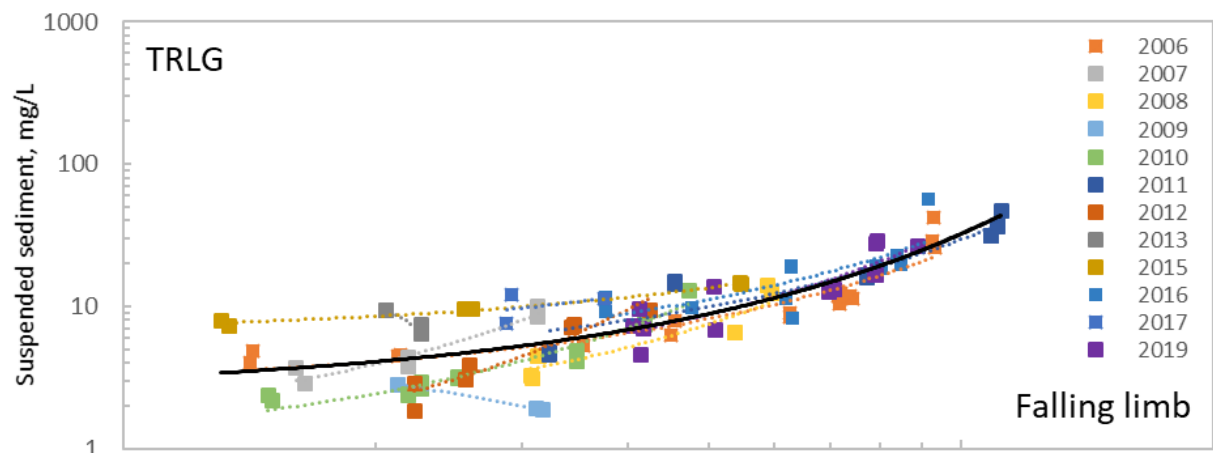
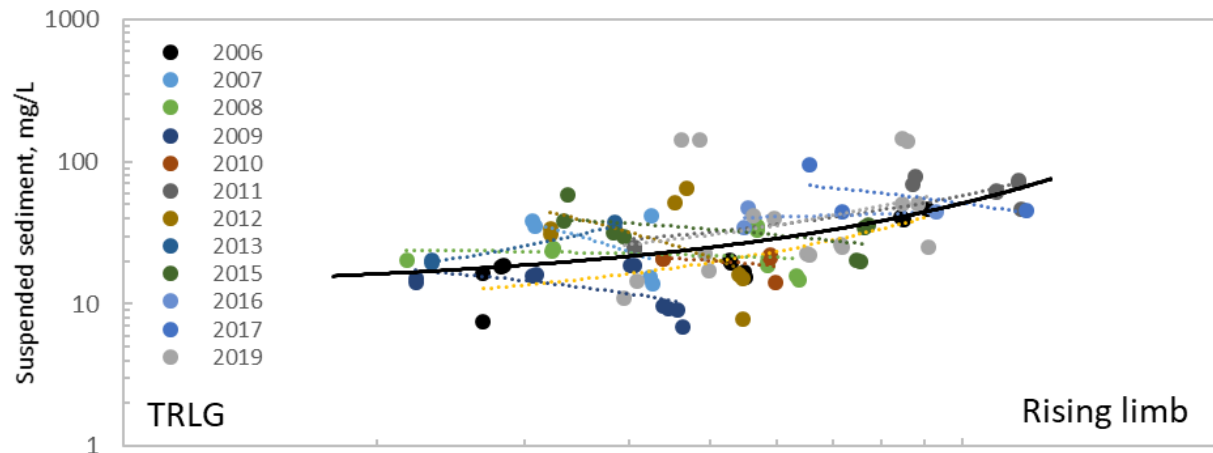


APPENDIX K. Exponential curves relating discharges that exceed critical flows for suspended sediment to concentrations at TRAL, TRLG, and TRDC.

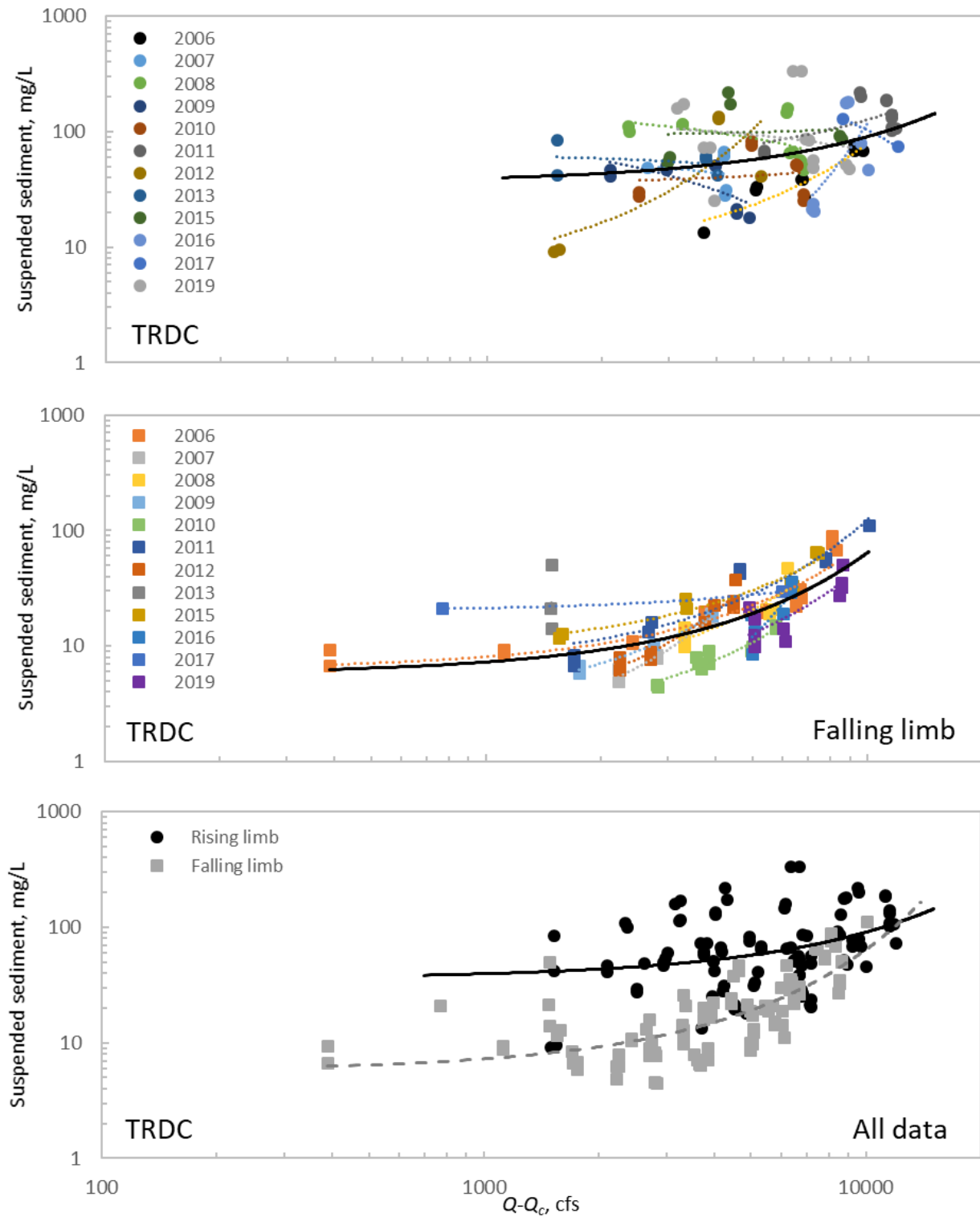
NOTE: Dotted lines are annual curves and solid lines are curves for the period of record at TRAL (2006–2016) and TRLG and TRDC (2006–2019).



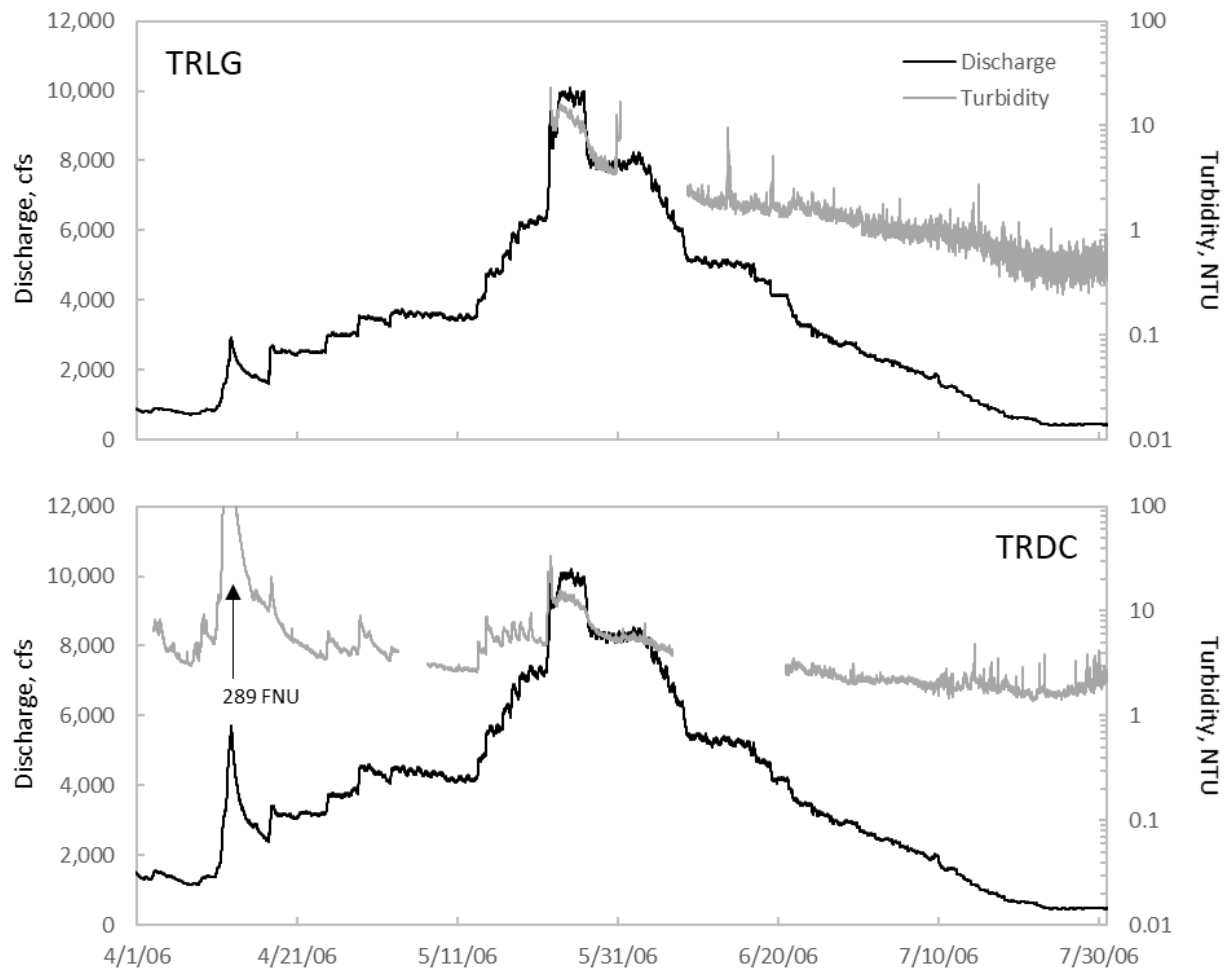
APPENDIX K. (continued)



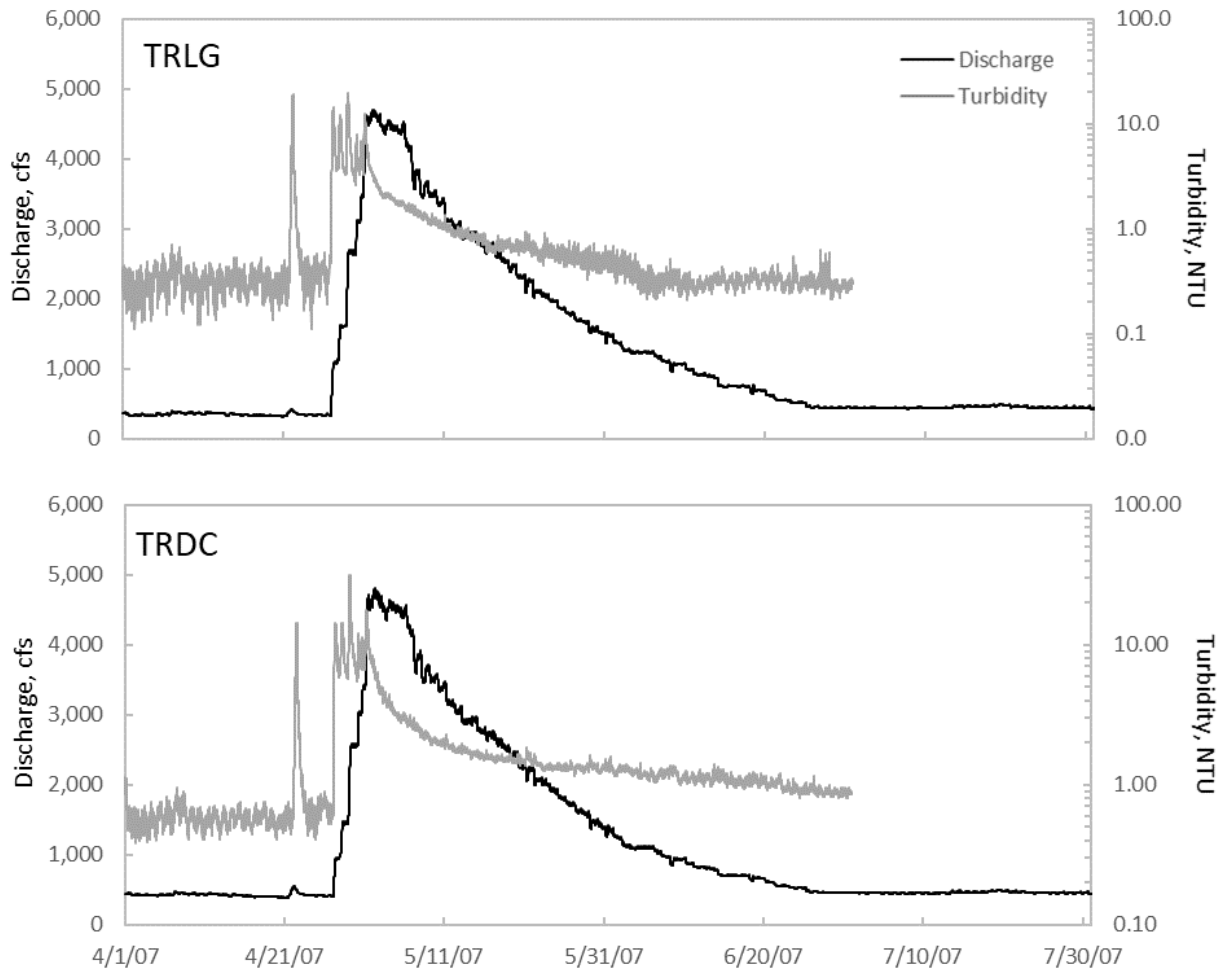
APPENDIX K. (continued)



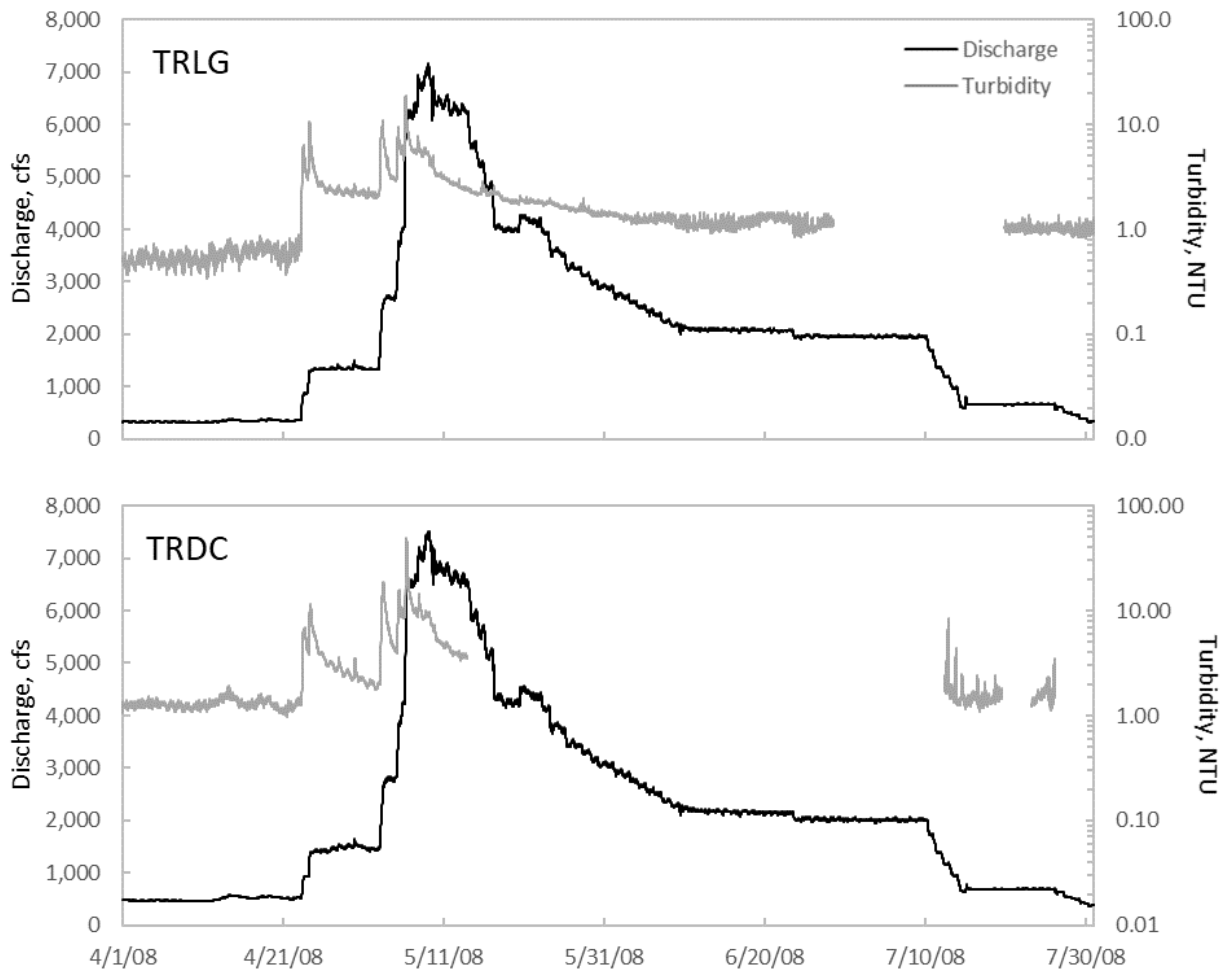
APPENDIX L. Turbidity and daily average discharges for spring flow releases at TRLG and TRDC.



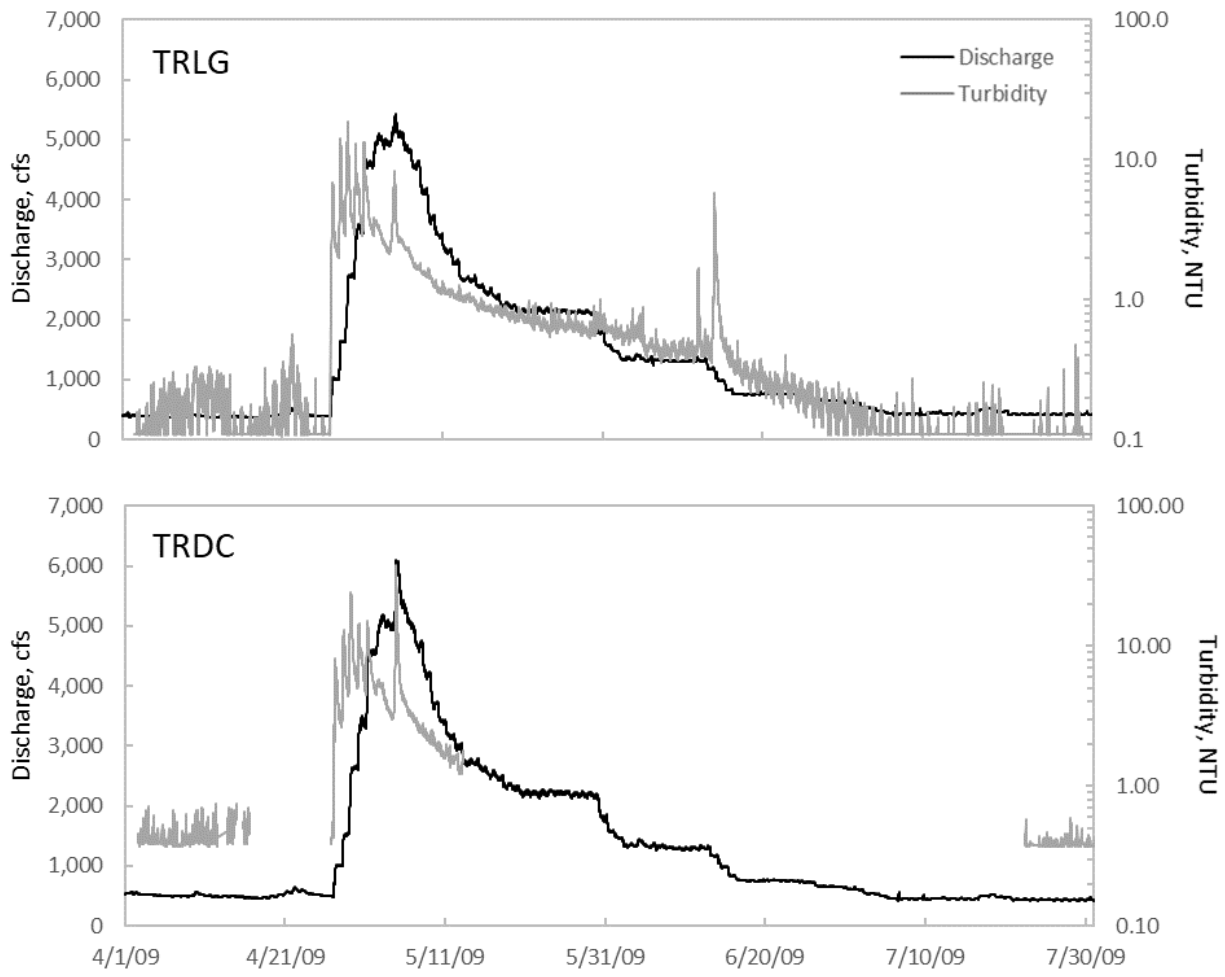
APPENDIX L. (continued)



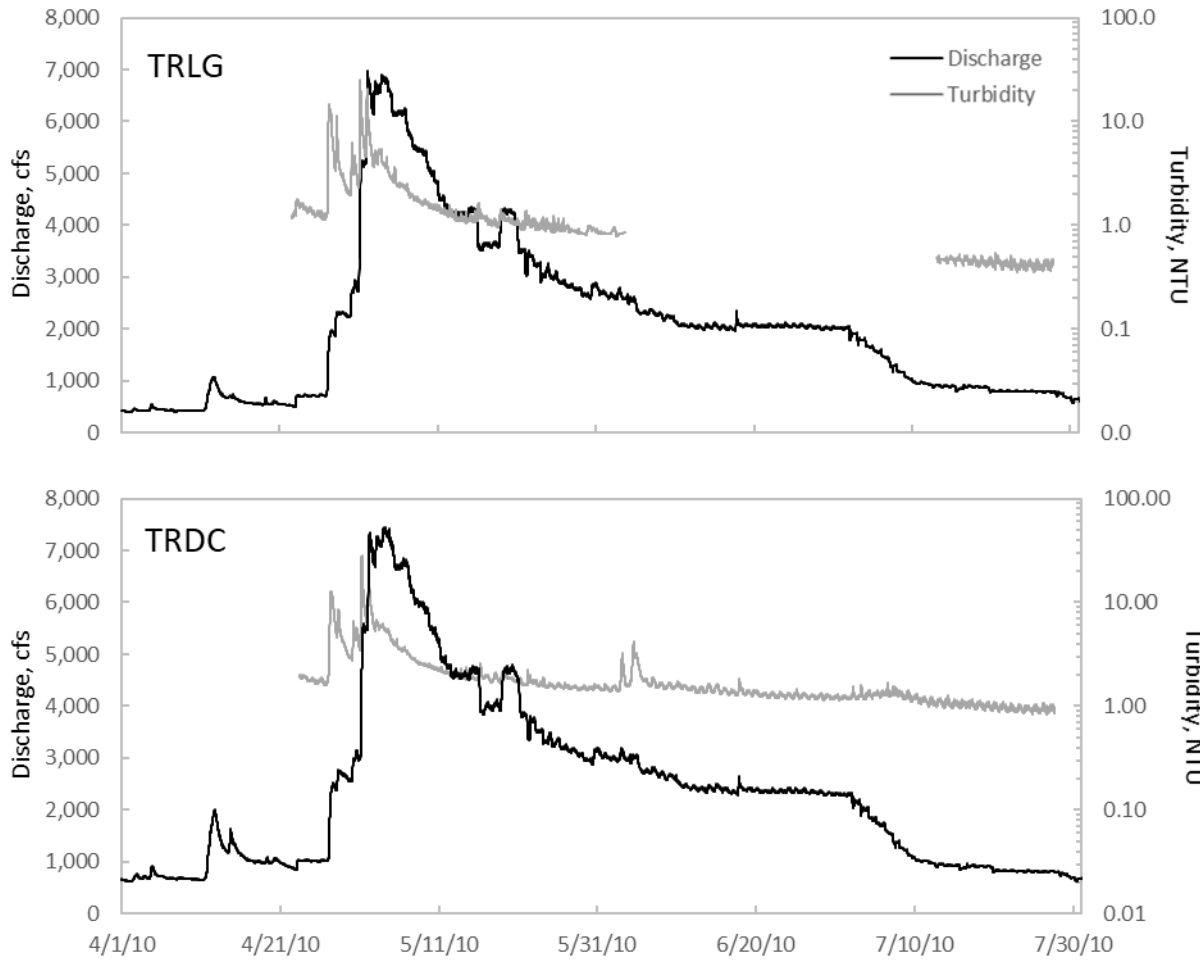
APPENDIX L. (continued)



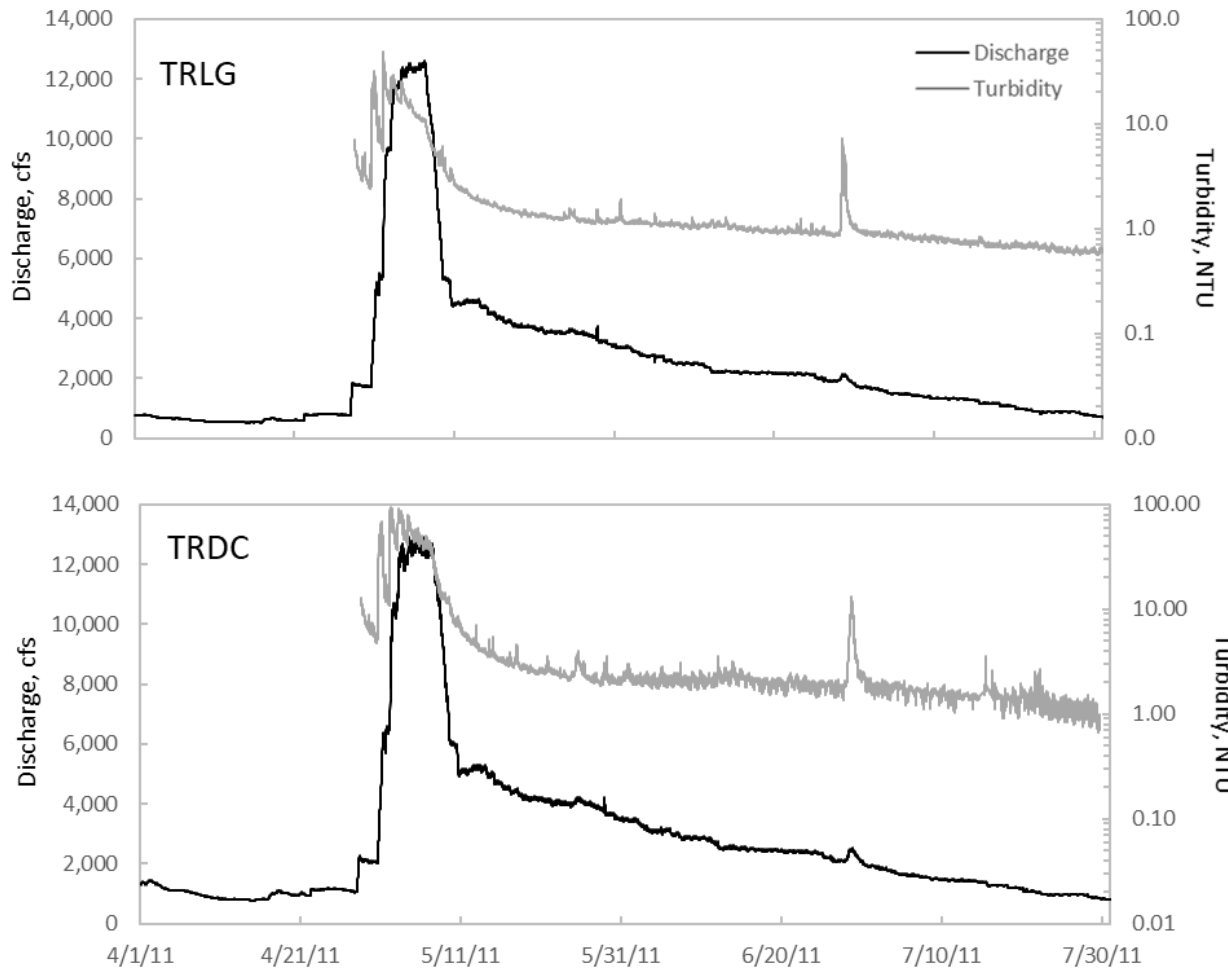
APPENDIX L. (continued)



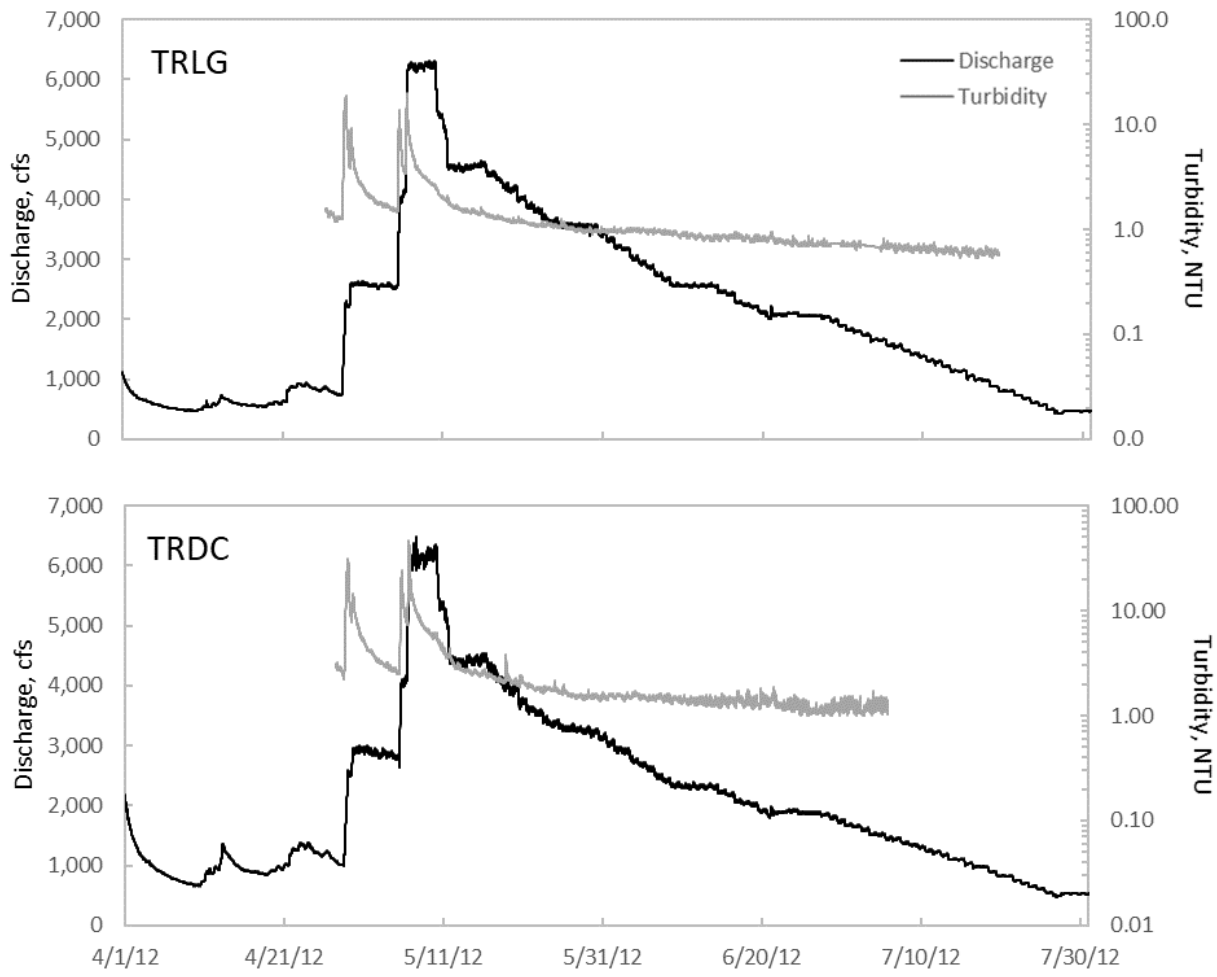
APPENDIX L. (continued)



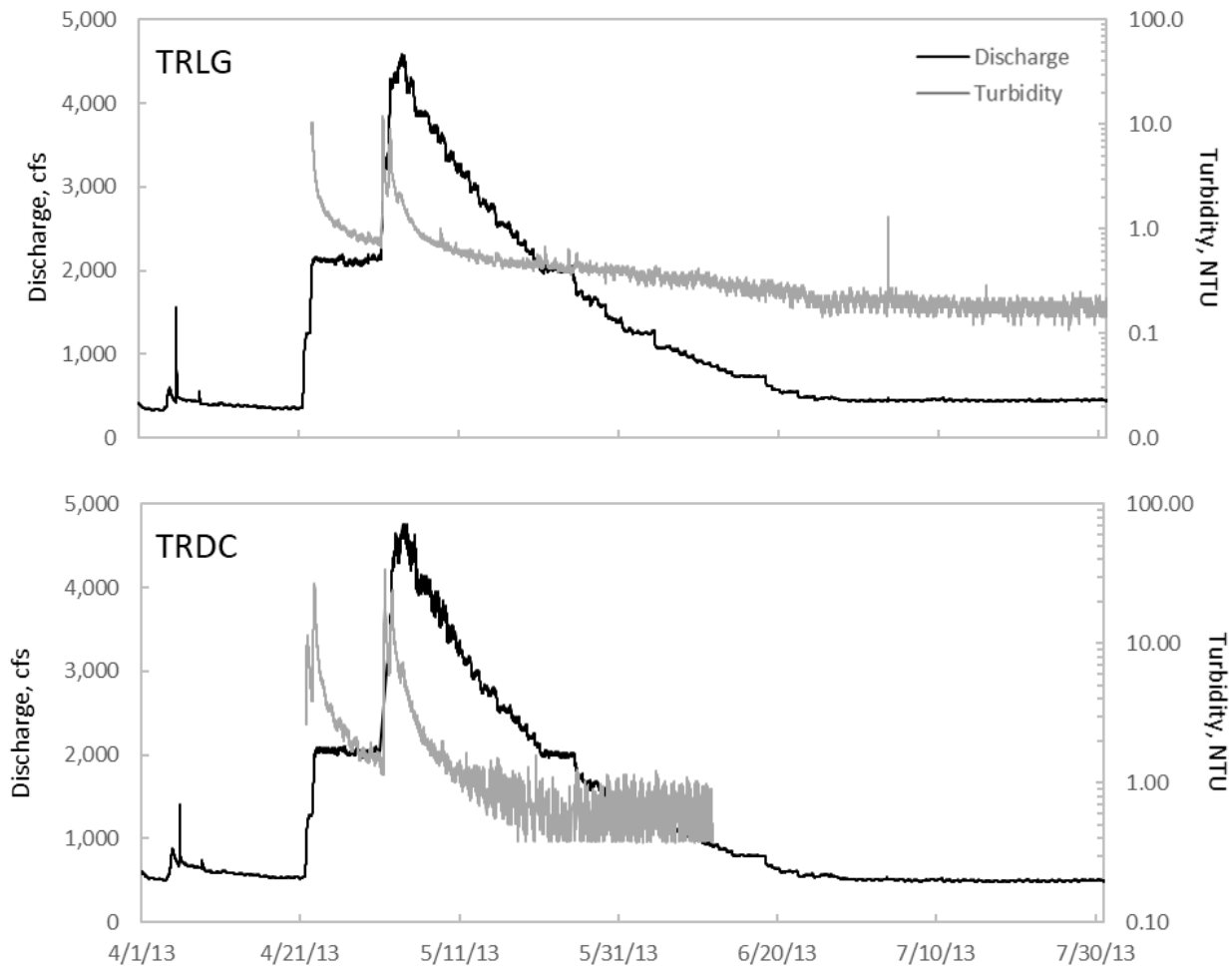
APPENDIX L. (continued)



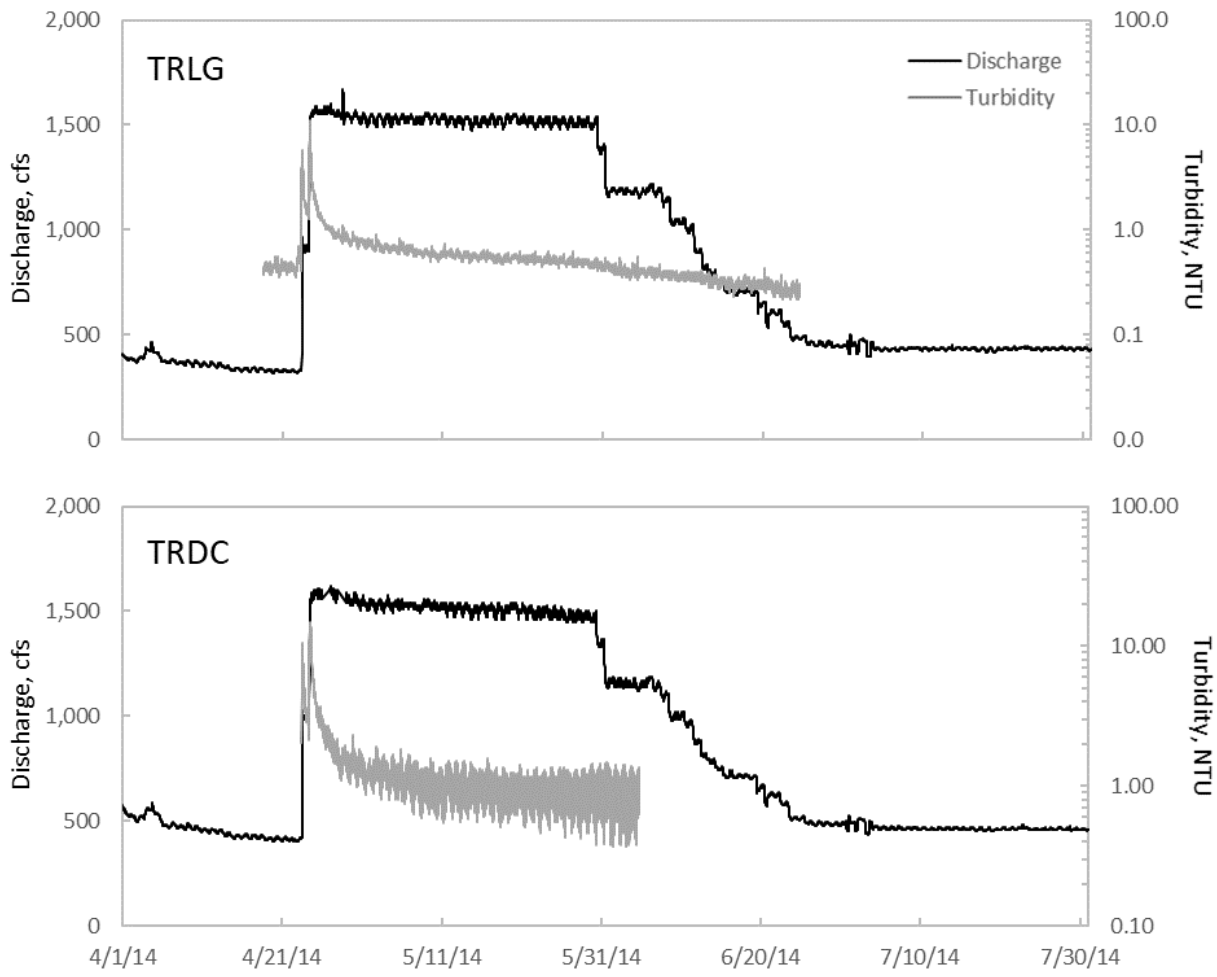
APPENDIX L. (continued)



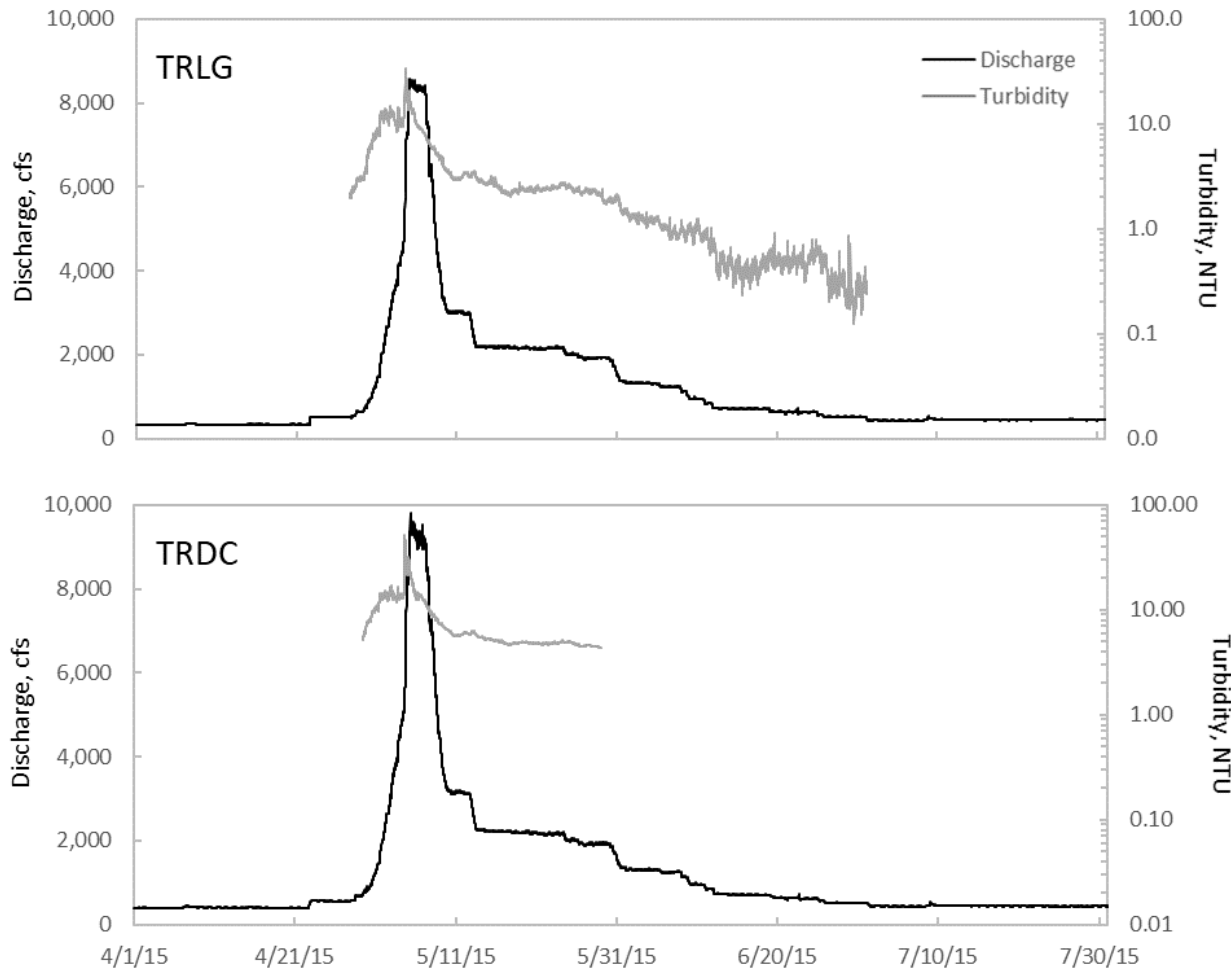
APPENDIX L. (continued)



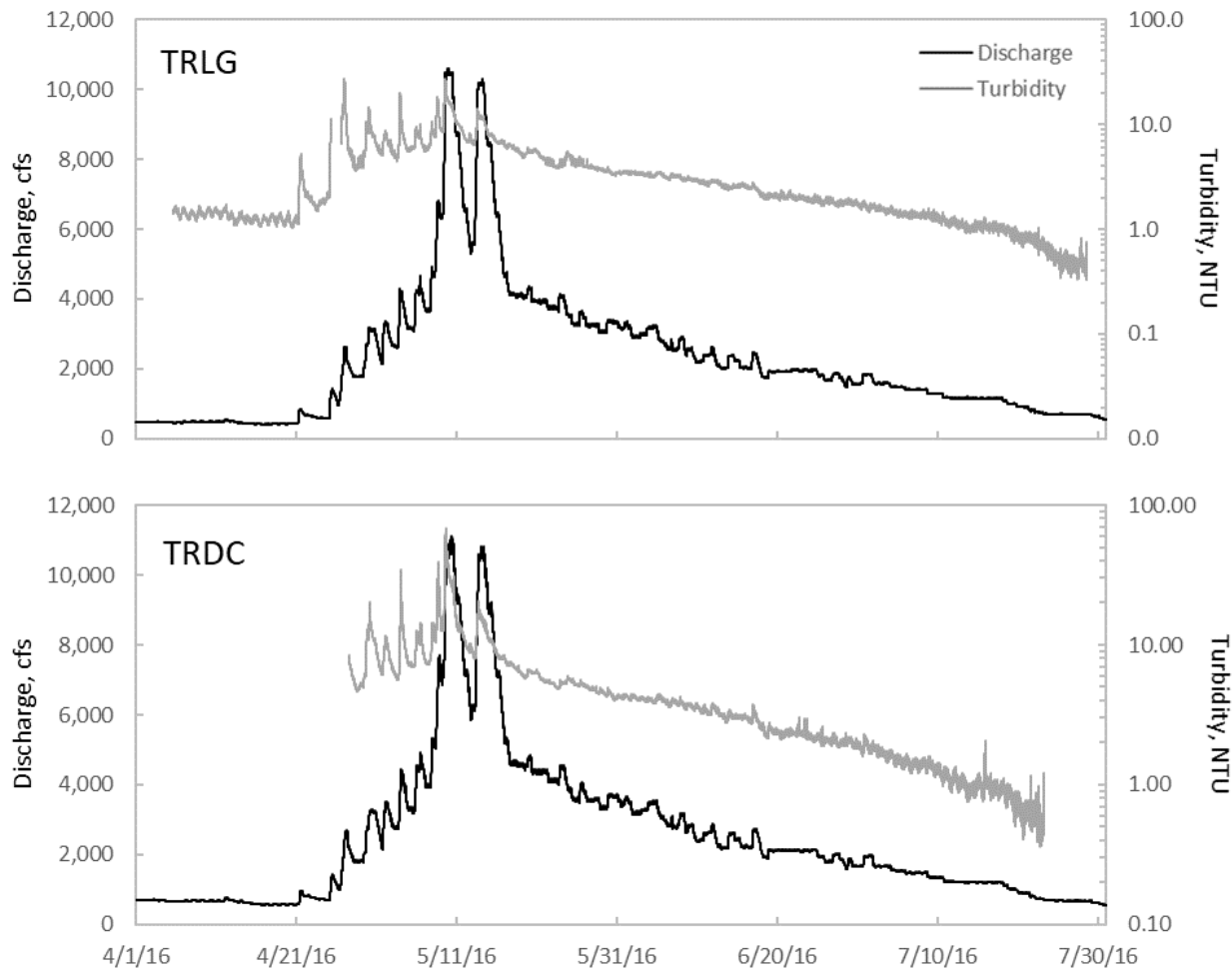
APPENDIX L. (continued)



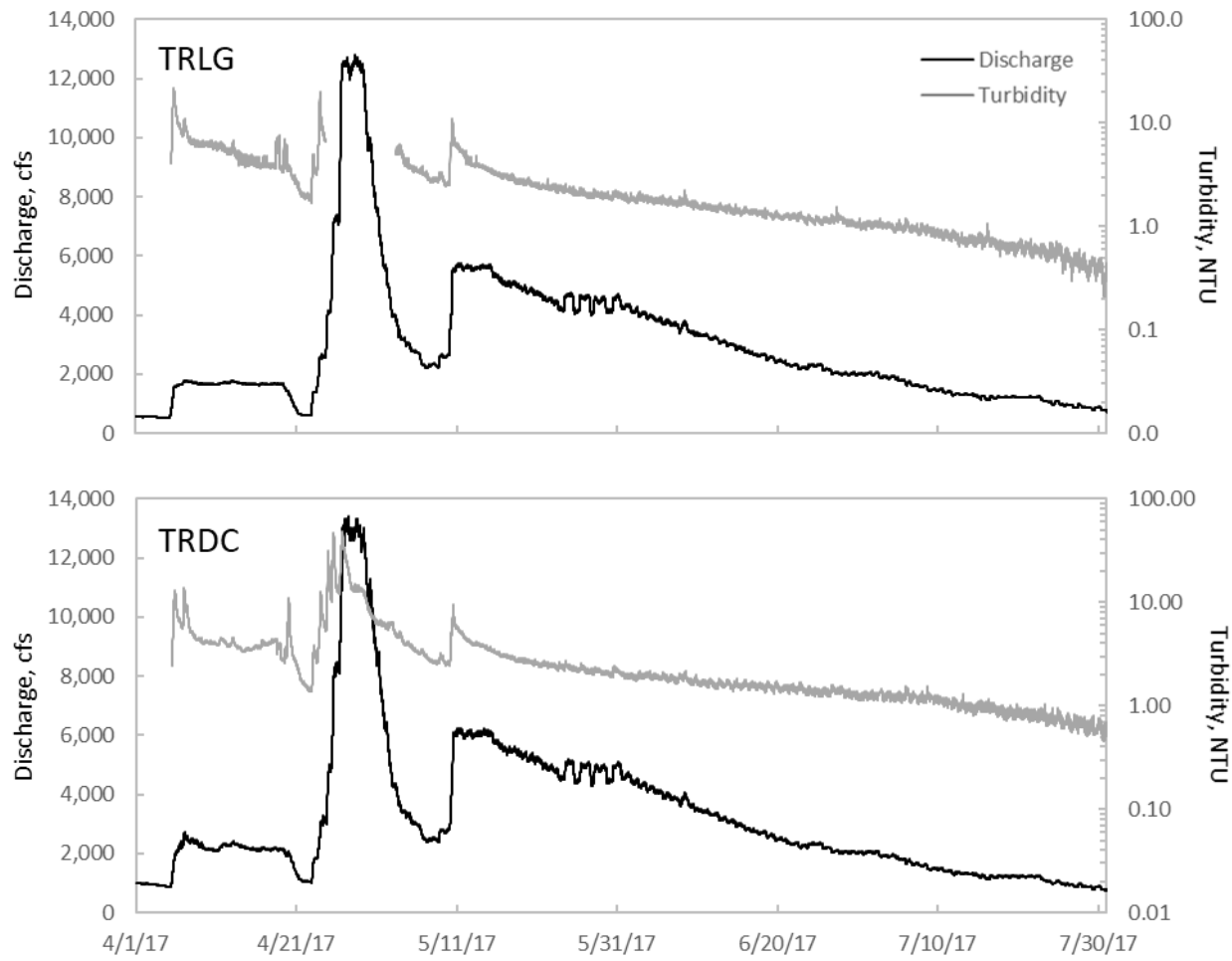
APPENDIX L. (continued)



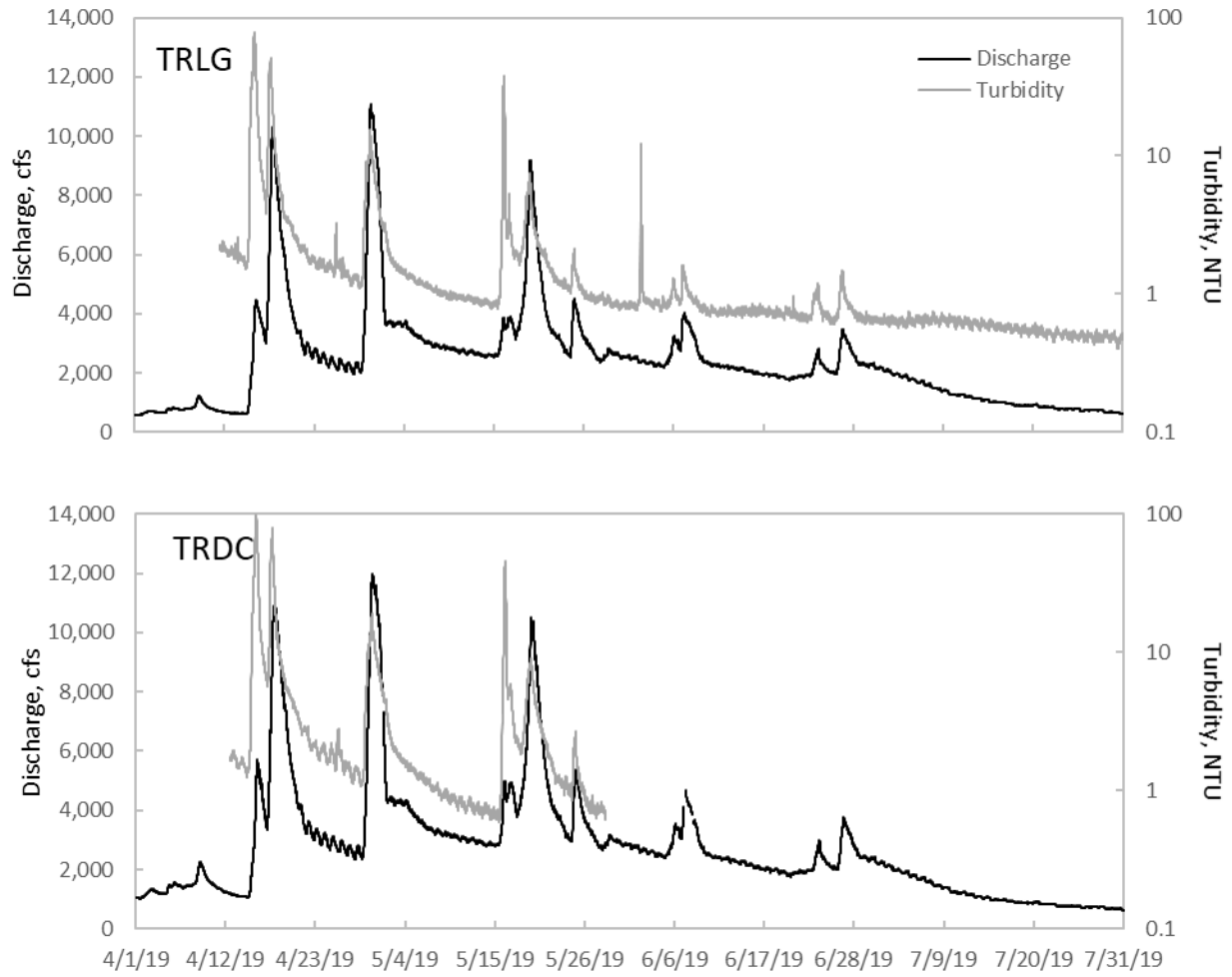
APPENDIX L. (continued)



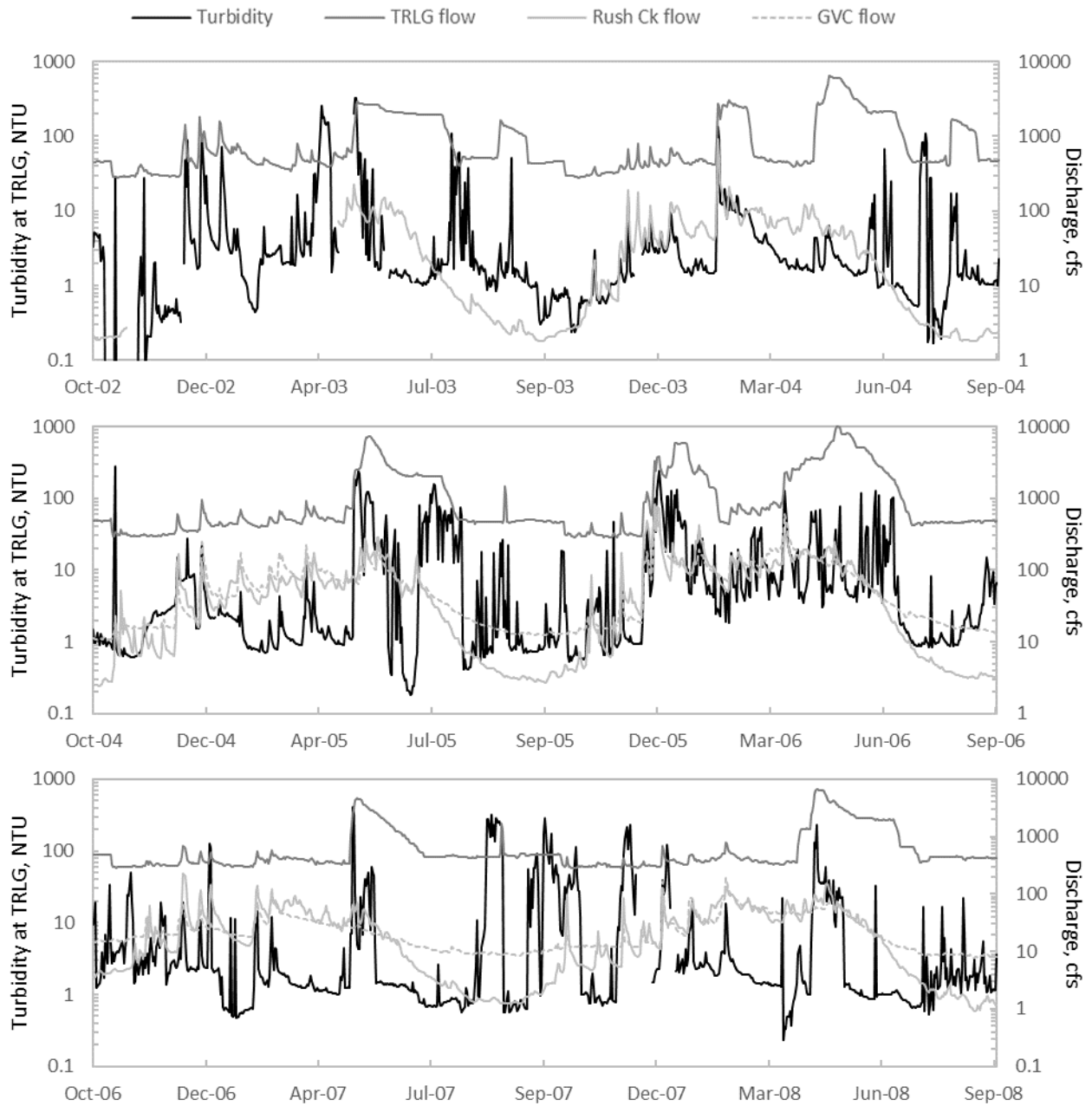
APPENDIX L. (continued)



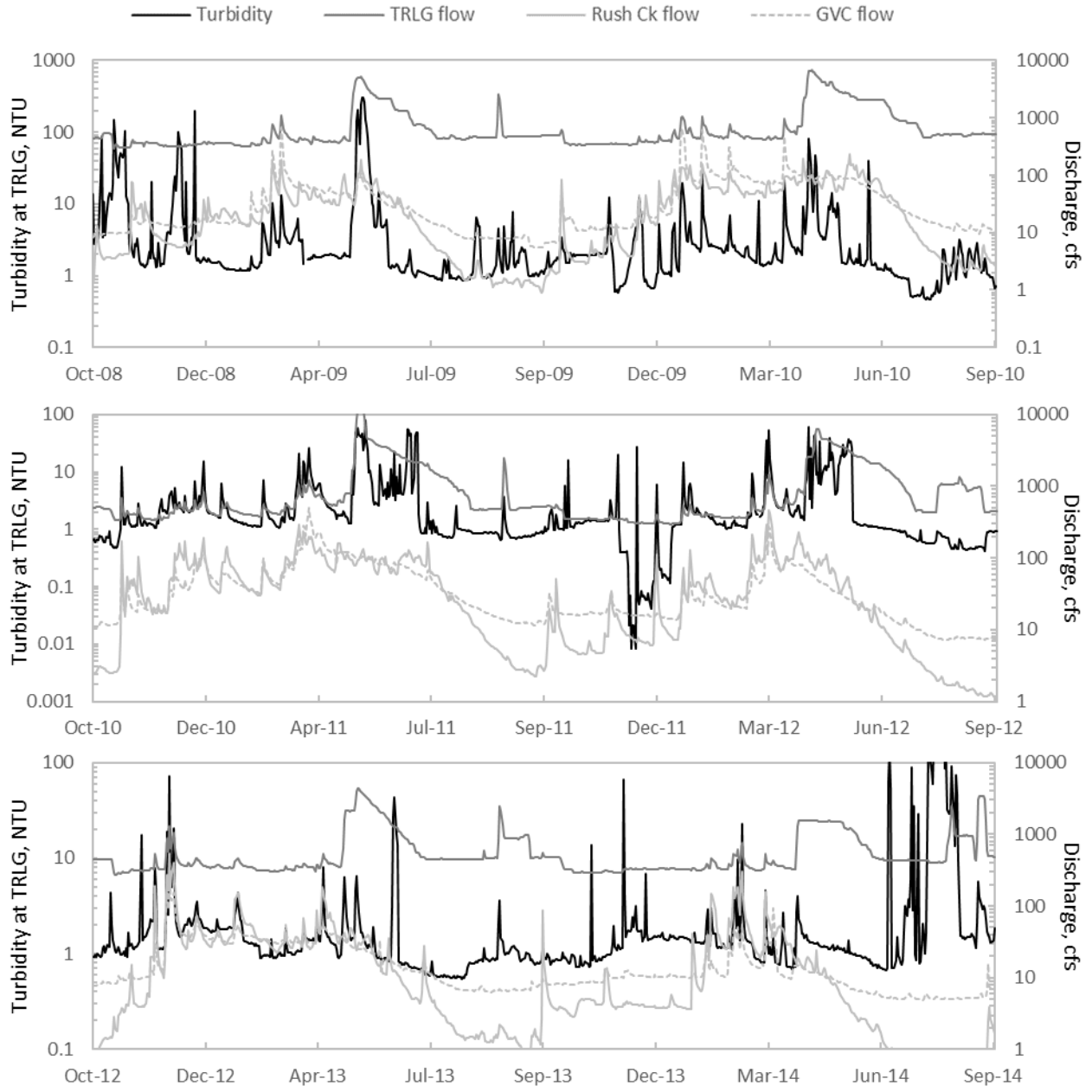
APPENDIX L. (continued)



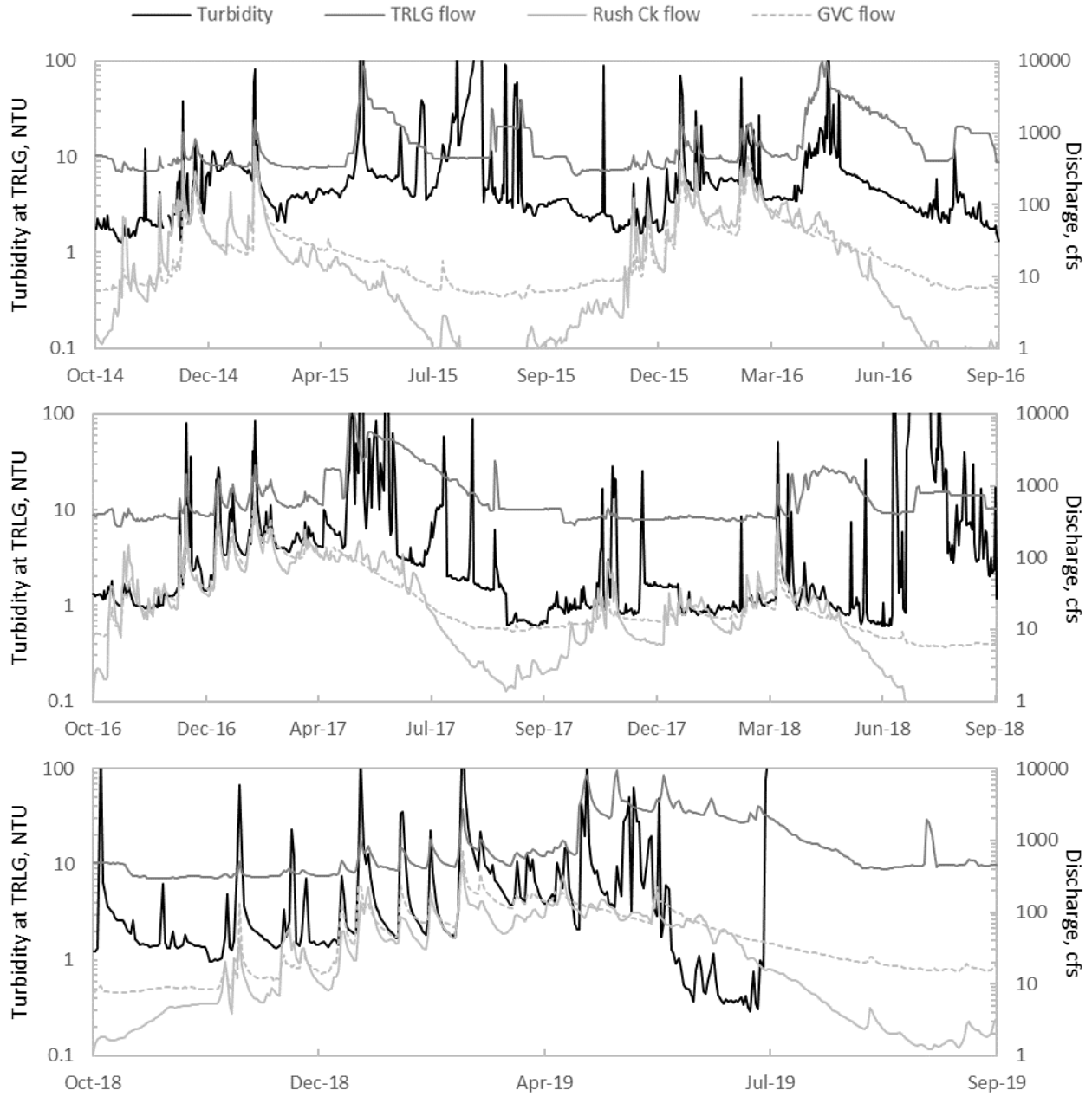
APPENDIX M. Turbidity and daily average discharges at TRLG, Rush Creek, and Grass Valley Creek (GVC).



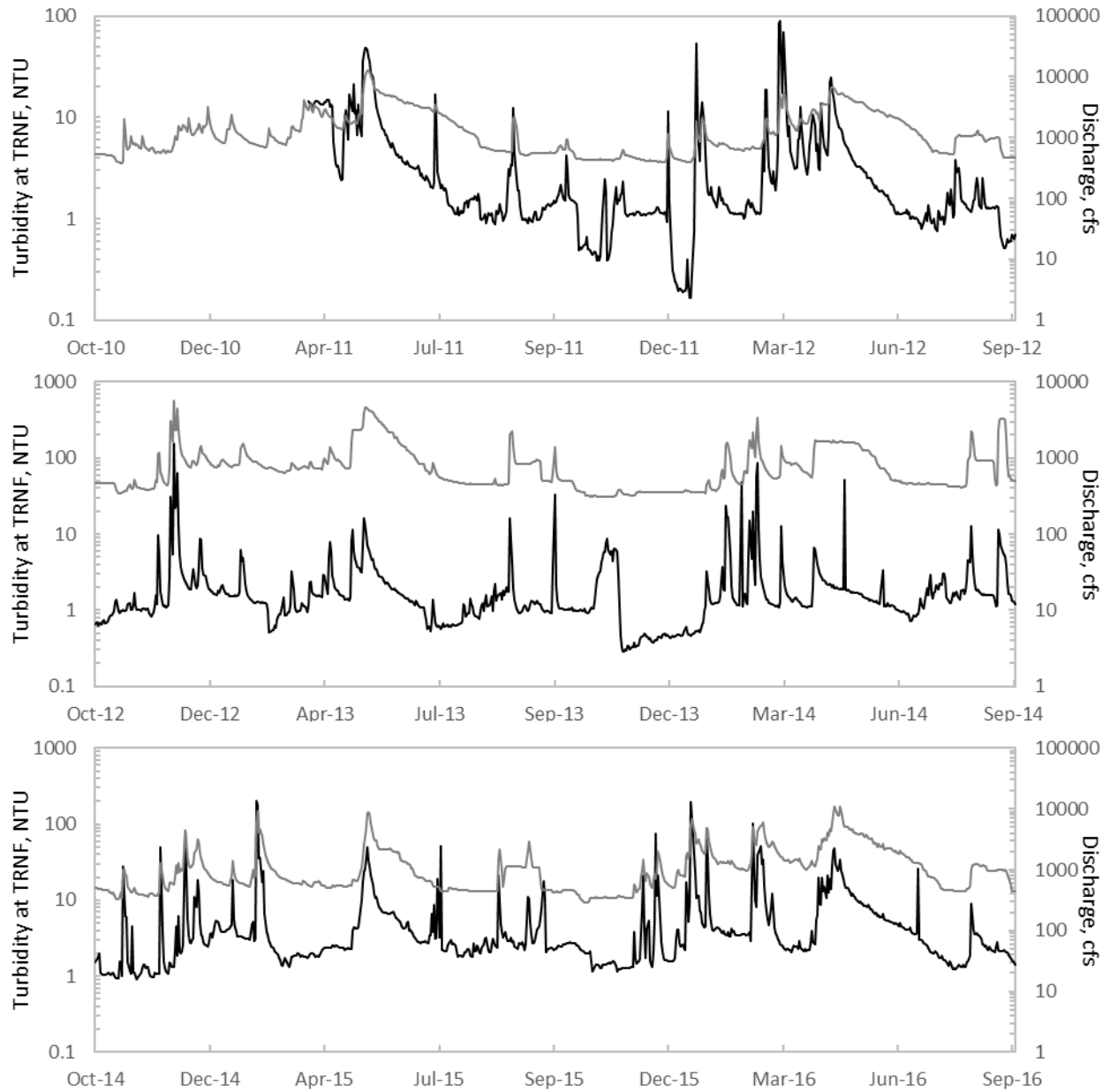
APPENDIX M. (continued)



APPENDIX M. (continued)



APPENDIX N. Turbidity (black line) and daily average flows on the Trinity River above the North Fork Trinity River (TRNF).



APPENDIX N. (continued)

